2015

Palaeoecology of the late Permian mass extinction and subsequent recovery

Foster, William J.

http://hdl.handle.net/10026.1/5467

PALAEOECOLOGY OF THE LATE PERMIAN MASS EXTINCTION EVENT AND SUBSEQUENT RECOVERY

by

WILLIAM JOSEPH FOSTER

A thesis submitted to Plymouth University

in partial fulfilment for the degree of

DOCTOR OF PHILOSOPHY

Earth and Environmental Sciences Doctoral Training Centre

August 2015

This copy of the thesis has been supplied on condition that anyone who consults it is understood to recognise that its copyright rests with its author and that no quotation from the thesis and no information derived from it may be published without the author's prior consent.

Acknowledgements

AUTHOR'S DECLARATION

At no time during the registration for the degree of Doctor of Philosophy has the author been registered for any other University award without prior agreement of the Graduate Sub-Committee.

Work submitted for this research degree at the Plymouth University has not formed part of any other degree either at Plymouth University or at another establishment.

Relevant scientific seminars and conferences were regularly attended at which work was often presented; external institutions were visited for consultation purposes and several papers prepared for publication.

Publications:

Foster, W.J. and Twitchett, R. J. 2014. Functional Diversity of marine ecosystems after the Late Permian mass extinction event. *Nature Geoscience* 8, 33-238.

Foster, W.J., Danise, S., Sedlacek, A., Price, G.D., Hips, K. and Twitchett, R.J. SUBMITTED. Eutrophication, sediment fluxes and salinity fluctuations delay the recovery of benthic invertebrates following the late Permian mass extinction event. *Palaeogeography, Palaeoclimatology, Palaeoecology*

Presentations and Conferences attended:

Foster, W.J., Danise, S. and Twitchett, R.J. Palaeoecology of benthic marine communities in the wake of the Late Permian mass extinction event. Palaeontological Association Annual Meeting, Leeds, United Kingdom (Oral Presentation).

Foster, W.J., Danise, S., Price, G.D. and Twitchett, R.J. 2014. Palaeoecology of the late Permian mass extinction event and subsequent recovery. Co-Evolution of Life and the Planet 2014 Conference, London, UK (Oral Presentation).

Foster, W.J. and Twitchett, R.J. 2014. Functional diversity of marine ecosystems after the late Permian mass extinction event. 4th International Palaeontological Congress, Mendoza, Argentina (Oral Presentation).

Foster, W.J. and Twitchett, R.J. 2013. Ecospace occupation across the Permian/Triassic boundary. Geological Society of America, abstracts with Programs Vol. 45, No.7, p.803. (Poster).

Foster, W.J. and Twitchett, R.J. 2013. Functional diversity of marine ecosystems after the late Permian mass extinction event. Palaeontological Association Annual Meeting, Zürich, Switzerland (Poster).

Word count of main body of thesis: 63,588

Signed …………………………

Date……………………………

Abstract

Palaeoecology of the late Permian mass extinction event and subsequent recovery

William Joseph Foster

Climate warming during the latest Permian is associated with the most severe mass extinction event of the Phanerozoic, and the expansion of hypoxic and anoxic conditions into shallow shelf settings. Our understanding of the magnitude, pattern and duration of the extinction event and subsequent recovery remains equivocal. Evidence suggests that the action of waves provided an oxygenated refuge, i.e. 'habitable zone', above wave base that may be limited to high latitudes, in association with a faster pace of recovery. In addition, advanced recovery faunas have been documented from the Induan and there is evidence from the pelagic realm that further biotic crises may have delayed the recovery of benthic organisms coinciding with large carbon isotope perturbations at the Lower Triassic sub-stage boundaries. To test these hypotheses, novel palaeoecological data was collected from localities in Hungary, northern Italy, and Svalbard. To understand better the ecological impact of the extinction, a database of all known benthic marine invertebrates from the Permian and Triassic periods was created, with each taxon assigned to a functional group based on their inferred lifestyle.

This study found that the skeletal and ichnofaunal assemblages consistent with advanced ecological recovery are limited to settings aerated by wave activity, which supports the habitable zone hypothesis. In the western Palaeotethyan sections it was found that the proximal end of the 'habitable zone' was limited by persistent environmental stress attributed to increased runoff that resulted in large salinity fluctuations, increased sedimentation rates and eutrophication creating an environment only favourable for opportunistic taxa. In the *Tirolites carniolicus* Zone, however, the 'habitable zone' expands into more proximal and offshore settings. This is associated with climate cooling in the late Spathian. The data also demonstrate that despite the taxonomic severity of the extinction, only one mode of life went extinct and only one subsequently evolved in the aftermath. Functional diversity was, however, reduced in particular regions and environmental settings, and recovery varied spatially and temporally.

In western Palaeotethys, benthic communities record evidence for biotic crises, such as reduced tiering in the Smithian, associated with Early Triassic carbon isotope excursions, but, until the Spathian there was no significant change in the composition of the benthic faunas.

Table of Contents

List of Figures

List of Tables

1. Introduction

The Permian-Triassic transition marks a time of major upheaval in the diversity and functioning of marine ecosystems leading to a major turnover of the marine communities. The late Permian mass extinction event (LPE), the most taxonomically and ecologically catastrophic extinction event of the Phanerozoic (Sepkoski, 2002; Stanley, 2007; Alroy et al., 2008; McGhee et al., 2004), occurred just prior to the Permian/Triassic (P/Tr) boundary; where 52% of families (Raup and Sepkoski, 1982), 78% of genera (Payne and Clapham, 2012) and 95% of species (Raup, 1993) are estimated to have gone extinct. The catastrophic nature of the LPE reduced taxonomic richness to levels not recorded since the Cambrian and led to the initial radiation of the 'modern' fauna that characterises our oceans today (Sepkoski, 1984; Sepkoski, 2002; Figure 1.1).
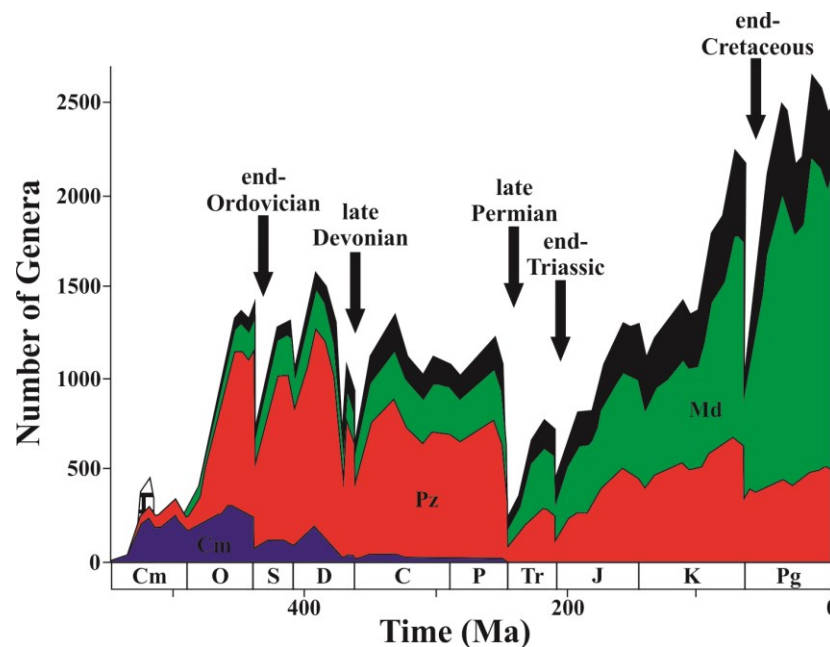
Figure 1.1: Generic-level diversity of both extant and extinct marine invertebrates during the Phanerozoic. The diversity curve is divided into four groups representing evolutionary faunas described by Sepkoski (1984): Cm = Cambrian fauna, Pz = Palaeozoic fauna and Md = Modern fauna, and soft-bodied and lightly sclerotized groups which are only rarely preserved as fossils (black proportion). Symbols for the x-axis indicate geological periods. After Sepkoski (2002).

Regional and local studies investigating the severity of the LPE have concluded that there is evidence of a series of extinction events spanning the late Permian *Clarkina yini* to *Isarcicella isarcica* conodont zones in South China (Zhao and Tong, 2010; Shen et al., 2011; Song et al., 2013; Clapham et al., 2013; He et al., 2015) and the upper *Hindeodus praeparvus* to the *H. parvus* conodont zone in northern Italy (Farabegoli et al., 2007; Crasquin et al., 2008). Recent U-Pb dating from the P/Tr Global Stratotype Section and Point (GSSP), Meishan section (Yin et al., 2011), suggests that this interval lasted ~60ka ±48ka (Burgess et al., 2014) with the main extinction pulse in south China and northern Italy occurring at the beginning of the extinction interval (Jin et al., 2000; Posenato, 2010; Wang et al., 2014).

The LPE also created largely vacant ecospace in reef environments and in deep infaunal tiers within the substrate (Twitchett and Wignall, 1996; Twitchett, 1999; Ausich and Bottjer, 2001; Flügel, 2002; Frasier and Bottjer, 2009; Hofmann et al., 2015b). After the LPE, transient reef ecosystems were composed of microbial mounds (Kershaw et al., 1999; Weidlich et al., 2003) that housed a microscopic fauna (Kershaw et al., 2011; Forel et al., 2013). It is not until the Smithian that reef-building metazoans are recorded in Lower Triassic sediments (Brayard et al., 2011). The diversity of reef-building metazoans again increases in the late Spathian, with the establishment of *Tubiphytes* (Payne et al., 2006b) and *Placunopsis* reef ecosystems (Pruss et al., 2007). Likewise the re-filling of ecospace in the deeper infaunal tier follows a stepwise pattern with benthic communities restricted to within a few centimetres of the sediment-water interface in the wake of the LPE, followed by an expansion into the deep infaunal tier during the Dienerian and Spathian (Twitchett and Wignall, 1996; Twitchett, 1999; Twitchett and Barras, 2004; Twitchett, 2006; Fraiser and Bottjer, 2009; Zonneveld et al., 2010; Chen et al., 2011; Hofmann et al., 2015b). Locally, therefore, the initial stages of recovery were underway during the Early Triassic.

Our understanding of the post-extinction recovery of marine ecosystems following the LPE is equivocal. At one extreme is the traditional view of a lengthy or delayed recovery (e.g. Hallam 1991; Payne et al., 2006a). This view is most evident in global-scale analyses; for example, it apparently took ca. 100 million years for family-level marine diversity to return to pre-extinction levels (Benton and Twitchett, 2003). Full recovery is typically described as occurring in the late Anisian, approximately eight million years after the LPE (Chen and Benton, 2012), and signalled by the return of many Lazarus taxa (Erwin and Pan, 1996), a marked increase in the diversity of bivalves (Posenato, 2008a) and other groups, reappearance of metazoan reef communities (Velledits et al., 2011) and reappearance of stenotopic hard-bottom dwellers (Posenato, 2002), amongst others.

Advances in radiometric dating have proven pivotal to improving our understanding of the gap between extinction and recovery. Prior to Ovtcharova et al. (2006) and Lehrmann et al. (2006b) no radiometric ages existed from the Dienerian to Illyrian and it was inferred from interpolation that the Early Triassic spanned ~8 Myr (Erwin, 1993).
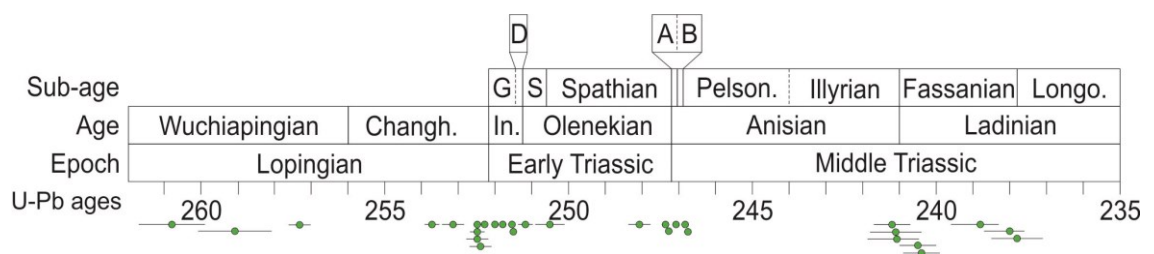
Figure 1.2: Late Permian-Middle Triassic timescale based on U-Pb radiometric dating studies: Mundil et al. (2004), Ovtcharova et al. (2006), Galfetti et al. (2007), Lehrmann et al. (2006), Brack et al. (2005), Pálfy et al. (2003), Shen et al. (2011), Burgess et al. (2014). Radiometric dates are marked by a green circle and error bars by horizontal black line. Abbreviations: Changh. = Changhsingian, G = Griesbachian, D = Dienerian, In = Induan, A = Aegean, B = Bithynian, Pelson = Pelsonian, Longo = Longobardian.

Recent radiometric dates (Ovtcharova et al., 2006; Lehrmann et al., 2006; Galfetti et al., 2007b), however, have shown that the Early Triassic lasted for 4.5 ±0.6 Myr, with the Spathian sub-stage spanning ~3 Myr (Figure 1.2). Therefore, the lag between extinction and recovery has been shortened.

1.1. Selectivity of the late Permian mass extinction

The LPE was highly selective with the 'Palaeozoic fauna' becoming severely reduced (Bush and Bambach, 2011). The dominant lifestyles among this fauna were erect and epifaunal sessile suspension feeders, most of which were also heavily calcified organisms with little inferred physiological control over mineralisation (Knoll et al., 2007). Song et al. (2014) also suggest that these Palaeozoic invertebrate groups may have had lower thermal tolerances than the "modern" fauna. These taxa never regained their former dominance and this permitted the rise of the 'modern fauna' (*sensu* Sepkoski, 1984), and an increasing stock of motile, infaunal and predatory marine animals throughout the Mesozoic (Aberhan et al., 2006).

One characteristic of the taxa that survived the extinction event is that their body size was significantly reduced, i.e. the Lilliput Effect (Twitchett, 2001; Twitchett, 2007; He et al., 2007; Wade and Twitchett, 2009; Metcalfe et al., 2011; Song et al., 2011; He et al., 2015). The Lilliput effect is only restricted to the immediate aftermath of the LPE (Twitchett, 2007), as individuals of the Early Triassic show size increases within the Induan (Metcalfe et al., 2011), and sizes of some taxa in the Spathian are comparable to the remainder of the Triassic (Brayard et al., 2010). In addition, those taxa that originated in the immediate aftermath were also of a small size compared to pre-extinction invertebrates (Twitchett, 2001; Twitchett, 2007; Metcalfe et al., 2011), e.g. heterodont bivalves (Hautmann and Nützel, 2005). Metcalfe at al. (2011) and Posenato et al. (2014) also show that even the opportunistic taxa that flourished in the wake of the LPE adapted by reducing their body size. Posenato et al. (2014) inferred that the

physiological adaptations, in particular the increase in the size of the lophophoral cavity of lingulid brachiopods across the LPE, were a response to reduced oxygen levels.

Palaeobathymetry has also been suggested as an important factor in the survival of some benthic invertebrate groups. In south China, the extinction of brachiopods shows an onshore-offshore trend where the onset of the LPE is interpreted to be more catastrophic and occur earlier in basinal settings than shallow platform settings (Chen et al., 2010b; Chen et al., 2011a; He et al., 2015). Furthermore, Clapham et al. (2013) found that, after the LPE, brachiopod dominance of marine communities was greater in shallower environments in northern Italy and the western US, whilst bivalves dominated assemblages in the deeper environments.

Payne and Clapham (2012) found that the LPE was relatively uniform between regions and latitudes and, therefore, neither local nor global abundance favoured survival, as would be expected during a mass extinction event (Harries et al., 1996). However, in well-studied sections in China and central Europe the impact of the LPE is slightly lower compared to the rest of the world. The higher survivorship in these areas is due to a few brachiopod species (e.g. Chen et al., 2006b) that may have also survived in other less-well studied regions (Erwin and Pan, 1996). A sampling bias, therefore, may be obscuring our understanding of the survival of the LPE (Allison and Briggs, 1993). Conversely, the survival and radiation of the bryozoans suggest that the mid- to high-latitude settings of the Boreal Ocean may have provided a refuge, as Induan bryozoans are only known from this region (Powers and Pachut, 2008).

1.2. Marine anoxia and euxinia

Strata that span the Permian-Triassic transition from sections around the globe show evidence of rapid sea-level rise, in addition to the large taxonomic losses (Hallam, 1991; Jin et al., 2000; Wignall and Twitchett, 2002b). Intensely bioturbated pre-extinction

sediments are overlain typically by laminated, pyrite-rich sediments that represent oxygen-restricted facies (Wignall and Hallam, 1992; 1993; Wignall and Twitchett, 1996; Wignall and Twitchett, 2002b; Thomas et al., 2004; Nabbefeld et al., 2010). These laminated sediments and the presence of pyrite framboids in shallow to deep water facies in the immediate extinction aftermath suggest anoxic conditions were widespread in Tethyan, Boreal and Panthalassan regions (Wignall and Twitchett, 2002b; Bond and Wignall, 2010; Grasby et al., 2013). Erwin (1993) and Hofmann et al. (2015b), however, suggest that the laminated sediments were due to the extinction of bioturbators rather than persistent anoxia.

Sections from Canada, Australia, India, Greenland and Svalbard that represent mid- to high-latitudes in the Boreal, Neotethys and Panthalassa oceans (Figure 1.3) contain small (<7μm) pyrite framboids that provide evidence for persistent anoxia, but their small diameter also suggests euxinic conditions (Bond and Wignall, 2010; Grasby et al., 2013). Evidence for the development of photic zone euxinia also comes from the presence of *Chlorobiaceae* (Green sulfur bacteria) biomarkers (Summons and Powell, 1986). *Chlorobiaceae* are anaerobes that use the light-harvesting pigments bacteriochlorophylls *c*, *d*, and *e*, carotenoids isorenieratene, chlorobactene and aryl isoprenoids to fix CO_2 with H_2S as the electron donor (Grice et al., 2005). Therefore, the presence of these pigments in the strata spanning the LPE can also be used to indicate photic zone euxinia (Summons and Powell, 1986). These pigments have been recorded in sediments spanning the Late Permian extinction in low to mid latitudes: Greenland (Hays et al., 2012), Svalbard (Nabbefeld et al., 2010), Canada (Hays et al., 2007), China (Grice et al., 2005; Cao et al., 2009) and Australia (Grice et al., 2005). The widespread occurrence of these pigments suggests widespread photic zone euxinia during and after the LPE. The Sverdrup Basin, Canada, however, lacks ceratenoid pigments suggesting that photic zone euxinia may not have been persistent in this basin

(Knies et al., 2012). Similarly, the presence of photic zone euxinia in eastern Panthalassa is equivocal (Algeo et al. 2010; 2012). The presence of benthic macroinvertebrates in sediments that show evidence of photic zone euxinia suggests that euxinic waters must have been episodic, as these animals would have required oxygen (Thomas et al., 2004; Grice et al., 2005).

1.3   Changes to the carbon cycle

Carbon isotope changes across the P/Tr boundary show a major disruption of the global carbon cycle near the extinction event, with a negative 4-7‰ $\delta^{13}C$ excursion lasting ~0.5 Ma (Korte and Kozur, 2010). This ^{13}C decline is a global phenomenon occurring in over 100 marine and terrestrial sections worldwide (Korte and Kozur, 2010). The maximum extent of the P/Tr isotope excursion (-1‰ to -2‰) occurs within the *H. parvus* Conodont Zone before returning to temporarily stabilising values of +1‰ to +2‰ in the Griesbachian. This excursion represents a rapid relative decrease in ^{13}C, which may represent a collapse in ocean primary productivity with delivery of organic matter rich in ^{12}C to the sea-floor, causing homogenisation of ocean carbon isotope values (i.e. a "Strangelove Ocean"; Rampino and Caldeira, 2005). A near cessation of primary productivity, which would be associated with a mass extinction of plankton, could lead to a rapid negative shift of ~2 to ~3‰ in ocean surface waters (Rampino and Caldiera, 2005). Meyer et al. (2011) investigated the isotopic gradient of $\delta^{13}C$ of the water column in south China across the extinction interval and throughout the Lower Triassic. These authors found that a strong isotopic onshore-offshore gradient of ~4‰ was established from the late Changhsingian and throughout most of the Lower Triassic suggesting that primary productivity was unusually high, rather than low. This high production may have been driven by nutrient fluxes into the oceans associated with the terrestrial extinction (Algeo et al., 2011; Wei et al., 2015).

Alternatively, the negative isotope excursion may have been caused by an injection of isotopically light carbon, i.e. depleted in ^{13}C. The different carbon-injection scenarios are debated and have been reviewed in Corsetti et al. (2005), Korte and Kozur (2010) and Payne and Clapham (2012). Although these authors have interpreted the $\delta^{13}C$ excursion to be the result of a carbon injection, the magnitude and isotopic composition of the released carbon are unknown because carbon-injection scenarios cannot be uniquely constrained by the magnitude of the $\delta^{13}C$ excursion alone (Payne and Clapham, 2012). The Lower Triassic is also characterised by three further carbon isotope excursions (Payne et al., 2004). The release of methane stored in methane hydrates may explain a catastrophic carbon injection at the P/Tr boundary (Richoz, 2006). Modern estimates, however, suggest that marine clatherate reservoirs require ~10 Myr to 'recharge' after a catastrophic release (Dickens, 2003), therefore, if this scenario explains the P/Tr boundary isotope excursion then alternative causes are needed to explain the later perturbations during the Lower Triassic. Alternatively, carbon injections from volcanism (i.e. the Siberian Traps) may explain the multiple negative isotope excursions as these release ^{13}C-depleted carbon, especially if associated with the destabilisation of methane from permafrost soils and intrusive magma causing the combustion of pre-Trap organic-rich sediments (Svensen et al., 2009; Korte et al., 2010).

1.4   Change in palaeotemperature

Oxygen isotopes can be used as a proxy for a palaeotemperature record because warmer oceans are enriched in $\delta^{16}O$ whilst in cooler periods oceans are depleted in $\delta^{16}O$ (Jouzel et al., 1994). This happens because water molecules formed of ^{16}O evaporate more easily. During glacial periods this water is then stored in the ice leading to ^{16}O depleted oceans.

Across the LPE the ratio of ^{16}O to ^{18}O in the apatite of conodonts increases from 22‰ to 19‰ and in brachiopods from -2‰ to -4‰ which suggests that sea surface temperature (SST) rose by ~8-11°C across the LPE with equatorial SST estimated at ~35°C after the extinction event (Kearsey et al., 2009; Joachimski et al. 2012; Schobben et al., 2014). Oxygen isotopes also show similar timings in the isotope excursions to the carbon isotopes in the late Permian and across the P/Tr boundary (Kearsey et al., 2009; Sun et al., 2012; Romano et al., 2012; Schobben et al., 2014).

These palaeotemperature estimates are all from equatorial settings in the Palaeotethys and Neotethys Oceans. To date, no high latitude oceanic basins have been investigated for a comparison. The unusual occurrence of calcareous red algae, that is normally restricted to hot equatorial settings, in a mid- to high-latitudinal setting (Wignall et al., 1998) suggests that higher latitudes experienced increased temperatures. A decrease in the latitudinal sea-surface temperatures gradient would have led to sluggish ocean circulation (Cubasch et al., 1992). Additionally, Brayard et al. (2006) suggest that ammonoid diversity reflects sea-surface temperatures and thus a pole to equator ammonoid diversity gradient reflects a latitudinal temperature gradient. Brayard et al. (2006) also show that the latitudinal ammonoid diversity gradient in the Griesbachian is severely reduced, suggesting that the sea-surface temperature gradient was also reduced.

1.5 Siberian Trap volcanism as the possible cause of the late Permian extinction

Meteorite impacts (Becker et al., 2001; 2004; Kaiho et al., 2001), H_2S outgassing (Kump et al., 2005) and volcanism from the Siberian Taps (Renne and Basu, 1991; Reichow et al., 2009) have been hypothesised as the cause/s of the LPE. The meteorite impact (Farley et al., 2005; Muller et al., 2005) and the H_2S outgassing scenarios (Harfoot et al., 2008; Meyer et al., 2008) have been discredited, whilst major climate
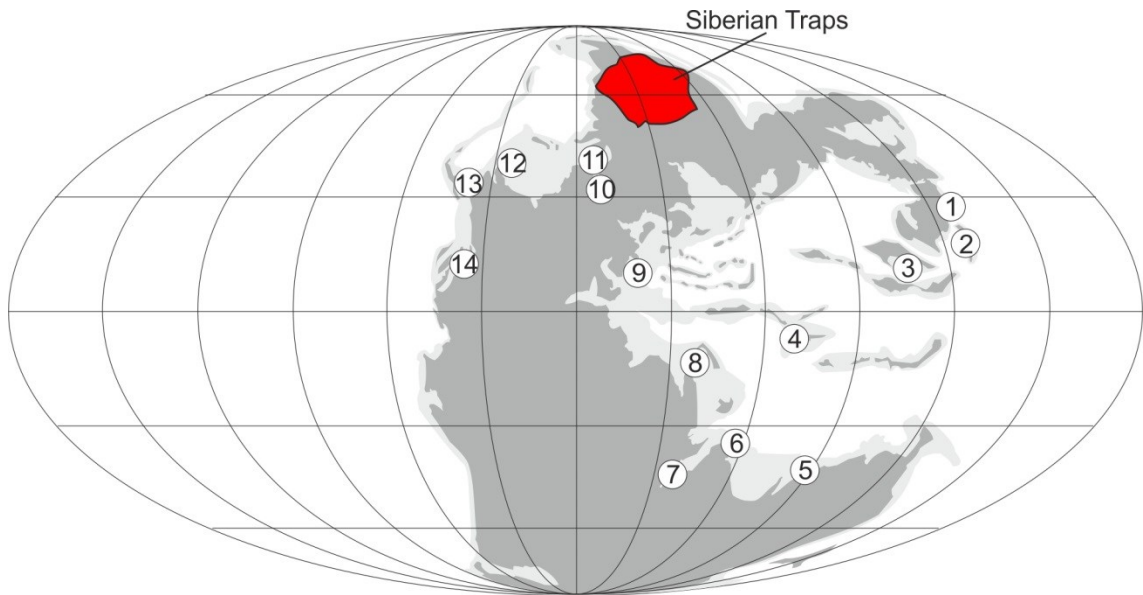
Figure 1.3: Palaeogeographic map of the Early Triassic period showing the palaeoposition of the Siberian Traps and the sites discussed in the text. 1 = Primorye, Russia; 2 = Kitakami Massif, Japan; 3 = south China; 4 = Tibet; 5 = Perth Basin, Australia; 6 = Kashmir, India; 7 = Madagascar; 8 = Oman; 9 = central Europe; 10 = East Greenland; 11 = Svalbard; 12 = Nunavut, Canada; 13 = British Columbia and Alberta, Canada; 14 = western US. Palaeogeographic reconstruction after Blakey, 2011.

warming triggered by Siberian Tap volcanism is the leading hypothesised cause of the LPE (Payne and Clapham, 2012).

According to radiometric dating, the formation of the Siberian Traps began in the late Changhsingian and persisted into the Middle Triassic, with the major phase of volcanism predating or synchronous with the LPE (Reichow et al., 2009; Figure 1.4). $^{40}Ar/^{39}Ar$ data put the onset of Siberian Trap volcanism at 253.5Ma with the main phase of activity at 251-247.5Ma (Reichow et al., 2009) and $^{40}Ar/^{39}Ar$ dates from the extinction horizon for Meishan (bed 25 to 28) are at 250.00 ±0.3Ma (Renne et al., 1995). U/Pb radiometric dates provide a more accurate estimate (Shen et al., 2011) but fewer exist for the Siberian Traps. Using U/Pb ages, the LPE at Meishan is dated as 251.9 ±0.037 (Burgess et al., 2014), whereas, Kamo et al. (2003) dated the lavas from the Noril'sk and Maymecha-Kotuy areas as slightly younger being deposited from

251.7 ±0.4 to 251.1 ±0.6 Ma. Shen et al. (2011) interpret this discrepancy as possibly due to interlaboratory bias related to the calibration of the tracer solutions used in the different laboratories. Siberian Trap volcanism also extends into the Triassic with the youngest known magmatism dated at 229 ±0.4Ma which suggests a possible role in delaying recovery during the Early and Middle Triassic (Kamo et al., 2003).

The Siberian Traps are the largest, Large Igneous Province (LIP) of the Phanerozoic (Wignall, 2001) and covered an area of 2.5 $x10^6$ km^2 (Reichow et al., 2009). Their eruptions would have led to a flux of large quantities of carbon and sulphate volatiles into the atmosphere. Svensen et al. (2009) additionally show that the magmatism from the Siberian Traps occurred over organic-rich shale and petroleum-bearing evaporites are estimated to have generated >100,000 gigatons of CO_2. This is hypothesised to have entered into the atmosphere via kilometre-sized pipe structures, along with, methyl chloride and methyl bromide that would have contributed to depletion of the ozone layer (Svensen et al., 2009; Black et al., 2014). This hypothesis is supported by mutated palynomorphs in late Permian rocks that are inferred to be a consequence of increased ultraviolet-B radiation associated with ozone depletion (Visscher et al., 2004; Beerling et al., 2007).

The large quantities of greenhouse gases emitted into the atmosphere and the persistence of volcanic activity could explain the rapid and long-term warming inferred at the time of the extinction (Kearsey et al., 2009; Sun et al., 2012; Schobben et al., 2014), leading to the chain of events that would have caused the LPE on land and in the oceans (Figure 1.5). The extreme warming would have caused plants with a C3 pathway to photorespirate rather than photosynthesise (Ellis, 2010) and changes to atmospheric circulation causing widespread environmental changes (Rees, 2002). The increase in CO_2, SO_2 and Cl into the atmosphere is likely to have led to acid rain (Wignall, 2001)
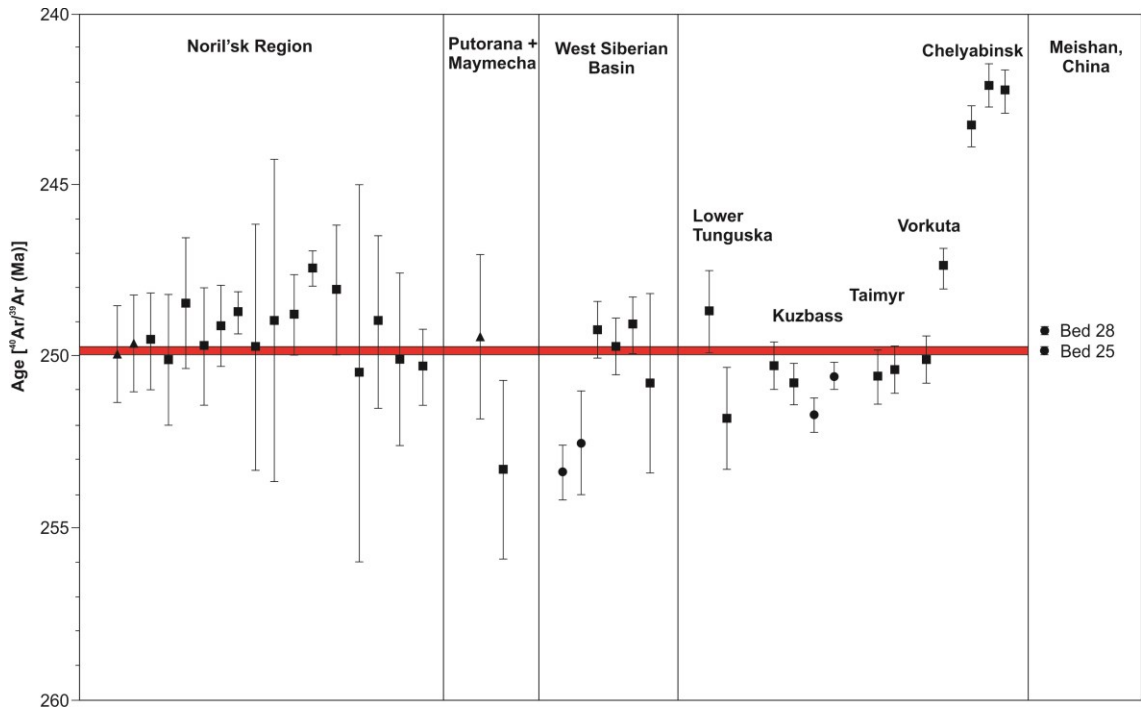
Figure 1.4: Radiometric ages for Siberian Trap volcanism and the late Permian mass extinction at the Meishan, Permian/Triassic GSSP. After Reichow et al. (2009). Red bar indicates the timing (including error bas) of the late Permian mass extinction.
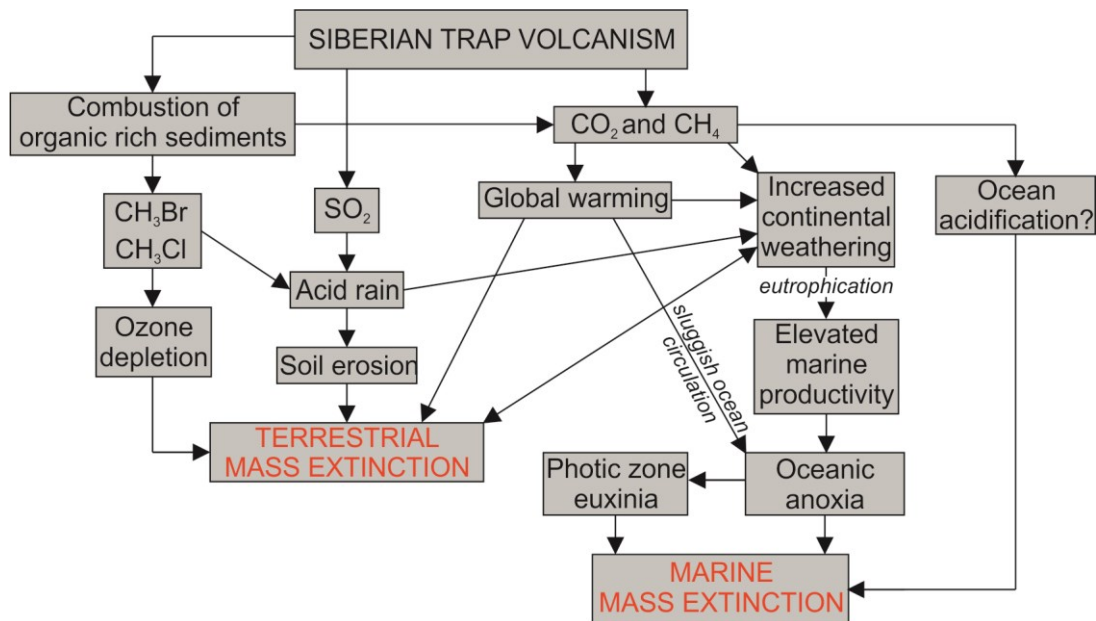
Figure 1.5: Flowchart model of cause-and-effect relationships during the LPE. Modified after Algeo et al. (2011).

that would cause soil degradation, increased soil erosion and increased chemical weathering that has been inferred in Antarctica (Sheldon, 2006) and Australia (Retallack, 1999).

These environmental changes would not have only been detrimental to the terrestrial realm but would have also caused environmental changes in the marine realm. The increase in weathering as a consequence of the terrestrial extinction, global warming and acid rain are hypothesised to have caused the increased sedimentation rates observed across the P/Tr boundary and throughout the Lower Triassic (Algeo and Twitchett, 2010). Furthermore, subsequent nutrient fluxes would have enhanced primary productivity as evidenced by an increase in phytoplankton biomarkers across the P/Tr boundary (Fenton et al., 2007; Nabbefeld et al., 2010), as well as increases in total organic carbon content (TOC) and phosphorous in the sediments (Nabbefeld et al., 2010; Wei et al., 2015). Eutrophication in shallow marine environments would also have led to seasonal hypoxia that may explain the observation of anoxic-dysoxic conditions in unusually shallow settings (Wignall and Twitchett, 1996; Bond and Wignall, 2010).

The long-term warming of global temperatures caused by the Siberian Traps would have caused a reduction in the pole-equator temperature gradient. This would have led to sluggish ocean circulation and expansion of the oxygen minimum zone and account for the interpretation of the establishment of photic zone anoxia and euxinia across the P/Tr boundary. The establishment of anoxic and euxinic shallow waters on the shelf would also explain the observed bathymetric selectivity of the LPE (Wignall and Twitchett, 1996; Beatty et al., 2008; Bond and Wignall, 2010; Zonneveld et al., 2010).

Boron and calcium isotope changes across the LPE have been interpreted as reflecting shallow water CO_2 and thus acidity (Payne et al., 2010; Clarkson et al., 2015) which has

been inferred to explain the physiological selectivity amongst organisms that excrete a calcified shell (Knoll et al., 2007). Calcium and boron isotope evidence for ocean acidification, however, is only recorded from the *H. parvus* and *I. isarcica* zones, respectively (Payne et al., 2010; Clarkson et al., 2015), which postdate the LPE. Furthermore, the boron isotope excursion occurs in the absence of a carbon isotope excursion that would be expected if more CO_2 were being pumped into atmosphere from further Siberia Traps volcanism. The boron isotope record may, therefore, indicate a change in salinity associated with changes in runoff rather than acidity (Hanehan et al., 2013). Thus conclusive evidence for ocean acidification as a cause of the LPE is lacking, but may be a factor in hypothesised subsequent extinctions.

1.6 Subsequent recovery

1.6.1 Pace of the recovery

Knowledge of the post-extinction recovery of marine ecosystems is incomplete and interpretations vary depending on the temporal, spatial, ecological or taxonomic scale of analysis and the parameters used to define or quantify 'recovery'. Furthermore geochemical and sedimentary anomalies (e.g. anoxia (Wignall and Twitchett, 2002b), eutrophication (Wei et al., 2015), high sea surface temperatures (Sun et al., 2012; Romano et al., 2012 and laminated sediments) have also been recorded throughout the Early Triassic. Therefore, an improved understanding of the recovery will be important to improving our understanding of the extinction event itself.

Marine species richness increased rapidly after the extinction event for pelagic animals, e.g. ammonoids, conodonts and fish (Orchard, 2007; Stanley, 2009; Scheyer et al., 2014), whereas the traditional view of the recovery of the benthic fauna is that recovery was much slower or delayed (e.g. Hallam, 1991). In addition, the benthic fauna that are characteristic of the Early Triassic are mostly cosmopolitan generalists, i.e.

opportunistic taxa that proliferated in the extinction aftermath, e.g. the genera *Claraia, Unionites, Promyalina, Eumorphotis, Lingularia* and *Microconchus* (Hallam and Wignall, 1997; Schubert and Bottjer, 1995; Harries et al., 1996; Rodland and Bottjer, 2001; Fraiser and Bottjer, 2007a; Fraiser, 2011; Zatoń et al., 2013).

At local scales, ecosystem recovery may be tracked using a palaeoecological or functional approach (e.g. Twitchett, 2006), analogous to that used to document local recovery from episodes of environmental stress in modern marine ecosystems (e.g. Steckbauer et al., 2011). Twitchett (1999) developed an ordinal scheme based on empirical data from the fossil record, to describe a step wise recovery of the marine benthic community from the initial post-extinction aftermath to the final recovery of the benthic fauna (Twitchett and Barras, 2004; Twitchett et al., 2004; Twitchett, 2006; Figure 1.6). The first stage of the model (Stage 1), which characterises most of the Griesbachian in northern Italy and the entire Induan of western USA (Twitchett et al., 2004), is defined by the presence of rare, small, simple fodinichnia (e.g. *Planolites*) of deposit feeding animals and the absence of vertical domichnia of suspension feeders as well as a low diversity and high dominance of shelly taxa, generally *Claraia* and *Unionites*. Stage 2, which is recorded from the late Griesbachian-Dienerian of Northern Italy and the Smithian of western USA, is characterised by the appearance of vertical domichnia of suspension feeders, e.g. *Arenicolites* and *Diplocraterion*, and increased infaunal tiering.

Stage 3 is defined by the presence of ichnotaxa attributed to the activity of burrowing crustaceans, such as *Rhizocorallium* and small *Thalassinoides*, and by a return of greater epifaunal tiering with the re-appearance of crinoids and bryozoans, and assemblages with >10 taxa. Fossil assemblages from shallow marine settings of the late Griesbachian-Dienerian commonly have these features, except they mostly lack representatives of the erect tier, therefore, reflecting a transient representation of Stage 3

of the Twitchett (2006) recovery model. Those lower Triassic assemblages that contain representatives of the erect tier probably reflect a more advanced recovery state and therefore this study has modified Stage 3 of Twitchett (2006) recovery model, which is divided into 3a (no erect tier) and 3b (erect tier; Figure 1.6). The full recovery is recorded by Stage 4, which is recorded in the Middle Triassic by a full recovery of pre-extinction ichnotaxa and degree of bioturbation with burrows of *Rhizocorallium* and *Thalassinoides* being >20mm, whilst shelly fauna return to larger size and more 'even' communities (Twitchett, 2006).

Advanced recovery, i.e. Stage 3b (Twitchett, 2006), has been documented from offshore seamount settings of Neotethys (Twitchett et al., 2004; Oji and Twitchett, 2015) and in mid-latitude shelf settings of the Boreal and Panthalassa Oceans (Lazutkina, 1963;
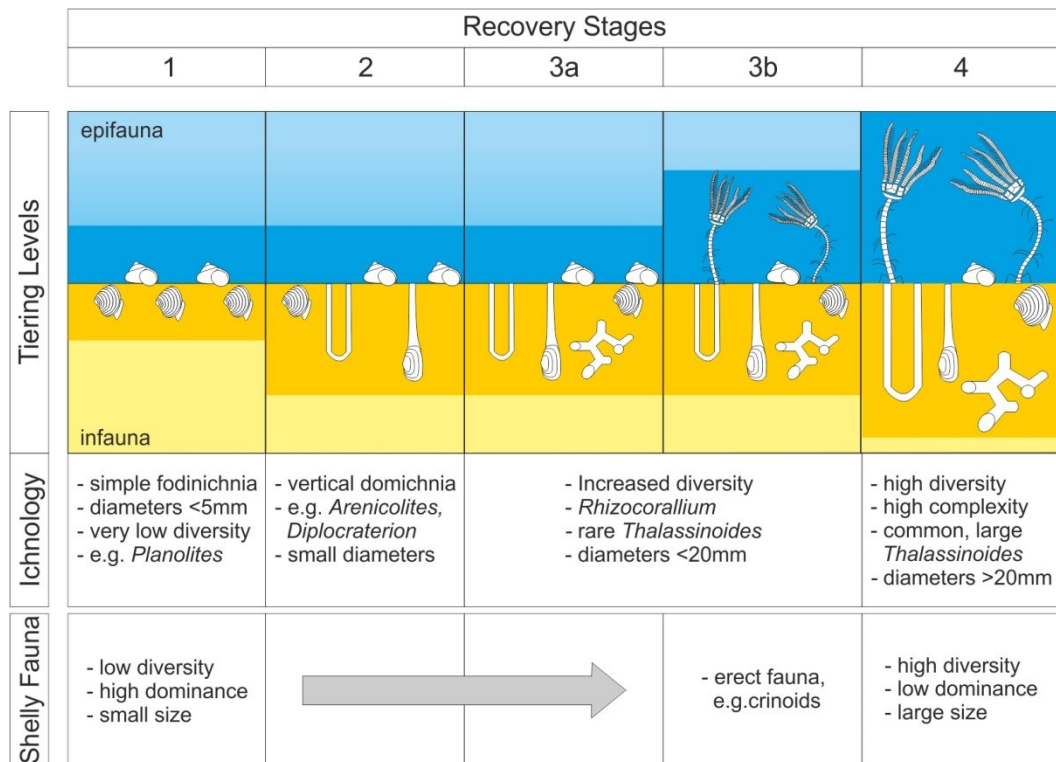
Figure 1.6: Empirical recovery model for the restructuring of benthic marine ecosystems following the late Permian mass extinction. Modified after Twitchett (2006).

Beatty et al., 2008; Zonneveld et al., 2010) by the second conodont zone of the Triassic, within a few hundred thousand years of the extinction. Shelf locations within the palaeotropics evidently took longer to reach the same stage (Twitchett et al., 2004), although some moderate recovery, i.e. Stage 3a, has been identified locally in the late Griesbachian (Hofmann et al., 2011; Hofmann et al., 2015a). The timing and pace of recovery of the benthos may, therefore, have varied locally between different habitats, locations and/or different taxonomic groups.

1.6.2 Latitudinal and regional variations in recovery

As a consequence of climate warming it is expected that higher latitudes will experience the greatest warming and thus greater ecological changes (Hoegh-Guldberg and Bruno, 2010). Mid- to high-latitudes, however, would still be expected to be habitable whereas relatively smaller temperature rises at low-latitude settings would be expected to be 'lethally hot' with a more hostile environment (Sun et al., 2012; Song et al., 2014). Therefore, although the extinction at mid- to high-latitude settings was still catastrophic (Payne and Clapham, 2012) it is probably unsurprising that the recovery of the benthos has been observed at a more rapid pace at higher latitudes (Wignall et al., 1998; Twitchett and Barras, 2004; Pruss and Bottjer, 2004a; Beatty et al. 2008; Fraiser and Bottjer, 2009; Zonneveld et al., 2010).

Faunas that are equivalent to Twitchett's (2006) Stage 3 have been reported from the late Griesbachian-Dienerian sites at Festningen, Svalbard (Wignall et al., 1998), Jameson Land, East Greenland (Twitchett and Barras, 2004), Nunavut and British Columbia, Canada (Beatty et al., 2008; Zonneveld et al., 2010) and Primorye, Russia (Shigeta et al., 2009), whereas, coeval faunas in tropical shelf settings record stages 1 or 2 (Schubert and Bottjer, 1995; Twitchett et al., 2004). Within these assemblages are groups such as bryozoans (Nakrem and Mørk, 1991; Powers and Pachut, 2008; Baud et al, 2008) that are rarely described from Early Triassic assemblages. In addition, the

most diverse ichnofaunal assemblage reported from the Smithian comes from a middle, southern latitudinal setting (Chen et al., 2012). A more rapid advanced recovery at higher latitudes has been attributed to the increased solubility of oxygen that would be expected in cooler waters of higher latitudes (Wignall and Twitchett, 2002).

Similarly advanced recovery faunas have, however, been recorded locally at lower latitudes during the Induan, e.g. mid-Griesbachian of Oman (Twitchett et al., 2004), Griesbachian of Persian Gulf (Knaust 2010), late Griesbachian of northern Italy (Hofmann et al., 2011) and late Griesbachian of China (Hautmann et al., 2011), indicating that advanced recovery was not restricted to higher palaeolatitudes. The apparent absence of a latitudinal aspect to the recovery may be due to a reduced latitudinal temperature gradient during the Induan, evidenced by a low ammonoid latitudinal diversity gradient (Brayard et al., 2006). On the other hand, Lower Triassic localities that have hitherto been investigated all occur within 50° of the palaeoequator and rocks deposited at even higher latitudes are currently unstudied.

Although recovery does not appear to vary with latitude the pace of recovery varies regionally. Initial recovery (e.g. increase in richness, ecological complexity or body size) in western US, south China and central Europe occurs by the third conodont zone in the Griesbachian (Hofmann et al., 2013b) compared with the second conodont zone in the Neotethys (Twitchett et al., 2004; Jacobsen et al., 2011). Wheeley and Twitchett (2005) also found that during the Griesbachian the size of gastropods from Oman, i.e. Neotethys, were larger, and assemblages more even than coeval assemblages from the Dolomites, Italy, i.e. western Palaeotethys. Ichnofaunal assemblages from the Neotethys and northwest Pangaean margin also show advanced recovery (e.g. presence of key taxa and increased richness) within the *H. parvus* Conodont Zone (Zonneveld et al., 2010; 2010c; Knaust 2010). Furthermore, based on the recovery of gastropods during the Smithian (Nützel and Schulbert, 2005) and complexity and diversity of benthic

communities in the Spathian (Hofmann et al., 2013a; Hofmann et al., 2015a) recovery in eastern Panthalassa was more advanced than in western Palaeotethys, even though they occupied similar palaeolatitudes.

This regional variation may be due to the differences in environmental settings or in key environmental parameters. For example, the south China sections represent deposition within a marginal sea (Chen et al., 2011b) where salinity may have been a controlling factor on the pace of recovery. Neotethyan seamounts were not influenced by increased runoff or high sedimentation rates in the Early Triassic (Algeo and Twitchett, 2010), which may explain their faster pace of recovery. Alternatively, this regional variability could be due to differences in the composition of pre-extinction communities between the different regions and/or a reflection of regional variation in the magnitude of extinction or ecological collapse (Jacobsen et al., 2011).

1.6.3 'Habitable zone' hypothesis

Early Triassic benthic assemblages are mostly described from a narrow range of sedimentary environments above wave base. Distal to these environments are laminated sediments with rare, small and low diversity faunas (Beatty et al., 2008). This led Beatty et al. (2008) to suggest that during the Early Triassic diverse benthos was restricted to settings from the upper shoreface to offshore transition, i.e. the 'habitable zone' hypothesis. Subsequent support for this hypothesis comes from the western US where benthic faunas from the Griesbachian, Smithian and Spathian are more diverse in wave aerated settings, i.e. the inner and mid-shelf, than below wave base (Mata and Bottjer, 2011; Hofmann et al., 2013a; Hofmann et al., 2013b; Hofmann et al., 2014; Pietsch et al., 2014).

Payne et al. (2006a) found that the percentage of skeletal material in the Nanpanjiang Basin decreased from 7.5% to <1% across the LPE, followed by a subsequent increase

in the Smithian and into the Middle Triassic. It is difficult, however, to distinguish if this is a result of changes in sedimentation, preservation or changes in the production of biotic grains. If it is mostly related changes in the production of biotic grains it would suggest that life became restricted to the platform setting in south China across the LPE with the oxygen minimum zone retreating during the Olenekian and into the Middle Triassic increasing the habitable area of Nanpanjiang Basin. Facies analysis of the Nanpanjiang Basin also suggests anoxic conditions during the Induan (Lehrmann et al., 2003; Galfetti et al., 2008) that would have been unfavourable for benthic colonisation thus supporting the habitable zone hypothesis.

The habitable zone hypothesis may, therefore also explain the observed pattern of extinction during the late Permian, as deeper shelf and basin settings show evidence for a single mass extinction event, e.g. Svalbard (Nabbefeld et al., 2010), Greenland (Twitchett et al., 2001), and China (Chen et al., 2010b; Chen et al., 2011b; He et al., 2015), whereas, shallower settings show multiple extinction events, e.g. Werfen Formation, Italy (Farabegoli et al., 2007; Posenato, 2009; Clapham et al., 2013) and China (Chen et al., 2010b; Song et al., 2013) associated with transgressions.

The narrow range of sedimentary environments containing these diverse faunas implies that bathymetric profiles were also a key component of the habitable zone hypothesis (Zonneveld et al., 2010). Narrow shelves or ramps may have been unable to support significant habitable conditions (Beatty et al., 2008), as these were likely to be more prone to fluctuations in sea-level and associated conditions beyond the habitable zone. Areas with broad shallow shelves supported a larger area of the habitable zone and were also less severely impacted by sea-level changes. This may explain why there is a faster pace of recovery in the broad shelf settings of the Pedigree-Ring-Kahntah sections than the narrow shelf setting of the Crooked River-Calais area (Zonneveld et al., 2010).

1.6.4   Temporal aspect to the recovery

Although the habitable zone hypothesis may explain survival of the benthos during the late Permian mass extinction, it does not explain why the constituent fauna are still characterised by an unusually small size with considerably lower diversities than faunas from the Middle and Late Triassic; for example, the most diverse benthic assemblages from the Early Triassic comprise 17 genera in the Griesbachian (Twitchett et al., 2004; Oji and Twitchett, 2015) and 22 genera in the Spathian (McGowan et al., 2009; Hautmann et al., 2013; Hofmann et al., 2013a) compared to 114 genera from the late Anisian (Stiller, 2001) or 123 genera in the late Triassic (Hausmann and Nützel, 2015). Thus even though the habitable zone provided an oxygenated refuge, this was still possibly environmentally stressed, as high CO_2 levels (Grard et al., 2005) and high sea surface temperatures (Sun et al., 2012) would have reduced the capacity of dissolved oxygen. The step-wise recovery in the complexity of benthic invertebrate communities (Twitchett et al., 2004) and their size (Metcalfe et al., 2011), may, therefore reflect the recovery of atmospheric oxygen. The results of a theoretical mass balance model, however, show that atmospheric oxygen declined between the Lower to Middle Triassic (Berner, 2005), which would suggest an alternative factor may have been controlling the recovery.

The carbon isotope record suggests that large environmental perturbations occurred at the Early Triassic sub-stage boundaries (Payne et al., 2004; Richoz, 2006; Grasby et al., 2013; Figure 1.7). Furthermore, the magnitude of the negative isotope excursion in the upper Smithian is greater than the P/Tr boundary (Payne et al., 2004). Oxygen isotopes from the apatite of conodonts suggests that large temperature perturbations coincide with these carbon isotope excursions (Sun et al., 2012; Romano et al., 2012) with the upper Smithian recording the hottest temperatures of the Early Triassic and the Dienerian/Smithian boundary representing a cooling interval of the Early Triassic (Sun

et al., 2012). Payne et al. (2004) hypothesised that these isotope perturbations represent environmental disturbances that directly inhibited biotic recovery. Support for this hypothesis comes from the pelagic realm where global diversity curves of ammonoid and conodont taxa show multiple extinctions at the Griesbachian/Dienerian, Smithian/Spathian and Spathian/Anisian boundaries (Orchard, 2007; Stanley, 2009). In addition, conodonts underwent a size decrease across the Smithian/Spathian boundary (Chen et al., 2013).

Payne and Kump (2007) suggest that multiple episodes of CO_2 release may account for the carbon cycle instability during the Early Triassic with a possible trigger being further eruptions from the Siberian Traps that erupted through the Lower and Middle
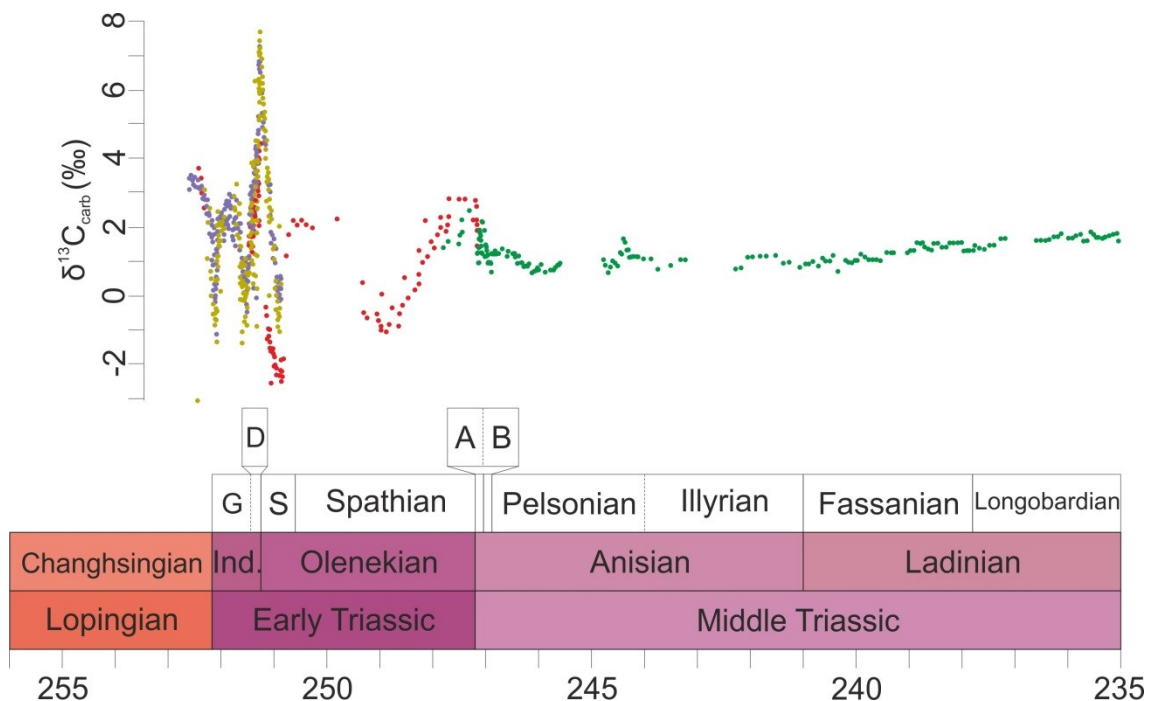
Figure 1.7: Carbon isotope data from the Nanpanjiang Basin, south China. Colours correspond to data from different sections. Modified after Payne et al. (2004), following the publication of new radiometric ages. Ind = Induan, G = Griesbachian, D = Dienerian, S = Smithian, A = Aegean, B = Bithynian.

Triassic (Kamo et al., 2003; Reichow et al., 2009). The coincidence of carbon cycle stabilisation with accelerated Middle Triassic biodiversity also supports the view that environmental perturbations delayed the faunal recovery following the LPE (Payne, 2005; Chen and Benton, 2012). Furthermore, new radiometric ages for the Early Triassic suggest that not only were there major environmental perturbations, but these occurred in rapid succession within the first 1.73myr of the Triassic (Ovtcharova et al., 2006; Shen et al., 2011).

Evidence from the benthic realm, however, is scarce. In Oman, a diverse Griesbachian fauna is overlain by a low diversity Dienerian fauna suggesting the diversity decreased across the Griesbachian/Dienerian boundary at this locality (Twitchett et al., 2004; Jacobsen et al., 2011). In addition, in Primorye, Russia, diverse assemblages from the late Griesbachian and early Dienerian are overlain by low diversity Smithian assemblages (Shigeta et al., 2009). Similarly, the relatively complex fauna from the Smithian in northeast Japan are overlain by laminated mudstones with a low diversity fauna (Kashiyama and Oji, 2004). These diverse faunas, however, are recorded from sediments that show evidence for wave activity, i.e. within the habitable zone, whereas the low diversity faunas are from settings below wave base, i.e. below the habitable zone, and the inference of a biotic crisis is equivocal as these changes can be accounted for by a facies change.

An important but largely neglected tool to investigate these observed patterns is the use of quantitative palaeoecology. To date it has been only applied in sections from the western US (e.g. Schubert and Bottjer, 1995; Hofmann et al., 2013a; Hofmann et al., 2013b; Hofmann et al., 2014; McGowan et al., 2009; Pruss and Bottjer, 2004a; 2004b; Mata and Bottjer, 2011; Pietsch et al., 2014), but these studies rarely span sub-stage boundaries and are only from a limited number of depositional settings. Further work in a range of depositional settings, across sub-stage boundaries and from other regions are

required to elucidate the rate and pattern of biotic recovery following the LPE and its relationship to environmental changes.

1.7   Aims of this study

The aim of this project is to collect novel palaeontological and geochemical data from a number of localities worldwide, spanning different environments and palaeolatitudes during the recovery of the LPE. Here palaeoecological studies were performed on shelly macrofauna and trace fossils through field sampling. Emphasis was placed on a quantitative analysis of the data, and importance given to the consideration of the quality of the rock-record and other potential biases. Palaeoecological changes have been compared between localities and correlated with palaeoenvironmental proxies.

The hypotheses that will be tested are:

  i.   'Habitable zone' hypothesis (*sensu* Beatty et al., 2008) that during the recovery of the LPE diverse benthic communities were restricted to settings aerated by wave activity between the upper shoreface and offshore transition, and limited to higher palaeolatitudinal settings.

  ii.   Carbon isotope variations represent subsequent biotic crises that directly delayed the recovery of benthic invertebrates (cf. Payne et al., 2004).

  iii.   Recovery was faster at higher latitudes (cf. Twitchett and Barras, 2004).

This study also aims to investigate how much ecospace was evacuated by the late Permian mass extinction and what were the dynamics of ecospace filling during the subsequent recovery.

2. Materials and Methods

Quantitative abundance data of fossil benthic invertebrates were collected from rocks that were deposited in mixed siliciclastic-carbonate ramp settings on the northwestern margin of the Palaeotethys Ocean (recorded at Aggtelek, Hungary; Lombardy and the Dolomites, Italy; Figure 2.1) and in a siliciclastic shelf setting from the Boreal Ocean (Spitsbergen, Svalbard; Figure 2.1). These data were analysed with multivariate statistical methods.

2.1 Study Sites and Geological Setting

2.1.1 Hungary

Hungary lies in the central part of the Carpathian Basin system, surrounded by the Alps, Carpathians and the Dinarides. The Pre-Cenozoic structure of the Carpathian Basin comprises the Tisza and Alpine-Carpathian-Pannonian (ALCAPA) structural megaunits separated by the Mid-Hungarian Sheer Zone (MHMU) (Kovács and Haas, 2010). Lower
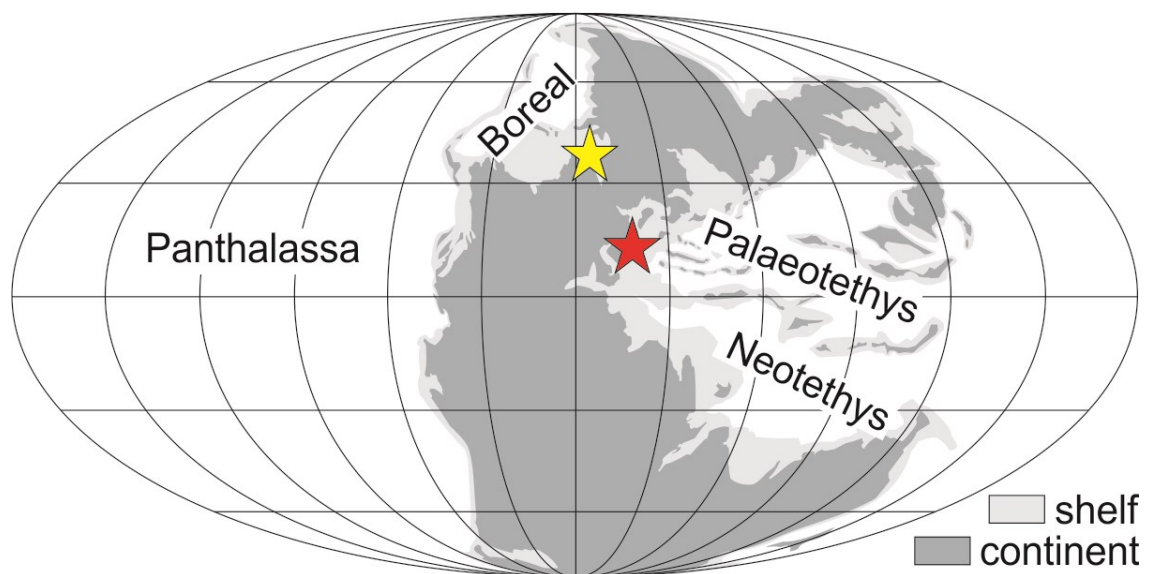
Figure 2.1: Global palaeogeography of the Late Permian. Showing the location of the western Palaeotethys study sites (red star) and Spitsbergen study sites (yellow star) (after Blakey, 2011).

Triassic marine deposits are known from three regions in Hungary, the: Balaton Highlands (within the Mid-Transdanubian Range), Bükk Mountains and the Aggtelek-Rudabánya Mountains.

Lower Triassic deposits of the Aggtelek-Rudabánya Mountains were located on the easternmost part of the Alpine-Carpathian shelf during the Late Palaeozoic and Early Mesozoic (Hips, 1998). Deposition took place on a homoclinal ramp during the Early Triassic, which evolved from a sabkha into a flat-topped carbonate platform by the Ladinian (Velledits et al., 2011). The Lower Triassic succession is represented by four formations: the Perkupa Evaporite Formation, Bódvaszilas Sandstone Formation, Szin Marl Formation and Szinpetri Limestone Formation (Figure 2.2). These are highly folded and faulted with, generally, the older deposits to the east and younger deposits to the west (Hips, 2001). The Lower Triassic succession of the Aggtelek-Rudabánya Mountains has been divided into three main facies: the Aggtelek, Szőlősardó and Bódva units (Hips, 1996b). Hips (1998) does not record a difference in the facies of the formations between the Aggtelek, Szőlősardó and Bódva units except in their uppermost part. Six stratigraphic sections were measured from the Aggtelek Unit, Aggtelek Karst: Perkupa Quarry, Perkupa Cemetery, Perkupa West, Szin Mill Quarry, Szin North and Szinpetri Quarry (Figure 2.3). Exposure is intermittent on densely wooded hillsides, which makes logging difficult, thus only 364m of the 800m Lower Triassic succession of Hips (1996b) was logged. Several boreholes in the Aggtelek Karst do exist, but stratigraphic logs from Hips (1990) show that these are highly deformed due to folding and, therefore, these cores were not sampled. Although these formations extend across the Hungarian-Slovakian border (Šimo and Olšavský, 2007), field visits in June 2012 to Vlkanová and Silica found no existing exposures.

Field visits to the Balaton Highland and Bükk Mountains did not yield any continuous exposures appropriate for this study (Appendix 2.1).

2.1.2 Northern Italy

Lombardy

In northern Italy, Upper Permian to Middle Triassic strata were investigated in two regions: Eastern Lombardy and the Dolomites. The Lower Triassic of northern Italy records deposition on the northwestern margin of the Palaeotethyan Ocean (Figure 2.1). Lithologically, the Lower Triassic successions of Lombardy and the Dolomites are similar, but have been assigned to two different formations: the Werfen Formation to the east and the Servino Formation to the west (Assereto et al., 1973). The Servino Formation extends from Campione d'Italia to Valli Giuducarie and in the foothills of the Tre Valli Bresciane, and due to Neoalpine underthrusting the Servino Formation is exposed on limbs of four anticlines: the Orobic, Trabuchello-Cabianca, Cedegolo and Camuna (Sciunnach et al., 1999; Figure 2.4). The Servino Formation facies differ from those of the Werfen Formation in that they represent a more marginal depositional setting and higher terrigenous content (Cassinis, 1968; Assereto et al., 1973). The Servino Formation is also more condensed than the Werfen Formation, being approximately 100-150m thick, and paraconformably overlies the Permian Verrucano Lombardo Formation (Assereto et al., 1973).

Two stratigraphic sections were investigated from the Camuna Anticline in eastern Lombardy: Path 424 and Maniva-Croce Domini road-cut through Mt. Rondenino (Figure 2.5). The Servino Formation on the Camuna anticline has been divided into seven members (Sciunnach et al., 1999), namely the: Prato Solaro Member, Praso Limestone Member, Ca'San Marco Member, Gastropod Oolite Member, Acquaseria Member, "Myophoria Beds" Member and "Upper Member" (Figure 2.2). The Mount Rondenino section is exposed in three outcrops. The southernmost exposes the Ca'San Marco Member to "Myophoria Beds", moving northwards, the next exposes the

		Lombardy	Dolomites	Aggtelek Karst	Svalbard West	Svalbard Central
Anisian		Carniola di Bovegno	Lower Serla Dolomite	Gutenstein	Bravaisberget Fm.	Botneheia Fm.
Lower Triassic – Olenekian – Spathian		"Upper Member"	San Lucano	Szinpetri Limestone	Kaosfjellet Member	Vendomdalen Member
		"Myophoria Beds"	Cencenighe	Szin Marl		
			Val Badia			
Lower Triassic – Olenekian – Smithian		Acquaseria	Campil	Bódvaszilas Sandstone	Iskletten Member	Lusitaniadalen Member
		Gastropod Oolite	Gastropod Oolite			
Lower Triassic – Induan – Dienerian		Ca'San Marco	Siusi		Selmaneset Member	Deltadalen Member
		Praso Limestone				
Lower Triassic – Induan – Griesbach.		Prato Solaro	Andraz Horizon	Perkupa Evaporite	Siksaken Member	
			Mazzin			
			Tesero			
Permian		Verrucano Lombardo	Bellerophon Fm.		Kapp Starostin Fm.	

Figure 2.2: Lithostratigraphic framework of the studied Lower Triassic successions. Lombardy after Sciunnach et al. 1999; Dolomites after Posenato, 2009; Aggtelek Karst after Hips, 1998 and Svalbard after Mørk et al. 1999. Griesbach. = Griesbachian.
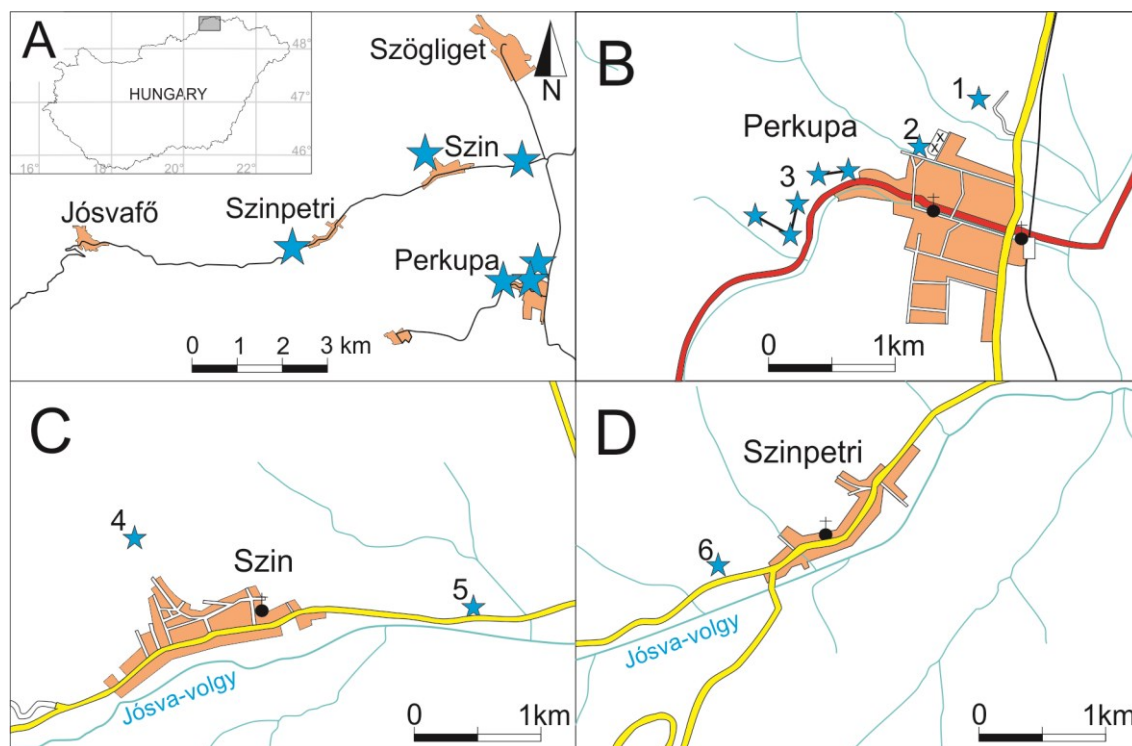
Figure 2.3: Locality maps of the study sites in the Aggtelek Karst. A) Study sites locations within the Aggtelek Karst. B) Perkupa: 1.Perkupa Quarry, 2.Perkupa Cemetery and 3.Perkupa West. C) Szin: 4.Szin North and 5.Szin Mill Quarry. D) Szinpetri: 6. Szinpetri Quarry.
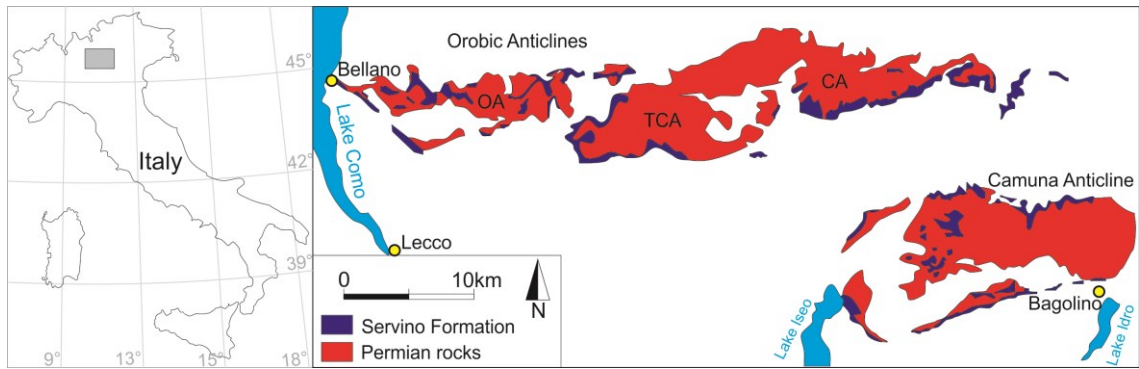
Figure 2.4: Simplified geological sketch of the Permian and Lower Triassic in the Lombardy region. It includes the Orobic anticlines: (OA) Orobic Anticline, (TCA) Trabuchello-Cabianca Aniticline and (CA) Cedegolo Anticline; and the Camuna Anticline (after Cassinis et al., 2007).

Acquaseria Member and the third exposes the "Myophoria Beds" (Figure 2.6). The Path 424 section provides a more complete succession, with few gaps, from the Permian Verrucano Lombardo Formation to the Middle Triassic Carniola di Bovegno Formation. In addition, the proposed type section of the Servino Formation at Passo Valdi, (Cassinis, 1968) was visited in 2012, but access, was difficult because of a recent rockfall and no sampling was attempted. Additionally, along Path 414 which runs parallel to the River Bruffione, beyond Passo Valdi (Figure 2.4), small patchy exposures of the cf. "Myophoria Beds" Member are present, but lack appropriate exposure for this study.

The Dolomites

The Dolomites are bounded by the Neogene Insubric Lineament to the north and by the Valsugana-Piere di Cadore Thrust to the south (De Zanche et al., 1993). The Lower Triassic succession of the Dolomites is represented by the Werfen Formation which is approximately 250m thick in the Adige Valley and up to 600-700m thick in the eastern Dolomites (Broglio Loriga et al., 1990). In the west, the Werfen Formation overlies the terrestrial Val Gardena Sandstone Formation and in the east it overlies the shallow

marine Bellerophon Formation (Bosellini and Hardie, 1973; Assereto et al., 1973; Massari et al., 1994; Broglio Loriga et al., 1990; Cassinis and Perotti, 2007; Posenato, 2010). In places, the upper part of the Werfen Formation is either uncomformably overlain by the late Anisian (Pelsonian-Illyrian) Richthofen Conglomerate or elsewhere conformably overlaid by the Lower Serla Dolomite Formation (Broglio Loriga et al., 1983, Neri and Posenato, 1985; Broglio Loriga et al., 1990). The Werfen Formation records deposition on a ramp with shallower deposits towards the southwest and deeper deposits towards the northeast (Massari et al., 1994). The lithostratigraphic framework of the Werfen Formation established by Broglio Loriga et al. (1983) and Neri and Posenato (1985), comprises nine members, the: Tesero, Mazzin, Andraz, Siusi, Gastropod Oolite, Campil, Val Badia, Cencenighe and San Lucano members (Figure 2.2; Posenato, 2008b).

Six stratigraphic sections exposing the Werfen Formation were investigated in the Dolomites: the Tesero, Val Averta, l'Uomo, Costabella, Rio di Pantl and the Siusi
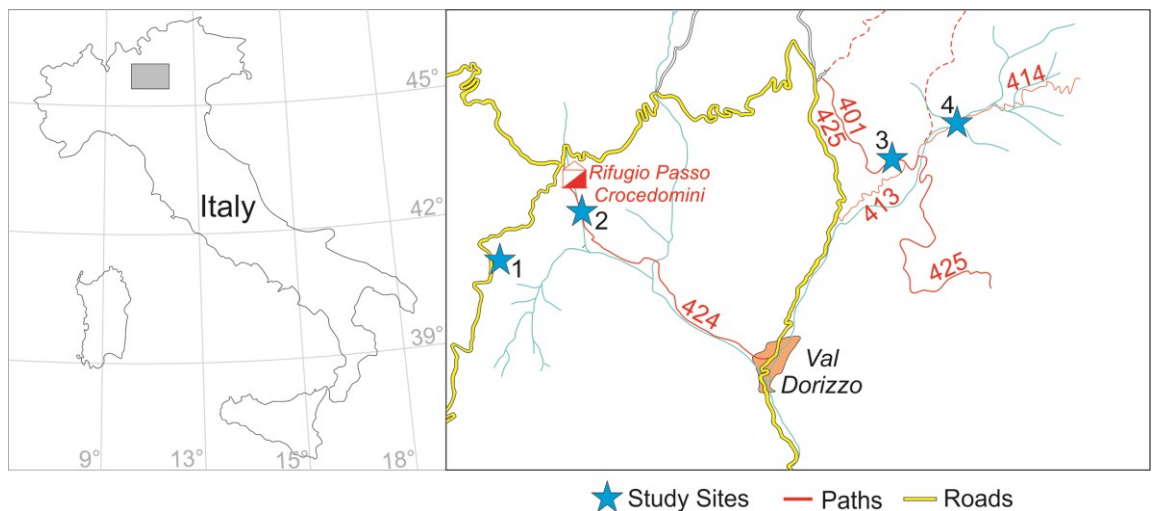
Figure 2.5: Locality maps of the study sites in Lombardy: 1.Mt.Rondenino road cut. 2. Path 424. 3. Passo Valdi. 4. Path 414.
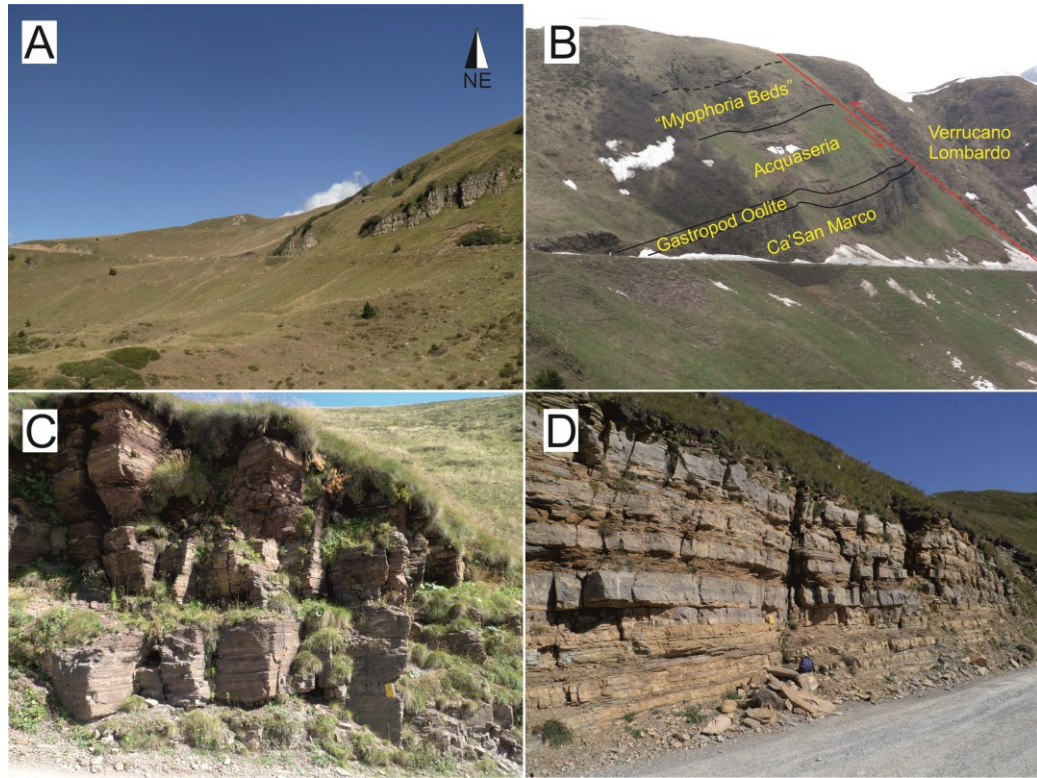
Figure 2.6: Photos from the Mt. Rondenino road-cut section. A) The entire Servino Formation exposure along the Mt. Rondenino road cut. B) The southernmost exposure showing the Ca'San Marco Member to the Strati a Myophoria Member. The faulted contact with the Permian Verrucano Lombardo Formation is shown. C) Exposure of the Acquaseria Member. D) Exposure of the "Myophoria Beds".

sections (Figure 2.7). Together, these sections provide a continuous exposure of the Werfen Formation from a similar depositional setting (i.e. a shallow homoclinal ramp with occasional restricted marine conditions; Massari et al., 1994).

2.1.3 Spitsbergen, Svalbard

The Lower Triassic succession of Svalbard occurs in three major structural terrains: around Sørkapp Land; within the major NNW-SSE fold belt in western Spitsbergen from Hornsund to Isfjorden; and east of this lineament, i.e. central Spitsbergen (Mørk et al., 1983; Harland, 1997). The Lower Triassic succession is 700m thick in western Svalbard to 200-300m thick in central and eastern Svalbard (Mørk et al., 1983; Mørk et

al., 1990; Mørk et al., 1999). These rocks are dominated by siliciclastic deposits which are coarser in the west and finer in the east. Deposition has been interpreted to have taken place upon a shallow shelf, deepening eastwards (Mørk et al., 1983; Wignall et al., 1998; Worsley and Mørk, 2001). These rocks were deposited in the Boreal Ocean at approximately 45°N in the Early Triassic whilst Svalbard was moving rapidly north (Hounslow et al., 2008a), in a humid climate of the northern temperate zone (Galfetti et al., 2007c).

Three stratigraphic sections were studied in Spitsbergen (Festningen, Deltadalen and Lusitaniadalen; Figure 2.8-2.9). The lithostratigraphic units differ between Festningen in the west and Deltadalen and Lusitaniadalen in central Spitsbergen (Figure 2.2). In western Spitsbergen two formations are described from the Lower Triassic, the: Vardebukta Formation (divided into the Siksaken and Selmaneset members) and the Tvillingodden Formation (divided into the Iskletten and Kaosfjellet members). In central Spitsbergen, instead, the Vikinghøgda Formation (divided into the Deltadalen, Lusitaniadalen and Vendomdalen members) represents the Lower Triassic (Figure 2.2). At the Festningen section, the upper part of the Permian Kapp Starostin and the lower part of the Vardebukta Formation were investigated. In central Spitsbergen, the Vikinghøgda Formation was studied in the river banks of Lusitaniadalen, Deltadalen and Duboisbreen tributary (Figure 2.9). The upper part of the Vikinghøgda Formation was investigated on the eastern slopes of the Vikinghøgda Mountain.

2.2 Field Techniques

Sedimentary logs were produced in the field for the Hungarian and Italian localities in May, June, July and September 2012, and June and July 2013, using the formation and unit/member definitions of Hips (1996b) for the Aggtelek Karst, of Sciunnach et al. (1999) for Lombardy and of Posenato (2008b) for the Dolomites (Figure 2.2).
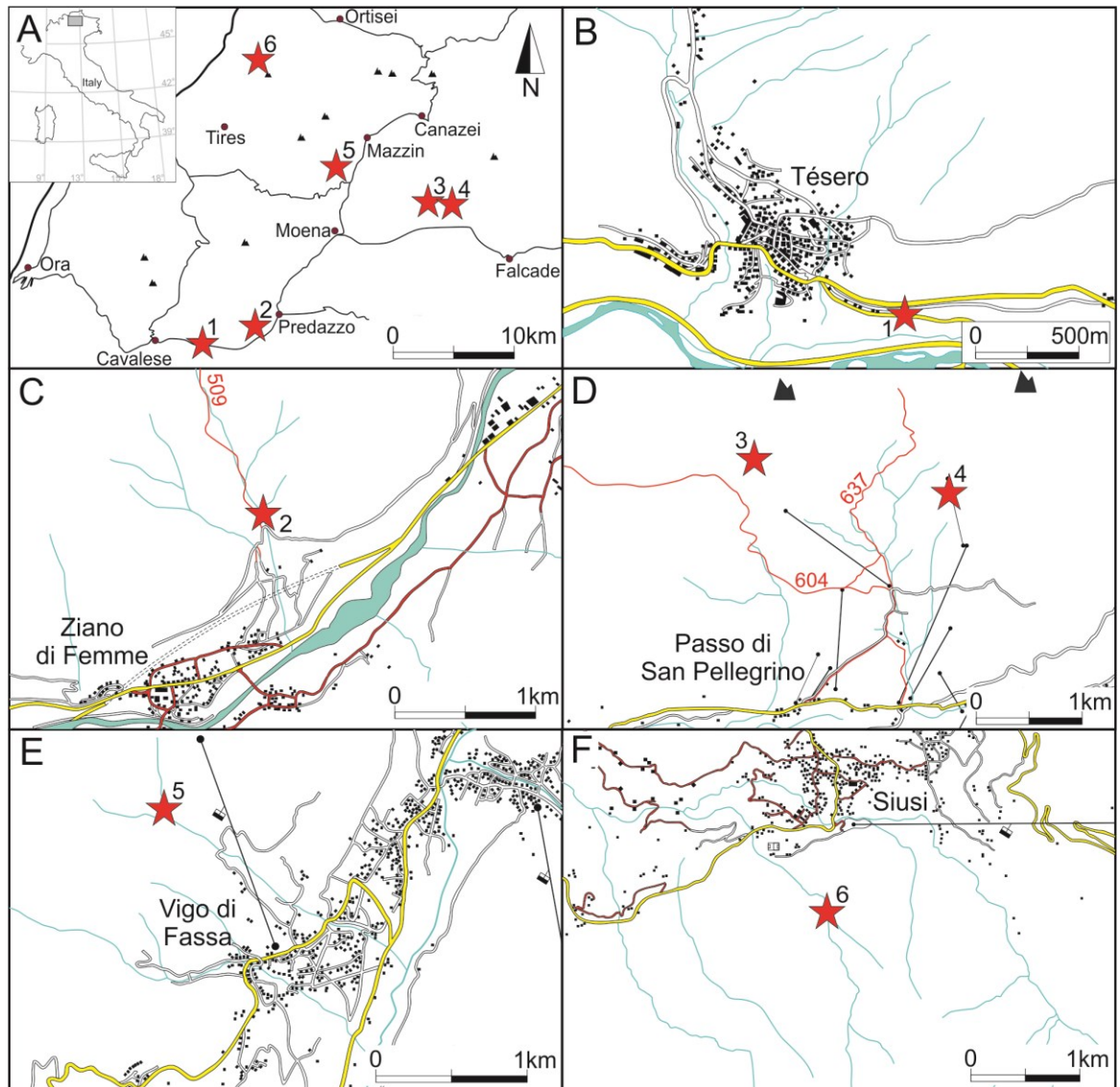
Figure 2.7: Locality map of the investigated sections of the Dolomites. 1) Tesero, 2) Val Averta, 3) Costabella, 4) l'Uomo, 5) Rio di Pantl, 6) Siusi.
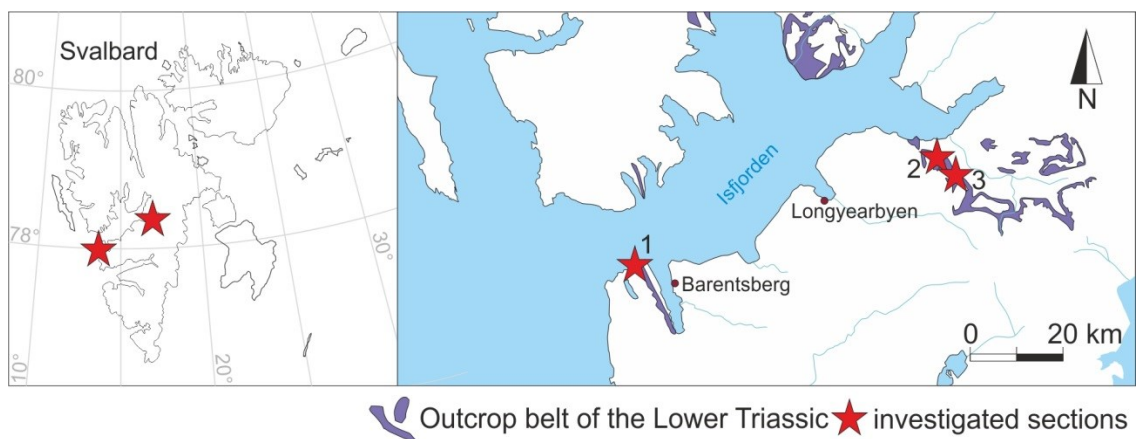
Figure 2.8: Locality map of the study sites of Spitsbergen, 1) Festningen, 2) Lusitaniadalen, 3) Deltadalen and Duboisbreen.
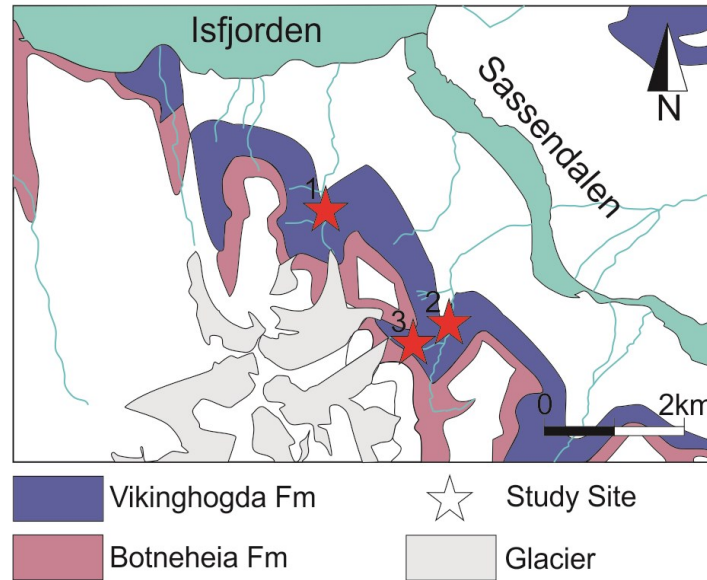
Figure 2.9: Locality maps of the study sites in central Spitsbergen: 1. Lusitaniadalen. 2. Deltadalen. 3. Duboisbreen tributary.

Unpublished sedimentary logs of R.J. Twitchett for Svalbard were modified in the field during August 2013. For Svalbard, the lithostratigraphic unit definitions follow Mørk et al. (1999). Lithologies, sedimentary structures, trace fossils and ichnofabric index (ii; Droser and Bottjer, 1993) were described for each measured bed. At the studied sections, all fossiliferous beds identified in the field were chosen for quantitative sampling of macrofossils. Cemented beds were sampled to produce polished slabs in the lab by collecting hand specimens 5cm across and 5cm thick. If the bed was thicker than a metre, a sample was collected every metre. Graded beds were sampled to include their base, middle and top. Laminated beds were sampled by collecting 2-3kg of bulk rock. In the field, bulk rock samples were then split parallel to bedding planes to reveal the fauna. Fossil material was identified and counted in the field with reference samples taken for lab preparation and further taxonomic identification. For Svalbard, samples were mechanically disaggregated in the lab. For bedding plane exposures, all preserved

fossil specimens within a 20cm x 20cm quadrat were counted, identified and measured with representatives of each taxon being sampled for further taxonomic identification.

In Lombardy, to resolve better the stratigraphy, 2-3kg bulk samples were collected for conodont biostratigraphy. Samples were collected from decimetre thick fossiliferous tempestite beds which have been described as yielding the most conodont elements in these successions (>100 per kg; Twitchett, 1997; 2000). Additionally, for chemostratigraphy the Val Averta (Dolomites) and Path 424 (Lombardy) sections were sampled by collecting small chips of fresh rock every 20cm.

2.3 Laboratory Techniques

2.3.1 Polished slab technique

The difficulty of removing and identifying small fossil shells from consolidated samples is a significant obstacle to detailed taxonomic investigation of those fossils not easily classified from thin sections (Payne et al., 2006a). Mechanical disaggregation is a common method for palaeoecological analysis (e.g. Schubert and Bottjer, 1995; Hautmann et al., 2011; Hofmann et al., 2013a; Hofmann et al., 2013b; Hofmann et al., 2013c; 2015; Pietsch et al., 2014), although McGowan et al. (2009) highlight that it is biased to small, common faunal components. In contrast, bedding plane analysis allows for greater spatial coverage increasing the chances of encountering rarer and/or larger elements of the fauna (McGowan et al., 2009).

The investigated sections do not, however, expose continuous bedding planes and the primary goal of this study is not detailed taxonomic analysis but to develop a quantitative understanding of local palaeoecological changes of the benthos with high stratigraphic resolution. A polished slab technique was, therefore, developed, which is an alternative approach from the thin section method of Payne et al. (2006a). Jacobsen et al. (2011) showed that the point-counting technique used by Payne et al. (2006a)

underestimates the taxonomic richness of the samples. An equal area approach as described by Jacobsen et al. (2011) is therefore used in this study.

There are several advantages of the polished slab technique over standard thin-sectioning. Polished slabs are larger and thus more likely to yield an appropriate number of identifiable bioclasts for statistical palaeoecological analysis. The procedure is also simpler, faster and it requires less equipment. In addition, the use of polished slabs allows for an accurate comparison of abundance among taxa of widely varying sizes and across a greater taxonomic range, and allows the inclusion of taxa that are too small (e.g. microconchids) to be counted using conventional methods (e.g. mechanical disaggregation) which may be the dominant component in some Lower Triassic beds (e.g. Zatoń et al., 2013). It also facilitates standardised sampling by allowing the investigator to search the same area of rock in each sample.

Samples were prepared following the acetate peel method of Wilson and Palmer (1989), without the final peel production step. Samples were cut perpendicular to the bedding plane surface using a diamond rock saw, and the surfaces ground flat using a diamond-encrusted grinding plate. To ensure a smoother surface, and to give better detail on the slab, the sample was then polished for 45 minutes using a Lapmaster 15 with silicon carbide dissolved in water. The sample was then washed to remove any excess silicon carbide. To enhance the relief between fossils and sediment the polished surfaces were then etched in 10% hydrochloric acid for ~10 seconds and then washed thoroughly with water, to remove excess acid. More siliciclastic samples were etched for ~20 seconds. The acid was changed after every 20 samples to maintain the 10% strength.

One representative individual of each species that was identified from bedding plane surfaces was sliced vertically. The distinguishing characteristics of each taxon in vertical section were then documented (Appendix 2.2), and used to identify specimens in the polished slabs. All identifiable fossils, were identified to the lowest taxonomic

level to which they could be confidently assigned (Appendix 2.2). The level of taxonomic resolution, therefore, varied between fossil groups, ranging from genus-level (e.g. bivalves) to phylum-level (e.g. foraminifera). A 5x5cm acetate sheet, divided into one hundred 5mm square divisions, was placed over the sample to aid counting, by preventing unintentional double counting of bioclasts. All the bioclasts within the quadrat were identified to measure taxonomic richness and tallied to obtain abundance data.

2.3.2 Conodont biostratigraphy

The conodont samples collected from Lombardy and the residues of four samples from Svalbard were processed by acid digestion using the buffered formic acid technique (Jeppsson and Anehus, 1995). The buffered formic acid technique was preferred over the acetic acid technique (Jeppsson et al., 1999) because it breaks down dolomite (Jeppsson and Anehus, 1995) and is a faster process. A buffered concentration of 9.6% was used in this study, which is below the maximum strength of 10.6%, determined by Jeppsson and Anehus (1995). For each gram of sample the solution was mixed using 1.29ml of 90% formic acid, 10.78ml of water, 0.22g of calcium carbonate and 0.013g of calcium phosphate. The starting pH of the solution was 2.2-2.3.

As the samples disaggregate, the released material acts as a buffer slowing the rate of dissolution. To obtain the maximum dissolution rates the sample was submersed in enough solution to maintain dissolution for 24 hours. The solution was renewed every 48 hours to ensure all of the solution had reacted. The residue was removed from the solution every 12 hours and was washed thoroughly with tap water to remove any excess solution, and to avoid crystal growth. The residues were then dried overnight at 40°C. Once dry, the residue was carefully sieved at 63μm, 125μm and 500μm. These fractions were then stored in glass vials. Only the >125μm fractions were used in the rest of the methods.

Heavy liquid (sodium-polytungstate; SPT) separation was used to concentrate conodonts prior to picking (following the method of Mitchell and Heckert, 2010). Plastic containers and tools were used as they do not react with SPT. The density of the SPT was ~2.8 g/ml. SPT was poured into a plastic beaker, and the sample was slowly poured into the liquid. The sample was then mixed for a few seconds to avoid the rafting of conodonts on top of floating grains. The mixture was then left to stand for a few minutes. A plastic spoon was used to slowly skim off the floating sample (float) which was placed into a funnel of 185nm filter paper, so the SPT could drain into a separate container (labelled dilute SPT). Once the SPT had drained from the float a small amount of distilled water was used to rinse the filter paper and sample of any remaining SPT. The filter paper and float was then dried at 40°C. The sediment that sank to the bottom of the container (sink) was then poured into a new piece of filter paper in the funnel and the same process was used as for float. The dilute SPT container was then placed into a hot water bath (below boiling), to evaporate the excess water. Once the SPT returned to a specific gravity of ~2.8g/ml the heavy liquid could be recycled. To prevent contamination, all equipment was thoroughly washed between samples and any spills of SPT were dissolved in deionised water and recovered. All conodont elements and other microfossils were picked from the sediment under an Olympus low-powered binocular microscope (up to x11 magnification) and using a paintbrush, placed into microslides.

2.3.3 Carbon and oxygen isotopes

Powders were drilled from a fresh surface of each sample, taking care to avoid signs of digenetic alteration, bioclasts and calcitic veins. For each sample, approximately, 400-1200μg of powder was put into a clean 10ml exetainer and sealed with a septum cap. The remaining head space was removed by flushing the exetainer with CP grade helium for 200 seconds at a flow of 40μl per minute. Subsequently, 0.15ml of anhydrous

phosphoric acid was injected through the septum into the sealed exetainer by using a disposable syringe and left for 2 hours to react fully. The resultant CO_2 was analysed for $\delta^{18}O$ and $\delta^{13}C$ on a heated Gilson Autosampler at 90°C connected to a carbonate MultiFlow, coupled with an IsoPrime isotope ratio mass spectrometer. Reference gas was measured using research grade CO_2 and calibrated against the V-PDB standard by using IAEA reference materials (NBS 19). The reproducibility of replicated standards was typically better than 0.1 ‰ (one standard deviation) for $\delta^{13}C$ and $\delta^{18}O$. Carbon- and oxygen-isotope values were calibrated against V-PDB and are reported in the standard ‰ notation. These samples were run at Plymouth University.

2.4 Palaeoecological analysis

The palaeoecological analysis was limited to benthic marine invertebrates, thus excluding ammonoids, conodonts, algae and foraminifera. Counting the number of individuals is complicated by the difference in disarticulation between different taxonomic groups, i.e. gastropods do not disarticulate whilst crinoids can disarticulate into thousands of elements. The common approach is, therefore, to use an estimate of the minimum number of individuals (MNI; Holland and Patzkowsky 2004). In this study a single individual of bivalves, brachiopods and ostracods was defined as comprising two opposing valves (i.e. left and right or brachial and dorsal) of equal size (mm resolution). In the absence of size data, a single individual is defined as comprising two opposing valves, or where no size data or valve orientation data was available, a single individual was defined as the number of valves divided by two. The number of gastropod individuals was equated to the number of individual apices. Each microconchid and scaphopod bioclast was considered to represent a separate individual.

As echinoderms can potentially disarticulate into hundreds or thousands of ossicles (e.g. Schubert et al., 1992; Twitchett et al., 2005), estimating their abundance is problematic. Schubert et al. (1992) calculated that approximately 1500 ossicles represent a

Holocrinus individual. This estimation is, therefore, used to calculate the MNI for crinoids. For ophiuroids, approximately thirty ossicles were counted from each arm in Early Triassic specimens from the Werfen Formation, Italy, (Hofmann et al., 2015a) and Changsing Formation, China, (Chen et al., 2004). To calculate the MNI for ophiuroids 150 ossicles are, therefore, used to represent an individual.

Twenty to thirty individuals have been recognised as the minimum required to begin to capture community signals for ecological analysis (Webb and Leighton, 2011; Patzkowsky and Holland, 2012). Therefore, samples with MNI <20 were removed from the analysis. The analysis was carried out at the finest taxonomic level. In localities where multiple methods were used, i.e. mechanical disaggregation and polished slabs, the analysis was carried out using the taxonomic resolution of the polished slab technique. For example, using the polished slab technique *Unionites* could only be identified to genus-level, whereas, using the mechanical disaggregation technique *Unionites* was identified to species-level, therefore the analysis was carried out at genus-level for *Unionites*. This allowed the different collection methods to be compared.

2.4.1   Ecological lifestyles

Each genus was assigned to a bin in the ecospace model of Bambach et al. (2007) based on its tiering, motility and feeding (Table 2.1), using data from extant relatives, previous publications and functional morphology. As some marine animals span different modes of life through ontogeny, each taxon was assigned a mode of life based on the adult life stages only, following Bambach et al. (2007). Each mode of life was assigned to the highest taxonomic resolution possible for each taxon, i.e. genus-level to order-level.

The assignment of modes of life follow the interpretations of Bush et al. (2007), e.g. even though scaphopods feed on foraminifera and could be considered predators,

Table 2.1: Ecologic categories for tiering, motility and feeding (after Bush et al., 2007).

Ecological category	Description	Examples
Tiering		
2. Erect	Benthic, extending into the water mass	Crinoids, some corals
3. Surficial	Benthic, not extending significantly upwards	Most gastropods
4. Semi-infaunal	Partly infaunal, partly exposed	*Pinna*
5. Shallow infaunal	Living in the top ~5cm of the sediment	*Lingula*
6. Deep infaunal	Living more than ~5cm deep in the sediment	*Pleuromya*
Motility		
1. Freely motile, fast	Regularly moving, unencumbered	Most arthropods
2. Freely motile, slow	As above, but strong bond to substrate	Gastropods, echinoids
3. Facultatively motile, unattached	Moving only when necessary, free-lying	Many clams
4. Facultatively motile, attached	Moving only when necessary, attached	*Holocrinus*
5. Non-motile, unattached	Not capable of movement, free-lying	Reclining brachiopods
6. Non-motile, attached	Not capable of movement, attached	Pedunculate brachiopods
Feeding		
1. Suspension feeding	Capturing food particles from the water	Lophophorates
2. Surface deposit feeding	Capturing loose particles from a substrate	Tellinid bivalves
3. Mining	Recovering buried food	Nuculid bivalves
4. Grazing	Scraping or nibbling food from a substrate	Many gastropods
5. Predatory	Capturing prey capable of resistance	Cephalopods
6. Other	e.g. photo- or chemosymbiosis, parasites	*Nucinella*

because foraminifera are "small buried food particles", Bush et al. (2007) defined scaphopods as miners. In addition, the assignment of some marine invertebrate groups to specific tiering, motility and feeding bins is problematic. All assignments were, therefore, made with reference to the most up-to-date or most widely accepted analysis.

2.4.2 Alpha Diversity

Alpha diversity, so named because it was originally measured with the Fisher alpha index (Fisher et al., 1943), is the diversity in an individual stand (sampling area) or community. In macroecology, alpha diversity is generally not measured with Fisher's alpha, but is regarded as richness (S) at the finest scale of observation. Richness is measured by counting the number of taxa in a sample. It is, however, very dependent on sample size and worker effort (Holland, 2010). Even when sample size is standardised, differences in S are controlled by differences in the rare taxa (Holland, 2010). The same is true, to a lesser extent, of many other standard diversity indices (e.g. Clarke and Warwick, 2001). Simpson's Diversity (D), on the other hand, can be used to generate

meaningful independent alpha and beta components, even when the community weights are unequal or sampling is uneven between samples (Jost, 2007). Here, richness and Simpson's Diversity were used in concert to understand how abundance contributes to changes in alpha diversity in a broad sense.

Simpson's D $(1 - \lambda)$ is an important diversity index that is related to the probability that any two randomly selected individuals from a population belong to the same taxon (Simpson, 1949; Equation 1).

Equation 1.

$$D = 1 - \lambda = 1 - \sum_{i=1}^{s} p_i^2$$

This is the inverse of Simpson's concentration (Simpson, 1949) and is often used as a measure of diversity (Jost, 2006).

Hurlbert's PIE is not biased by sample size or richness and uses Simpson D to calculate the probability of an interspecific encounter (Equation. 2).

Equation 2.

$$\Delta_1 = N \times D/(N - 1)$$

(Hulbert, 1971; Olszewski, 2004)

Where N is the number of individuals.

Simpson's D and Hurlbert's PIE are measures of evenness, not diversity (Olszewski, 2004; Jost, 2006; Holland, 2010), i.e. the probability that any two randomly selected individuals from a population belongs to the same taxon (Simpson, 1949). Simpson's D, however, can also be transformed into an effective diversity (Equation 3), which allows the impact of evenness on richness to be quantified:

Equation 3.

$$\text{Simpson Diversity } \Delta = 1/(1 - \Delta_1)$$

(Jost, 2006; 2007)

Diversity metrics are not independent of abundance: *S* provides information on the rare tail of the taxon abundance distribution; whereas Simpson's Δ reflects the abundant end of the distribution (Holland, 2010).

The Kruskal-Wallis test was used to investigate differences in the median diversity between different formations and members, facies, lithology, collection method and setting. *P*-values of <0.05 were used to reject the null hypothesis that the samples are taken from populations with equal medians. The Kruskal-Wallis test was used instead of the Analysis of Variance (ANOVA), as it does not assume a normal distribution. The analyses for investigating diversity were performed using PAST 2.17c (Hammer and Harper, 2001). Computing the Kruskal-Wallis test in PAST also computes multiple comparisons using Mann-Whitney pairwise tests. The Mann-Whitney *U* test also does not assume a normal distribution and tests that the medians between two samples are different.

2.4.3 Multivariate analyses

For multivariate elaboration, samples that only contain species found in no other sample were removed because they would have zero similarity to any other sample and would plot randomly in an ordination and as outliers in a cluster analysis. Relative, rather than absolute, abundances were used as multiple collection methods were used. Most of the samples are dominated by a few taxa, and so the relative abundance data were square-root transformed to de-emphasise the influence of the most dominant taxon (Clarke and Warwick, 2001).

Hierarchical agglomerative clustering (cluster analysis), using an unweighted pair-group average cluster model (Clarke and Warwick, 2001), was applied to recognise those species that tend to co-occur in samples and to group together samples of similar taxonomic composition using the Bray-Curtis similarity matrix. The similarity profile test (SIMPROF) was applied to determine significant differences between the clusters (Clarke and Warwick, 2001). This technique is a permutation test of the null hypothesis that a specified set of samples, which are not *a priori* divided into groups, do not differ from each other in multivariate structure. Here, 999 permutations were applied to calculate a mean similarity profile, 999 simulated profiles were generated, and the chosen significance level is 0.05.

The resulting clusters of samples were analysed through a similarity percentages routine (SIMPER) to determine which species were responsible for the greatest similarity within groups (Clarke, 1993). The species identified by the analysis as typifying each group are (i) those that occur at a similar relative abundance in each sample within the group, so that the standard deviation of their contribution (Sd) is low; and (ii) those where the ratio between the average similarity within the group (Sim) and Sd is high (Clarke, 1993). This method enabled the identification of groups of samples that contain a similar suite of taxa in similar proportions (i.e. ''biofacies'' sensu Ludvigsen et al., 1986), and also to identify their characteristic species.

Non-metric multidimensional scaling (nMDS) was then applied to visualise trends and groupings of the samples. Shepard diagrams were produced for the ordinations to investigate the stress of the plot. Stress measures the departure of points from the best fitting increasing regression line. Thus, when rank order relationships are exactly preserved the stress is zero (Clarke and Warwick, 2001). Stress, therefore, indicates the quality of the nMDS plot with values of <0.05 showing an excellent representation of

the data; <0.1 good representation; <0.2 acceptable representation for 2D plots only and >0.3 unsatisfactory representation (Clarke and Warwick, 2001).

The permutational ANOVA and MANOVA (PERMANOVA) were used to compare the benthic assemblages between the different factors: facies, sub-stages, lithologies, formations and sampling methods. PERMANOVA is a routine for testing the simultaneous response of one or more variables to one or more factors in an analysis of variance (ANOVA) experimental design, on the basis of any resemblance measure, using permutation methods (Anderson, 2001; Anderson et al., 2008). One advantage of this technique over traditional ANOVA and MANOVA is that is does not assume a normal distribution of the data, also a one-way PERMANOVA maintains the dissimilarity distances for the analysis (Anderson, 2001). A disadvantage of the PERMANOVA test is that it provides a pseudo F-statistic which is dependent on the degrees of freedom and cannot necessarily be compared across studies. In a PERMANOVA routine the P-value is of interest and is used as a measure of strength of evidence with respect to any particular null hypothesis. In some situations there are not enough possible unique permutations to get a reasonable test (Anderson, 2001), and so Monte Carlo P-values were also calculated. Significance was taken at the 0.05 level (Manly, 2006). PERMANOVA tests the null hypothesis that the centroids of the groups, as defined by the space of a chosen resemblance measure, are equivalent.

When multiple variables, e.g. formation, stage, sampling method, sedimentary facies or lithology, showed significant differences, they were then subjected to pair-wise comparisons. This is useful when findings are no *a priori* and a causal element of a factor is wanted to be known. This is done by performing a (two-tailed) t test, where the greater the t statistic, the greater the evidence against the null hypothesis of no difference in community structure between the two groups. In PRIMER the routine for pair-wise tests also produces a triangular matrix containing the average resemblances

between samples that are either in the same group or in different groups. 999 permutations were generated, and the chosen significance level is 5%.

PERMANOVA tests if the difference in the position of the centroids is significant, whereas a test of homogeneity of dispersions (PERMDISP) is a routine for testing multivariate dispersions (Anderson, 2001). This is useful because two samples may have a similar centroid in multi-dimensional space and PERMDISP demonstrates whether they have significantly different dispersions.

Cluster, ordination and PERMANOVA analyses were performed with the software PRIMER 6.1.15 & PERMANOVA 1.0.5.

3. Aggtelek Karst, Hungary

3.1 Stratigraphy

Detailed descriptions of the stratigraphic framework of the Lower Triassic succession in the Aggtelek Karst are given by Hips (1996a; 1996b). Hips (1996b) and Hips and Pelikán (2002) found that the Lower Triassic ammonoid and bivalve zonations presented for the Werfen Formation were also applicable for the "Gemer-Bükk area", i.e. Aggtelek Karst (Figure 3.1).
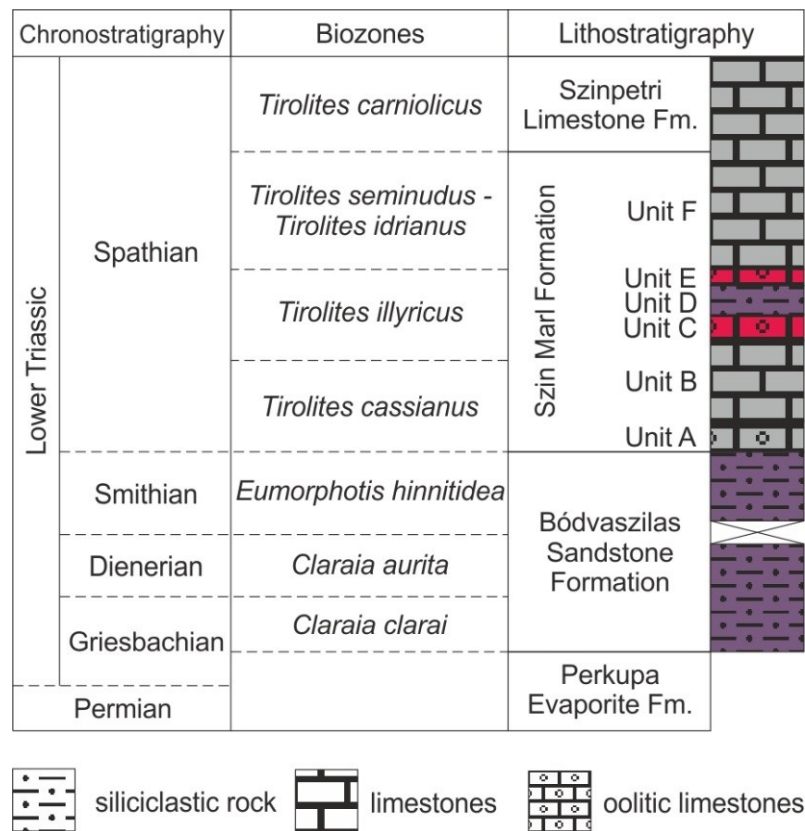
Figure 3.1: **Stratigraphic subdivision of the Lower Triassic of the Aggtelek Karst.** Vertical subdivision is proportional to thickness; after Hips 1996b. Biostratigraphy for the Griesbachian, Dienerian and Smithian follows the bivalve biozonation of the Werfen Formation, Dolomites (Posenato, 2008b). Biostratigraphy for the Spathian follows the ammonoid biozonation of the Werfen Formation, Dolomites, Csopak Marl Formation, Bakony, and the Muć section, Croatia (Posenato, 1992). Modified after Hips (1998).

Bódvaszilas Sandstone Formation

The only age-diagnostic fossils from the Bódvaszilas Sandstone Formation are bivalves. At the base of the Bódvaszilas Sandstone Formation Hips (1996b) records *Claraia clarai* and correlates initial deposition with the late Griesbachian *C. clarai* zone of the Siusi Member, Werfen Formation. In this study, at the base of this formation the index fossils *Claraia clarai* and in the basal 4m *Claraia wangi-griesbachi* occur. Following the bivalve biozonation of Broglio Loriga et al. (1990) the ranges of *C. clarai* and *C. wangi-griesbachi* do not overlap in the Werfen Formation. In this study (Chapter 4), however, the ranges of these bivalves overlap in the Werfen Formation at the top of the mid-Griesbachian Mazzin Member. The overlap of the ranges of *C. clarai* and *C. wangi-griesbachi* observed in the basal 4m of the Bódvaszilas Sandstone Formation, therefore, suggests that initial deposition of the formation correlates between the mid-Griesbachian upper part of the Mazzin Member and the late Griesbachian transgression at the base of the Siusi Member, Werfen Formation. The findings of this study, therefore, agree with Hips (1996b) and infer that the Permian/Triassic boundary occurs in the underlying Perkupa Evaporite Formation (Hips, 1996b), which is not exposed in the Aggtelek Karst (personal observation).

Currently there is no formal definition for recognising the Griesbachian/Dienerian boundary. *Claraia aurita*, however, is used as an index fossil of the Dienerian in the Werfen Formation due to its occurrence within the *Gyronites* ammonoid Zone in Iran (Nakazawa, 1977). The identification of *C. aurita* and closely related species (e.g. *Claraia wangi* and *C. griesbachi*) is problematic. As they are all characterised by mostly orbicular to prosocline outline and fine commarginal sculpture, which may only be faintly developed (Hofmann et al., 2015a). The small-sized (~2mm to 2cm) and almost smooth forms from the Werfen Formation have been described as *C. wangi-griesbachi* whereas *C. aurita* have been distinguished by well-developed commarginal

ornamentation (Broglio Loriga et al., 1983). The taxonomic determination of *C. wangi-griesbachi*, however, has been questioned by Hofmann et al. (2015a), who highlights that size is not a standard taxonomic criterion and preservational effects on the ornamentation makes it difficult to define robust criteria to separate *C. wangi-griesbachi* from *C. aurita.* The ranges of *C. wangi-griesbachi* and *C. aurita* have not yet been observed to overlap and although the size of *C. wangi-griesbachi* and *C. aurita* do overlap they are significantly different ($p = <0.01$; Appendix 3.1). Therefore, based on the differences of strength of sculpture and the stratigraphic gap (in the absence of a facies change), this study considers *C. wangi-griesbachi* to be a subspecies of *C. aurita.*

The first occurrence of *C. aurita* sensu stricto occurs at 42m above the base of the Perkupa Quarry section and is used to determine the Griesbachian/Dienerian boundary in this study. The ranges of the index fossils *C. clarai* and *C. aurita* overlap in the western Palaeotethys, and the boundary between the *C. clarai* and *C. aurita* biozones is defined by the first occurrence of *C. aurita*.

The Induan/Olenekian boundary is defined as the boundary between the *Eumorphotis multiformis* and *E. hinnitidea* zones (Posenato, 2008b). These index fossil ranges overlap and the FAD of *E. hinnitidea* is used in the Werfen Formation to indicate the Smithian (Posenato, 2008). In this study *E. multiformis* and *E. hinnitidea* first occur together in the upper part of the Bódvaszilas Sandstone Formation at the base of the Perkupa Cemetery section. The Induan/Olenekian boundary is also defined by a carbon isotope perturbation to +6‰ and a transgression in the Werfen Formation (De Zanche et al., 1993; Horacek et al., 2007a; Posenato, 2008b). Due to the lack of carbonate and organic material in the Bódvaszilas Sandstone Formation a carbon isotope investigation was not possible in this study. *E. hinnitidea*, therefore, is used to indicate the Smithian sub-stage.

Szin Marl Formation

In the western Palaeotethys, ammonoids are only known from the Spathian (Posenato, 1992; 2008b). The first appearance of ammonoids occurs at the base of the Szin Marl Formation (Hips, 1996b) and, following Posenato (1992), the first appearance of *Tirolites cassianus* within Unit A of the Szin Marl Formation indicates the first ammonoid zone of the Spathian (Figure 3.1). The Smithian/Spathian boundary, therefore, has been inferred to occur at the boundary between the Bódvaszilas Sandstone and Szin Marl formations (Hips, 1996b). In the upper part of Unit B of the Szin Marl Formation, Hips, (1996b) records the ammonoid *Diaplococeras liccanum*, which in the Werfen Formation occurs in the Spathian Val Badia Member. A single occurrence of the ammonoid *Dinarites dalmatinus*, reported by Hips, (1996b), in unit F of the Szin Marl Formation enables correlation to unit C of the Cencenighe Member of the Werfen Formation in the Dolomites (Posenato, 2008b) and, following Posenato (1992) the mid-Spathian *T. seminudus-T. idrianus* Zone.

Szinpetri Limestone Formation

The ammonoids *T. carniolicus* and *Stacheites* cf. *floweri*, reported by Hips (1996b), in the lower part of the Szinpetri Limestone Formation correlate with the late Spathian *T. carniolicus* zone (Posenato, 1992). In addition, strontium isotopes from the Szinpetri Limestone at Szin North indicate a late Spathian age ($\delta^{87/86}$Sr 0.708162, Alexa Sedlacek, personal communication 2015; Korte et al., 2003).

The Lower/Middle Triassic boundary is poorly constrained in the study area, because age diagnostic fossils are absent. The Jósvafő Member, Gutenstein Formation, represents dark grey mudstones and overlies the Szinpetri Limestone Formation. The uppermost beds of the Jósvafő Member contain the foraminifera *Glomospira densa* which has been used to infer an Aegean-Bithynian age (Hips, 2003; 2007). The

Spathian/Anisian boundary, therefore, is inferred to occur between the Szinpetri Limestone and Gutenstein formations (Hips, 2007).

3.2   Facies Analysis

Detailed descriptions of the facies and ramp evolution of the Lower Triassic succession in Aggtelek are given by Hips (1996b; 1998) and Kovács et al. (1989). This study follows Hips (1998), who recognised sixteen facies, eight of which were observed in this study (Table 3.1; Figures 3.2-3.3).

Facies 1: Purple siltstones with desiccation cracks and wave ripples (tidal-flat facies).

Description: Mainly purplish-red laminated siltstones, interbedded with (1-3cm) brown and occasionally green, very fine- to fine-grained flaser bedded sandstones. Occasional thinly bedded (1-2cm), graded sandstone beds are also present. The laminated siltstone beds occasionally display desiccation cracks, wave-formed ripple marks, wrinkle marks and small domes (ø=2-5cm). Convex-up bivalves are recorded on siltstones that lack desiccation cracks and within the sandstone beds. In the upper part of the Perkupa Quarry, *Diplocraterion* burrows are common in the siltstones (Figure 3.4). This facies occurs in the lower part of the Bódvaszilas Sandstone Formation.

Interpretation: This facies is interpreted to represent a tidal-flat facies, recording mudflats and sand flats deposited in the supratidal to intertidal zone (Hips, 1998). The siltstones with desiccation cracks were deposited in the high intertidal/low supratidal zone where they were subaerially exposed. Wave-formed ripples and flaser-bedded sands were formed in the intertidal zone of the tidal flat. Graded sandstones, i.e. tempestites, were deposited from waning storm currents (Tucker, 2001). The predominance of fine-grained sediments (siltstones) indicates deposition in a low-

Table 3.1: Sedimentary facies and depositional environments for the Lower Triassic succession of the Aggtelek Karst. After Hips (1998).

Facies	Lithology	Sedimentary structures	Depositional Environment
1	Purple siltstones, very fine- to fine-grained (1-3cm) sandstones.	Laminated siltstones and flaser bedded sandstones. Desiccation cracks, ripple marks, wrinkle marks and small domes on the siltstones.	Tidal-Flat
2	Purple siltstones, green clay, brown sandstones and (1-2cm) grey packstones.	Laminated siltstones with ripples, wrinkle marks, and small ball and pillow structures (~5cm diameter). Massive and graded sandstones.	Inner ramp, shallow subtidal
3	Brown sandstones and purple siltstones.	Thick-bedded sandstones with large ball and pillow structures. Thin-bedded, graded sandstones. Hummocky and hummocky cross-stratified, fine grained sandstones. Wave rippled siltstones.	Mid-ramp, deep subtidal
4.1	Varicoloured (orange, black and yellow) oolitic grainstones.	Hummocky tops and hummocky cross-stratification. Ooids with bioclast fragments as nuclei.	Oolitic shoal and storm sheets
4.2	Red oolitic pack- and grainstones, Bedded grey wackestones and brown and purple siltstones.	Thick oolitic beds with erosive bases. Bedded wackestones. Laminated siltstones.	Oolitic storm sheets
5.1	Grey fine-grained sandstones, sandy wackestones and light yellow siltstones.	Hummocky and swaley cross stratification with planar bases. Laminated siltstones.	Mid-ramp, sand storm sheets
5.2	Green, bedded fine grained sandstones. Green sandy limestones and siltstones.	Hummocky cross stratification, grading and erosive bases. Large ball and pillow structures. Laminated siltstones.	Mid-ramp, storm sheets

6.1	Purple and green siltstones and sandy limestones.	Laminated and bioturbated siltstones. Gutter casts on the base of limestone beds or as lenses within siltstones. Cross-laminated sandy limestone beds.	Outer ramp, distal storm layers
6.2	Grey, silty limestones, very-fine sandy limestones and grey crinoidal packstones	Laminated silty limestones. Thin-bedded sandy limestones. Crinoidal packstones. Small ball and pillow structures.	Outer ramp, distil storm layers
7	Beige, green-tinted silty limestone. Green marls.	Laminated marls. Current ripples and glauconite on the thin-bedded silty limestones.	Outer ramp, low-energy
8	Light grey wackestones and dark grey packstones.	Wackestones are intensely bioturbated (ii4–5) overprinting original sedimentary structures.	Outer ramp, bioturbated

energy environment such as a lagoon behind a protecting barrier (Reading and Collison, 1996).

Facies 2: Inner ramp, lower shoreface.

Description: Massive and graded brown sandstones (1-16cm) interbedded with purple wavy-and parallel-laminated siltstones which occasionally contain small (<5cm diameter) ball and pillow structures. Occasionally between the wavy siltstones are green clay laminae (1-3mm) with moulds of bivalves. The siltstones contain abundant wrinkle marks, occasional wave-formed ripple marks and are also bioturbated by oblique (45°) *Rhizocorallium* c.f. *jenense* burrows. Bivalves are disarticulated and convex up and occur as thin coquinas on top of siltstone beds and within sandstone beds. In the Szin Marl, thin (1-2cm) dark grey packstone beds with convex-up bivalves and microconchids are intercalated within the silts. This facies occurs in the lower part of the Bódvaszilas Sandstone and Unit A and D of the Szin Marl Formation.

Interpretation: These sediments were deposited in shallow subtidal environments, in the shoreface zone (above fair-weather wave base (fwwb)). Graded sandstones were deposited during a waning-flow following storm events. Ball and pillow structures represent water escape processes following the rapid deposition of sand (Lowe, 1975). The pre-dominance of fine-grained sediments suggests deposition took place in a low-energy environment such as a lagoon behind a protecting barrier (Reading and Collison, 1996).

Facies 3: Cross-stratified sandstones alternating with laminated siltstones (Mid ramp, deep subtidal facies).

Description: This facies is characterised by thick-bedded (25-60cm) brown sandstones, interbedded with thinly bedded (2-10cm) sandstones and siltstones. The thinly bedded sandstones are mostly graded and parallel-laminated, occasionally massive, and are

interbedded by thin (1-2cm) of siltstones and green marls. The thicker packages of siltstones contain small ball and pillow structures. Thicker sandstone beds have sharp planar bases and are massive. Some of these sandstone beds have rippled surfaces and display hummocky cross-stratification throughout. At the base of the Perkupa Cemetery section, a 60cm sandstone bed contains ball and pillow structures that span the entire bed. Convex-up bivalves occur on the thin beds of sandstone and siltstone. The siltstone beds are rippled and contain *Arenicolites* and *Skolithos*. In the thick sandstone beds the fauna are randomly orientated. This facies is found throughout the Bódvaszilas Sandstone Formation.

Interpretation: This facies is interpreted as representing storm sheets in a mid-ramp environment (above storm weather wave base (swwb)). Planar and hummocky-cross stratified beds were formed as a result of storm wave activity and deposition in a mid-ramp environment, i.e. between fwwb and swwb. The graded sandstone beds are associated with a waning-flow during storm deposition.

At the base of the Perkupa Cemetery section, large (60cm) ball and pillow structures occur, which are associated with water escape processes due to a density difference following the rapid deposition of sands. Twitchett (1999) recognised that large ball and pillow structures characterise the base of the Campil Member in the Dolomites and suggested that their basin-wide, potentially synchronous, distribution may reflect large-scale tectonic activity. Furthermore, Smithian strata from the margin of the Palaeotethys are associated with a 'Campil Event' where marly-carbonate lithologies are replaced by red terrigenous clastics in shallow marine environments (Broglio Loriga et al. 1990). Tectonic activity during the Smithian, therefore, may have caused a temporary increase in the supply of clastic material to the mid-ramp environment associated with topographic changes causing increased run-off. This would have led to a lowering of the
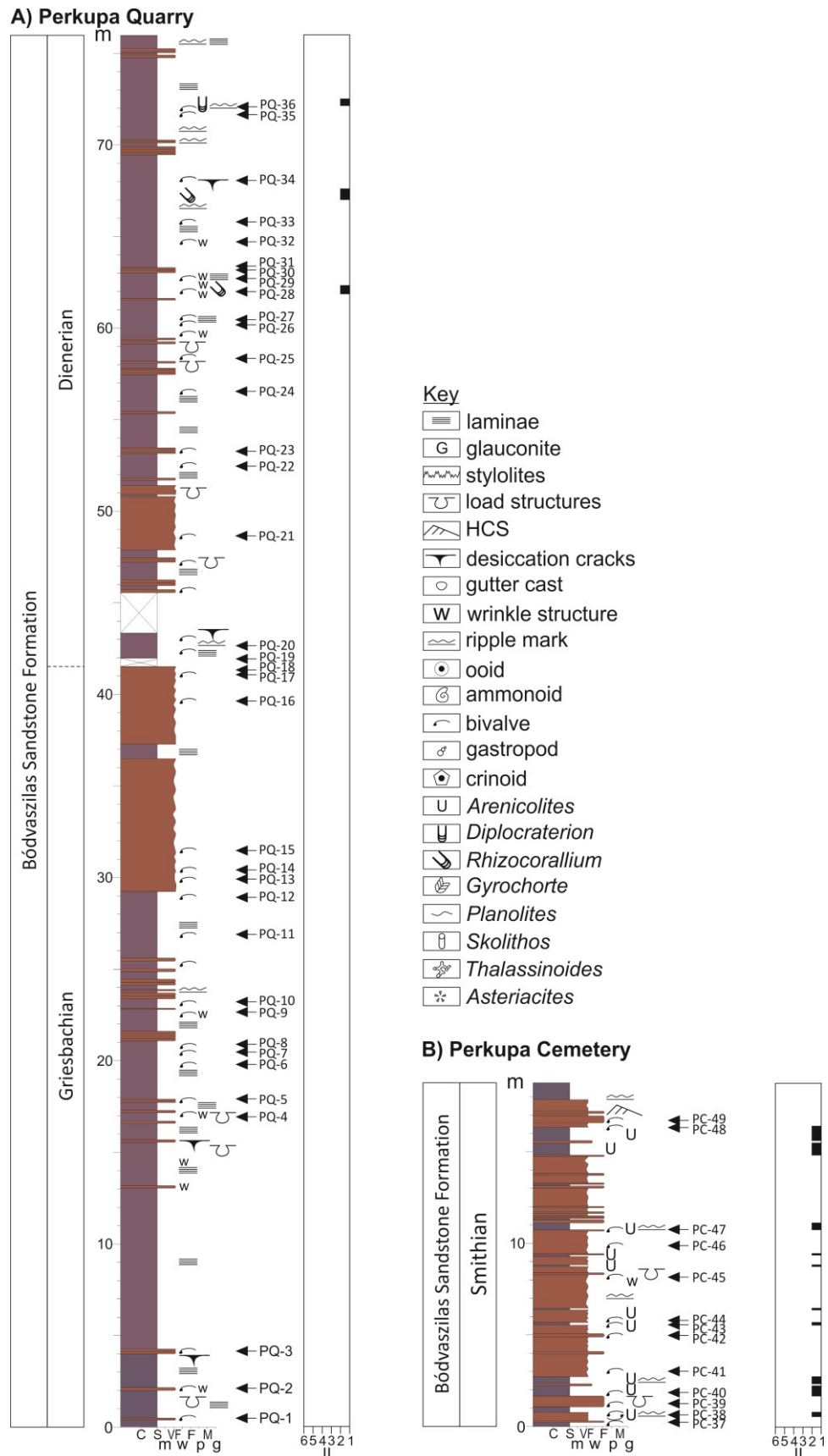
Figure 3.2: Logs of the Aggtelek Karst that show the facies and stratigraphic intervals of the Lower Triassic. A) Perkupa Quarry section, B) Perkupa Cemetery section. II = Ichnofabric Index (Droser and Bottjer, 1993). Colour in the lithology column refers to the rock colour observed in the field.
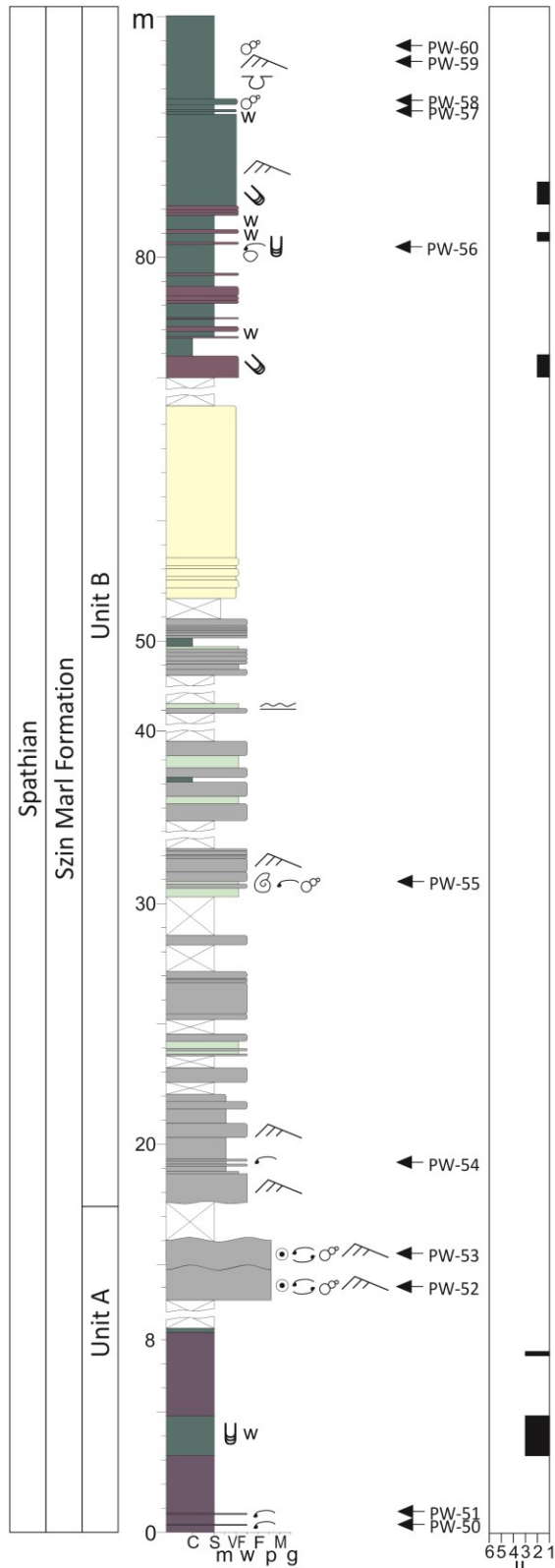
Figure 3.2. Continued: C) Perkupa West, D) Perkupa Vineyard.
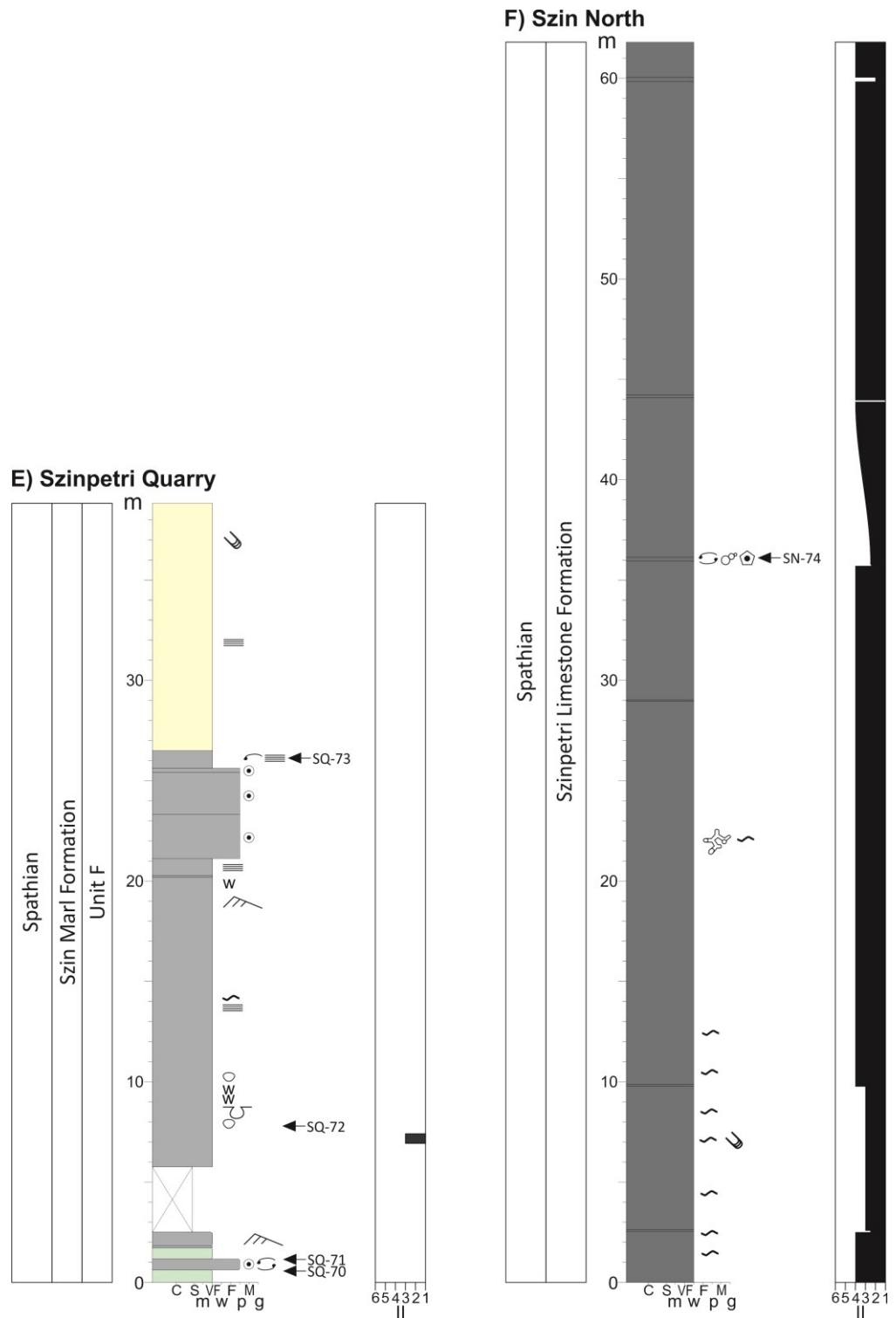
Figure 3.2. Continued: E) Szinpetri Quarry, F) Szin North.

salinity and this facies may, therefore, represent deposition in a brackish environment (Twitchett, 1999).

Facies 4: Oolitic limestones (Oolitic shoal facies).

Description: This facies is split into two subfacies.

Sub-facies 4.1: Orange, black and yellow, 20-220cm thick, oolitic grainstones characterise this sub-facies. These beds have hummocky tops, erosive bases and are sometimes cross-bedded. The beds contain a large quantity of thick, black, recrystallised bivalve shell fragments and other bioclasts that are randomly orientated. Thin shell fragments occur as nuclei of ellipsoidal ooids that show distinct layering and faint radial structures. These beds weather light grey and contain abundant stylolites. This sub-facies occurs in Unit A and F of the Szin Marl Formation.

Sub-facies 4.2: This sub-facies is characterised by 20-130cm thick, red oolitic grainstones and packstones with erosive bases. Most of the ooids are formed around thin shell fragments. The bivalves within these beds have thick black shells and occur mostly convex up and parallel to the bedding. These oolitic grainstones are interbedded with 18-20cm thick grey wackestones and decimetre beds of laminated brown and purple siltstones. *Diplocraterion* is abundant on the bedding surfaces of the siltstone beds. These beds also contain stylolites that appear to extenuate bedding. This sub-facies characterises Unit C of the Szin Marl Formation and Hips (1996b) also describes this sub-facies from Unit E of the Szin Marl Formation.

Interpretation: The ooids were formed in a high-energy environment on the inner ramp. The sediment was produced and accumulated in wave-agitated zones forming oolitic shoals (the beds that show cross bedding in sub-facies 4.1). Beds that lack cross-bedding have a sheet-like structure and have erosive bases were redeposited as tempestites in a mid-ramp environment. The alternations of these oolitic beds,

sandstones and wackestones also suggest storm-influenced deposition below fwwb. The bivalve fauna represents shallow-water benthos that lived on high-energy shoals (cf. Posenato, 1985). The red colour of the ooids in facies 4.2 comes from iron oxides that would have formed in an oxidised environment. The lining of iron oxide around bioclasts suggests the fauna were also transported from an oxygenated high-energy inner shelf environment (cf. Assereto and Rizzini, 1973).

Facies 5: Sandy limestone tempestites (Mid-ramp, storm sheets facies).

Description: This facies is split into two subfacies.

Sub-facies 5.1: Grey fine sandstones and fine sandy wackestones which weather light yellow, are interbedded with laminated yellowish grey siltstones. The sandy limestones have hummocky and swaley cross bedding and sharp planar bases. Large (>1cm) poorly preserved gastropods, bivalves and ammonoids occur within the sandy limestone beds. This sub-facies occurs at the base of Unit B in the Szin Marl Formation. This facies corresponds to sub-facies (3) of the *storm sheet facies* in Hips (1998).

Sub-facies 5.2: This sub-facies has a distinctive green colour in fresh and weathered rock, and comprises bedded fine sandstones (1-10cm thick), sandy limestones (1-10cm thick) and beds (centimetre-metre) of laminated siltstones. Thick beds of siltstones are more dominant in this sub-facies than sub-facies 5.1. The green colour in the sandy limestones comes from glauconite up to 1mm in diameter. Large well preserved gastropods are abundant in this facies and occur within the siltstone and sandy limestone beds. Throughout this facies there are large ball and pillow structures that from beds of deformed siltstones and sandy limestones up to 2m thick.

Interpretation: These deposits reflect a storm-wave agitated depositional environment in the mid-ramp between fwwb and swwb. Hummocky cross-stratified beds are thought to be the result of storm-generated oscillatory flows, or combined flows (waves plus

currents), produced by the passage of storms and are associated with deposition between fwwb and swwb (Tucker, 2001). The laminated siltstones between the HCS beds represent deposition in a low-energy environment in a more distal setting of the mid-ramp. The formation of glauconite is usually associated with an open-marine environment with low sedimentation rates (Huggett and Gale, 1997). The predominance of siltstone beds in facies 5.2 suggests an environment in a lower energy setting on a more distal part of the mid-ramp than facies 5.1.

Facies 6: Alternating limestones and siltstones (Outer ramp facies with distal storm layers).

Description: This facies is split into two subfacies.

Sub-facies 6.1: This sub-facies is characterised by 16-68cm beds of bioturbated purple and green siltstones that are interbedded with 4-11cm wacke- and packstones. Gutter casts either occur at the base of limestone beds or as limestone lenses within the siltstones. Gutters are commonly straight or slightly meandering in nature and trend NE-SW. Hips (1998) describe cross-laminations in the sandy limestone beds. The packstones often contain abundant crinoid ossicles. The siltstones are bioturbated (ii2-3) with *Diplocraterion, Rhizocorallium, Skolithos, Planolites* and *Asteriacites*. Covex-up bivalves occur convex-up within the sandy limestone beds. This sub-facies occurs in the upper part of Unit B in the Szin Marl Formation.

Sub-facies 6.2: Characterised by laminated grey silty limestones and thin-bedded very fine sandy limestones interbedded with grey, graded crinoidal packstones and wackestones. Small ball and pillow structures occur. *Planolites* and wrinkle marks occur on bedding planes. Hips (1998) also reports foraminifera, ammonoids, conodonts and rare bivalves from this facies, which, occurs in Unit B and F of the Szin Marl Formation.

Interpretation: Deposition took place in a low-energy environment occasionally agitated by storm activity. Sandy limestone beds and graded crinoidal packstones were deposited during storm events. The predominance of fine-grained material suggests deposition in a low-energy environment below mean swwb in the outer ramp. Gutter casts, cross-lamination and graded limestones occurred during storms and are the results of storm reworking and deposition from waning flow (Bhattacharya and Bhattacharya, 2011).

Facies 7: Thin bedded silty limestones (Low-energy outer ramp). Is made up of thinly bedded (<1cm) pale yellowish grey, pale green silty limestones. Low amplitude (<1cm) symmetrical ripples can occasionally be observed on some bedding planes. Glauconite is occasionally observed within the beds that are rarely bioturbated by oblique (45°) *Rhizocorallium* cf. *jenense*. Some 20-80cm thick beds of green laminated marls occur.
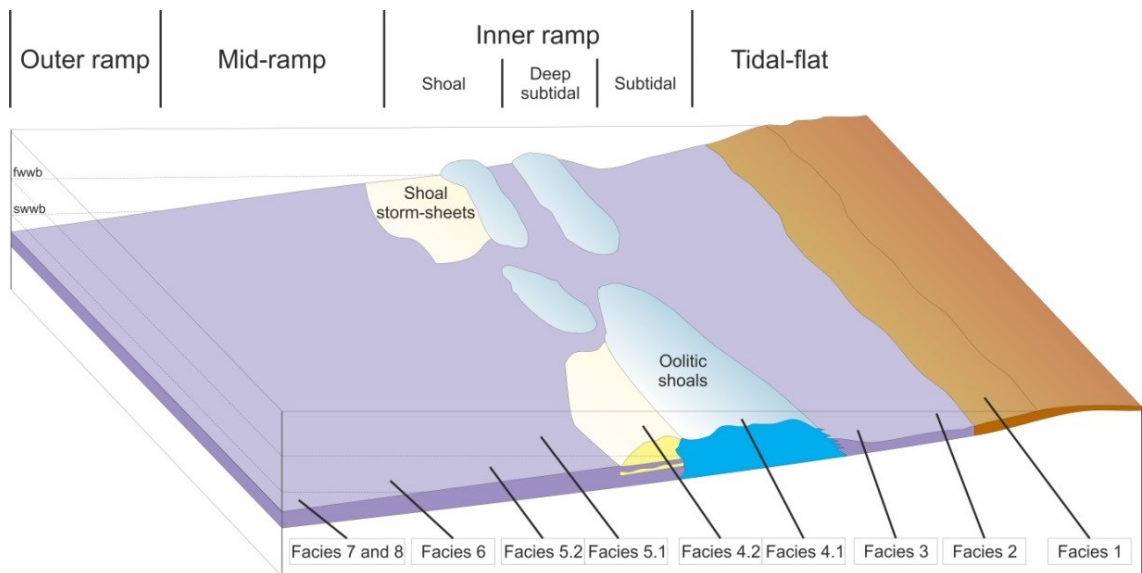
Figure 3.3: Schematic facies interpretation for the Aggtelek Karst showing the position of facies. 1 – Tidal-flat, 2 – Inner ramp, shallow subtidal, 3 – Mid-ramp, deep subtidal, 4 – Oolitic shoal, 5 – Mid-ramp, storm sheets, 6 – Outer ramp with distil storm layers, 7 – Low-energy outer ramp, 8 – Outer ramp.
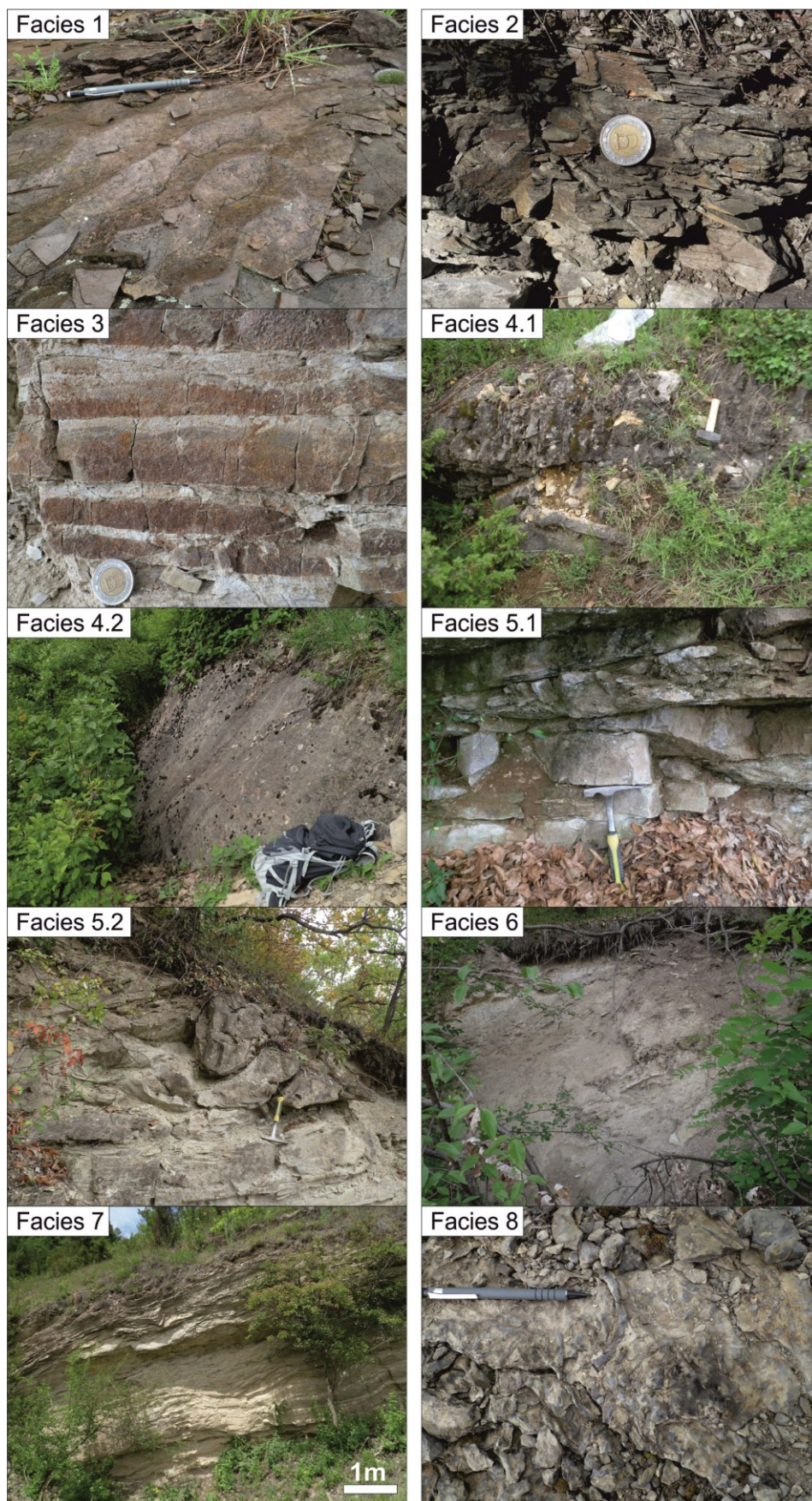
Figure 3.3 continued: 1 – Tidal-flat, 2 – Inner ramp, shallow subtidal, 3 – Mid-ramp, deep subtidal, 4 – Oolitic shoal, 5 – Mid-ramp, storm sheets, 6 – Outer ramp with distil storm layers, 7 – Low-energy outer ramp, 8 – Outer ramp.

Interpretation: This environment was below storm wave base and the sediments were deposited from suspension under low energy conditions. The low-amplitude of the ripples suggests that they were probably formed by storm-induced currents below wave base. Rare glauconite pellets were probably transported from shallower settings settling from suspension in the outer ramp environment.

Facies 8: Bioturbated limestones (Outer ramp facies).

Description: This is characterised by light grey, well bioturbated (ii4-5) wackestones. Bioturbation has destroyed original sedimentary structures. *Thalassinoides, Rhizocorallium* and *Planolites* traces are present on bedding planes. A few dark grey, ~5cm thick, wackestones and packstones contain a rich fauna including: bivalves, gastropods, crinoids, ophiuroids and microconchids. The bivalves in the limestones are articulated, the echinoderms, however, are disarticulated. Poorly preserved bivalves and ammonoids are present on some bedding planes. Hips (1996b) also reports ostracods and foraminifera from this facies. This facies is observed in the Szinpetri Limestone Formation.

Interpretation: This facies was interpreted as a low-energy lagoon by Hips (1996), however, the lack of shallowing observed between Unit F and the Szinpetri Limestone led to a reinterpretation by Hips (1998) of an outer ramp setting below swwb. The predominance of fine grained rocks suggests deposition took place in a low-energy environment below mean swwb. Hips (1998) also interpreted the dark grey colour of the limestone beds, strong bioturbation and low taxonomic diversity as an indicator of dysaerobic conditions. The presence of high diversity faunas, complex ichnofauna, high ichnofabric indices and infaunal taxa, however, suggest that this facies was deposited under well-oxygenated conditions (Savrda and Bottjer, 1991).

3.3 Ichnology

Ten ichnogenera were identified from the Aggtelek Karst, including an unidentified cubichnia (Figure 3.4). The Bódvaszilas Sandstone Formation is characterised by low ichnogeneric diversity, small burrows and infrequent bioturbation. Ichnofabric indices (ii, Droser and Bottjer, 1993) of the Bódvaszilas Sandstone Formation are low (ii1-2). No bioturbation was recorded in the Griesbachian. The Dienerian lower shoreface and tidal flat deposits were almost undisturbed with only 1% of the strata exhibiting weak (ii2) bioturbation. In contrast, 30% of the Smithian strata are weakly (ii2) bioturbated (Figure 3.5). Burrow diameters in the Bódvaszilas Sandstone Formation are small (average 3mm; max 7mm; Figure 3.6), average burrow depth is 19mm (maximum depth 30mm). In the Dienerian only *Diplocraterion* and *Rhizocorallium* were observed, whereas, in the Smithian *Skolithos* and *Arenicolites* were also recorded.

The Spathian Szin Marl Formation records an increase in the ichnogeneric diversity and complexity but is also characterised by small burrow diameters and infrequent bioturbation. In the outer ramp facies no bioturbation was recorded (Figure 3.5). In the mid-ramp facies seven ichnogenera were recognised: *Planolites, Rhizocorallium, Diplocraterion, Catenichnus, Skolithos, Asteriacites* and an unidentified cubichnia, whereas, in the shoal and protected inner ramp deposits only *Diplocraterion* and *Gyrochorte* were observed (Figure 3.5). The problematicum of Hips (1996b) is identified as *Laevicyclus* and occurs in the mid-ramp in Unit B of the Szin Marl Formation. The presence of *Gyrochorte* in inner ramp settings represents an increase in the complexity of trace fossil behaviour compared with the Bódvaszilas Sandstone Formation that lacked evidence for grazing activity. In the Szin Marl Formation, however, only 7% of the strata are disrupted by weak (ii2-3) bioturbation. Burrow diameters are also small (average diameter: 5mm; Figure 3.6) and the maximum burrow depth recorded was 10mm.

Figure 3.4: Trace fossils from the Lower Triassic of the Aggtelek Karst. A) *Arenicolites* (white arrow) and *Skolithos* (black arrow), Bódvaszilas Sandstone Formation. B) *Diplocraterion* (black arrow), Bódvaszilas Sandstone Formation. C) *Rhizocorallium* cf. *jenense*, Bódvaszilas Sandstone Formation. D) *Diplocraterion*, Bódvaszilas Sandstone Formation. E) *Gyrochorte* (black arrow) and *Arenicolites* (white arrow) Unit D Szin Marl Formation. F) unidentified cubichnia, Unit B Szin Marl Formation. G) *Thalassinoides*, Szinpetri Limestone Formation. H) *Arenicolites obtusus,* Unit B Szin Marl Formation. I) wrinkle marks, Bódvaszilas Sandstone Formation. Scale bar = 10mm, coin = 10mm.

The Szinpetri Limestone Formation records an increase in the extent of bioturbation, an increase in burrow diameter and an increase in the complexity of trace fossils. 99% of the Szinpetri Limestone Formation is disturbed by bioturbation with 94% of the formation showing extensive (ii4) bioturbation (Figure 3.5). Four ichnogenera were recognised: *Thalassinoides, Planolites, Rhizocorallium* and the problemticum *Laevicyclus* (Figure 3.4). *Thalassinoides* and *Rhizocorallium* from the Szinpetri Limestone Formation, represent the first recorded activity of crustaceans in the Lower Triassic succession of the Aggtelek Karst. The average burrow diameter is still small (6mm), but the maximum burrow diameter increases to 25mm (Figure 3.6). Burrow depth also increases in the Szinpetri Limestone Formation, but does not exceed 10cm. In addition, wrinkle marks that were recognised from tidal mudflat to outer ramp environments of the Bódvaszilas Sandstone and Szin Marl formations were not recorded in the Szinpetri Limestone Formation suggesting that the evidence for the presence of microbial mats has disappeared by the late Spathian.
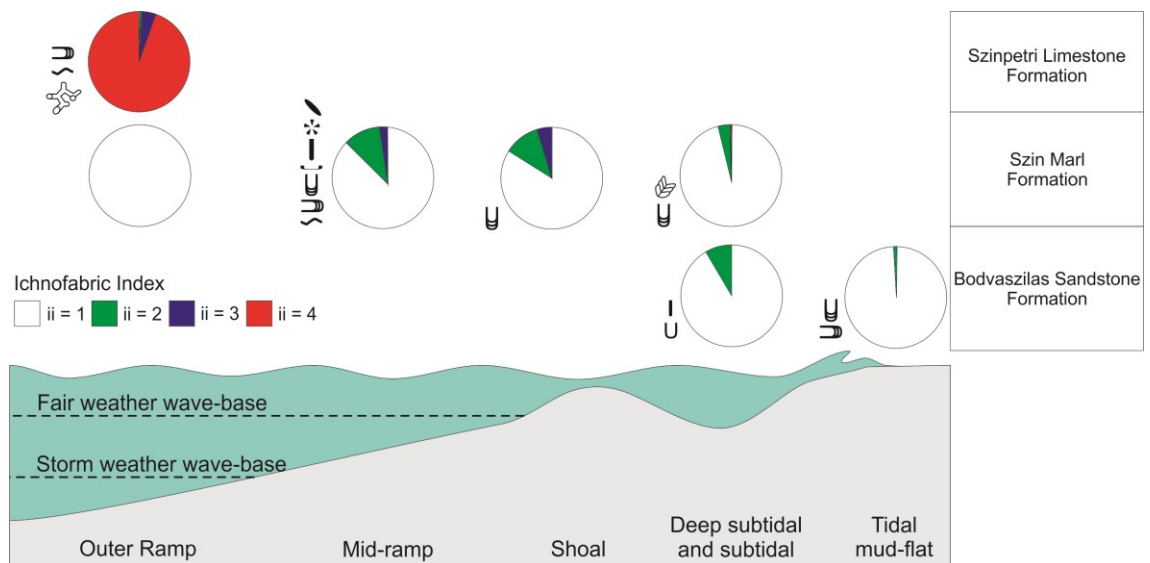
Figure 3.5: Proportion of bioturbated sediment between the different Lower Triassic formations of the Aggtelek Karst and the distribution of trace fossils. Trace fossil symbols as in figure 3.2.
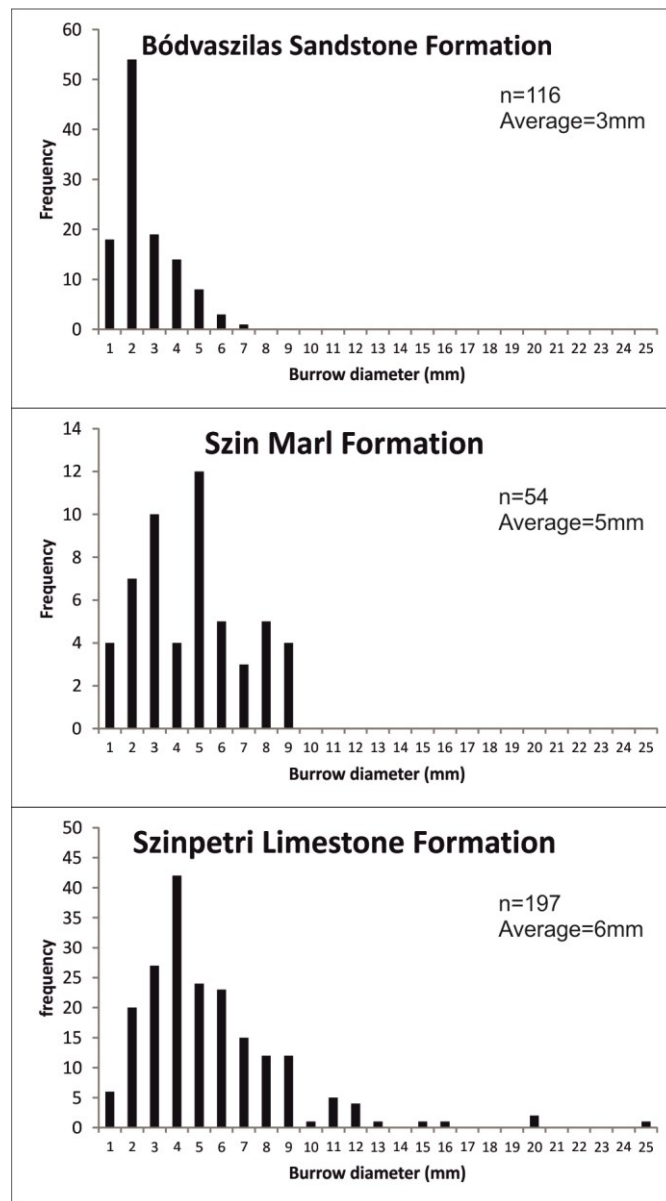
Figure 3.6: Histograms of the burrow diameter of the Lower Triassic Formations of the Aggtelek Karst.

3.4 Palaeoecological results

3.4.1 Alpha Diversity

In the Aggtelek Karst, 26 species from 16 genera were identified from 82 samples and 5,458 specimens of the Lower Triassic succession (Figure 3.7-3.8; Table 3.2), and recorded the presence of bivalves, gastropods, microconchids, crinoids, ophiuroids, brachiopods and scaphopods. Microgastropod packstones and grainstones that are

common in other Lower Triassic strata (e.g. Fraiser and Bottjer, 2004) were not observed in the Aggtelek Karst. The MNI per sample ranges from 1 to 163, and 45 samples have a large enough abundance (>20 MNI) for quantitative analysis (Appendix 3.2).

The alpha diversity indices record changes along a temporal and environmental gradient: the lowest values are recorded in the siliciclastic inner and mid-ramp settings of the Bódvaszilas Sandstone (S = 2–5; Δ = 1.1-3.9) and Szin Marl (S = 4; Δ= 2.7) formations, and the highest in the carbonate oolitic shoal to mid-ramp settings of the Szin Marl Formation (S = 1-7; Δ = 1-3.7) and the outer ramp setting of the Szinpetri Limestone (S=11; Δ = 7.4). The significant differences between the formations, sub-stages, and lithologies (Figure 3.9) are due to a greater number of facies sampled in the Szin Marl Formation compared with the Bódvaszilas Sandstone Formation. There are no significant changes in Simpson Diversity however (Figure 3.9), which suggests that the significant differences in species richness are due to the changes in the rare taxa.

Within the Szin Marl Formation, species richness is significantly higher in the oolitic shoal facies association than in other facies, but Simpson diversity is not significantly different between the different facies (Figure 3.9). Therefore, the higher diversity in oolitic shoal facies is driven by an increase in the number of rare taxa. Benthic fauna, excluding rare crinoid ossicles, were not recorded in the outer ramp environment until Unit F of the Szin Marl Formation. Only two samples were collected from outer ramp facies, the one from the Szinpetri Limestone Formation shows the greatest alpha diversity values recorded in this study (S=11; Δ = 7.4).

Eleven modes of life were identified from the Aggtelek Karst (Table 3.2). Changes in functional diversity also vary along temporal and environmental gradients: the siliciclastic inner ramp and deep subtidal settings of the Bódvaszilas Sandstone and Szin
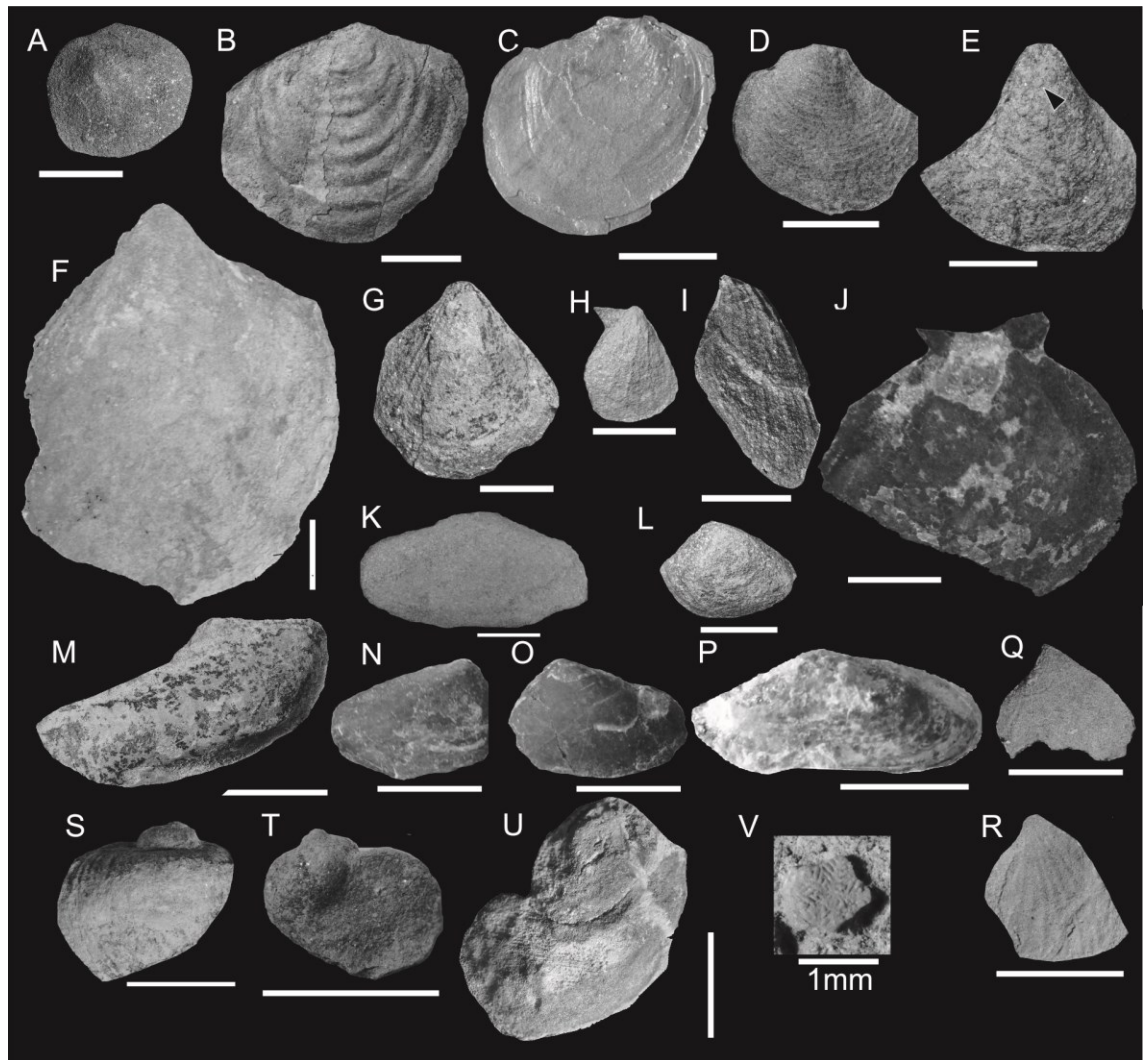
Figure 3.7: **Fossil invertebrates from the Lower Triassic of the Aggtelek Karst.** A) *Claraia wangi-griesbachi*, Perkupa Quarry 0.5m. B) *C. clarai*, Perkupa Quarry. C) *C. clarai*, Perkupa Quarry. D) *C. aurita*, Perkupa Quarry. E) *C. aurita* encrusted with microconchids (black arrow), Perkupa Quarry. F) *Eumorphotis kittli*, Szinpetri Quarry. G) *E. multiformis*, Perkupa Cemetery. H) *E. multiformis*, Perkupa Cemetery. I) *E. venetiana*, Perkupa Cemetery. J) *Scythentolium tirolicum*, Perkupa Vineyard. K) cf. *Unionites canalensis*, Perkupa Quarry. L) cf. *U. fassaensis*, Perkupa Cemetery. M) *Bakevellia* cf. *incurvata*, Perkupa West. N) *Neoschizodus ovatus*, Perkupa vineyard. O) *N. ovatus*, Perkupa Vineyard. P) "*Homomya*", Perkupa Vineyard. Q-R) *Costatoria costata*, Szinpetri Quarry. S-T) *Natiria costata*, Perkupa West. U) *Werfenella rectostata*, Perkupa West. V) *Holocrinus*, Perkupa Vineyard. Scale bar = 10mm except V.
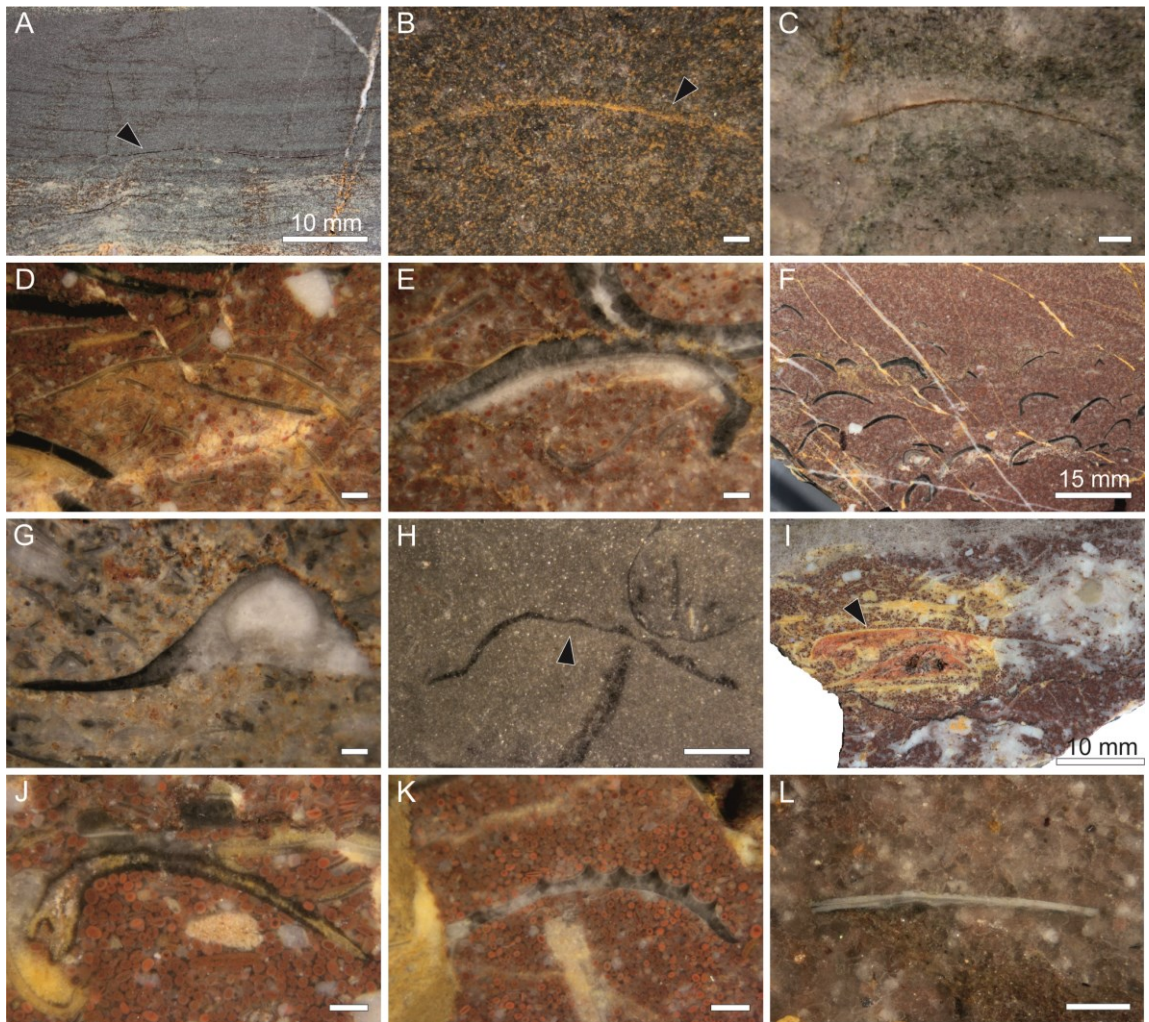
Figure 3.8: Polished slabs displaying the fauna recognised from the Lower Triassic of the Aggtelek Karst. All specimens are photographed under water. A) *Claraia clarai*, Perkupa quarry section. B) *Claraia aurita*, Perkupa quarry section. C) cf. *Unionites*, Perkupa west section. D) *Eumorphotis*, Perkupa Vineyard. E) *Neoschizodus ovatus*, Perkupa Vineyard. F) *Neoschizodus ovatus*, Perkupa Vineyard. G) *Bakevellia* cf. *incurvata*, Perkupa West. H) *Bakevellia* with costae, Szin North. I) *Scythentolium tirolicum*, Perkupa Vineyard. J) cf. *Homomya* sp., Perkupa Vineyard. K) *Costatoria costata*, Perkupa Vineyard. L) *Lingularia* sp., Perkupa cemetery. Scale bar = 1mm, except A, F and I.
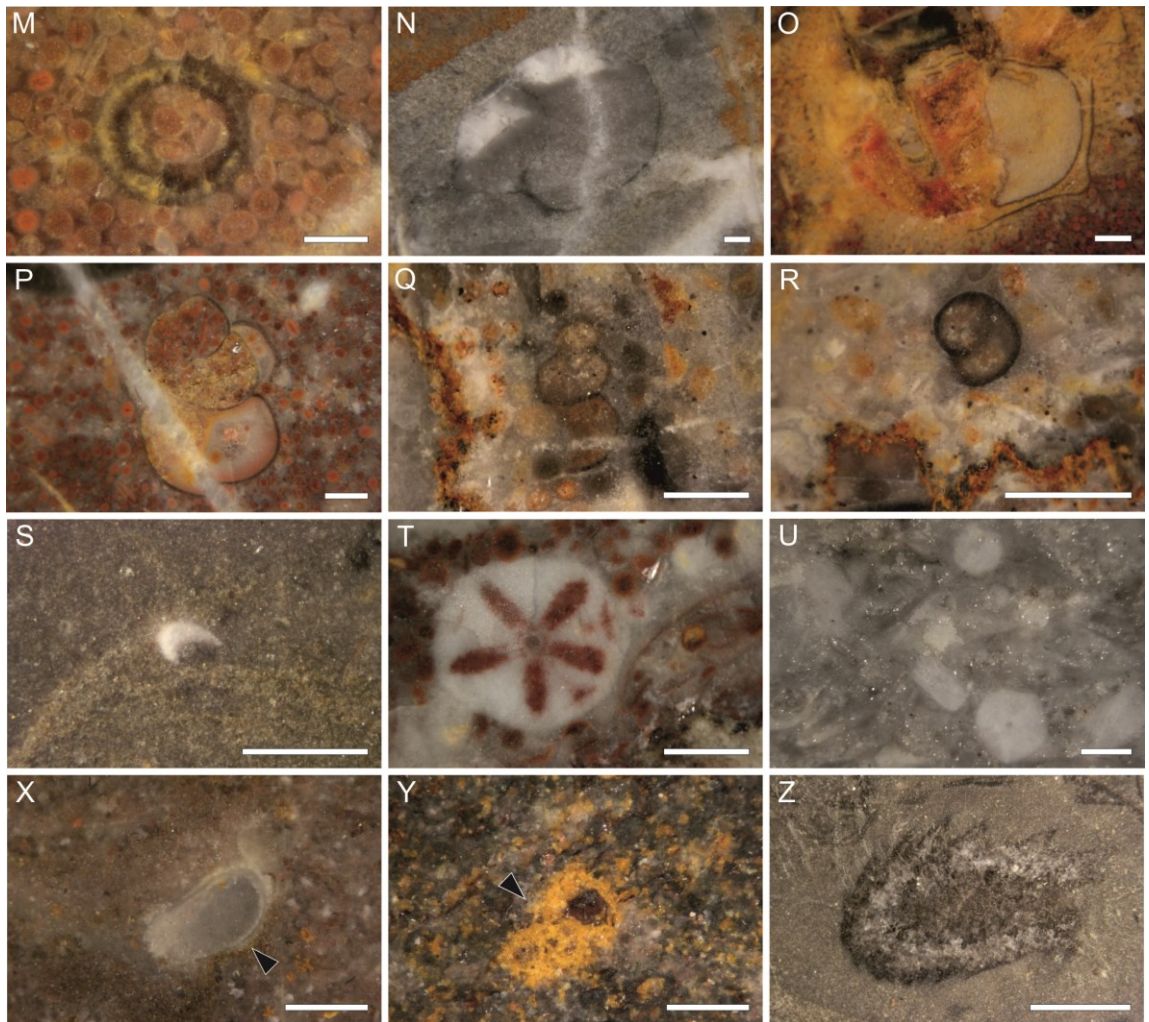
Figure 3.8: continued. M) *?Dentalium* sp., Perkupa Vineyard. N) *Natiria costata*, Perkupa west. O) Gastropod Indet. A., Perkupa Vineyard. P) *Coelostylina werfensis*, Perkupa vineyard. Q) *Coelostylina werfensis*, Szinpetri quarry. R) transverse section of a gastropod, Szinpetri quarry. S) Ophiuroid ossicle, Szin north section. T) *Holocrinus* sp., Perkupa Vineyard. U) *Holocrinus* sp., Perkupa vineyard. X) Microconchid, Perkupa cemetery. Y) Microconchid, Perkupa quarry. Z) Problematicum (c.f. Porifera), Szin north. Scale bar = 1mm.

Table 3.2: List of all recorded taxa and their mode of life. Modes of life after Foster and Twitchett, (2014). T = Tiering, M = Motility, F = Feeding. Tiering: 2 = erect, 3 = epifaunal, 4 = semi-infaunal, 5 = shallow infaunal. Motility: 2 = slow, 4 = facultative, attached, 3 = facultative, unattached, 5 = unattached, 6 = attached. Feeding: 1 = suspension feeding, 2 = surface deposit feeding, 3 = miner, 4 = grazer, 5 = predator.

Species	Group	Mode of life			Taxonomic Identification after
		T	**M**	**F**	
Bakevellia with costae	Bivalve	4	4	1	Neri and Posenato (1985)
Bakevellia c.f. *incurvata*	Bivalve	4	4	1	Kolar-Jurkovšek et al. (2013)
Claraia aurita	Bivalve	3	4	1	Nakazawa (1977)
Claraia clarai	Bivalve	3	4	1	Nakazawa (1977)
Claraia sp.	Bivalve	3	4	1	
Claraia cf. *wangi-griesbachi*	Bivalve	3	4	1	Broglio Loriga et al. (1983)
Costatoria costata	Bivalve	5	3	1	Broglio Loriga and Posenato (1986)
Eumorphotis hinnitidea	Bivalve	3	6	1	Broglio Loriga and Mirabella (1986)
Eumorphotis kittli	Bivalve	3	6	1	Broglio Loriga and Mirabella (1986)
Eumorphotis multiformis	Bivalve	3	6	1	Broglio Loriga and Mirabella (1986)
Eumorphotis venetiana	Bivalve	3	6	1	Broglio Loriga and Mirabella (1986)
Neoschizodus laevigatus	Bivalve	5	3	1	Neri and Posenato (1985)
Neoschizodus ovatus	Bivalve	5	3	1	Neri and Posenato (1985)
cf. *Homomya* sp.	Bivalve	5	3	1	Neri and Posenato (1985)
Scythentolium tirolicum	Bivalve	3	5	1	Neri and Posenato (1985)
cf. *Unionites canalensis*	Bivalve	5	3	1	Shigeta et al. (2009)
cf. *Unionites fassaensis*	Bivalve	5	3	1	Shigeta et al. (2009)
Gastropod sp. A	Gastropod	3	3	1	
Coelostylina werfensis	Gastropod	3	3	1	Nutzel and Schulbert (2005)
Natiria costata	Gastropod	3	2	4	Neri and Posenato (1985)
Werfenella rectostata	Gastropod	3	2	4	Nutzel (2005)
Lingularia sp.	Brachiopod	5	4	1	Posenato et al. (2014)
Holocrinus sp.	Crinoid	2	4	1	Kashiyama and Oji (2004)
Ophiuroidea	Ophiuroid	3	2	1/2	Glazek and Radwański (1968)
Dentalium	Scaphopod	4	2	3	
Microconch	Micronchida	3	6	1	Zaton et al., (2013)

Taxonomic alpha diversity
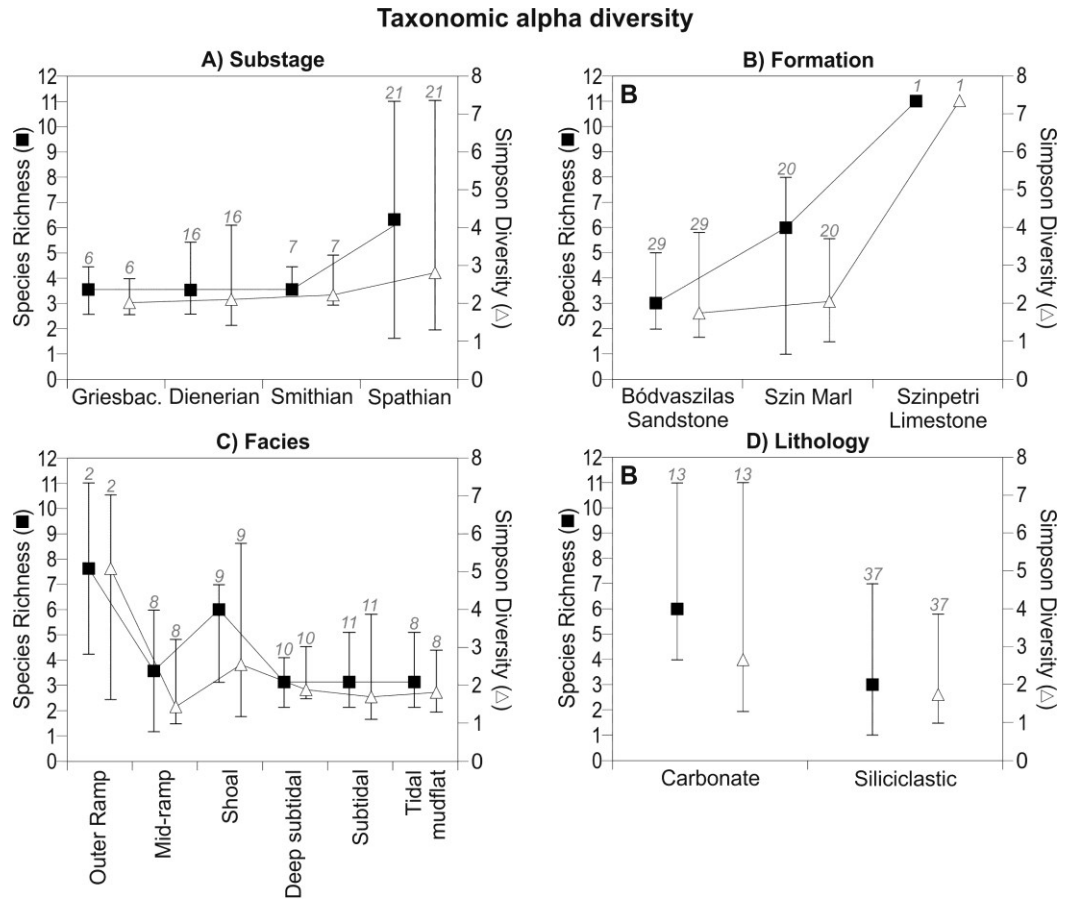
Figure 3.9: Box plots showing the changes in alpha diversity. A) Sub-stage, B) Formation, C) Facies and D) Lithology. Black squares represent median taxonomic richness and white triangle represents median Simpson Diversity. The maximum and minimum values are shown with short horizontal lines. Grey italics indicate the number of samples.

Marl formations recorded lower alpha diversity than the carbonate shoal and mid-ramp settings of the Szin Marl and outer ramp of the Szinpetri Limestone formations (Figure 3.10). The Kruskal-Wallis test shows that these differences are significant, except between changes in the Simpson diversity of samples between different facies (Figure 3.10). This suggests that the increase in functional diversity in shoal and mid-ramp settings is driven by the increase in rare modes of life, e.g. semi-infaunal slow-moving miners.
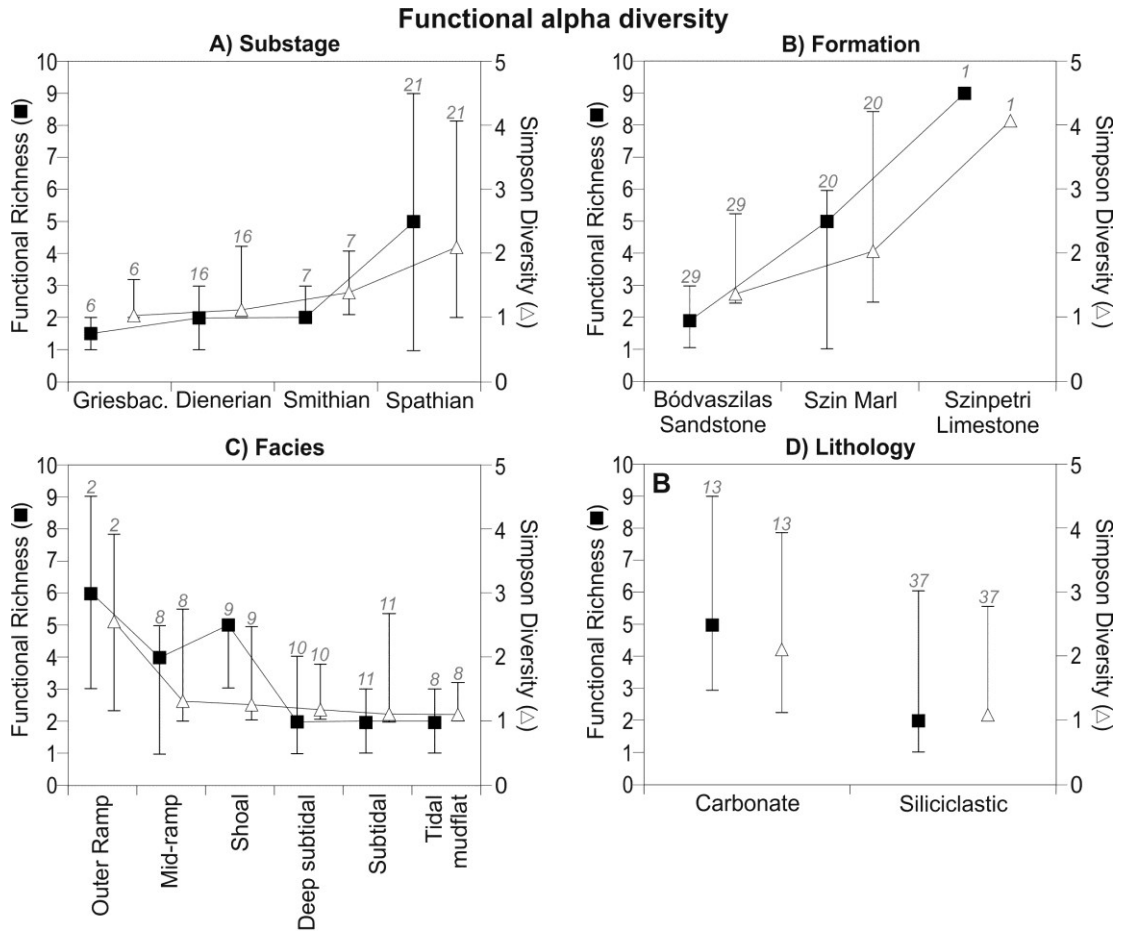
Figure 3.10: Box plots showing the changes in functional alpha diversity. A) Sub-stage, B) Formation, C) Facies and D) Lithology. Black squares represent median functional richness and white triangle represents median Simpson Diversity. The maximum and minimum values are shown with short horizontal lines. Grey italics indicate the number of samples.

3.4.2 Changes in taxonomic composition

The cluster analysis shows that two broad sample clusters at a similarity of around 40% (Figure 3.11). The first comprises samples from the Bódvaszilas Sandstone Formation and one from the outer ramp facies of the Szin Marl Formation, and is characterised by the dominance of the bivalve *Unionites* and the absence of gastropods. The second comprises samples from the Spathian Szin Marl and Szinpetri Limestone formations (Figure 3.11) and is characterised by samples dominated by the bivalve *Neoschizodus ovatus* or the large gastropod *Natiria costata*. The SIMPROF test applied to the cluster

analysis recognised five statistically distinct groups, (A-E; Figure 3.11) that, together with the SIMPER analysis enabled the identification of the trophic nucleus within each group of samples and the definition of five biofacies (Figure 3.11; Appendix 3.3).

The main axis of the ordination (nMDS1) mostly reflects temporal changes through the studied site, with Griesbachian samples on the left side of the diagram, through to Spathian samples on the right (Figure 3.12). The stress value for the nMDS ordination is 0.07, which gives confidence that the two dimensional plot is an accurate representation of the sample relationships (Clarke and Gorley, 2006). Induan samples, overlap and most samples from the Smithian group close to the Induan samples on the nMDS plot (figure 3.12A). The distinction between the Induan and Smithian samples is due to taxonomic turnover (i.e. from *Claraia* in the Induan to *Eumorphotis* in the Smithian). This is supported by the pairwise comparisons of the PERMANOVA and PERMDISP results that indicate only Spathian samples are significantly different (Figure 3.12A; Appendix 3.4).

The increased heterogeneity (i.e. sample dispersal) in the Spathian is mainly due to increased facies variation (Figure 3.12b). The dispersion of samples within individual facies, excluding deep subtidal facies, is low, showing that the composition of samples within lithofacies is homogenous. The PERMDISP results also record no significant difference in the dispersion of samples within the different facies ($p = 0.38$). The PERMANOVA shows no significant interaction in the effects of sub-stage and facies on the variability in these assemblages ($p = 0.61$), due to a low number of facies associations recognised in the Bódvaszilas Sandstone Formation. Therefore, the increased taxonomic heterogeneity recognised in the Spathian is due to increased facies heterogeneity.

The only facies that was recognised and quantitatively sampled in both the Bódvaszilas Sandstone and Szin Marl formations is the deep subtidal facies. The Szin Marl

Formation sample is significantly distinct from the other pre-Spathian samples and is characterised by a very different fauna, i.e. *Bakevellia* not *Unionites*. The pre-Spathian samples are from siliciclastic rocks, whereas, the Spathian samples are from a carbonate lithology. This suggests that even though there is a significant change in the benthic communities that occupied the deep subtidal depositional environment between pre-Spathian and Spathian times, the significant differences may be due to different lithologies.

Temporal benthic community changes within the Spathian can also be recognised. The outer ramp depositional environment of the Szin Marl Formation contains a less diverse and compositionally different fauna to that of the Szinpetri Limestone Formation (Figure 3.12). The composition of the Szin Marl, outer-ramp sample occurs within the *Eumorphotis* biofacies (Figure 3.12c) and shows greater similarity to the samples from the Bódvaszilas Sandstone Formation. The younger Szinpetri Limestone outer-ramp sample, however, shows a greater resemblance to the Szin Marl mid-ramp and oolitic shoal environments. This shows that the fauna that occupied shallower environments during deposition of the Szin Marl Formation expanded into outer-ramp environments during deposition of the Szinpetri Limestone Formation in the late Spathian.
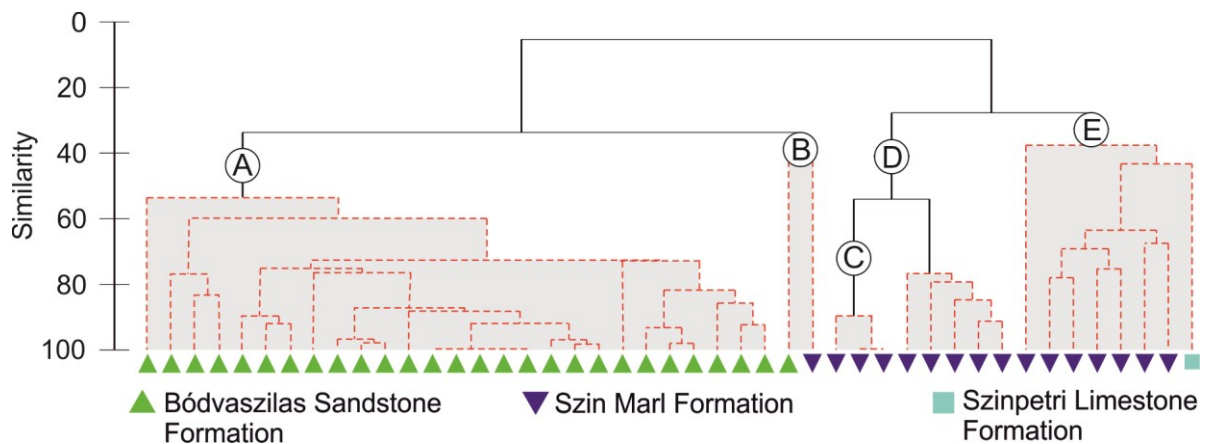
Figure 3.11: The cluster analysis together with the SIMPROF test, identified 5 groups of samples which are statistically distinct (red lines). The 5 groups have been interpreted as different benthic biofacies.
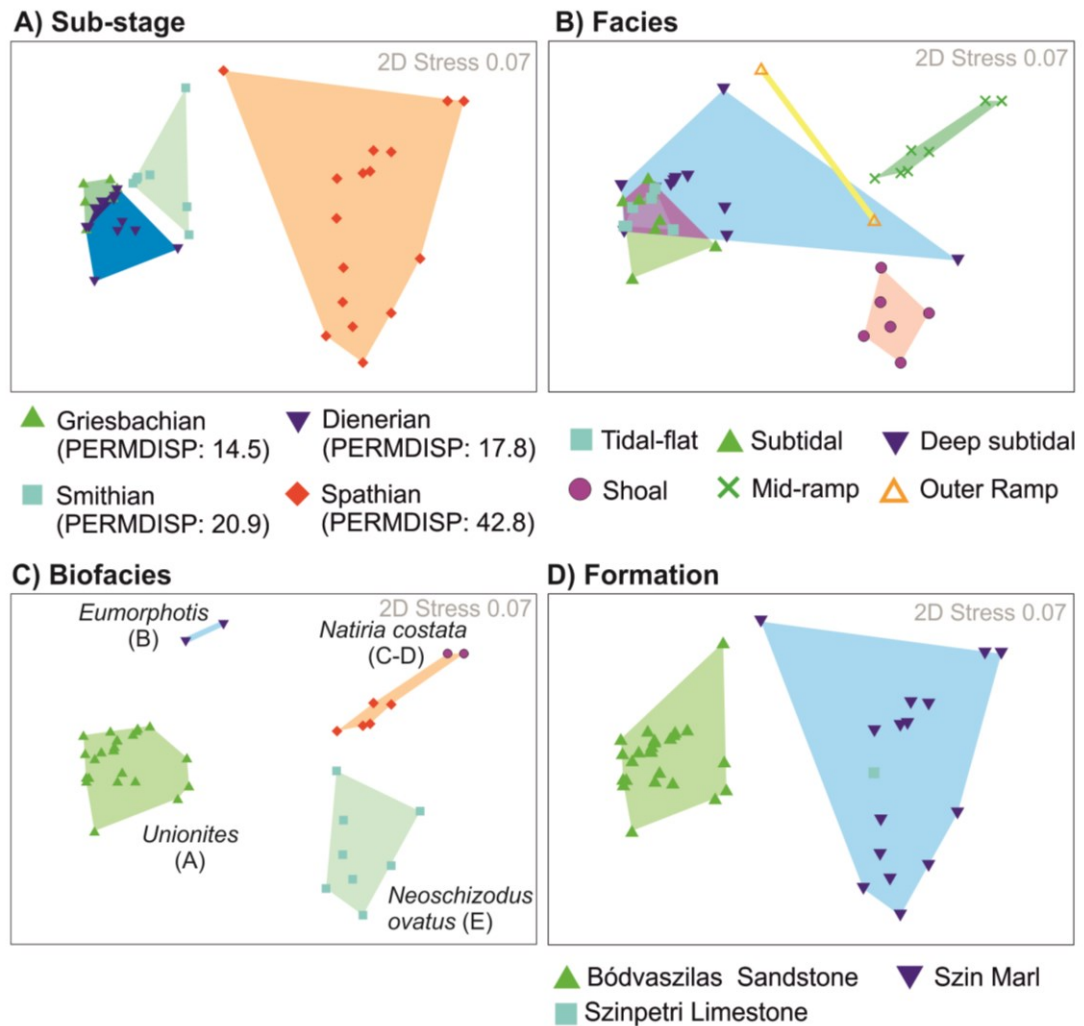
Figure 3.12: nMDS ordination of samples. A) samples are grouped according substage, B) samples are grouped according to lithofacies; C) samples are grouped according to biofacies and D) according to their formation.

3.4.3   Changes in ecological composition

Cluster analysis based on ecological composition shows two major groups, one characterised by infaunal, facultatively motile, unattached, suspension feeders and the other by epifaunal, slow-moving, grazers (Figure 3.13). Group 1 does not separate according to the sampled formation, in contrast to the taxonomic analysis. Group 2, however, is restricted to the Szin Marl Formation. Instead, the division is due to the sampled facies, where infaunal bivalves, i.e. Group 1, occur in all the facies except the mid-ramp which is dominated exclusively by slow-moving grazers, i.e. Group 2. The

SIMPROF test recognises 7 significantly different biofacies (Figure 3.13; Appendix 3.5).

The stress values for the nMDS ordination is 0.05, which gives confidence that the two dimensional plot is an accurate representation of the sample relationships (Clarke and Gorley, 2006). The samples in the nMDS plot (Figure 3.14a) group into the two clusters that were recognised in the cluster analysis, i.e. Groups 1 and 2. Although a temporal aspect to the clustering is not recognised, the Griesbachian, Dienerian and Smithian samples overlap in the nMDS plot, but the Spathian samples do not (Figure 3.14). The Spathian samples are more diverse and contain a greater number of modes of life within the samples (Figure 3.14). Therefore, even though there is no strong temporal trend, there is a temporal aspect to distribution of ecofacies. The results of the PERMANOVA show that the differences are significant (p=0.001; Appendix 3.5). The same is apparent for the disparity of samples in the nMDS plot, where the samples of the Bódvaszilas Sandstone Formation are homogenous and it is not until the Spathian Szin Marl and Szinpetri Limestone formations that heterogeneity significantly increases (PERMDISP p= 0.001, Figure 3.14).
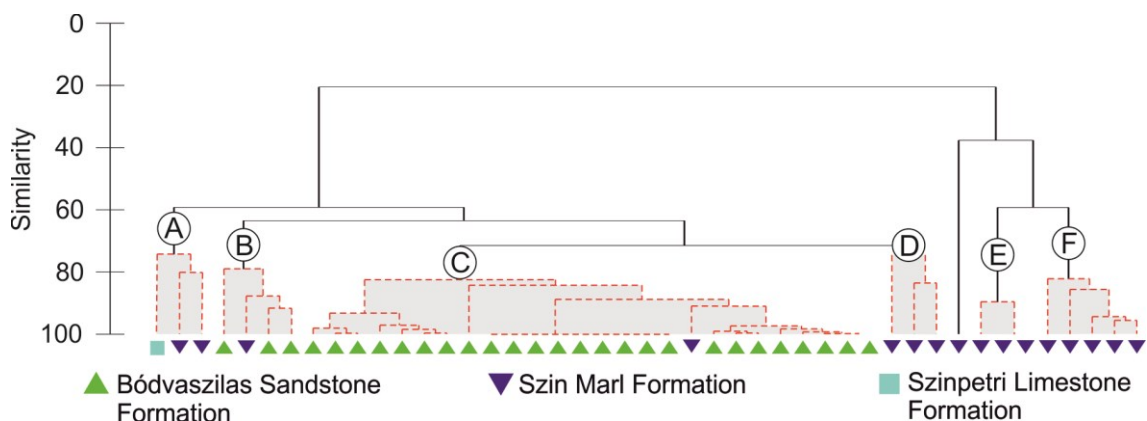
Figure 3.13: The cluster analysis performed on species labelled according to their mode of life (or functional diversity as you say below), together with the SIMPROF test, identified 6 groups of samples which are statistically distinct (red lines). The 7 groups have been interpreted as different ecofacies.
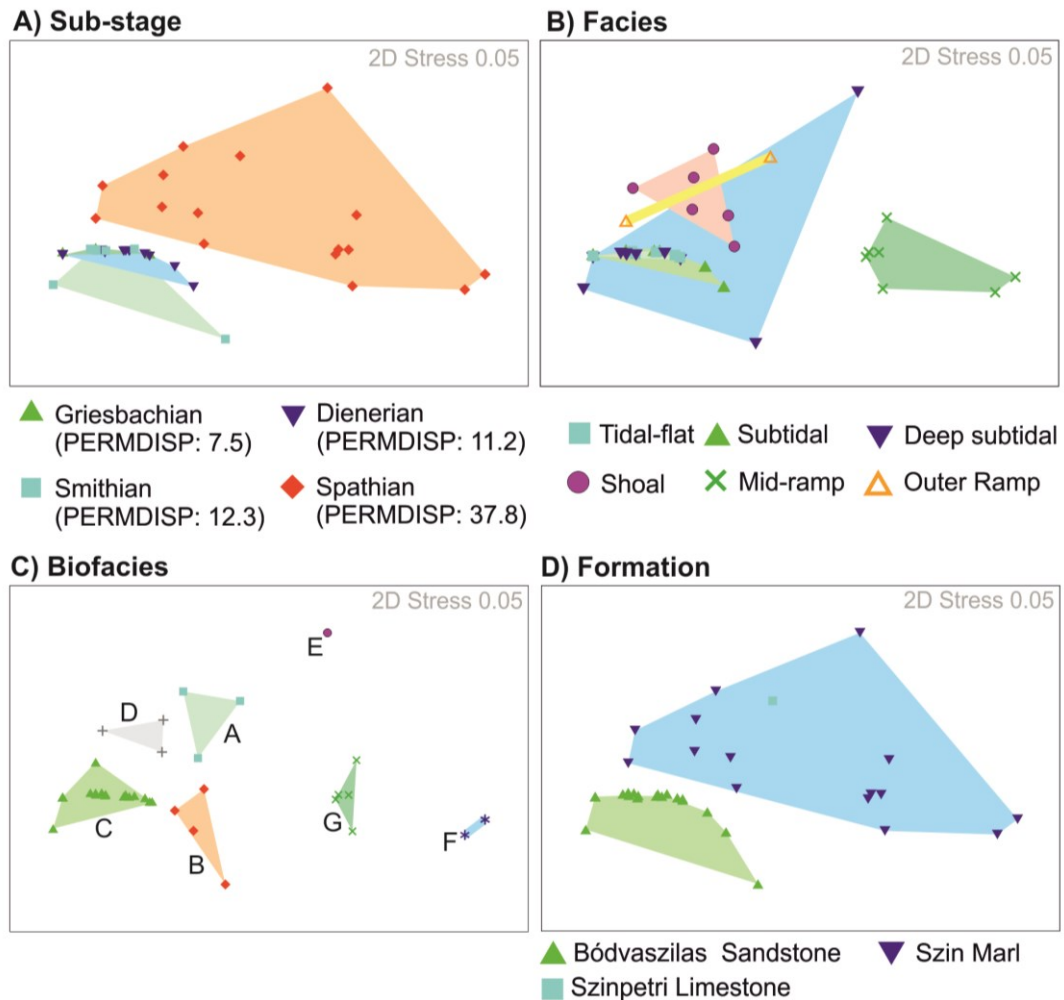
Figure 3.14: nMDS ordination for functional diversity of samples. A) samples are grouped according sub-stage, B) samples are grouped according to lithofacies, C) samples are grouped according to biofacies and D) samples grouped according to formation.

3.5   Discussion

A Delayed Recovery

Previous studies investigating the response of benthic marine communities to the late Permian extinction have shown that in the absence of anoxia advanced stages of recovery may be recorded locally by the second Triassic conodont zone, i.e. *Isarcicella isarcica* Zone, of the Griesbachian (Twitchett et al., 2004). Wave aeration of shallow marine environments is inferred to have allowed survival during the late Permian anoxic

event and subsequent recovery in habitats above wave base, at least outside the tropics (Beatty et al., 2008; Zonneveld et al., 2010). Initial deposition of the Bódvaszilas Sandstone Formation occurred during the late Griesbachian in an oxygenated inner ramp environment, as indicated by the purple colour of the sediment (Hips, 1996b), yet the benthic assemblages from these deposits have low alpha taxonomic (S = 2-4; Δ = 1-3) and ecological diversities (S =1-3; Δ =1-2).

A late Griesbachian biotic crisis has been hypothesised (Stanley, 2009), associated with a transgression and regional anoxia (Wignall and Hallam, 1993), and negative carbon and oxygen isotope excursions (Payne et al., 2004; Sun et al., 2012). A decline in conodont and ammonoid diversity supports this hypothesis (Brayard et al., 2006; Orchard, 2007; Stanley, 2009). In the Neotethys, the appearance of anoxia caused a collapse of rapidly recovering benthic ecosystems and a change from high evenness/high diversity to low evenness/low diversity skeletal assemblages that led Twitchett et al. (2004) and Jacobson et al. (2011) to infer a mid-Induan (end-Griesbachian) regional crisis related to a sea-level transgression. In the present study, however, no significant differences in the composition, ecological structure or alpha diversity of shelly benthic marine assemblages are recorded across the Griesbachian/Dienerian boundary in the Bódvaszilas Sandstone Formation. The only recorded changes to the benthic ecosystem are the first appearances of *Diplocraterion* and short, obliquely oriented (~45°) *Rhizocorallium* in the Dienerian. The appearance of these ichnotaxa, and their small size, represents a small increase in infaunal tiering and the return of domichnia consistent with early recovery (Stage 2 of Twitchett et al., 2004; Twitchett 2006).

The absence of a Late Griesbachian biotic crisis in the Aggtelek Karst indicates that it is not a global event, at least among the benthos. A critical aspect of the Hungarian record is that there is no facies change across the Griesbachian/Dienerian boundary. Localities

in Neotethys that record a Late Griesbachian benthic biotic crisis, such as Wadi Wasit in Oman (Twitchett et al., 2004), also record a major change to deeper, more oxygen-restricted facies. In these locations, the supposed "crisis" may simply reflect expected ecological change along an onshore-offshore diversity gradient and the successive sampling of shallow and then deeper-water benthic assemblages. This interpretation is supported by Hofmann et al.'s (2013b) study of the Griesbachian/Dienerian boundary of the Dinwoody Formation, USA, which found that high diversity/high evenness faunas were restricted to settings that were influenced by wave activity, i.e. the habitable zone, with low diversity/low evenness faunas in outer ramp environments.

Eutrophication, sediment fluxes and salinity fluctuations

Based on the distribution of trace fossils, Beatty et al. (2008) limited the proximal end of their habitable zone to the upper shoreface to swash zone, where high turbidity and shifting sediments suppress benthic colonisation and reduces preservation potential. Song et al. (2014), however, limited their 'refuge zone' to 'mid-waters' due to high temperatures in Early Triassic equatorial shallow waters that may have excluded benthic invertebrates due to thermal stress. Other environmental stressors in shallow marine environments likely to exclude or restrict benthic invertebrates during the Early Triassic include large salinity fluctuations (Posenato, 1985; 2008b; Nützel and Schulbert, 2005); high sedimentation (Algeo and Twitchett, 2010); eutrophication (Algeo and Twitchett, 2010); desiccation stress (Petes et al., 2007); increased ocean surface pH and $CaCO_3$ saturation (Fraiser and Bottjer, 2007b; Payne et al., 2010).

The benthic communities of the Bódvaszilas Sandstone Formation are characterised by the bivalve genera *Unionites, Eumorphotis* and *Claraia*, lingulid brachiopods and microconchids, which are frequently described as eurytopic opportunistic taxa that thrived in stressed environments in the wake of the late Permian mass extinction event (Schubert and Bottjer, 1995; Twitchett, 1999; Rodland and Bottjer, 2001; Posenato,

2008a; Hautmann et al., 2011; Fraiser, 2011; Zatoń et al., 2013; Posenato et al., 2014). The lack of unequivocally stenohaline taxa suggests that salinities were outside the normal marine range during deposition of the Bódvaszilas Sandstone Formation. One consequence of increased global temperatures is an increase in runoff and evaporation (Labat et al., 2004), which could lead to greater salinity fluctuations in nearshore environments that would increase osmoregulation stress (Verschuren et al., 2000) impeding the distribution of stenohaline animals, such as crinoids.

Increased sedimentation rates and the subsequent development of eutrophication in nearshore environments would also be a likely consequence of increased runoff (Peizhen et al. 2001). The entire thickness of the Bódvaszilas Sandstone Formation in the Aggtelek Karst is not known due to faulting and folding, but its minimum thickness is 250m (Hips, 1996b). The minimum average linear accumulation rate for the Griesbachian-Smithian interval is therefore, 187 m per myr which is comparable to the elevated sedimentation rates recognised in shelf settings elsewhere during the Early Triassic (Algeo and Twitchett, 2010). The Bódvaszilas Sandstone Formation lacks grazing taxa, and contains abundant wrinkle structures which suggest an absence of grazing activity. The lack of grazing animals may be due to frequent sediment influxes burying and killing off their food source.

Eutrophication may negatively affect grazers as it provides unfavourable conditions for macrophytes, creating a shift in the communities of primary producers to microbial mats and free floating algae (Grall and Chauvaud, 2002). On the other hand, eutrophication has been found to favour stationary suspension feeders that can tolerate seasonal hypoxia during calm water periods, as it increases the availability of food (Loo and Rosenberg, 1989; Carmichael et al. 2012). Nutrient-overloading will also favour the widespread development of algal mats in shallow marine environments (Bonsdorff et al. 1997; Pihl et al. 1999), resulting in summer hypoxia and an increased decomposition of

organic material contributing to higher amounts of CO_2 (Cai et al., 2011). In modern shelf seas, eutrophication is widely acknowledged as a major threat to marine ecosystems and can create 'dead zones' from the inner to outer shelf in excess of 20,000 square kilometres (Diaz and Rosenberg, 2008; Cai et al., 2011).

Shallow shelf settings from the Neotethys, Boreal Ocean, northeast Panthalassa and China also record evidence for an increase in total organic carbon (TOC), phosphorous and barium supporting the interpretation that primary productivity increased across the late Permian mass extinction and into the Lower Triassic (Shen et al., 2014; Wei et al., 2015). In the neighbouring Dolomites where a similar fauna to that observed in the Aggtelek Karst can be observed (Hofmann et al., 2015a), the rock records an enrichment of $\delta^{34}S$ across the late Permian mass extinction and into the Griesbachian, Dienerian and Smithian sub-stages (Horacek et al., 2010b). The $\delta^{34}S$ signature at least partly reflects phosphorous recycling, which is vital for maintaining high primary productivity (Mort et al., 2007), this would provide additional support for the increase in primary productivity across the LPE. A synergy of large salinity fluctuations, elevated sedimentation and eutrophication may therefore explain why Bódvaszilas Sandstone exhibits low diversities and communities dominated by the cosmopolitan suspension feeding bivalves *?Unionites, Claraia* and *Eumorphotis*.

Spathian recovery

Globally, the Spathian marks an advanced recovery phase for the benthos following the late Permian extinction event, with increasing diversity, re-establishment of deep and erect tiers, and evidence of increased predation (Schubert and Bottjer, 1995; Twitchett, 1999; 2006; Twitchett et al., 2004; Posenato, 2008a; Hofmann et al., 2013a; 2014; 2015a). This global pattern is reflected locally by the Spathian Szin Marl faunas, which record significantly greater richness and the re-establishment of erect and deep infaunal tiers. The taxa *Holocrinus* and cf. *Homomya* that, respectively, represent these tiers are,

however, relatively small and thus probably did not occupy the full range of available ecospace above and below the sediment-water interface as recorded in the Anisian (Hagdorn and Velledits, 2006; Figure 3.15). In addition, 'Homomya' has only been recorded in Unit C of the Szin Marl Formation suggesting that it is restricted to wave-agitated environments. Disarticulated *Holocrinus* ossicles have been identified from the mid- to outer-ramp (Hips, 1996b), but their original living habitat is hard to determine because their small size and robustness makes them easy to transport over large distances (Baumiller, 2001). Crinoid ossicles from the Szin Marl Formation are only found in storm beds suggesting that their living habitat may have been restricted to settings above wave base, i.e. the habitable zone.

The observed Spathian recovery signal is likely due, at least in part, to a greater number of facies in the Szin Marl Formation. Prior to the Spathian, only facies from stressed inner and mid-ramp environments were sampled. Inner ramp settings represented by units A and D of the Szin Marl Formation still reflect high stress, as inferred from low ichnofabric indices (Figure. 3.6), but no body fossils were recovered from these units to compare with the Bódvaszilas Sandstone Formation. The rest of the Szin Marl Formation, on the other hand, records strong habitat differentiation with different biofacies representing each sedimentary facies. This contrasts with the time-equivalent Virgin Limestone Formation from the western USA (Hofmann et al., 2013a). The most diverse assemblages are associated with oolitic shoals, and these habitats are not recorded prior to the Spathian in the Aggtelek Karst. Faunal changes in mid- and outer ramp settings from the Griesbachian to Smithian are currently unknown, and the onset of local recovery in those environments may have possibly occurred prior to the Spathian.
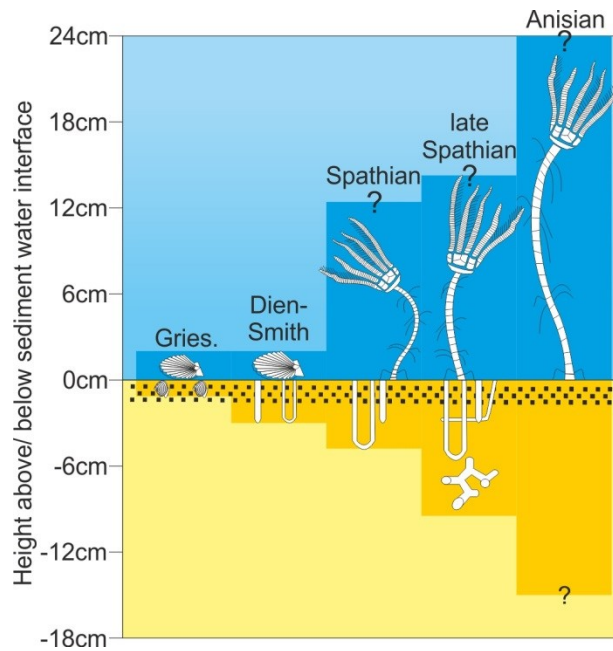
Figure 3.15: Local tiering above and below the substrate following the late Permian mass extinction in the Aggtelek Karst. Question marks refer to the uncertainty concerning the height of *Holocrinus* as no complete specimens have been found. Tiering in the Anisian from Hagdorn and Velledits (2006) and Baumiller and Hagdorn (1995) for the erect tier, and from the German Muschelkalk for the infaunal tier (Knaust 2007). Gries. = Griesbachian, Dien = Dienerian, Smith = Smithian, Spath = Spathian.

The high diversity reported in shoal and mid-ramp environments is consistent with a 'habitable zone' between the lower shoreface and offshore transition as recorded in the Sverdrup Basin, Canada (Beatty et al., 2008; Zonneveld et al., 2010) and in the Virgin Limestone Formation, western USA (Mata and Bottjer, 2011). Deposits distal to this habitable zone are characterised by low taxonomic and ecological diversities in the USA and Canada. Benthic faunas in Aggtelek do not appear in the settings below wave base until the late Spathian, and are characterised by low alpha diversities.

Late Spathian recovery pulse

Only a single sample was recovered from the late Spathian Szinpetri Limestone Formation, yet this sample had the highest alpha diversity values of all studied samples.

Compared to the outer ramp sample from Unit F of the Szin Marl Formation from the same facies, this sample records higher alpha diversity, both taxonomically and ecologically, and includes skeletal groups associated with advanced recovery, i.e. crinoids. Bioturbation intensity rises to levels (ii4-5) not recorded elsewhere in the Aggtelek Lower Triassic succession, and the occurrences of *Thalassinoides* and *Rhizocorallium*, which represent crustacean activity, indicate advanced recovery (cf. Twitchett and Barras, 2004; Twitchett 2006). Advanced recovery in the late Spathian has also been observed globally with increased burrow sizes in northern Italy (Twitchett and Wignall, 1996; Twitchett 2007), south China (Chen et al., 2011) and Svalbard (Worsley and Mørk, 2001); increased burrow depths (Twitchett 1999); intense bioturbation in northern Italy (Twitchett and Wignall, 1996; Twitchett and Barras, 2004) and the Bükk Mountains, Hungary (Hips and Pelican, 2002); conifer-dominated forests on land (Looy et al., 1999); the establishment of reefs on the Great bank of Guizhou, China (Payne et al., 2006b), *Placunopsis* bioherms in western USA (Pruss et al., 2007).

Globally, these advances in ecological recovery in the late Spathian coincide with a decline in temperature or a change from low to normal salinity (Sun et al., 2012; Romano et al., 2012), the subsequent re-establishment of strong latitudinal temperature gradients (Brayard et al., 2006) and oxic conditions in the outer ramp (Grasby et al., 2013), related to improved ocean circulation. This would have led to a retreat of the oxygen minimum zone and expansion of the habitable zone into the outer shelf environment. The fossil assemblages of the Szinpetri Limestone have a similar structure to those of the oolitic shoal and mid-ramp settings of the underlying Szin Marl Formation (Figure 3.12), and have faunal elements (i.e. *Costatoria costata*) in common with the outer ramp setting of the Szin Marl Formation. This suggests that the benthic fauna from shallower settings rapidly recolonised the outer ramp environment once it

became better oxygenated, and supports the hypothesis that rapid refilling of vacated seafloor by surviving taxa occurred before novel functional morphologies could evolve (Erwin et al., 1987). The recovery of benthic invertebrates recorded in this study area is limited mostly to molluscs and crinoids during the Early Triassic, and recovery of other groups, (i.e. sponges, corals, echinoids and brachiopods) is not recorded locally until the Anisian (Hips, 2007; Velledits et al., 2011).

4. Dolomites, Italy

4.1 Stratigraphy

Detailed investigations of the stratigraphy of the Werfen Formation were published by Neri and Posenato (1985), Broglio Loriga et al. (1983; 1986; 1990), Posenato (1992), Scholger et al. (2000), Perri (1991), Perri and Farabegoli (2003), Horacek et al. (2007a) and Posenato (2008b), Figure 4.1. Here, new key finds of macrofauna and a novel carbon isotope curve for the Spathian (Figure 4.1-4.3) are incorporated to resolve better sub-stage boundaries in the Werfen Formation.

Late Permian mass extinction and the Permian/Triassic boundary

The base of the Triassic is defined by the Global Stratotype Section and Point (GSSP) in Meishan, China, with the first occurrence of the conodont *Hindeodus parvus*, i.e. the base of bed 27c of Meishan section D (Yin et al., 2001). Three sections investigated in this study span the Permian/Triassic boundary: the l'Uomo, Tesero and Siusi sections. Conodonts in the Tesero Member are rare and so the range of *H. parvus* is poorly constrained in the Dolomites (Posenato, 2008b). In the Tesero section, *H. parvus* occurs 11m above the base of Werfen Formation (Nicora and Perri, 1999). This position for the Permian/Triassic boundary has been described as anomalously high and the occurrence of *H. parvus* as "stratigraphically perched" due to unfavourable conditions (Nicora and Perri, 1999; Perri and Farabegoli, 2003). This is supported by the occurrence of the conodont *Isarcicella changxingensis* which is described as having a short stratigraphic range spanning the Permian/Triassic boundary in South China (Wang, 1995; Kozur 1996). *I. changxingensis* occurs 1.3m above the base of the Werfen Formation and has been used by previous authors, e.g. Groves et al. (2007), to define the P/Tr boundary at the Tesero section (Figure 4.2). At the Siusi section, *H. parvus* first occurs 1.45m above the base of the Werfen Formation (Horacek et al., 2010a; Figure 4.2). At the nearby, slightly diachronous, Bulla section (i.e. Kraus et al., 2009) *H. parvus* first occurs 1.3m

above the base of the Werfen Formation (Perri and Farabegoli, 2003). At l'Uomo, however, conodonts have not been investigated.

In the absence of conodonts, the carbon isotope record has been used to infer the position of the Permian/Triassic boundary (e.g. Korte and Kozur, 2010). At Meishan, a carbon isotope minimum occurs 10cm below the FAD of *H. parvus* (Shen et al., 2011) and at the Bulla section the first negative isotope excursion from +4‰ to +1‰ (Horacek et al., 2007a; Korte and Kozur 2005) occurs 50cm below the FAD of *H. parvus* (Farabegoli et al., 2007). The carbon isotope profiles then rise briefly to ~1.5‰ coincident with the FAD of *H. parvus* at the Siusi and Bulla sections (Figure 4.2; Korte and Kozur, 2005) before reaching a minimum, -2.5‰, in the lower part of the Mazzin Member (Horacek et al., 2007a; Kraus et al., 2009). The unpublished isotope curve from l'Uomo (R.J. Twitchett and G.D. Price) indicates that the P/Tr boundary occurs ~2m above the base of the Werfen Formation (Figure 4.2). The carbon isotope curve from the Tesero section (Magaritz et al., 1988; Groves et al., 2007) supports the interpretation of Nicora and Perri (1999) that the conodont *I. changxingensis* may represent the Permian/Triassic boundary at ~1.5m into the Werfen Formation.

The late Permian mass extinction occurs below the Permian/Triassic boundary. In the Dolomites it has been identified by foraminifera, algae and brachiopods and occurs within the basal beds of the Tesero Member (Assereto et al., 1973; Broglio Loriga et al., 1988; Farabegoli et al., 2007; Groves et al., 2007; Posenato, 2010). Farabegoli et al. (2007) and Farabegoli and Perri (2012) have inferred three separate extinction events from the late Changhsingian into the Triassic *H. parvus* conodont Zone, similar to the extinction interval recognised at Meishan (Shen et al., 2011). This extended extinction interval corresponds to the first ~2m of the Tesero Member at the Bulla and Siusi sections and occurs ~3.5m above the base of the Tesero Member at the Tesero section (Farabegoli et al., 2007; Farabegoli and Perri, 2012). Based on the confidence intervals
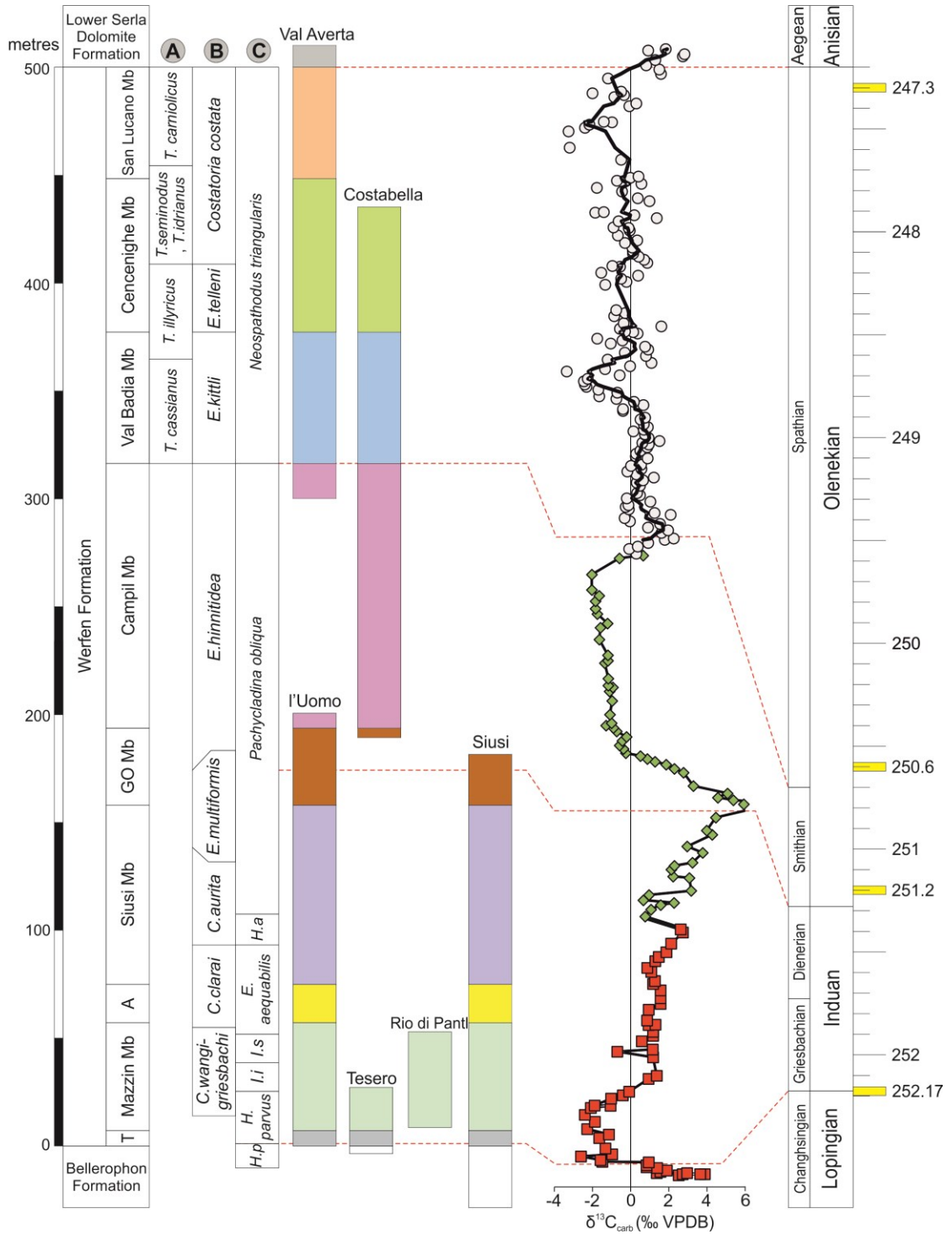
Figure 4.1: Stratigraphic framework for the Dolomites. Lithostratigraphy and relative thicknesses after Posenato (2008b). A: Ammonoid biozones after Posenato (1992). B: Bivalve biozones after Broglio Loriga et al. (1990). C: Conodont biozones after Perri and Farabegoli (2003): *H.p – Hindeodus praeparvus*, *I.i – Isarcicella isarcica*, *I.s – Isarcicella staeschei*, *H.a – Hadrodontina anceps*. Chemostratigraphy: from Bulla section (red squares) and, l'Uomo section (green diamonds; Horacek et al., 2007a) and Val Averta section (grey circles; this study). Radiometric ages (yellow bars) from Shen et al. (2011), Ovtcharova et al. (2006), Lehrmann et al. (2006b) and Galfetti et al. (2007b). Colours in the sections highlight the different lithostratigraphical units.

of foraminiferal ranges from the Bulla and Tesero section, however, Groves et al. (2007) inferred a single extinction event ~1-1.5m into the Tesero Member (Figure 4.2). At the l'Uomo section, Permian algae and foraminifera are only known from the basal oolitic bed (Broglio Loriga et al. 1986b), below the $\delta^{13}C$ excursion, and may indicate the late Permian mass extinction (Figure 4.2).
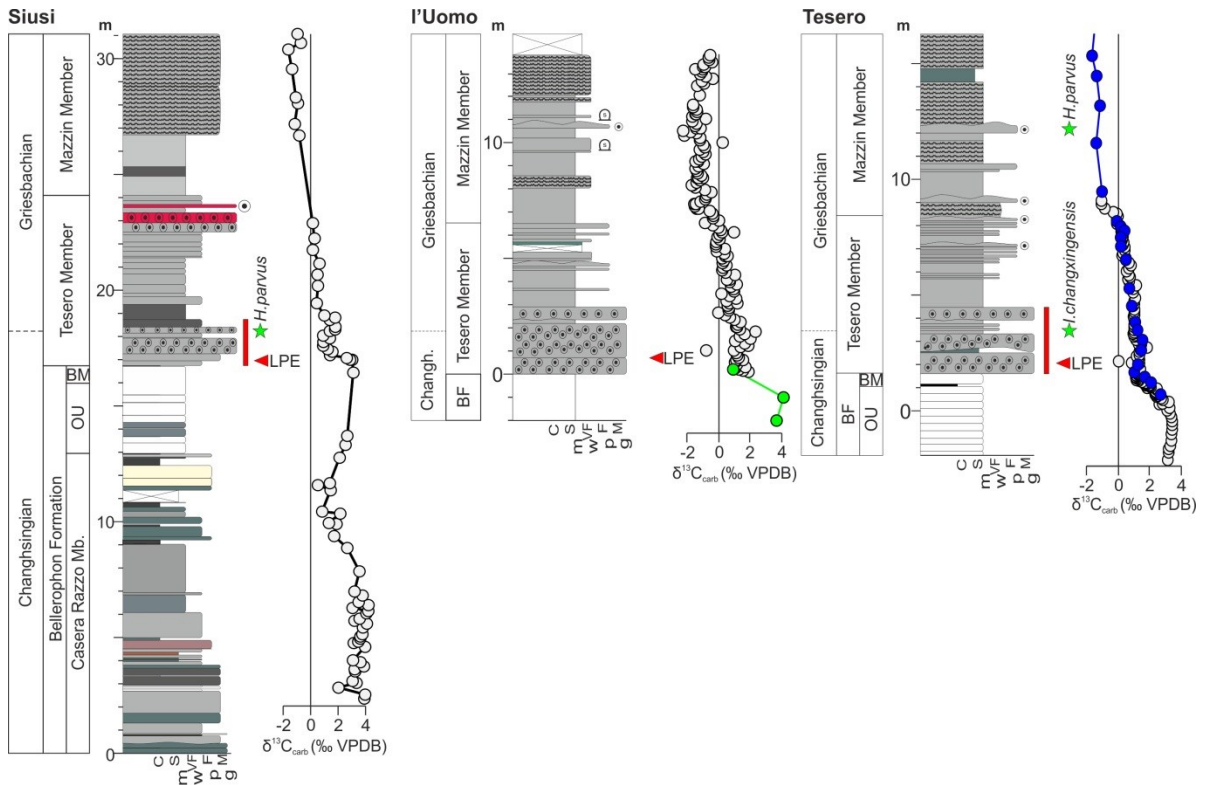
Figure 4.2: The Permian-Triassic transition in the studied sections of the Dolomites. Siusi section: the LPE from Groves et al. (2007); extinction interval (red bar) inferred from the nearby Bulla section (Farabegoli et al., 2007); carbon isotopes from Kraus et al. (2009) and Siegert et al. (2011); the FAD of *Hindeodus parvus* after Horacek et al. (2010a). l'Uomo section: LPE the last occurrences of Permian foraminifera and algae (Broglio Loriga et al., 1986); carbon isotope profile is unpublished data from R.J. Twitchett and G.D Price (grey circles); carbon isotopes after Horacek et al. (2007a) (green circles). Tesero section: LPE and carbon isotopes (grey circles) after Groves et al. (2007); carbon isotopes (blue circles) after Korte and Kozur (2005); extinction interval after Farabegoli and Perri, (2012); conodont FADs after Perri and Farabegoli (2003). LPE = late Permian mass extinction event. Changh = Changhsingian. BF = Bellerophon Formation. BM = Bulla Member. OU = Ostracod Unit. For key see Figure 4.4.

Griesbachian/Dienerian boundary

The FAD of the bivalve *Claraia aurita* sensu stricto is used by Posenato, (2008b) to indicate the base of Dienerian. *Claraia aurita* sensu stricto is correlated with the Dienerian *Gyronites* Ammonoid Zone (Nakazawa, 1977) and first appears locally in Unit C of the Siusi Member (Broglio Loriga et al., 1990). *C. aurita* sensu lato is also recorded from the Mazzin Member, but these specimens are considered to represent a separate subspecies (see Chapter 3). The FAD of the conodont *Hadrodontina anceps* has also been used to indicate the base of the Dienerian (Algeo et al., 2007), which also occurs at the base of Unit C of the Siusi Member (Perri, 1991). In terms of magnetostratigraphy, the *H. anceps* zone in the Dolomites corresponds to a period of normal polarity (Schloger et al., 2000; Hounslow et al. 2008a). In Iran, the Griesbachian/Dienerian boundary is defined by the FAD of the ammonoid *Proptychites* and the conodont *Neospathodus dieneri* (Gallet et al., 2000), and also occurs within a normal polarity zone (Hounslow et al., 2008a). Therefore, based on the FADs of *C. aurita* s.s and *H. anceps* the Griesbachian/Dienerian boundary in this study is placed at the lithological boundary between Units B and C of the Siusi Member.

Induan/Olenekian boundary

In the proposed type sections of the Induan/Olenekian boundary in the Tethyan realm, the first appearances of the conodont *Neospathodus waageni* and the ammonoids *Flemingites* and *Euflemingites* mark the base of the Smithian (Tong et al., 2003; Orchard, 2007). None of these taxa have been recognised from the Dolomites. The carbon isotope record has been described as recording a peak of +6‰ and +8‰ near the Induan/Olenekian boundary (Payne et al., 2004; Meyer et al., 2011; Burgess et al., 2014). The first appearance of *Ns. waageni* in the Guandao section described by Payne et al. (2004), however, occurs during the negative isotope excursion that follows this
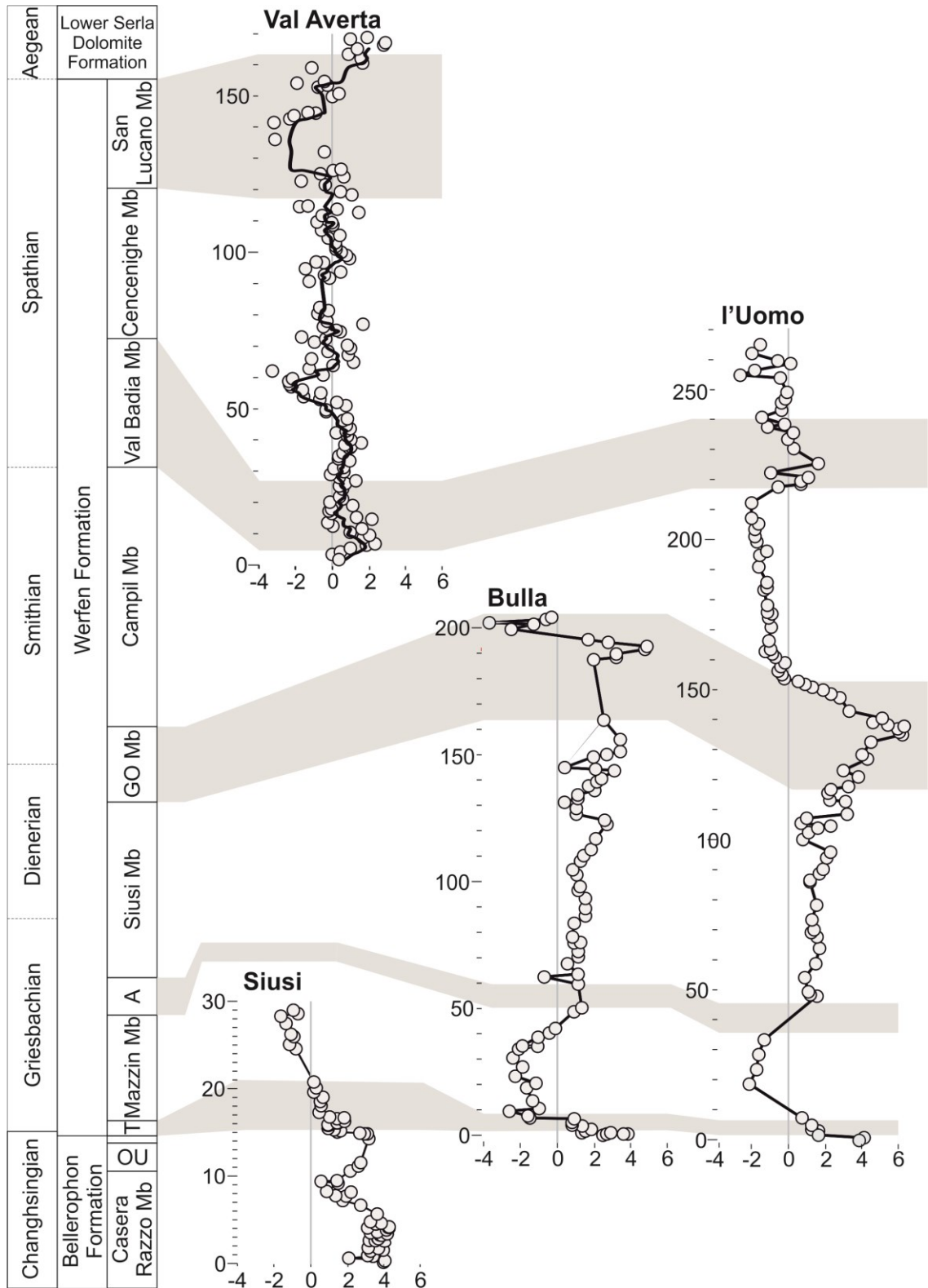
Figure 4.3: Carbon isotope profiles for the Werfen Formation, Dolomites. Lithostratigraphical correlations are shown by shaded bars. Carbon isotope profile of the Siusi section after Kraus et al. (2009) and Siegert et al. (2011). Carbon isotope profiles of the l'Uomo and Bulla sections after Horacek et al. (2007a). The Val Averta carbon isotope profile (this study) with a 5-point moving average line to reduce noise. T = Tesero Member, A = Andraz Member, LSD = Lower Serla Dolomite Formation.

positive isotope peak. The same is recorded in Neotethys (Richoz, 2006). At the Jiarong and Zuodeng sections, China, however, the positive isotope peak occurs with the FAD of *Ns. waageni* (Sun et al., 2012). Based on an extensive review of the chemostratigraphic and biostratigraphic data, Posenato (2008b) placed the Induan/Olenekian boundary above the supratidal unit in the lower part of the Gastropod Oolite Member (previously included in the Siusi Member) associated with the carbon isotope peak. This study follows Posenato (2008b) and the I/O boundary is placed at the boundary between Units A and B of the Gastropod Oolite Member.

Smithian/Spathian boundary

Locally, the base of the Spathian is defined by the FAD of the ammonoid *Tirolites cassianus* which occurs at the base of the Val Badia Member (Krystyn, 1974; Broglio Loriga et al., 1990). The base of the Spathian is also marked by a positive isotope peak of +1‰ (Payne et al., 2004; Galfetti et al., 2007c). Horacek et al. (2007a) identified the isotope peak just above the supratidal facies between the Campil and Val Badia Members at the l'Uomo section. The novel carbon isotope data from this study section also record a peak above the supratidal unit at the top of the Campil Member at the Val Averta (Figure 4.3). In this study the Smithian/Spathian boundary is therefore placed at the Campil/Val Badia Member boundary.

Lower/Middle Triassic boundary

The Lower/Middle Triassic boundary has been placed by many authors around the Werfen/ Lower Serla Dolomite formational boundary (e.g. Neri and Posenato, 1985; De Zanche and Farabegoli, 1982; Broglio Loriga et al., 1990; Posenato, 1992; Posenato, 2008b). The Lower Serla Dolomite and San Lucano Member, however, lack age-diagnostic fossils and therefore a precise biostratigraphic correlation cannot be made. At the Spathian/Aegean boundary in China, carbon isotope values rise from +2‰ in the

mid-Spathian to +4‰ within the Aegean (Payne et al., 2004; Sun et al., 2012). The new carbon isotope profile from Val Averta shows a comparable increase in carbon isotope values of ~2-3‰ across the Werfen/Lower Serla Dolomite boundary (Figure 4.3), confirming previous interpretations that the formation boundary correlates with the Lower/Middle Triassic boundary.

4.2 Facies analysis

4.2.1 Werfen Formation

Detailed descriptions of the sedimentology and shelf evolution of the Werfen Formation are given by Broglio Loriga et al. (1983; 1986; 1990). Collectively, sections of the Werfen Formation represent a broad range of environments between and within members from outer shelf to supratidal environments, on a storm-influenced shelf in the western Palaeotethys. Here, seven facies from the supratidal zone to outer shelf were recognised in the investigated sections (Table 4.1; Figure 4.4-4.10).

Facies 1: Tepee-structured siltstones (supratidal).

Description: This is characterised by light red laminated siltstones frequently containing tepee structures (Figure 4.10). In the Andraz Member at the Siusi section a 4cm thick conglomerate bed intercalates with the tepee-structured silts. This conglomerate contains white, silty, angular clasts (up to 2cm) that are laminated. The clasts are supported within a brown silty matrix and are poorly sorted.

This facies is observed in the Andraz Member, Unit B of the Cencenighe and in the San Lucano Member.

Interpretation: Tepee structures form when deposits are subaerially exposed and are commonly found in tidal-flat carbonates (Wright and Burchette, 1996). The terrigenous grains were deposited in an oxidised state as indicated by the red colour of the sediments. The colour of the rocks likely comes from ferric iron which only forms in

oxidising conditions and is frequently present within sediments of semi-arid environments (Tucker, 2001). Broglio Loriga et al. (1983) have also identified mudcracks within some laminated siltstones. Facies 1, therefore, is interpreted to have formed in a tidal-flat with prevailing supratidal conditions. This follows previous interpretations (Broglio Loriga et al., 1983; 1990). The conglomerate bed from the Andraz Member is interpreted to have been deposited following inundation during a major storm event, i.e. hurricane.

Facies 2: Wavy, flaser and lenticular bedded siltstones and sandstones (peritidal).

Description: Laminated red siltstones that are occasionally bioturbated (ii2-3) by small stuffed burrows, *Planolites* and *Skolithos*. The siltstones are interbedded with thin red, yellow, brown and blue fine-grained, wavy and flaser-bedded sandstones. The thin sandstone beds of this facies are interbedded with facies 5. Occasionally thin (1-4cm) vuggy sandy dolomite beds with erosive bases, herringbone cross-bedding and convex-up bivalves also intercalate. The bedding surfaces of these sandstones often have wrinkle marks.

This facies is observed in Unit A of the Gastropod Oolite Member, Units B and C of the Cencenighe Member and in the San Lucano Member.

Interpretation: The bedded dolomitic sandstones were deposited in a peritidal sand-flat setting with the dolomite produced through evaporitic pumping in an arid/ semi-arid climate (Haas et al., 2012). Flaser, wavy and lenticular bedding represent deposition on a tidal-flat where there are fluctuations in sediment supply or wave activity (Flemming, 2012). The cross-laminated sands in the lenticular and wavy-bedded sands indicate that these are most likely low-energy tidal current deposits and mud drapes accumulate on the forsets and bottom sets during the slack water periods that follow (Komatsu et al., 2014). The presence of herringbone cross-bedding in the sandstones also provides

Table 4.1: Summary of sedimentary facies of the Werfen Formation, Dolomites.

Facies	Lithology	Sedimentary structures and fossils	Depositional Environment
1	Red siltstones	Tepee structures.	Supratidal
2	Red and bluish grey siltstones alternating with varicoloured sandstones.	Siltstones: laminated, bioturbated (ii2) by small stuffed burrows, *Skolithos* and *Planolites* Sandstones: wavy and flaser bedding.	Peritidal
3.1	Red and brown sandstones alternating with grey red siltstones, interbedded by grey packstones.	Siltstones: laminated or bioturbated (ii2-3) by *Diplocraterion, Planolites* and *Skolithos* Sandstones: cross-stratification, load structures and ripples.	Shallow subtidal, inner shelf
3.2	Grey wackestones interbedded by grey siltstones.	Siltstones: bioturbated (ii3-5) by *Skolithos, Planolites, Diplocraterion* and *Rhizocorallium*. Wackestones: randomly orientated fauna and ripples.	Shallow subtidal, inner shelf
3.3	Red siltstones interbedded by fine sandstones.	Siltstones: alternations of laminations with wrinkle marks and bioturbated (ii2-4) by *Rhizocorallium, Skolithos, Planolites*,	Shallow subtidal, inner shelf
3.4	Green siltstones interbedded with grainstones.	Siltstones: planar-laminated Grainstones: contains ooids, crinoids and convex-up bivalves.	Shallow subtidal, intershoal areas, inner ramp
4.1	Grey oolitic limestones separated by thin green marls.	Packstones and grainstones contain ooids, algae, foraminifera, gastropods, microconchids, bivalves and brachiopods.	Oolitic shoal
4.2	Purple oolitic grainstones.	Thick beds (19-206cm) with hummocky tops. Contains ooids and randomly orientated fauna: bivalves, crinoids ossicles, microconchids and bivalves. Gastropod chambers filled with smaller gastropods or ooids. Bivalves are recrystallised with thick black shells.	Oolitic shoal
4.3	Brown oolitic grainstones.	Thick beds (up to 200cm). Contains ooids and randomly orientated fauna: bivalves, ophiuroids, microconchids and rare crinoids.	Oolitic shoal

5.1	Grey oolitic pack- and grainstones.	5-20cm beds with hummocky tops and erosive bases. Contains: ooids with the nuclei replaced by rhomboidal dolomite, gastropods, shell fragments and convex-up bivalves.	Oolitic shoal storm sheets
5.2	Red-pink oolitic pack- and grainstones	10-63cm beds with hummocky tops and graded in the upper few centimetres. Contains ooids, flat pebbles, randomly orientated fauna including bivalves, microconchids, ostracods and shelly fragments. Gastropod chambers filled with smaller gastropods or ooids.	Oolitic shoal storm sheets
5.3	Brown oolitic pack- and grainstones and fine grained red sandstones.	Contains: ooids, flat pebbles, randomly orientated bivalves.	Oolitic shoal storm sheets
6.1	Grey silty mudstones interbedded by packstones.	Mudstones: Bioturbated (ii2) in the Mazzin Member by *Planolites* Bioturbated (ii2) in the lower Siusi Member by *Thalassinoides, Lockeia, Diplocraterion, Catenichnus* and *Planolites* . Wrinkle marks on bedding planes. Packstones: randomly orientated bivalves, microconchids, ostracods, lingulids, gastropods and ophiuroids.	Mid-shelf with storm sheets
6.2	Grey silty mudstones interbedded by packstones.	Mudstones: Bioturbated (ii3-5) by *Thalassinoides* and *Planolites* . Packstones: randomly orientated bivalves, microconchids, ostracods, lingulids, gastropods and ophiuroids	Mid-shelf with storm sheets
6.3	Brown and grey siltstones alternating with red packstones	Siltstones: laminated, convex-up bivalves, wrinkle marks and load structures. Packstones: rippled tops and gutter casts at their bases. Contains ooids, gastropods and randomly orientated bivalves.	Mid-shelf with storm sheets
6.4	Grey siltstones interbedded with packstones	Siltstones: laminated or weak bioturbation (ii2) by *Skolithos* and *Planolites* . Load structures. Gastropods and convex-up bivalves. Packstones: flat pebbles, ophiuroid ossicles, randomly orientated bivalves.	Mid-shelf with storm sheets
7	Dark grey carbonate mudstones	Stylolaminated or stylonodular bedding, erosive bases, randomly orientated bivalves.	Outer ramp 'debris flows'

Figure 4.4: Stratigraphic section, position of samples (arrows) and ichnofabric indices (ii) at the Siusi section. Lithostratigraphy follows Posenato (2008b) and Mette and Roozbahani (2012). The occurrence of *H. parvus* (after Horacek et al., 2010) marks the Permian/Triassic boundary. LPE = late Permian extinction. The position of the late Permian mass extinction is interpreted from the nearby Bulla section after Groves et al. (2007). OU – Ostracod Unit. BM = Bulla Member. Colour in the lithology column refers to the rock colour observed in the field.

Figure 4.4. continued.

Figure 4.5: Stratigraphic section, position of samples (arrows) and ichnofabric indices (ii) at the Tesero section. Lithostratigraphy after Posenato (2008b). BF = Bellerophon Formation. OU = Ostracod Unit. B = Bulla Member. For key see Figure 4.4.
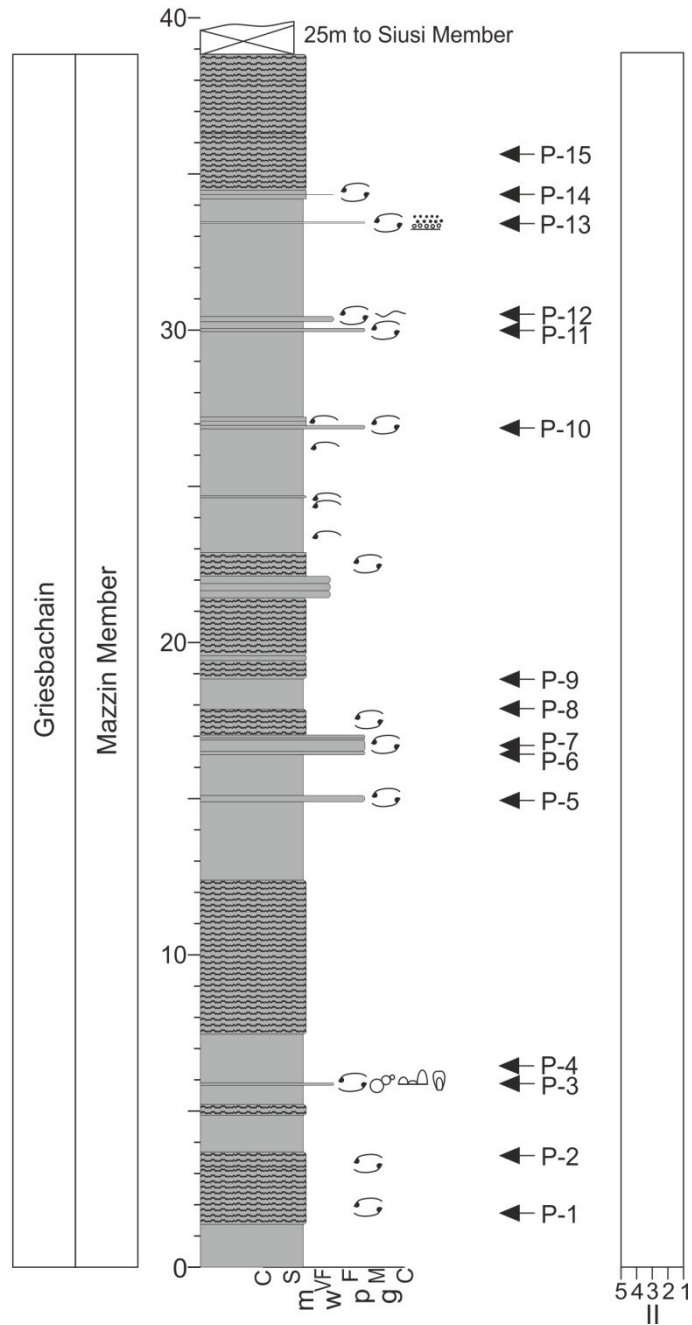
Figure 4.6: Stratigraphic section, position of samples (arrows) and ichnofabric indices (ii) at the Rio di Pantl section. Lithostratigraphy after Posenato (2008b). For key see Figure 4.4.
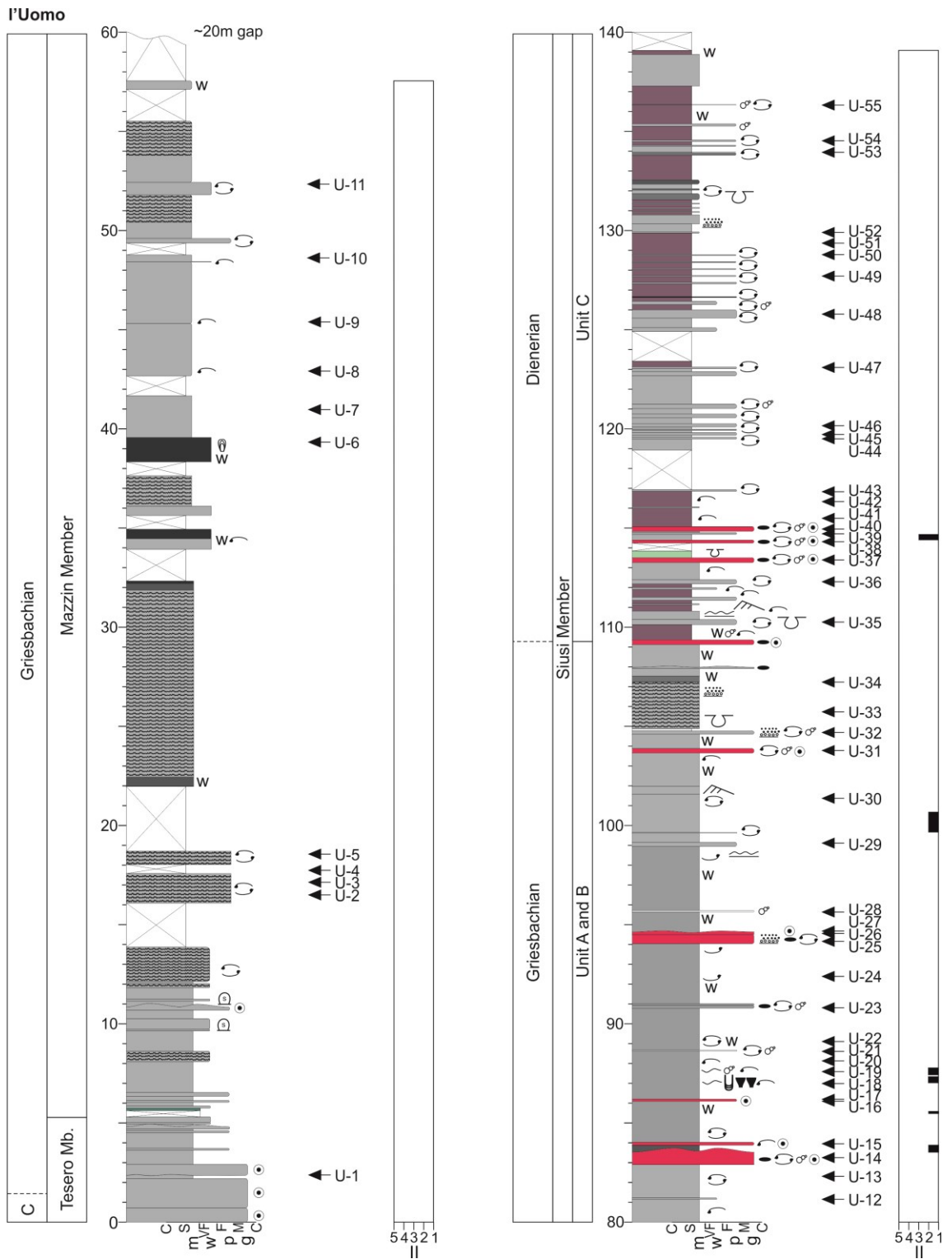
Figure 4.7: Stratigraphic section, position of samples (arrows) and ichnofabric indices (II) at the l'Uomo section. Lithostratigraphy after Posenato (2008b). For key see Figure 4.4.
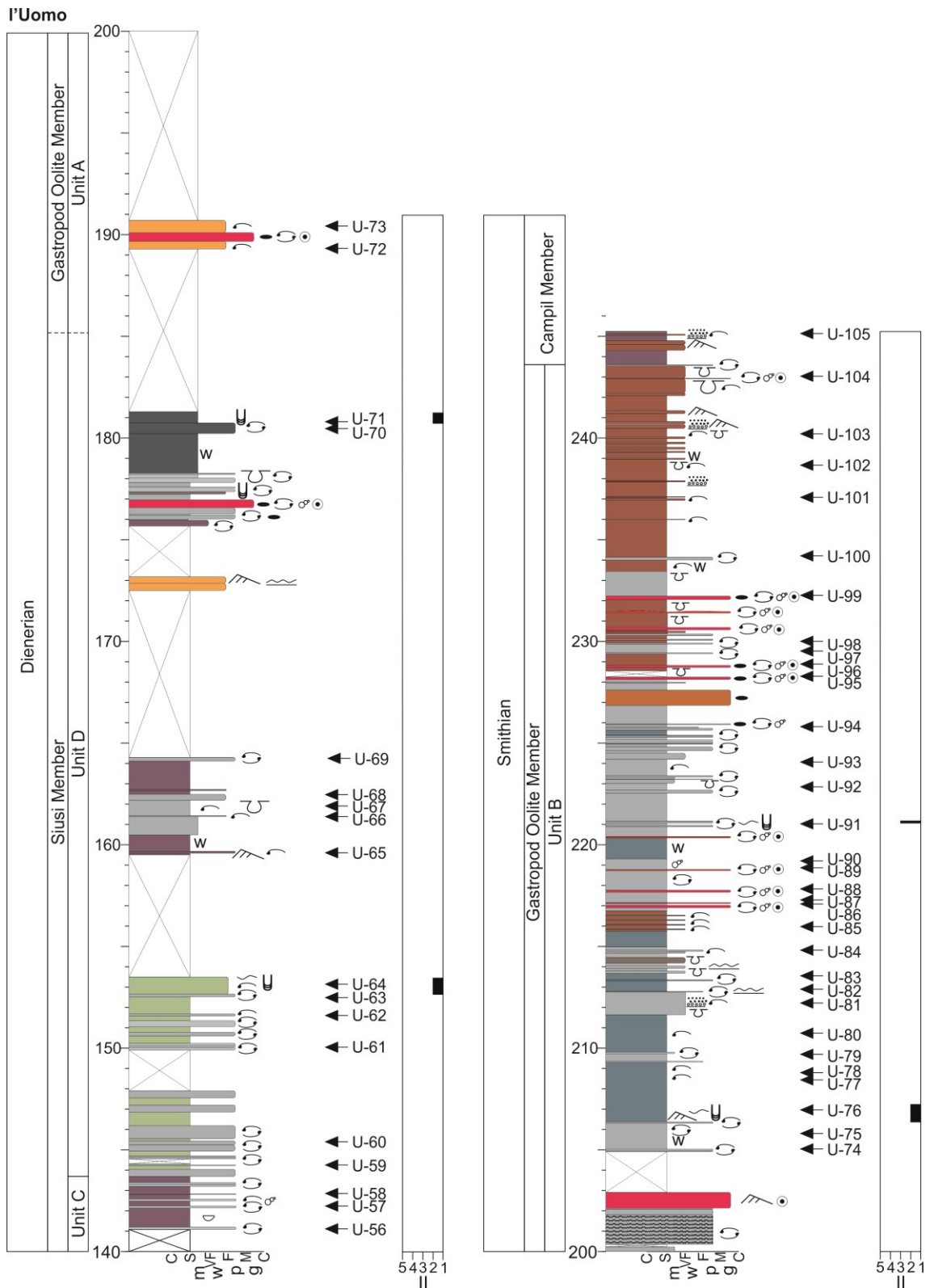
Figure 4.7 continued.
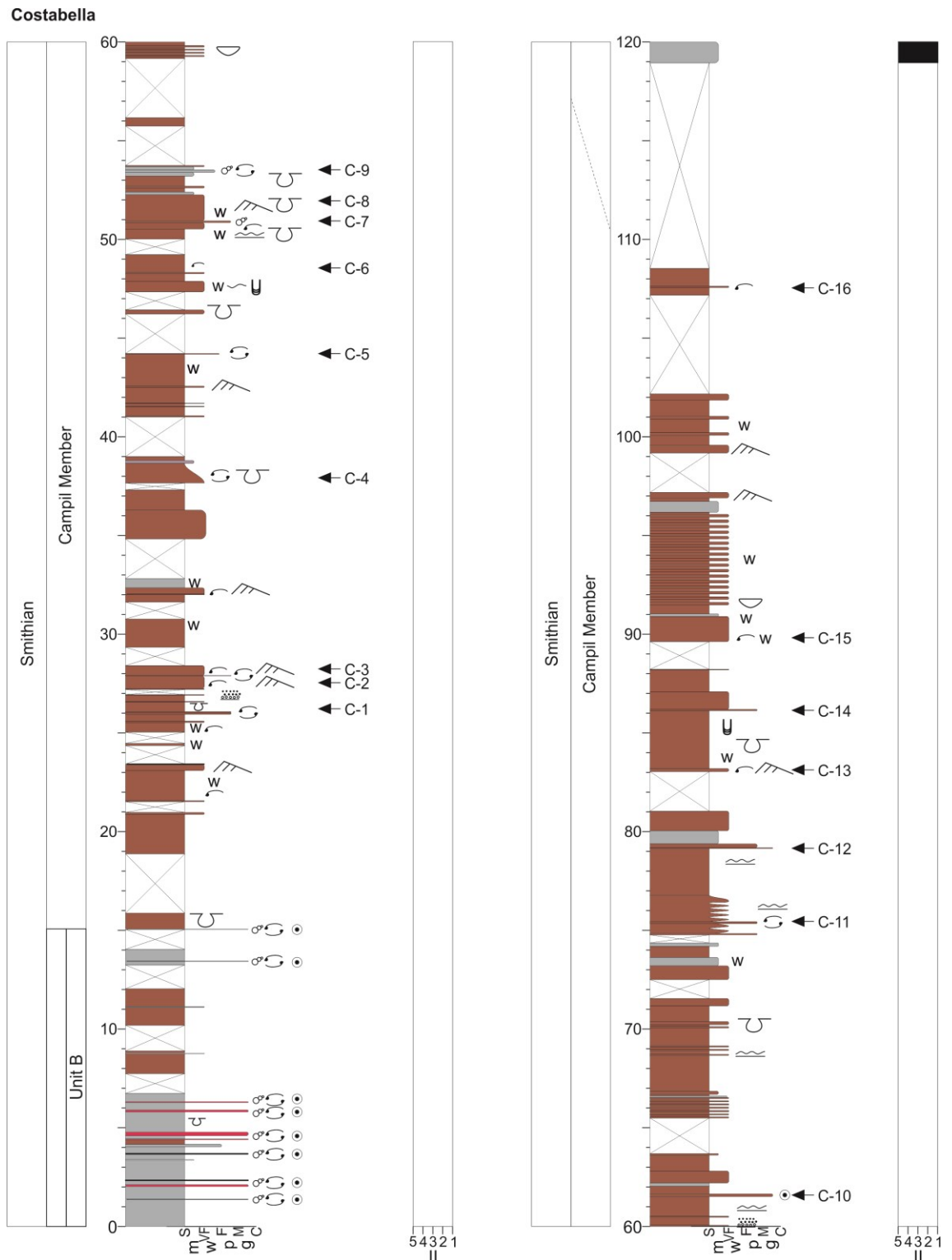
Figure 4.8: Stratigraphic section, position of samples (arrows) and ichnofabric indices (II) at the Costabella section. Lithostratigraphy after Posenato (2008b). For key see Figure 4.4.
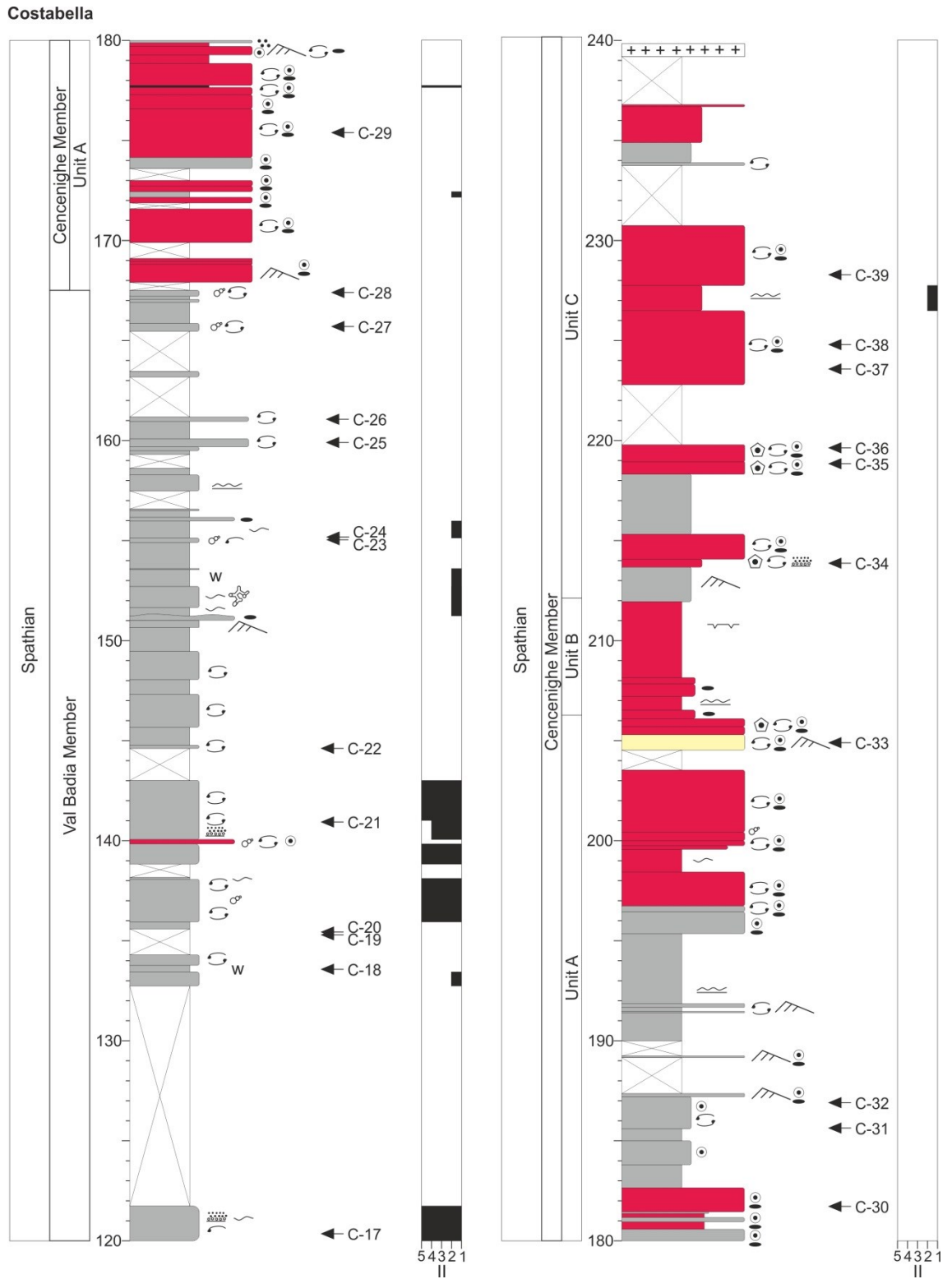
Figure 4.8 continued.
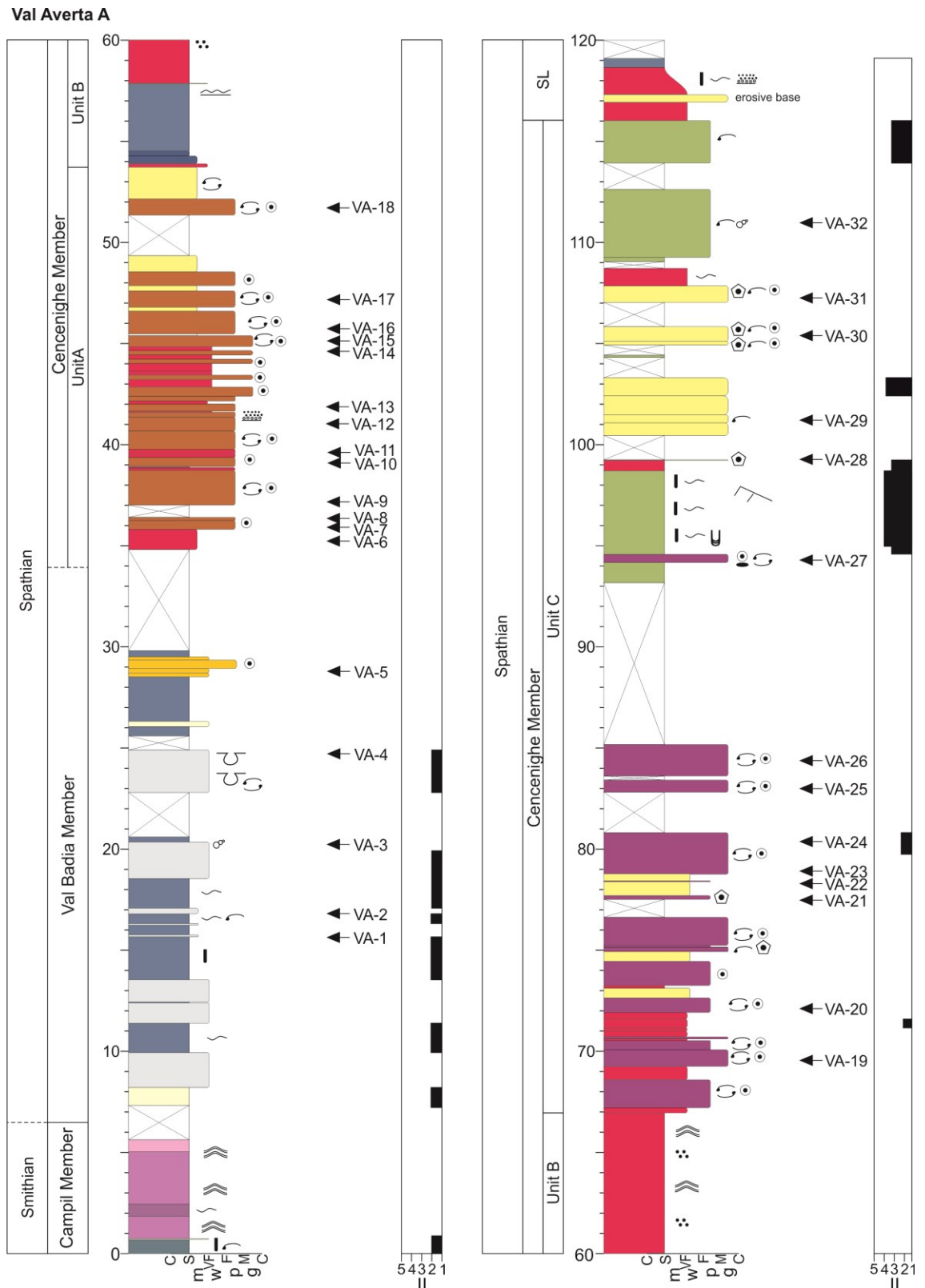
Figure 4.9: Stratigraphic section, position of samples (arrows) and ichnofabric indices (II) at the Val Averta section. Lithostratigraphy after Posenato (2008b). For key see Figure 4.4.
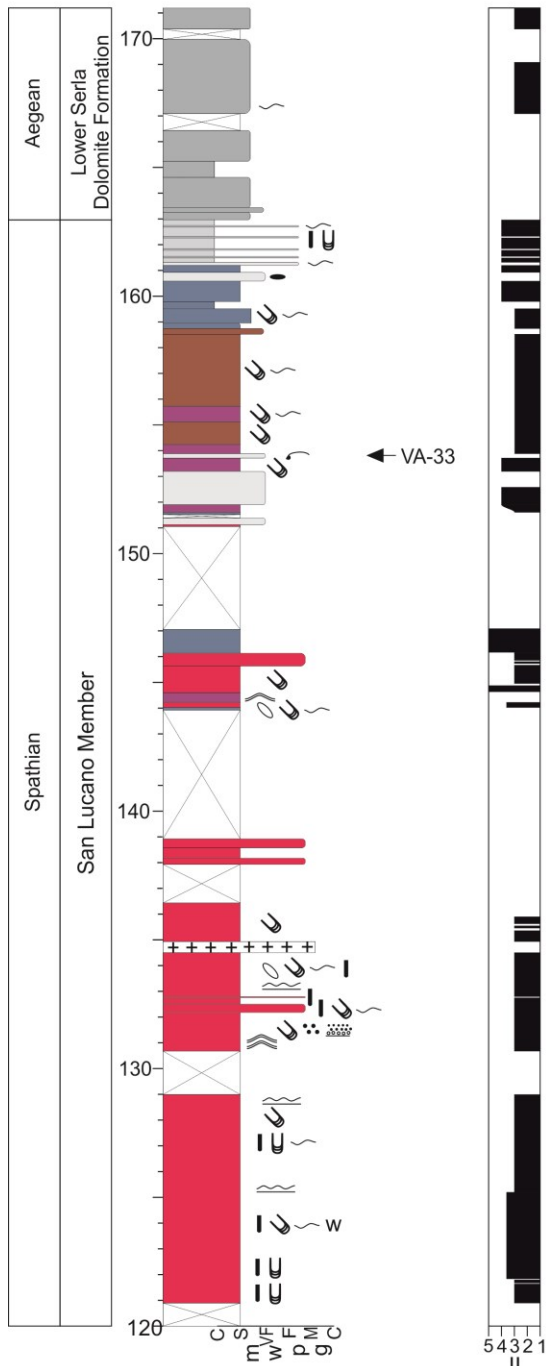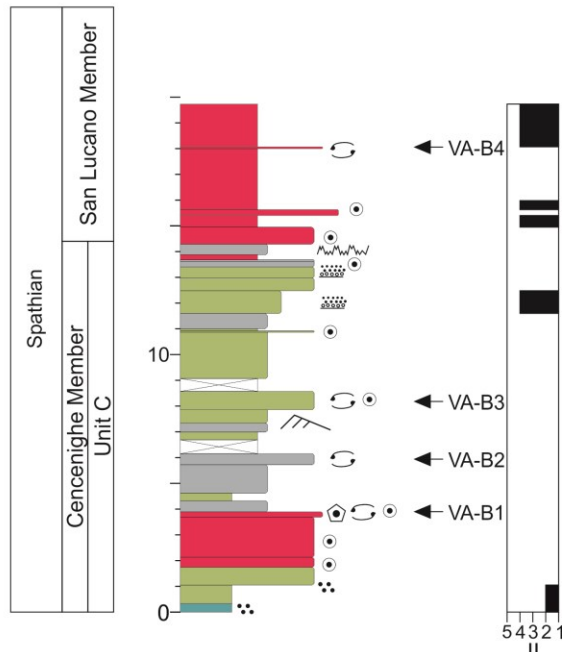
Figure 4.9 continued.

evidence for tidal influence during the accumulation of these sediments (Broglio Loriga et al., 1983). The alternation of this facies with facies 5 suggests the landward re-deposition of shoals during storms.

Facies 3: Alternating limestones/sandstones and siltstones (subtidal inner shelf).

<u>Description</u>: This facies can be subdivided into four subfacies:

Sub-facies 3.1: Fine- to medium-grained green, red or brown bedded (1-10cm) sandstones interbedded with sandy grey packstones and planar-laminated siltstones. The sandstone beds have cross-laminations and have symmetric ripples on their surface. These beds are also characterised by abundant convex-up bivalves, *Diplocraterion*, *Planolites* and *Skolithos*. In the Campil Member ophiuroid ossicles also occur within the sandstones. Occasionally ball and pillow structures also occur. The sandy packstones contain gastropods, microconchids, scaphopods and bivalves. The packstones are also graded and contain randomly orientated bivalves.

Sub-facies 3.2: Beds up to 1m thick of bluish grey sandy wackestones are interbedded by thin grey siltstone beds. The wackestones contain ripple structures and contain randomly orientated bivalves. The siltstones are bioturbated (ii3-5) by *Skolithos, Planolites, Diplocraterion,* and *Rhizocorallium*. These beds are also interbedded with thin oolitic purple and red packstones that contain randomly orientated bivalves.

Sub-facies 3.3: Red siltstones with alternations of laminations and persistent bioturbation (ii4-5) by *Rhizocorallium, Skolithos, Diplocraterion, Planolites* and *Lockeia*. The siltstones are interbedded with thin fine-sandstones, containing convex-up bivalves and small ball and pillow structures. Bedding planes of sandstones also occasionally have wrinkle marks.

Sub-facies 3.4: Green laminated siltstones interbedded with thin (1-6cm) oolitic grainstones. The oolitic grainstones contain vugs, crinoids and convex-up bivalves.

Interpretation: This facies is interpreted to have taken place in a shallow subtidal zone, within the intershoal areas, on the inner ramp. In a broad sense grain size reflects hydraulic energy of the environment with coarser sediments transported by faster flowing currents and winnowing of fine-grained material (Tucker, 2011). The dominance of well-sorted sandstones in this facies suggests deposition in a wave agitated environment on the inner shelf (Tucker, 2011). The presence of ripple cross-laminae in the sandstone beds also indicate wave-generated oscillatory flows and the co-occurrence of planar laminae of finer sediments indicates an environment prone to variance in current velocity (Zonneveld et al., 2010b). Indications for tidal reworking were not observed. Thin lenses of graded sandstones with randomly orientated bivalves, bioclasts fragments, erosive bases, and flat pebbles represent deposition during the waning flow phases of storm events. The ball and pillow structures formed by water escape processes following the rapid deposition of sand (Lowe, 1975). The presence of crinoids in subfacies 6 indicates stenohaline conditions during deposition. This facies alternates with oolitic shoal facies 4 and 5, suggesting deposition took place within intershoal areas on the inner shelf.

Facies 4: Thick cross-bedded oolitic grainstones (oolitic shoal).

Description: This facies is characterised by thick (up to 2m) cross-bedded oolitic grainstones and can be divided into three subfacies:

Sub-facies 4.1: Thick bedded (25-145cm), grey oolitic pack- and grainstones. These beds are usually cross-bedded but occasionally no sedimentary structures are preserved. These beds contain algae, foraminifera, gastropods, microconchids, bivalves and articulate brachiopods. Bivalves occur convex-up within the oolitic beds. The nuclei of

ooids are recrystallised with rhomboidal dolomite that appears as orange flecks in the field. The thick oolitic beds are separated by thin (1-2cm) green marls. This subfacies occurs in the Tesero Member.

Sub-facies 4.2: Thick beds (19-206cm) of purple oolitic pack- and grainstones. These thick beds have erosive bases and alternate with beds (10-46cm) that grade from oolitic packstones into cm-bedded sandstones. Some of the oolitic beds have hummocky tops and some others have *Planolites* burrows on bedding surfaces. Within the oolitic limestones crinoids, microconchids and randomly orientated bivalves occur. The shells of bivalves are recrystallised, thick and black. Some gastropods have their chambers filled by other smaller gastropods or ooids whilst other gastropods are filled with micrite. The nuclei of the ooids of this subfacies are either shell fragments or replaced by rhomboidal dolomite.

Sub-facies 4.3: Thick beds (up to 2m) of reddish brown oolitic pack- grainstones. These beds contain bivalves, ophiuroids, microconchids and occasionally crinoids. The bivalve shells are recrystallised, thick and white and are randomly orientated. Bivalve fragments form the nuclei of ooids. Occasional cross-bedding and flat pebbles are recorded within the beds. The bivalves and stylolites give the appearance of bedding approximately every 5cm.

Interpretation: The presence of ooids and cross-bedding suggests sediments were produced and accumulated in wave-agitated zones on the inner ramp. The ferroan dolomite that is commonly found replacing the nuclei of the ooids suggests initial deposition in a restricted lagoon (Assereto and Rizzini, 1975). The coating of the grains in subfacies 2 and 3 with iron oxides suggests reworking in a well-oxygenated environment (Assereto and Rizzini, 1975). Grading in the top of some of the oolitic beds suggest deposition in a lower-energy setting probably associated sea-level change.

This facies is interpreted have been deposited on the outer inner ramp where waves agitated the seafloor allowing the formation and build-up of oolitic shoals and reworking of the fauna, forming lenticular masses that probably stood no more than a few metres above the seafloor.

Facies 5: Hummocky and graded oolitic limestones (oolitic shoal storm sheets).

Description: This facies is characterised by graded oolitic pack- and grainstones with hummocky tops and can be split into three subfacies:

Sub-facies 5.1: Bedded (5-20cm) grey oolitic pack- and grainstones. Occasionally, ooids are replaced by rhomboidal dolomite that appears as orange flecks in the field. These beds are graded and often display hummocky tops and erosive or sharp bases. Gastropods, convex-up bivalves and shell fragments occur within the beds. This subfacies occurs in the Tesero and Mazzin members.

Sub-facies 5.2: Thick beds (10-63cm) of oolitic-intraclastic-bioclastic grainstones and packstones. It is also characterised by its reddish staining due to the high ankerite content (Broglio Loriga et al., 1990). Ooids are not always preserved and often replaced by rhomboidal dolomite. The tops of these beds often have hummocky tops and are graded in the upper few centimetres. Flat pebbles occur as isolated clasts within the grainstones and are roughly parallel to the bedding. These beds also contain randomly orientated fauna including bivalves, gastropods, microconchids, ostracods, and a large proportion of shelly fragments. Gastropods may have other smaller gastropods preserved inside. Bioclasts are coated red and the fragments form the nuclei of ooids.

Sub-facies 5.3: Alternation of thin bedded (3-24cm) brown oolitic packstones, grainstones and fine-grained red sandstones. Within the oolitic limestones flat pebble

and randomly orientated bivalves occur. The base of the limestone beds is sharp and planar.

Interpretation: Lack of cross-bedding and the sheet-like geometry of the oolites suggest that they represent redeposited amalgamated lobes of shoals (cf. Hips, 1998). The intercalation of this facies with Facies 3 suggests the landward re-deposition of shoals, whereas the intercalation of this facies with Facies 6 suggests the seaward re-deposition of shoals. The hummocky tops, erosive bases and grading of the beds in this facies suggests deposition took place during waning conditions of storm events. Ferroan dolomite is likely to have been formed on the landward side of shoals with the formation of iron oxides around grains occurring during the reworking of sediments in a more oxygenated setting (Assereto and Rizzini, 1975). Flat pebbles are probably extraclasts derived from a more proximal (peritidal?) setting (Wignall and Twitchett, 1999). Sub-facies 5.2 is occasionally interbedded with the distal mid-shelf facies in the lower Siusi Member and appear out of sequence. Deposition, therefore, probably took place during intense storm events, e.g. hurricanes. The restriction of Sub-Facies 5.1 to the Tesero and Mazzin members and the grey colour of the sediments may be a result of deposition in an anoxic environment as indicated by low Th/U ratios (<2; Wignall and Twitchett, 1996).

Facies 6: Alternations of laminated siltstones/ mudstones with thin-bedded limestones (mid-shelf).

Description: this facies is characterised by laminated siltstones or carbonate mudstone interbedded with thin-bedded (<10cm) limestones and can be subdivided into four subfacies:

Sub-facies 6.1: laminated to cm-bedded grey carbonate silty mudstones interbedded by thin-bedded (1-5cm) wackestones and packstones. In the Tesero Member the laminated

silty carbonate mudstone is occasionally green. The siltstones occasionally have ripples and the degree of bioturbation within this subfacies differs between the members of the Werfen Formation. In the Tesero and Mazzin members, only *Planolites* is recorded and the sediments are mostly laminated. In the lower Siusi Member *Thalassinoides, Lockeia, Diplocraterion, Catenichnus* and *Planolites* occur and the sediments are periodically slightly bioturbated (ii2). In addition, wrinkle marks are present on bedding surfaces of Tesero, Mazzin and Siusi members. Bivalves, microconchids, ostracods, lingulids, gastropods and ophiuroids may occur within the packstones. Stromatolites were recorded in the Mazzin Member.

Sub-facies 6.2: As for sub-facies 6.1. This sub-facies, however, is well bioturbated (ii3-5) by *Thalassinoides* and *Planolites*. Wrinkle marks are rarely observed in this sub-facies.

Sub-facies 6.3: This subfacies has an increased siliciclastic content and is characterised by laminated brown, purple or grey siltstones interbedded by thin (1-5cm) light-red packstones frequently forming coarsening-up packages. Within the siltstones convex-up bivalves and wrinkle marks can be observed. Ball and pillow structures are also common. The packstones have rippled tops, gutter casts at their bases, and contain ooids, gastropods and randomly orientated bivalves. Rhomboidal dolomite occurs inside a few of the gastropod chambers.

Sub-facies 6.4: Laminated grey siltstones or carbonate mudstones are less frequently interbedded with thin (1-3cm) grey packstones than sub-facies 6.1. The siltstones are weakly bioturbated (ii2-3) by *Skolithos* and *Planolites*. The siltstone beds also contain ball and pillow structures, gastropods and convex-up bivalves. The packstones contain flat pebbles, ophiuroid ossicles and randomly orientated bivalves.

Interpretation: Low-energy conditions between storms are indicated by the accumulation of finer sediments. The beds with preserved trace fossils were deposited in the mid-ramp setting during fair-weather conditions in an oxygenated environment (Török, 1998). The lack of bioturbation in the Tesero and Mazzin members suggest deposition in an anoxic environment supported by Th/U ratios <2 (Wignall and Twitchett, 1996). The alternations of weakly bioturbated and laminated mudstones in the lower Siusi suggest alternations of oxic and anoxic conditions. The ripples that occur may have been produced by storm-induced currents. The alterations of siltstones and carbonate mudstones may be explained by changes in sediment supply (Elrick, 1995). The thin beds, small size of bioclasts and parallel bedding of packstones suggest deposition during storms in a distal mid-ramp (Török, 1998). The gutter casts on the base of packstones would have been formed by storm-induced bottom currents (Török, 1998). The presence of rhomboidal dolomite with a few of the gastropods suggests some of the bioclasts were transported from the inner shelf during storm events. The facies is interpreted as a mid-shelf environment with storm sheets.

Facies 7: Stylonodular limestones (Outer ramp 'debris-flow').

Description: This facies is characterised by light grey wavy (i.e. stylolaminated/ stylonodular) and non-parallel bedded mudstones and wackestones. The beds are 35cm to over a metre thick with either sharp or erosional bases. These beds also contain bivalves which are randomly orientated throughout, although convex-up bivalves dominate near the top. These beds also contain gastropods, microconchids and ostracods but they are not as conspicuous as the bivalves. Grading was not observed in these beds, however, Wignall and Twitchett (1999) describe imperceptible grading at the top of these beds or ripples. This facies alternates with Facies 6 in the Mazzin and Siusi members.

Interpretation: Low-energy conditions between storms is indicated by the accumulation of finer sediments and the rare, thin event beds suggest distal infrequent storm influence and deposition below storm wave base. The lack of typical storm features such as convex-up bivalves and flat pebbles in this facies led Wignall and Twitchett (1999) to propose slow-moving turbulent flows probably triggered by storm events as the process responsible for the deposition of this facies. Th/U ratios from Wignall and Twitchett (1996) suggest that this facies was also deposited in an anoxic benthic environment.

Some authors suggest that this facies is bioturbated (Broglio Loriga et al. 1986; Noé, 1987; Farabegoli and Perri, 2012) and therefore represents oxygenated conditions (Farabegoli and Perri, 2012). This facies is similar to the 'Wellenkalk facies' of the Muschelkalk of the Netherlands and Germany (Knaust, 1998; Pöppelreiter, 2002) which is interpreted as a bioturbated oxygen-depleted environment on the outer ramp. Circular
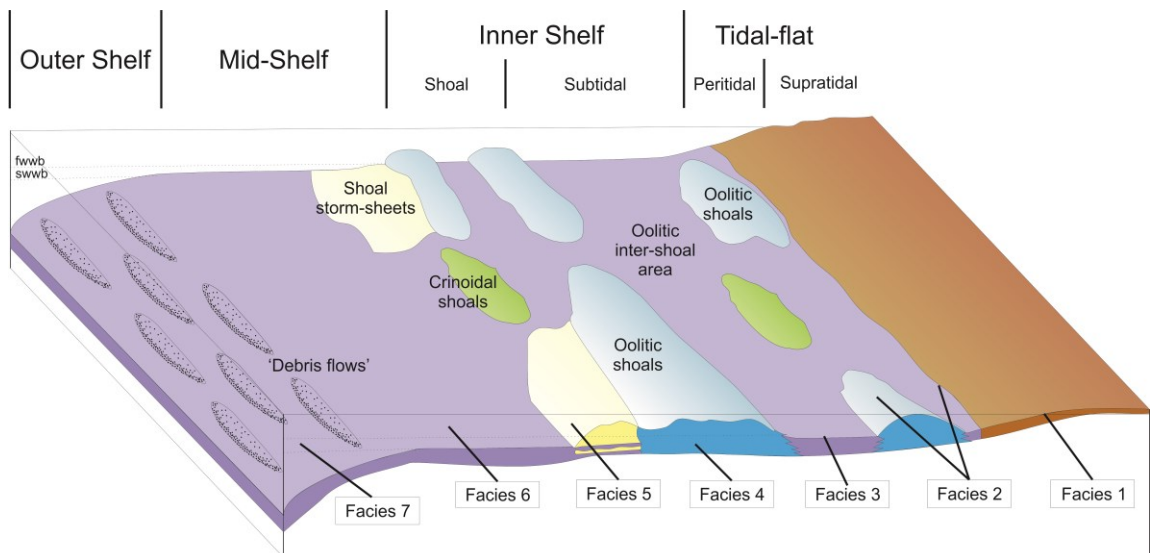
Figure 4.10: Schematic facies interpretation for the Werfen Formation, Italy, showing the position of facies. 1 – Supratidal, 2 – peritidal, 3 – shallow subtidal, inner shelf, 4 – Oolitic shoal, 5 – Mid-shelf, oolitic storm sheets, 6 – Mid-shelf with storm sheets, 7 – Outer shelf 'debris flows'. Crinoidal shoals were only observed in the Cencenighe Member, see text.

Figure 4.10 continued: Scale bar in Facies photos 1-3 and 6 is 15cm and in Facies photos 4, 5 and 7 is 1mm.

nodules that may represent *Planolites* in cross section have been reported from this facies (Wignall and Hallam, 1992), however, no unequivocal identifications have yet been made. In addition, a similar facies has been recognised from the Hungarian

Mushelkalk ramp (mottled limestone 'slope facies' of Török, 1998). Török (1998), however, identified the mottled texture of the rock as a product of diagenesis and recrystallization related to the steepening of the homoclinal ramp due to tectonism. Therefore, because no unequivocal evidence for bioturbation has been recorded from this facies in the Werfen Formation, it is interpreted have been deposited on the outer shelf with tectonism or high sedimentation creating debris-flows.

4.2.2 Bellerophon Formation

The upper part of the Bellerophon Formation was only recorded in the Siusi and Tesero sections. Deposition took place on a proximal shelf and has previously been described by Bosselini and Hardie (1973), Farabegoli et al. (2007) and Posenato (2010). Here, three facies were recognised from the Bellerophon Formation from the upper shoreface to mid-shelf.

Facies BF 1: Beige, bioturbated, marly dolomite (Upper shoreface-estuarine).

Description: This facies is characterised by thick beds of beige dolomitic marly and grey-green medium calcareous sandstones. This facies is strongly bioturbated (ii3-4) by vertical Y-shaped burrows. In addition, *Rhizocorallium* are present (R.J. Twitchett, personal communication 2015). The burrows within the beds contain large vugs.

Interpretation: Previous workers have identified this unit as a peritidal environment based on the presence of mudcracks, dolomitised nodular fabric and the eurotypic nature of microfossil assemblages (Bosselini and Hardie, 1973; Newton et al., 2004; Farabegoli et al., 2007; Mette and Roozbahani, 2012). Vertical Y-shaped burrows have previously been described as root traces (Hallam and Wignall, 1999; Farabegoli et al., 2007). Here the vertical Y-shaped traces are interpreted as *Psilonichnus lutimuratus* (associated with the activity of crustaceans; Figure 4.11), because, if the burrows were

plant roots, the traces would be expected to branch as they go deeper into the bed. The traces at the Siusi section, however, are the inverse and branch as you move up the bed.

The presence of *Psilonichnus lutimuratus* and *Rhizocorallium* would also support an upper shoreface-estuarine facies which is associated with the burrowing activity of crustaceans in estuarine environments (Nesbitt and Campbell, 2006). The presence of dolomite may also indicate a shallow marine environment if they were formed penecontemporaneously as they commonly form on arid tidal flats via reflux and evaporitic pumping (Haas et al., 2012) and in evaporitic lagoons via reflux and with the mediation of microbes (McKenzie and Vasconcelos, 2009). This facies is interpreted as an upper shoreface environment.

Facies BF 2: Alternations of sandstones and shales (Inner shelf storm sheet).

Description: This is characterised by thick bedded (50-100cm) grey silty dolomitic wacke-packstones and medium grained green vuggy sandstones separated by thin shales. These beds are moderately bioturbated (ii2-3) by *Skolithos* and *Diplocraterion* and vugs are restricted to within the burrows (Figure 4.11). Some beds show normal grading. The tops of these beds are hummocky and are separated by thin (<1cm) black shales. Within these beds algae, brachiopods, bivalves and gastropods are observed. Occasionally these beds alternate with red silt- and sandstones. These beds contain abundant plant fragments and fish remains that infill *Thalassinoides* burrows.

Interpretation: Hummocky and graded beds would have been deposited during storms. Mette and Roozbahani (2012) suggest that the abundance of plant fragments in this facies suggests freshwater influxes and associated periods of hypohaline conditions. Farabegoli et al. (2007) also interpreted the lack of fusulinid foraminifera and eurytopic foraminifera as indicating a shallow salinity-controlled environment. The presence of red silt- and sandstones is interpreted as representing deposition on or just below a tidal

mud-sandflat. This facies is interpreted as a shallow subtidal setting on the inner-shelf with storm sheets.

Facies BF 3: *Zoophycos*-bioturbated wackestones (Mid-shelf).

Description: This is represented by beds of light grey moderate to strongly bioturbated (ii3-4) mud-wackestones. These beds are bioturbated by poorly preserved *Zoophycos* (Figure 4.11) and sedimentary structures are not preserved.

Interpretation: These beds are interpreted as representing a more distal setting than Facies BF 2 based on the low amounts of siliciclastic material and are inferred to have been deposited in a mid-shelf environment below fwwb.

Figure 4.11: Facies from the Bellerophon Formation, Siusi section. Facies BF1) *Psilonichnus lutimuratus* from the upper shoreface/estuarine facies. Facies BF2) *Skolithos* burrows filled with large vugs from the inner shelf facies. Facies BF3) *Zoophycos* burrows from the mid-shelf facies. Scales: pencil is approximately 15cm; hand ~10cm.

4.3 Palaeoecological results

4.3.1   Alpha diversity

In the Dolomites, 39 different benthic invertebrate taxa were identified from 333 samples from the upper Changhsingian and Lower Triassic (Table 4.2; Figure 4.12-4.14), representing bivalves, gastropods, microconchids, ostracods, brachiopods, scaphopods, ophiuroids and crinoids. The MNI ranges from 1 to 867 per sample, and 182 samples have a large enough abundance (i.e. MNI >20) for quantitative analysis (Appendix 4.1).

Taxonomic richness does not increase with time but changes across member boundaries, associated with carbon isotope fluctuations (Figure 4.15; 4.3). The Mazzin Member is relatively diverse, with 14 taxa recorded. Excluding the Siusi and San Lucano members, this diversity is comparable to the rest of the Werfen Formation (Figure 4.15A). Additionally, the highest origination rates are observed in the Mazzin Member (54%; Figure 4.15A) associated with the appearance of ophiuroid ossicles and the Triassic taxa *Lingularia yini, Claraia aurita, C. clarai, Polygyrina* sp., *Neoschizodus laevigatus*, cf. *Unionites canalensis,* cf. *U. fassaensis* and *Eumorphotis* spp. Sample diversity, on the other hand, is significantly lower in the Mazzin Member than in the lower and mid-Siusi, Campil, Val Badia or Cencenighe members (Figure 4.15B; Appendix 4.2). Taxonomic richness and sample diversity significantly rise into the lower and mid-Siusi Member where they reach peak values for the entire Werfen Formation (Figure 4.15A). This increase is associated with high origination and low extinction rates (Figure 4.15A), and follows an overall gradual rise in carbon isotope values (Figure 4.3).

The negative isotope excursion within unit D of the Siusi Member below the Siusi/Gastropod Oolite Member boundary (Figure 4.3), coincides with elevated

Table 4.2: List of all recorded taxa and their mode of life. Modes of life after Foster and Twitchett, (2014). T = Tiering: 2 = erect, 3 = epifaunal, 4 = semi-infaunal, 5 = shallow infaunal. M = Motility: 2 = slow, 4 = facultatively motile, attached, 3 = facultatively motile, unattached, 5 = unattached, 6 = attached. F = Feeding: 1 = suspension feeding, 2 = surface deposit feeding, 3 = miner, 4 = grazer, 5 = predator.

Species	Group	Mode of life			Identification after
		T	M	F	
Brachiopod sp.	Brachiopod	3	6	1	
Rhynchonellid sp.	Brachiopod	3	6	1	
Lingularia spp.	Brachiopod	5	4	1	Posenato et al. (2014)
Lingularia borealis	Brachiopod	5	4	1	Posenato et al. (2014)
Lingularia yini	Brachiopod	5	4	1	Posenato et al. (2014)
Bivalve sp. A	Bivalve	3	6	1	
Bivalve sp. B	Bivalve	3	6	1	
Bivalve sp. C	Bivalve	3	6	1	
Bivalve sp. D	Bivalve	5	3	1	
Avichlamys tellinii	Bivalve	3	6	1	Neri and Posenato (1985)
Bakevellia spp.	Bivalve	4	6	1	Neri and Posenato (1985)
Bakevellia with costae	Bivalve	4	6	1	Neri and Posenato (1985)
Claraia aurita	Bivalve	3	4	1	Nakazawa (1977)
Claraia clarai	Bivalve	3	4	1	Nakazawa (1977)
Claraia stachei	Bivalve	3	4	1	Nakazawa (1977)
Claraia wangi-griesbachi	Bivalve	3	4	1	Broglio Loriga et al. (1983)
Costatoria costata	Bivalve	5	3	1	Nakazawa (1977)
Eumorphotis	Bivalve	3	6	1	Broglio Loriga and Mirabella (1986)
Eumorphotis multiformis	Bivalve	3	6	1	Broglio Loriga and Mirabella (1986)
Neoschizodus laevigatus	Bivalve	5	3	1	Neri and Posenato (1985)
Neoschizodus ovatus	Bivalve	5	3	1	Neri and Posenato (1985)
Scythentolium sp.	Bivalve	3	5	1	Neri and Posenato (1985)
cf. *Unionites canalensis*	Bivalve	5	3	1	Shigeta et al. (2009)
cf. *Unionites fassaensis*	Bivalve	5	3	1	Shigeta et al. (2009)
Holocrinus	Crinoid	2	4	1	Kashiyama and Oji (2004)
Ophiuroidea	Ophiuroid	3	2	2/5	Glazek and Radwański (1968)
cf. *Plagioglypta*	Scaphopod	4	2	3	Nützel and Schulbert (2005)
Allocosmia	Gastropod	3	3	1	Posenato (1985)
Coelostylina werfensis	Gastropod	3	3	1	Nützel and Schulbert (2005)
Pseudomurchisonia kokeni	Gastropod	3	3	1	Nützel and Schulbert (2005)
Polygyrina sp.	Gastropod	3	3	1	Nützel and Schulbert (2005)
High-spied gastropod sp. A	Gastropod	3	3	1	
cf. *Worthenia*	Gastropod	3	3	1	
Murchisoniina with costae	Gastropod	3	3	1	
Bellerophontidae	Gastropod	3	2	2	Kaim and Nützel (2011)
Bellerophontidae with costae	Gastropod	3	2	2	Kaim and Nützel (2011)
Werfenella rectecostata	Gastropod	3	2	4	Nützel (2005)
Natiria costata	Gastropod	3	2	4	Neri and Posenato (1985)
Gastropod sp. A	Gastropod	3	2	4	
Ostracod	Ostracod	3	2	2	
Microconch	Microconchid	3	6	1	Zatoń et al., (2013)

Figure 4.12: Gastropods and microconchids from the Werfen Formation, Dolomites. A) *Coelostylina werfensis*, Siusi Member, U-27. B) Murchisoniina with costae, Siusi Member, S-36. C) *Polygyrina* sp., Siusi Member, U-45. D) *Polygyrina* sp., Siusi Member, U-27. E) *Polygyrina* sp. A with *Postcladella kahlori* filling the shell cavity (pink spirals) Siusi Member, S-40. F) cf. *Worthenia*, Campil Member, C-5. G) *Pseudomurchisonia kokeni*, Siusi Member, S-55. H) *Allocosmia* sp., Cencenighe Member, VA-28. I) Gastropod sp. A, Siusi Member, U-49. J) Bellerophontidae, Siusi Member, S-66. K) Bellerophontid assemblage, Siusi Member, S-69. L) *Natiria costata*, Cencenighe Member, VA-5. M) Microconchid, Siusi Member, S-74. N-O) - cf. *Plagioglypta* sp., Siusi Member, S-73. Scale bar = 1mm.
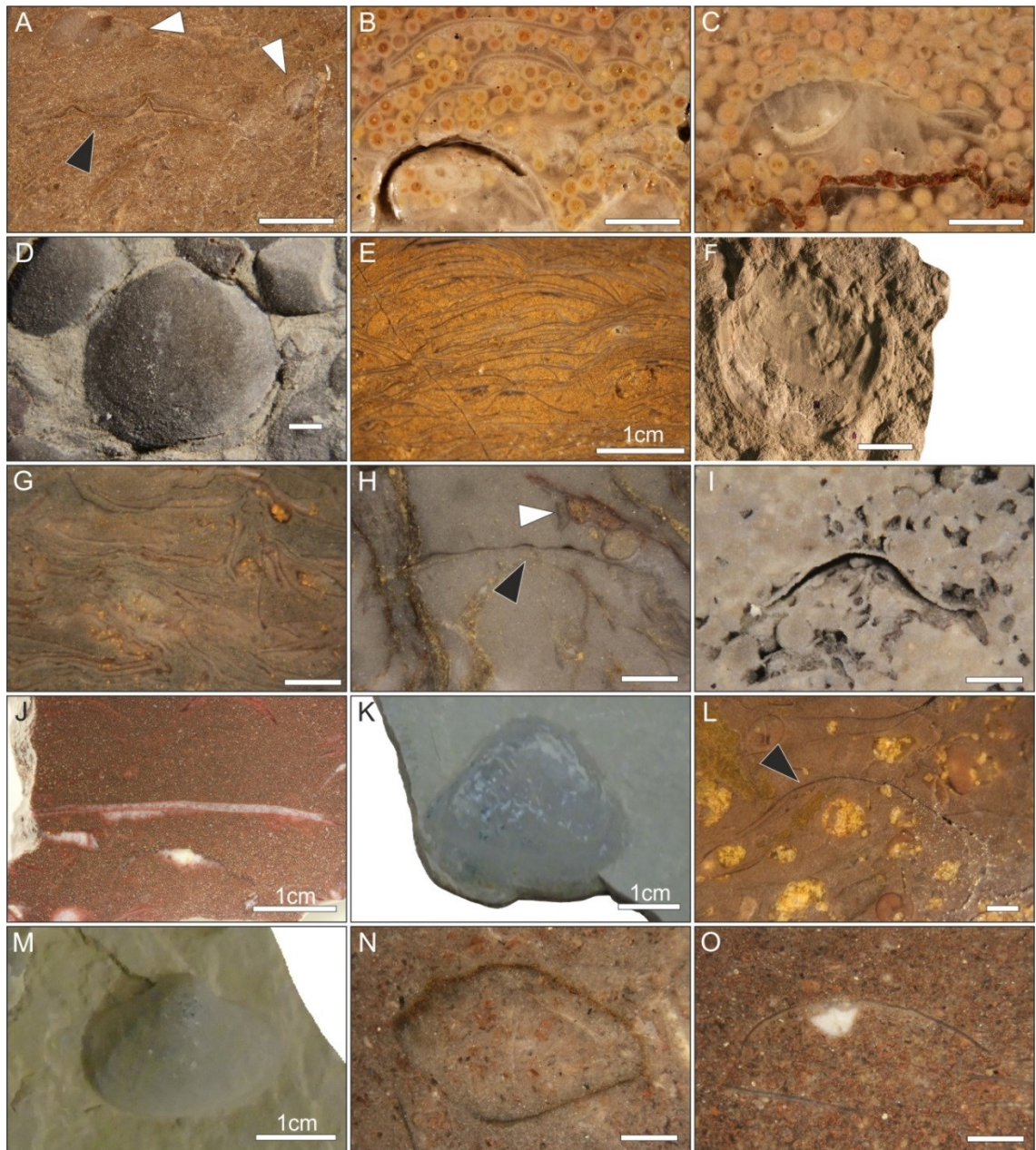
Figure 4.13: Benthic invertebrates from the Werfen Formation, Dolomites. A) Bivalve sp. B (black arrow) and *Coelostylina werfensis* (white arrow), Mazzin Member, U-5. B) Bivalve sp. B, Tesero Member, S-7. C) Bivalve sp. C, Tesero Member, T-1. D) *Claraia aurita* sensu lato, left valve, Mazzin Member, U-S1. E) *Claraia aurita* sensu lato assemblage, Mazzin Member, P-5. F) *Claraia clarai*, right valve, Mazzin Member, S-15. G) *Claraia* c.f. *stachei*, S-48. H) *Eumorphotis* (black arrow) and a microconchid encrusted on another bivalve shell (white arrow), S-87. I) *Bakevellia*, Cencenighe Member, VAB-1. J) *Scythentolium*, Cencenighe Member, C-39. K) Myophoriidae sp. A, Siusi Member, U-64. L) Myophoriidae sp. A. Siusi Member, S-79. M) cf. *Unionites canalensis,* Siusi Member, U-64. N) articulated cf. *Unionites*, Campil Member, C-1. O) cf. *Unionites* and ophiuroid ossicle, Campil Member, C-9. Scale bar = 1mm.
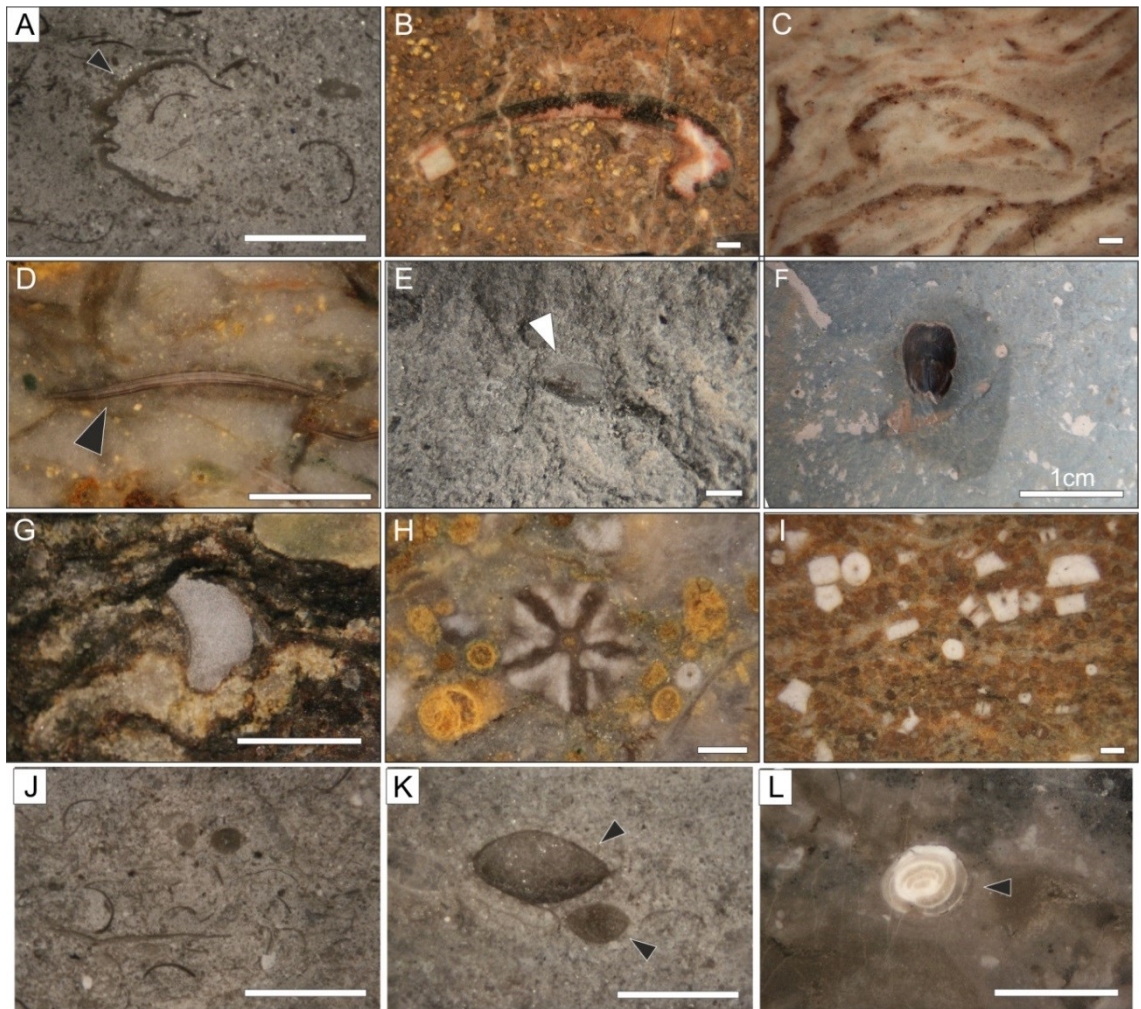
Figure 4.14: Benthic invertebrates from the Werfen Formation, Dolomites. A) Rhynchonellid sp. A (black arrow), Bellerophon Formation, S-4. B) *Neoschizodus ovatus*, Cencenighe Member, C-37. C) *Neoschizodus ovatus*, San Lucano Member, VAB-4. D) *Lingularia*, Gastropod Oolite Member, S-87. E) *Lingularia yini* (white arrow), Mazzin Member, S-S3. F) *Lingularia borealis*, Siusi Member, S-8. G) Ophiuroid ossicle, Siusi Member, S-72. H) *Holocrinus* ossicle, Cencenighe Member, C-34. I) *Holocrinus* ossicles, Cencenighe Member, C-38. J) Ostracods, Bellerophon Formation, S-4. K) Ostracod (black arrow), Bellerophon Formation, S-4. L) Foraminifera, Bellerophon Formation, S-1. Scale bar = 1mm.

extinction rates (28%; Figure 4.15A) between Unit C and D of the Siusi Member, with the disappearance of Bivalve sp. C, *Claraia* and bellerophontids. In addition, median species richness and Simpson Diversity significantly declines (p=0.02; Appendix 4.2). Origination and extinction rates are low throughout the Gastropod Oolite Member (Figure 4.15A), where, there

is a cluster of positive and negative isotope excursions (Figure 4.3). The Campil Member, is associated with only two new originations and a similar standing diversity to the Gastropod Oolite Member, however, median sample diversity significantly increases (p = 0.001; Figure 4.15).

The positive perturbation at the Campil/Val Badia member boundary, i.e. the Smithian/Spathian boundary, is not associated with significant difference in sample or standing diversity but elevated extinction (29%) and origination rates (29%; Figure 4.15) are recorded. Three of the four taxa that disappear across the boundary are microgastropods (<2cm) species: *Polygyrina* sp.*,* cf. *Worthenia* and Gastropod sp. A. Two of the four new taxa recorded in the Val Badia Member are notably larger (>2cm) gastropod species: *Natiria costata* and *Werfenella rectecostata*. In unit C of the Cencenighe Member there is a significant increase in median sample richness (p = <0.001) and origination rates (Figure 4.15A).

The species richness and Simpson diversities of siliciclastic and carbonate samples are not significantly different (Figure 4.16B). Additionally, when the samples are grouped according to facies, there is no significant difference ($p = 0.24$) in the species richness of samples (Figure 4.16A). Pairwise comparisons demonstrate that the Simpson Diversity of samples from the inner shelf and oolitic shoal settings are, however, significantly lower than those of other sedimentary facies (Appendix 4.3).

There are no significant differences in richness or Simpson Diversity between the sedimentary facies in the Griesbachian, Smithian or Spathian (Appendix 4.2). The mid-shelf sedimentary facies, however, shows a significant increase between the Griesbachian and Dienerian (p=<0.001; Figure 4.16). Also in the Dienerian there is significant difference between environmental settings: species richness and Simpson diversity are significantly lower in the inner shelf than in the mid-shelf (p=<0.01). The

median richness of inner shelf assemblages does, however, significantly increase between the Dienerian and Smithian (p=0.02; Figure 4.16C).

4.3.2   Alpha functional diversity

Eleven different modes of life were recognised in this study (Table 4.2). Functional richness increases between the Tesero, Mazzin and Siusi members, reaching seven modes of life in the Siusi Member, before declining in the Gastropod Oolite Member to four modes of life (Figure 4.17A). This decline is associated with the disappearance of *Claraia,* bellerophontids and scaphopods in the upper Siusi Member, and the loss of epifaunal, facultative motile, attached, suspension feeders; epifaunal, slow-moving, surface deposit feeders; semi-infaunal, slow-moving, miners. The recovery of two modes of life in the Campil Member is associated with the reappearance of ophiuroids and the first records of semi-infaunal, stationary attached, suspension feeders (e.g. *Bakevellia*) in this study. The further increase in functional richness between the Campil and Val Badia members (Figure 4.17A) is associated with the first record of erect, facultatively motile, suspension feeders, i.e. crinoids, and epifaunal, slow-moving, grazers (e.g. *Werfenella*).

Median sample richness shows similar trends; increasing from the Tesero to Siusi members, with the Siusi Member being significantly more functionally rich than the Mazzin and Tesero members (Figure 4.17B; Appendix 4.2). Functional richness then significantly declines into the Gastropod Oolite Member and significantly increases again in the Campil Member (Figure 4.17B: Appendix 4.2). No significant changes are recorded in the Simpson functional diversity between the members of the Werfen Formation (Figure 4.17; Appendix 4.2), suggesting that differences in species richness is controlled by rare taxa.
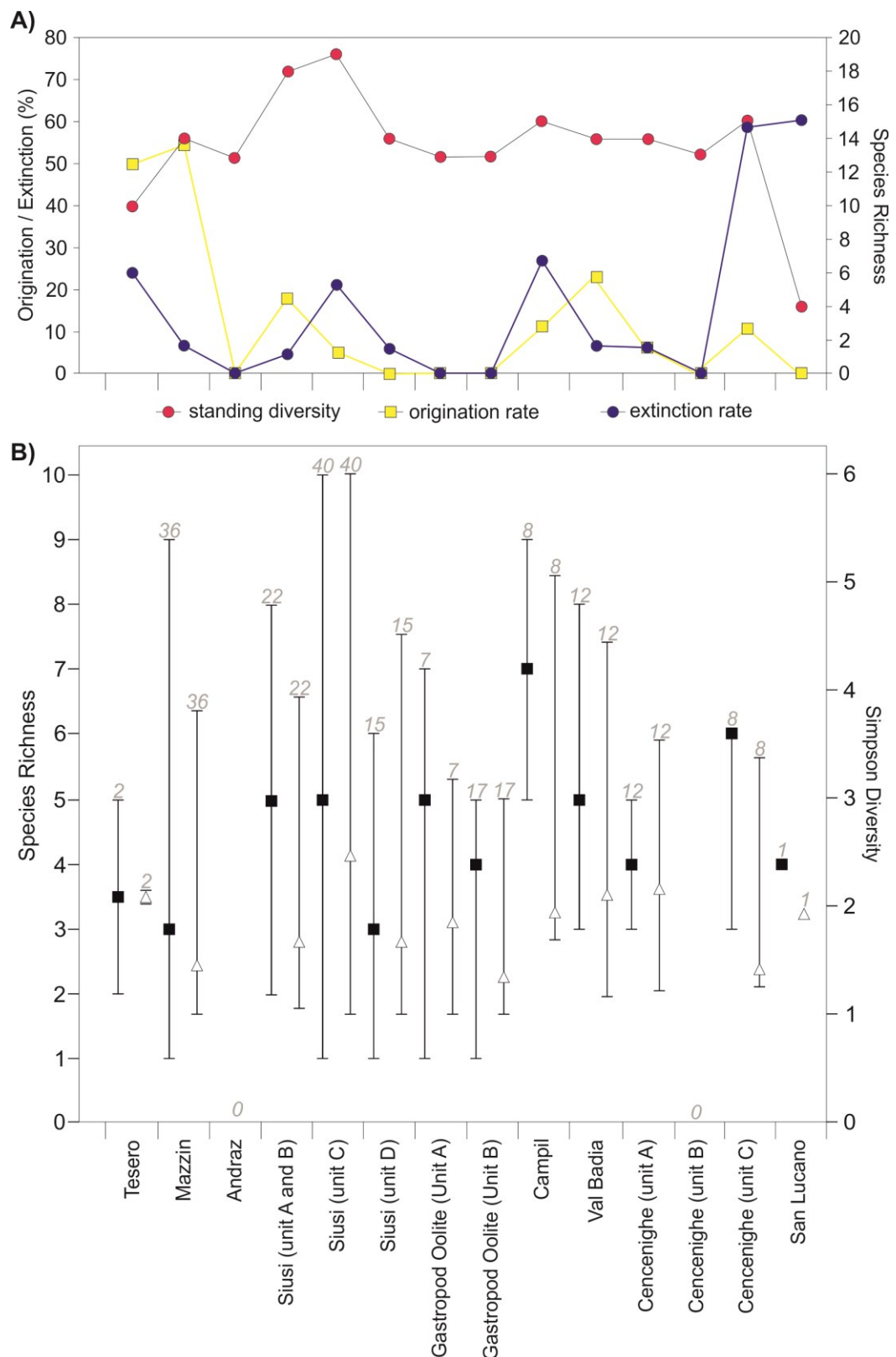
Figure 4.15: Changes in alpha diversity between each member and unit of the Werfen Formation. A) Changes in standing diversity of each member/unit and the local origination and extinction rates for the Werfen Formation. B) Median species richness (black squares) and median Simpson Diversity (white triangles) for each member/unit. The minimum and maximum values are shown with short horizontal lines.

The functional richness and Simpson functional diversities of siliciclastic and carbonate samples are not significantly different (Figure 4.18B). Functional richness does not vary significantly between different depositional settings ($p = 0.60$; Figure 4.18A). The Simpson diversity of inner ramp and shoal sedimentary facies, were however significantly less diverse than outer shelf and peritidal sedimentary facies (Figure 4.18A; Appendix 4.4). Even when the facies are split between the different sub-stages the Griesbachian, Smithian and Spathian do not show a significant difference in functional richness between the different sedimentary facies (Figure 4.18C; Appendix 4.4). In the
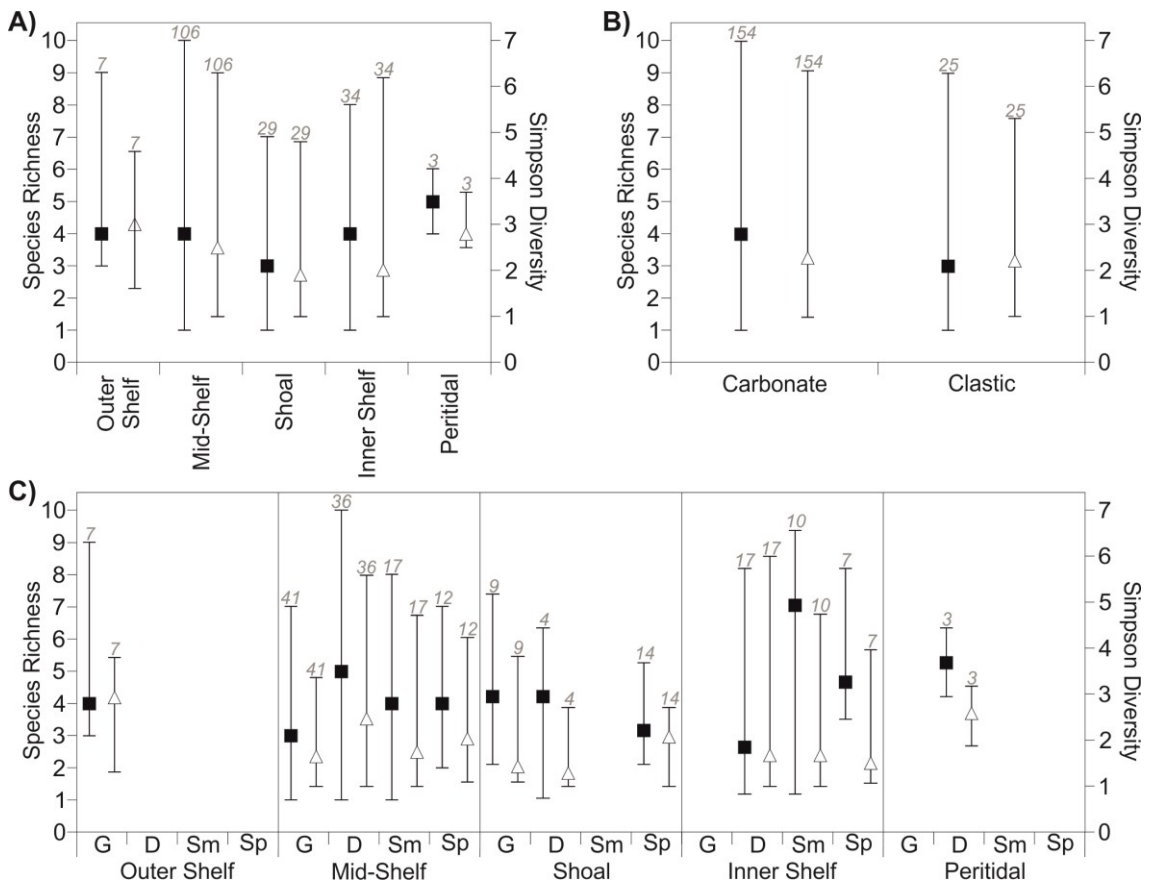
Figure 4.16: Changes in alpha diversity between each (A) sedimentary environment, (B) lithology and (C) sedimentary environment for each sub-stage. Black squares = Median species richness. White triangles = Simpson Diversity. The minimum and maximum values are shown with short horizontal lines. G = Griesbachian, D = Dienerian, Sm= Smithian, Sp = Spathian.

Dienerian, however, species richness is significantly lower in the inner shelf (p = 0.01; Appendix 4.4). In addition, during the Griesbachian, the Simpson diversity values are significantly higher in outer shelf sedimentary facies (p= 0.01; Appendix 4.4). The
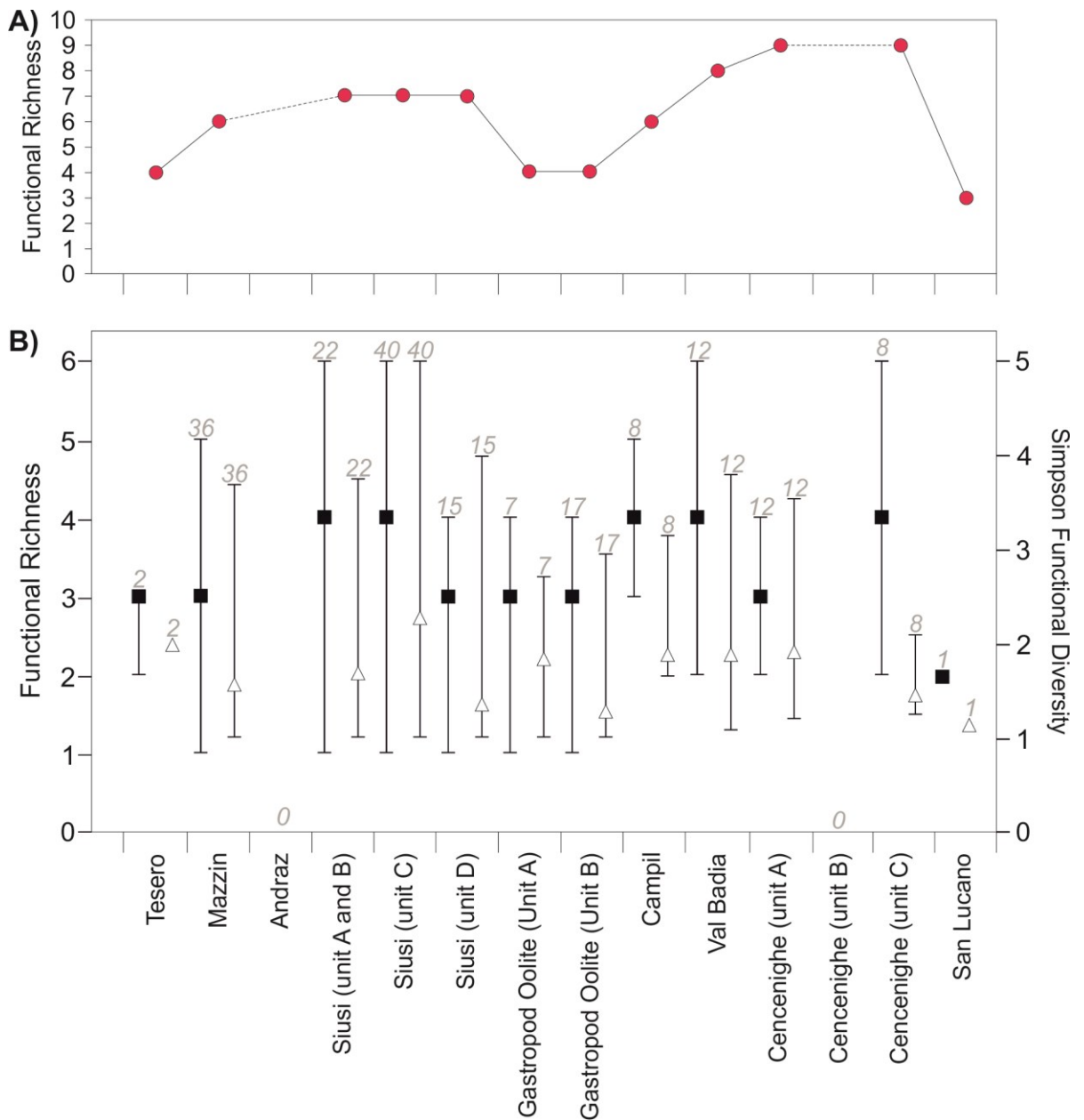
Figure 4.17: Functional alpha diversity in the Werfen Formation, Italy. A) Standing functional richness, i.e. the number of modes of life recorded in each stratigraphic time bin. B) Median sample functional richness (black squares) and median sample Simpson functional diversity (white triangles). The minimum and maximum values are shown as horizontal lines. The number of samples in each stratigraphic bin is shown in grey.

functional richness and Simpson functional diversity of mid-shelf sedimentary facies significantly increases between the Griesbachian and Dienerian (p = <0.001), whereas, the functional richness of inner shelf facies does not increase significantly until the Spathian (p = <0.001; Figure 4.18C).
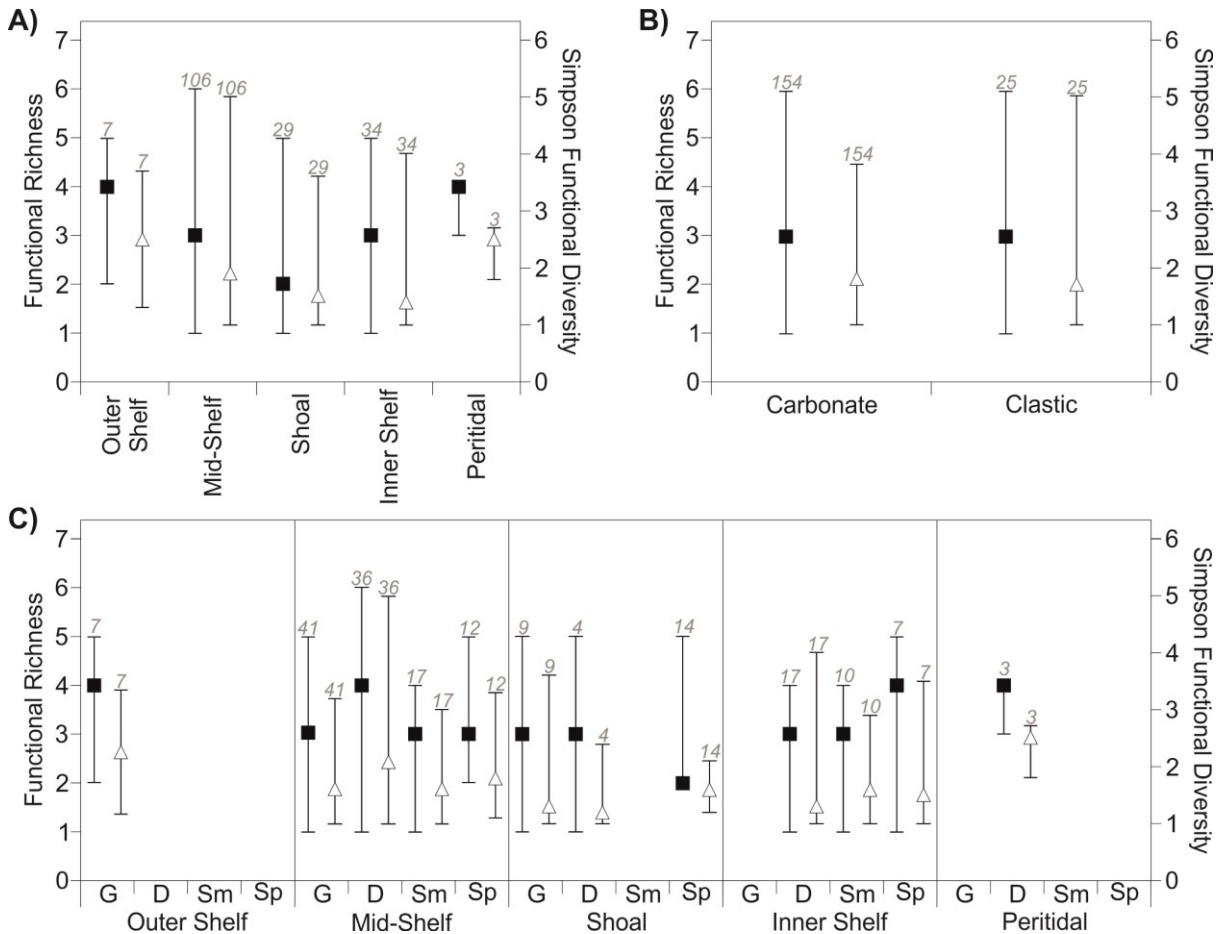
Figure 4.18: Functional alpha diversity between different environmental settings. **A)** Median functional richness and median Simpson functional diversity of samples between sedimentary environments. **B)** Median functional richness and median Simpson functional diversity of samples between carbonate and siliciclastic rocks. **C)** Median functional richness and median Simpson functional diversity of samples between sedimentary environments divided into sub-stage. The minimum and maximum values are shown with short horizontal lines. The number of samples in each stratigraphic bin is shown in grey. G = Griesbachian, D = Dienerian, Sm= Smithian, Sp = Spathian.

4.3.3   Changes in taxonomic composition

The cluster analysis shows five broad groups at low similarity (<20%) that are divided into 24 quantitative biofacies recognised by the SIMPROF analyses (Figure 4.19; Appendix 4.5). Group 1 includes a single sample from the Tesero Member dominated by bivalve sp. A (A; Figure 4.19). Group 2 is dominated by ostracods (B) and *Claraia aurita* (C) which are limited to the Bellerophon Formation and Mazzin Member (Figure 4.19). Group 3 comprises samples from the Siusi Member and a single biofacies (D) which is dominated by *C. clarai* (Figure 4.19). Group 4 includes samples from the Tesero, Mazzin, Siusi, Gastropod Oolite and Campil members, as well as a single sample from the Val Badia Member (Figure 4.19). This comprises 15 biofacies dominated by: *Plagioglypta* (E); *Unionites* (J-K); Bellerophontids, ostracods, *Unionites* and microconchids (L-O); *Coelostylina* (P); *Lingularia* (Q) and microconchids (R-S). Group 5 comprises almost all of the Spathian samples and a single Siusi Member sample and indicate biofacies dominated by *Natiria costata* (T) or *Neoschizodus ovatus* (U-X).

The nMDS plots have stress values of 0.18 which suggests that they are a good representation of the data (Clarke and Gorley, 2006). The distribution of samples along the horizontal axis follows almost precisely their stratigraphic order (Figure 4.20 A-B). Samples from the Tesero, Mazzin, Siusi, Gastropod Oolite and Campil members overlap in the centre of the ordination (Figure 4.20 A-C) because of the common occurrence of *Unionites*, *Coelostylina* and microconchids. The PERMANOVA results show that significant differences occur between the centroids of all members of the Werfen Formation ($p = 0.001$), except between the Gastropod Oolite and Campil members and the Cencenighe and San Lucano Members (Figure 4.20 A-C; Appendix 4.6).
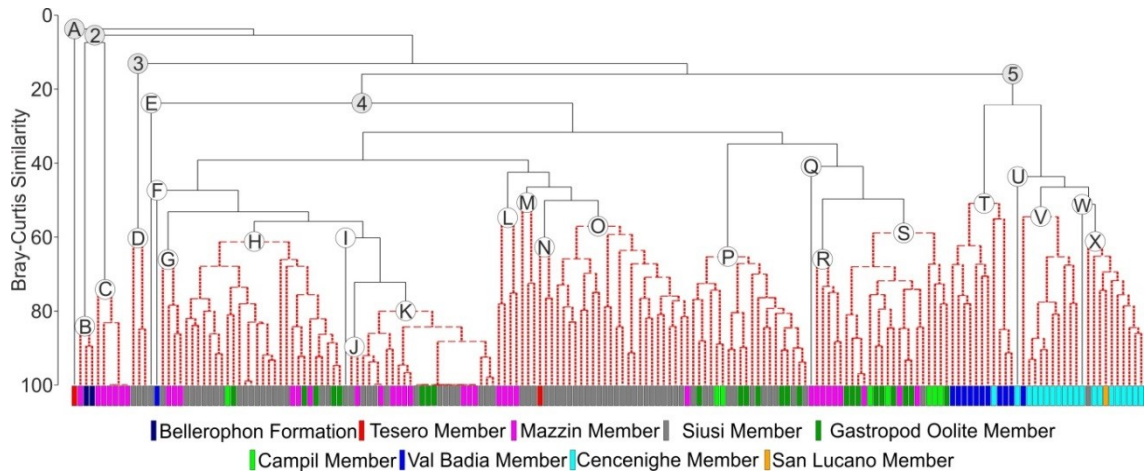
Figure 4.19: Taxonomic cluster analysis. The cluster analysis, together with the SIMPROF test, identified 24 groups of samples which are statistically distinct. The 24 groups have been identified as representing different biofacies and the SIMPER analysis (Appendix 4.5) has identified the taxa that constitute the nucleus of biofacies. The different biofacies are labelled from A to X and the five main groups of biofacies are labelled 1 to 5 and shaded grey, A is the same as 1.
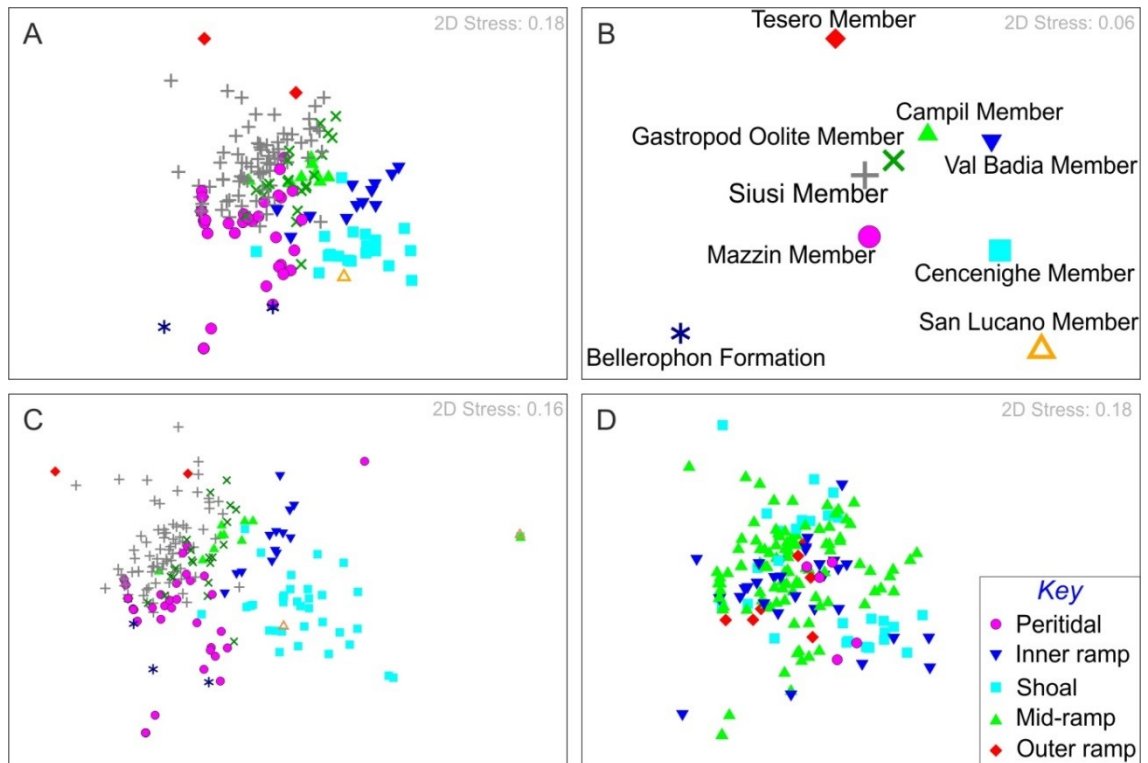
Figure 4.20: nMDS ordination of samples. A) The ordination of samples using the minimum number of individuals (MNI) grouped by stratigraphic unit. Colours and symbols as in B. B) Ordination of stratigraphic unit centroids using MNI. C) The ordination of samples using the number of bioclasts divided by stratigraphic unit. Colours and symbols as in B. D) The ordination of samples using the MNI divided by sedimentary environment.

The Bellerophon Formation, Tesero Member and San Lucano Member have too few samples, (<3), for a comparison of sample dispersion (Table 4.4). The PERMDISP results show that the dispersion of samples is significantly different between the remaining members of the Werfen Formation (p=0.001). Pair-wise comparisons show that the Mazzin Member samples are significantly more dispersed in the ordination than the remainder of the Werfen Formation (Table 4.4). The Siusi Member samples are also significantly more dispersed than the Campil and Val Badia members. The Campil and Val Badia members, however, have fewer samples (Figure 4.4) and this difference may therefore be a sampling artefact.

Table 4.3: PERMDISP results for sedimentary facies within each Lower Triassic sub-stage.

	N	PERMDISP
Griesbachian		
Shoal	9	42.0
Mid-shelf	42	48.4
Outer shelf	7	35.1
Dienerian		
Peritidal	3	13.3
Inner shelf	17	33.6
Shoal	4	33.3
Mid-shelf	36	35.2
Smithian		
Inner shelf	10	34.3
Mid-shelf	17	34.3
Spathian		
Peritidal	<3	n/a
Inner shelf	4	36.0
Shoal	14	26.2
Mid-shelf	12	30.4

Table 4.4: the PERMDISP results between the members of the Werfen Formation.

	Tesero Mb.	Mazzin Mb.	Siusi Mb.	GO Mb.	Campil Mb.	Val Badia Mb.	PERMDISP	N	N of biofacies
Mazzin Mb.	0.49						45.1	36	10
Siusi Mb.	0.66	**<0.01**					39.4	77	12
GO Mb.	0.82	**<0.01**	0.34				36.2	24	5
Campil Mb.	0.70	**<0.01**	**<0.01**	0.10			25.1	8	4
Val Badia Mb.	0.97	**<0.01**	**<0.01**	0.48	0.20		32.0	12	2
Cencenighe Mb.	0.89	**<0.01**	0.20	0.72	0.20	0.72	34.4	20	4
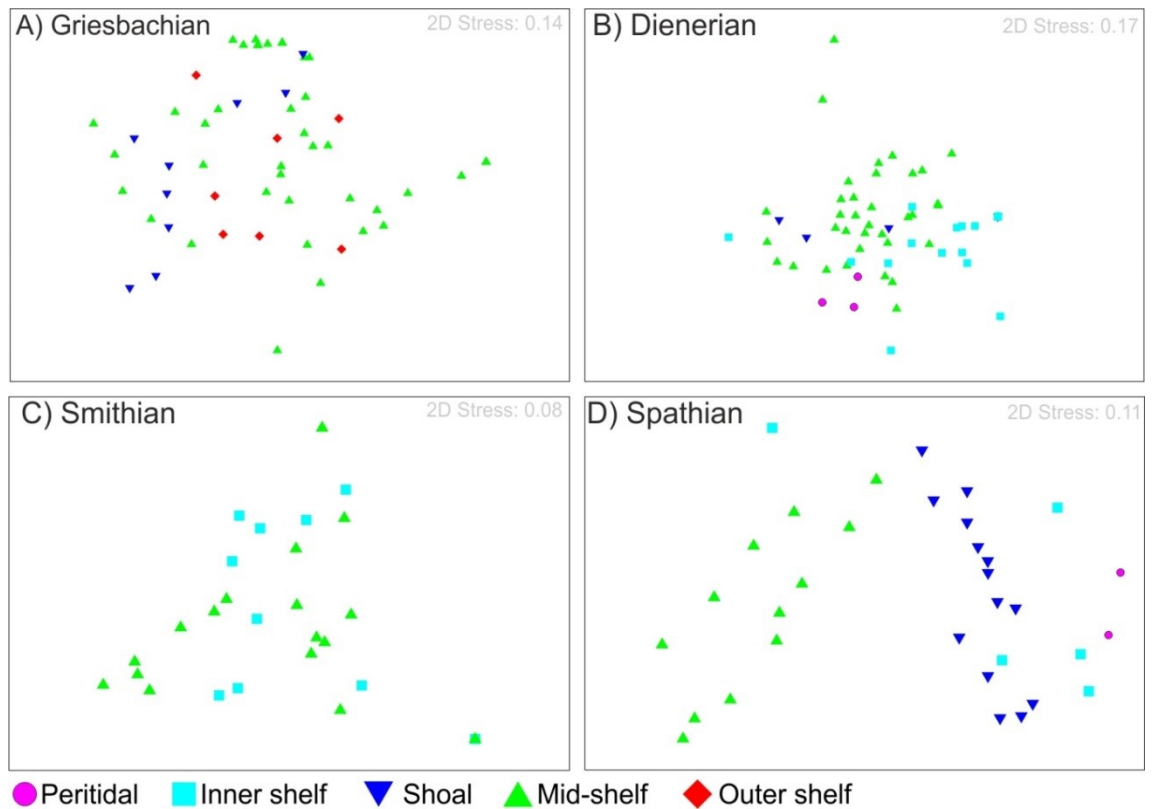
Figure 4.21: nMDS ordination of samples grouped according sedimentary facies within each Lower Triassic sub-stage.

When the samples are grouped according to their depositional environment, the samples are highly dispersed with large overlaps and, therefore, no noticeable trends (Figure 4.20D). When the samples are binned according to sub-stage no trends are observed until the Spathian (Figure 4.21), where there appears to be an environmental gradient with samples from the mid-shelf sedimentary facies plotting on the left of the ordination, through shoal and inner shelf to peritidal towards the right of the diagram (Figure 4.21D). A two-way PERMANOVA between sub-stage and sedimentary facies also shows that sub-stage and sedimentary environment are significant ($p = 0.01$) in affecting the taxonomic composition of samples in the nMDS ordination (Figure 4.21). Therefore, the main factor controlling changes in taxonomic composition is time.
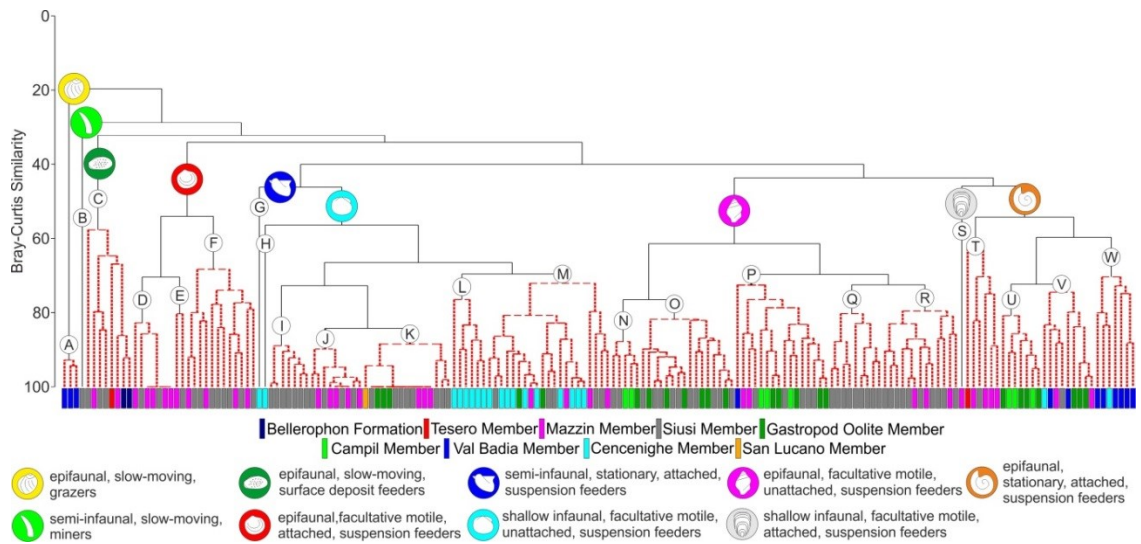
Figure 4.22: cluster analysis based on modes of life. The cluster analysis, together with the SIMPROF test, identified 23 groups of samples which are statistically distinct. The 9 groups have been identified as representing different biofacies.
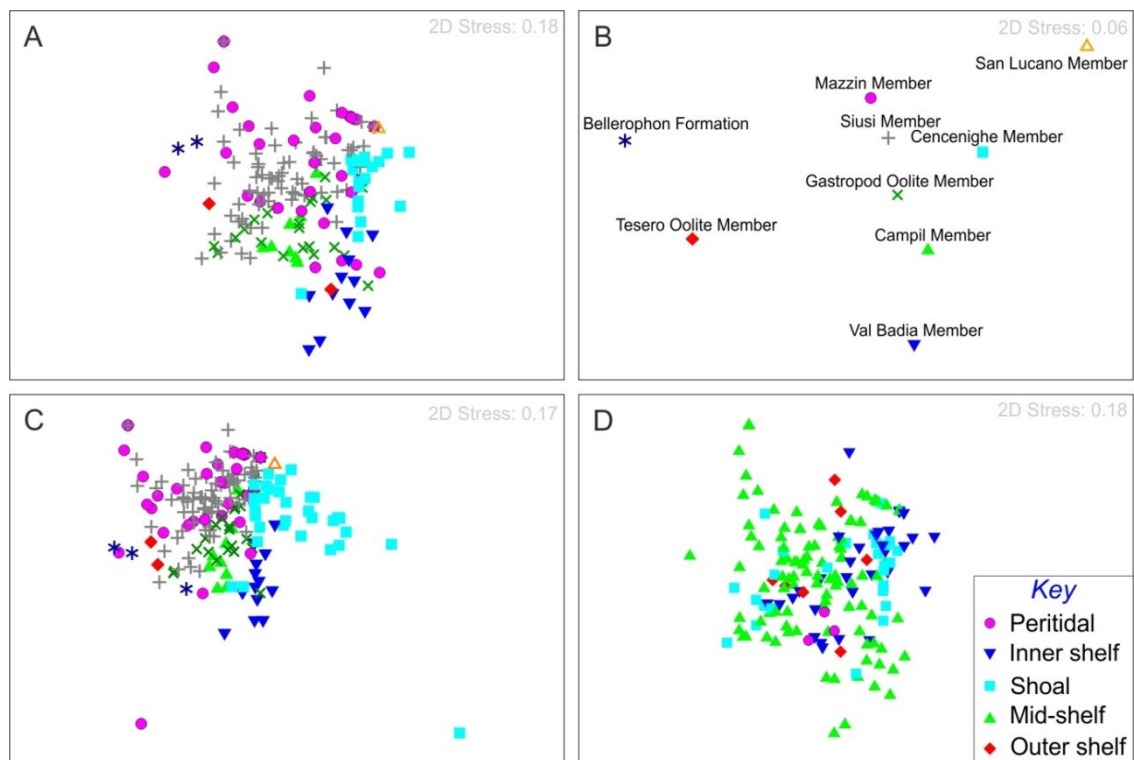
Figure 4.23: nMDS ordinations of the samples, with species labelled according to their ecospace category. A) The ordination of samples using the minimum number of individuals (MNI) grouped by stratigraphic unit. Colours and symbols as in B. B) Ordination of stratigraphic unit centroids. C) The ordination of samples using the number of bioclasts grouped by stratigraphic unit. Colours and symbols as in B. D) The ordination of samples using the MNI divided by sedimentary environment.

Echinoderm-dominated biofacies

If the total number of specimens per sample is used to reconstruct relative abundances rather than MNI, the ordination of samples shows similar relationships, but the samples are more dispersed (Figure 4.20C). The bioclasts analysis also increases the number of quantitative biofacies from 24 to 35 (Appendix 4.7). The increased number of biofacies is attributed to the increased variability in the relative abundance of echinoderms. Echinoderm-dominated biofacies were not recognised using the MNI approach, whereas, using the number of bioclasts two of the biofacies are dominated by echinoderms: an ophiuroid-dominated biofacies which appears in the lower Siusi, Campil and Val Badia members, and a *Holocrinus* biofacies that dominates samples in Unit C of the Cencenighe Member (Appendix 4.7). The increased abundance of ophiuroids also means that the Val Badia Member samples now cluster with the Siusi, Gastropod Oolite and Campil members (Appendix 4.7).

4.3.4   Changes in ecological composition

The cluster analysis, SIMPROF test and the SIMPER analysis made on functional groups shows that there are 23 quantitative ecofacies that are dominated by one of nine modes of life (Figure 4.22). There is no temporal trend to the distribution of ecofacies. Ecofacies dominated by shallow-infaunal, facultatively motile, unattached, suspension feeders or epifaunal, stationary, attached, suspension feeders are recorded from the Tesero to San Lucano members. On the other hand, a few of the ecofacies are stratigraphically restricted: ecofacies C (dominated by epifaunal, slow-moving, surface deposit-feeders) is restricted to the Bellerophon Formation, Tesero, Mazzin and Siusi members; ecofacies W (dominated by epifaunal, stationary, attached, suspension feeders) is restricted to the Mazzin Member; ecofacies D-F (dominated by epifaunal, facultatively motile, attached, suspension feeders) only occur in the Mazzin and Siusi

members; ecofacies A (dominated by epifaunal, slow-moving, grazers) only occurs in the Val Badia Member; ecofacies R and T (dominated by epifaunal, facultatively motile, unattached, suspension feeders and epifaunal, stationary, attached, suspension feeders, respectively) occurs from the Mazzin to Campil Member only (Figure 4.22).

The nMDS plots (Figure 4.23) have stress values of 0.18 which suggests that they are a good representation of the data (Clarke and Gorley, 2006). Overall the horizontal axis of the ordination mostly reflects a stratigraphical control to their distribution with older samples towards the left of the plot and younger samples towards the right (Figure 4.23B). The PERMANOVA shows that these differences are significant (p= 0.001). For sedimentary facies, however, no trends are observed (Figure 4.23).

A two-way PERMANOVA between sub-stage and sedimentary facies shows a significant difference (p=0.001) suggesting that there is both a temporal and an environmental aspect to the ordination results. The nMDS plots of sedimentary facies
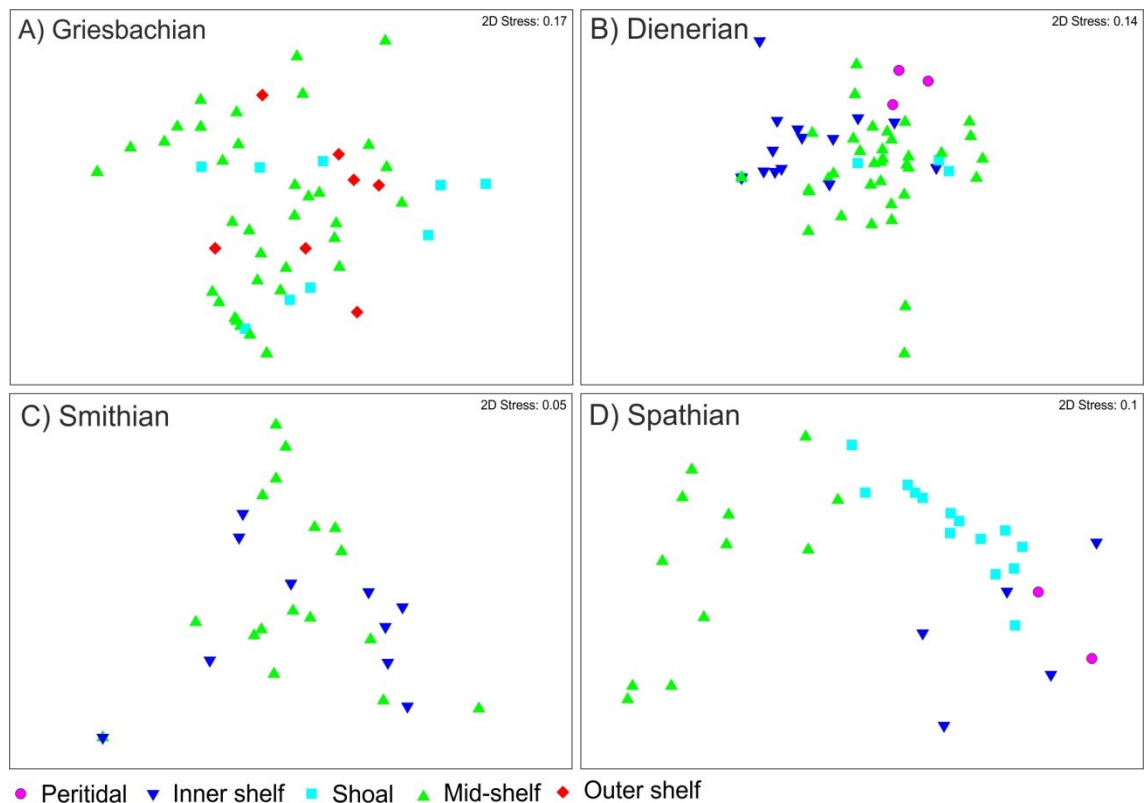
Figure 4.24: nMDS ordination of samples grouped according sedimentary facies within each Lower Triassic sub-stage, with species labelled according to their mode of life.

within each sub-stage (Figure 4.24), however, only show an environmental gradient in the Spathian. The pair-wise comparisons of sedimentary facies within each stage also show that there is significant difference in the Dienerian and Spathian (Appendix 4.8).

4.4   Discussion

Diverse faunas from hypoxic facies of the Mazzin and Siusi members.

The late Permian mass extinction event is considered to be represented in the Dolomites by four events from the base of the Bulla Member, Bellerophon Formation, to the first appearance of *Hindeodus parvus*, i.e. Permian/Triassic boundary, (Farabegoli et al., 2007; Farabegoli and Perri, 2012) which in this study occur in the lower half of the Tesero Member. The subsequent Mazzin and lower Siusi members have been interpreted as representing oxygen-restricted mid- and outer shelf environments (Wignall and Twitchett, 1996). The initial stages of benthic recovery have previously been hypothesised as occurring in the Dienerian (Twitchett, 1999; Twitchett et al., 2004). The Mazzin Member, however, records high 'origination' rates and high standing diversity, as well as taxonomic and ecological compositions comparable to the oxygenated facies of the Siusi Member. A high standing diversity and compositional similarities between the Mazzin and Siusi members was also found by Hofmann et al. (2015a).

Units A and B of the Siusi Member also record oxygen-restricted facies (Wignall and Twitchett, 1996) and are characterised by high origination rates, as well as taxonomic and functional compositions comparable to subsequent oxygenated facies of the Siusi Member. The lower Siusi Member also records increased bioturbation and ichnodiversity (Twitchett and Wignall, 1996; Twitchett, 1997; Hofmann et al., 2011; this study). The assemblages from the Mazzin and lower Siusi members occur with evidence for storm deposition, i.e. in storm beds. The fauna recorded from the Mazzin

and lower Siusi members, therefore likely represents the rapid colonisation of the sea-floor in the distal mid-shelf following storm events that temporarily oxygenated the seafloor. In addition, the debris flows and tempestites recorded in the outer shelf would have transported the fauna from the storm-dominated shelf into the outer shelf environment. Alternatively, the fauna colonised the sediment below wave base in-between periodic upwelling of deeper anoxic waters (Zonneveld et al., 2010a). The restriction of fauna to storm deposits in the distal mid-shelf supports the distal end of the proposed 'habitable zone' hypothesis (Beatty et al., 2008; Zonneveld et al., 2010a).

Even between the similar oxygen-restricted distal mid-ramp facies of the Mazzin and lower Siusi members there are differences in the fauna, with increased size (Twitchett and Wignall, 1996; Twitchett, 2007; Metcalfe et al., 2011), increased sample diversity (Figure 4.15), increased ichnodiversity (Twitchett and Wignall, 1996; Twitchett, 1997; Hofmann et al., 2011), and an increased standing diversity (Figure 4.15) in the lower Siusi Member. Previous studies investigating the response of benthic marine communities to the late Permian extinction have shown that in the absence of anoxia, the recovery of benthic communities (i.e. increased tiering, diversity, size and the presence of indicator taxa) occurs by the second conodont zone, i.e. *Isarcicella isarcica* Zone, of the Griesbachian (Twitchett et al., 2004), or by the late Griesbachian (Chen et al., 2006b; Chen et al., 2007; Chen et al., 2010b; Beatty et al., 2008; Shigeta et al., 2009; Fraiser and Bottjer, 2009; Knaust, 2010; Zonneveld et al., 2010a; Kaim et al., 2010; Hautmann et al., 2011; Hofmann et al., 2011; Clapham et al., 2013; Hofmann et al., 2013b). The same trend is observed in the Werfen Formation, where recovery in the lower Siusi Member occurs in the late Griesbachian *Hadrodontina aequabilis* Zone. This late Griesbachian recovery in the Dolomites also corresponds with increased carbon isotope values (Horacek et al., 2007a). This may correspond with the return to

more favourable environmental conditions during the Griesbachian allowing for initial recovery following the late Permian mass extinction.

Hofmann et al. (2011), based on the recovery model of Twitchett (2006), suggested that the recovery of the benthic realm had recorded similar levels globally by the late Griesbachian. The lower Siusi Member, however, lacks the same ecological complexity as observed in the *I. isarcica* Zone of Oman (Twitchett et al., 2004), as there are no representatives of the erect tier, no articulate brachiopods, sample diversity is half as much as in Oman, and gastropods are larger in Oman (Twitchett et al., 2004; Wheeley and Twitchett, 2005; Oji and Twitchett, 2015). The level of recovery in Oman was, therefore, at a more advanced state than in the Werfen Formation. The episodic oxygen-restriction of the seafloor during the Griesbachian in the Dolomite region may, therefore, have still hindered the recovery of local benthic communities following the late Permian mass extinction. This suggests that the recovery was not as globally synchronous as Hofmann et al. (2011) propose.

Upper Siusi Member biotic crisis

The boundary between Unit C and D of the Siusi Member corresponds to a regression from a mid-shelf to inner shelf environment, a carbon isotope negative excursion and a 28% extinction in opportunistic taxa, e.g. *Claraia,* and 'dead clade walking' taxa, like bellerophontids (Kaim and Nützel, 2011). Hofmann et al. (2015a) also recognised this biotic crisis in the Werfen Formation, but also included *Pseudomurchisonia kokeni* and *Coelostylina werfensis* as going extinct during this interval. Nützel and Schulbert (2005), however, describe these taxa from the Smithian of the Werfen Formation and in the present study, these taxa were abundant even into the Cencenighe Member (Appendix 4.1).

Twitchett (2000) and Posenato (2008b) show that the upper Siusi Member is often misidentified as the Campil Member due to lithostratigraphical similarities, at least when exposure is limited. Based on correlation of carbon isotope records between the Gartnerkofel-1 core (Magaritz and Holser, 1991) and the western Dolomites (Horacek et al., 2007a) it appears that this may have affected the interpretation of the Gartnerkofel-1 core. This means that the decline in bioturbation intensity in the upper part of the Gartnerkofel-1 core (Twitchett and Wignall, 1996) correlated to the Campil Member may actually correspond to the regression associated with the upper Siusi Member. The reduction in bioturbation, elevated extinctions and the subsequent decline in sample diversity into the Gastropod Oolite member (Figure 4.15) may, therefore, be the first evidence for a late Dienerian biotic crisis associated with the negative isotope excursion. At the same time, widespread anoxia is recognised from marine platforms in China (Galfetti et al., 2008), India (Galfetti et al., 2007a) and Pakistan (Hermann et al., 2012; Romano et al., 2012) and sea surface temperatures increased (Romano et al., 2012). Further environmental deterioration in the upper Dienerian, therefore, may have been global, although no environmental deterioration has yet been recorded from the Dolomites.

The subsequent Gastropod Oolite Member records no new taxa and no extinctions but nevertheless records the Induan/Olenekian positive isotope peak, followed by a negative isotope excursion (Horacek et al., 2007a; Posenato, 2008b). Although the composition of the benthic faunas in the Smithian Gastropod Oolite and Campil members is similar to those of the Induan, suggesting that the late Dienerian crisis and the subsequent environmental changes during deposition of the Gastropod Oolite Member did not cause a major disruption to the benthic invertebrate community, the Gastropod Oolite Member is less rich functionally than the Mazzin and Siusi members (Figure 4.17). Functional diversity is an important proxy for the health of marine ecosystems (Dineen et al.,

2014), therefore, the low functional diversity of the Gastropod Oolite Member suggests that benthic marine ecosystems were stressed during the Induan/Olenekian, transition in association with a cluster of rapid positive and negative isotope excursions. In addition, the taxa that occur and dominate assemblages from the Mazzin, Siusi and Gastropod Oolite members are characterised as cosmopolitan opportunists or generalists (Schubert and Bottjer, 1995; Fraiser and Bottjer, 2004; Fraiser et al., 2005; Fraiser, 2011), and so, the lack of recovery of endemism and complex specialists may explain why there is no significant change to the benthic marine community.

Campil Event

Continuous warming during the Smithian (Sun et al., 2012; Romano et al., 2012) and/or changes in the topography of the hinterland (Twitchett, 1999) may have caused the increased siliciclastic content in the upper Gastropod Oolite and Campil members that resulted from increased humidity, weathering and runoff (Haas et al., 2012). In addition, the base of the Campil Member is characterised by large load structures (~50cm) and Twitchett (1999) hypothesises that if these loaded horizons were caused by liquefaction during earthquake activity then it would suggest large-scale tectonic activity during the Smithian that could have produced major topographic changes in the hinterland which would have affected clastic input (Twitchett, 1999). In the Bódvaszilas Sandstone Formation, Hungary, which was affected by high sedimentation rates, taxonomic assemblages exhibit low diversities and are dominated by cf. *Unionites* (see Chapter 3). In the clastic beds of the Campil Member the same is observed (Hofmann et al., 2015a), which supports previous suggestions, e.g. Twitchett, (1999) and Posenato (2008b) that high sedimentation rates, eutrophication and salinity fluctuations caused a biotic crisis during the Smithian in the western Palaeotethys.

Despite a dominance of siliciclastic deposits, some carbonate beds are recorded in the Campil Member (Figure 4.8). Nine quantitative samples were collected from these

carbonate beds and they record the highest median alpha diversity recorded in the Werfen Formation. The taxonomic and functional composition of the assemblages is comparable to the lower part of the Werfen Formation (Figure 4.20). The Campil Member also records an increase in origination rates (Figure 4.15A) including the appearance of two modes of life (epifaunal, unattached, suspension feeders and semi-infaunal, stationary, attached, suspension-feeders) associated with the radiation or immigration of the bivalves *Avichlamys, Leptochondria, Scythentolium* and *Bakevellia* (Posenato, 2008a; Hofmann et al., 2015a). In addition, the size of cf. *Unionites* increases into the Campil Member (Metcalfe et al., 2011) and *Asteriacites* (formed by ophiuroids) also occur (Leonardi, 1935; Twitchett and Wignall, 1996). The Smithian 'Campil Event' therefore, represents a restriction of diverse benthic assemblages during periods of high sedimentation and increased runoff (cf. Twitchett, 1999) but does not record an overall biotic crisis.

Smithian/ Spathian event and subsequent recovery

Pelagic global diversity declines across the Smithian/Spathian boundary (Orchard, 2007; Stanley, 2009) and conodonts decrease in size (Chen et al., 2013), associated with a positive carbon and oxygen isotope peak and high sea surface temperatures (Sun et al., 2012; Romano et al., 2012), but a Smithian/Spathian event has not been recognised in the benthos (Hofmann et al., 2014; Hofmann et al., 2015a). Taxonomic compositions of assemblages in the Spathian are, however, significantly different from those of the Smithian (Figure 4.20), and the Smithian/Spathian boundary in this study is characterised by elevated extinction and origination rates (Figure 4.15). A shift in taxonomic composition across the Smithian/Spathian boundary in the western USA has been attributed to the increasing relative abundance of previously rare taxa (Hofmann et al., 2014). In the Dolomites, on the other hand, the changes are better attributed to taxonomic turnovers, with the extinction and decrease in dominance of small

gastropods, *Polygyrina* sp. A*, Coelostylina werfensis,* cf. *Worthenia* and *Pseudomurchisonia kokeni,* and the origination and dominance of *Natiria costata* and *Werfenella rectecostata*. If due to a biotic crisis, this change is limited to a few metres of rock that occurred in the upper Smithian or lowermost Spathian. Yet, a single inner shelf sample from the top of the Val Badia Member comprises a cf. *Unionites* biofacies and is not significantly different from the *Unionites* biofacies recorded prior to the Spathian. This suggests that harsh environmental conditions in inner shelf settings persisted into, at least, the lower Spathian.

Advanced biotic recovery following the late Permian extinction is inferred to have occurred in the Spathian (Twitchett and Wignall, 1996; Twitchett, 1999; Twitchett et al., 2004). This is associated with increased ichno- and skeletal faunal richness, ichnotaxa associated with the activity of infaunal crustaceans, increased bioturbation, increased burrow depth, increased burrow diameter and the recovery of stenohaline high tier filter feeders taxa such as crinoids. This study also shows that the recovery of the onshore-offshore gradient in taxonomic assemblages occurs in the Spathian, i.e. increase in β-diversity (Figure 4.21). The mid-shelf Val Badia Member records a very similar fauna to the Spathian mid-ramp Szin Marl Formation, Hungary (Chapter 3) composed of ophiuroid and crinoid ossicles, microconchids, *Natiria costata, Eumorphotis and Bakevellia*. Diverse mid-shelf deposits from the western USA also show similar faunal assemblages dominated by *Eumorphotis* and *Bakevellia* (Hofmann et al., 2013a). The recovery during the Spathian may be associated with an increased latitudinal temperature gradient and cooler global temperatures (Brayard et al., 2006) allowing improved ocean circulation and the initial retreat of the oxygen minimum zone, and reduction in sedimentation rate (Table 4.5). The reduction in sedimentation rate may provide an explanation for a shift from infaunal suspension feeding to motile, epifaunal, grazing across the Smithian/Spathian boundary in the mid-shelf environment.

Table 4.5: Changes in the linear sedimentation rate during deposition of the Werfen Formation.

Stage/ sub-stage	Thickness (m)	Duration (myr)	Sedimentation rate (m/myr)
Siusi section			
Induan	146	0.9	162
l'Uomo and Costabella section			
Induan	198.5	0.9	221
Smithian	146	0.6	243
Val Averta section			
Spathian	157	3.4	46

In addition, stenohaline taxa, e.g. crinoids, and *Neoschizodus ovatus*, appear and dominate assemblages in the Spathian, suggesting that large salinity fluctuations associated with high sedimentation rates and increased runoff, previously restricting stenohaline taxa (Posenato, 2008b), were not present in the Spathian.

Shallow subtidal environments in the Werfen Formation only appear to have recovered in the late Spathian. Comparing the ichnofaunal richness and level of bioturbation between the peritidal and shallow subtidal horizons in the upper Campil Member (late Smithian), Unit B of the Cencenighe Member (Mid-Spathian) and San Lucano Member (late Spathian) shows that improvements do not occur until the San Lucano Member. In addition, crinoid ossicles are not abundant, i.e. dominate bioclasts assemblages, in the subtidal and peritidal shoals, until unit C of the Cencenighe Member. Biofacies dominated by grazers were not recognised in the inner shelf settings of the mid- to late Spathian Cencenighe and San Lucano members, but there is a reduction in the abundance of wrinkle structures and trace fossils such as *Gyrochorte* serve as evidence for the re-establishment of grazing in these shallow environments. A reduction in sedimentation would have led to reduced stress on grazing modes of life (Algeo and Twitchett, 2010) facilitating their recovery. It would also have provided favourable habitats for macrophytes and the re-establishment of oligotrophic conditions that would

have favoured the recovery of benthic invertebrates. Recovery within the Spathian have also been recorded elsewhere with increased burrow sizes in northern Italy (Twitchett and Wignall, 1996; Twitchett, 2007), south China (Chen et al., 2011) and Svalbard (Worsley and Mørk, 2001); intense bioturbation in northern Italy (Twitchett and Wignall, 1996; Twitchett and Barras, 2004), the Bükk Mountains, Hungary (Hips and Pelican, 2002) and Aggtelek Karst, Hungary (Chapter 3); conifer-dominated forests on land (Looy et al., 1999); the establishment of reefs on the Great bank of Guizhou, China (Payne et al., 2006b); and *Placunopsis* bioherms in western USA (Pruss et al., 2007) in the late Spathian.

The recovery recorded in the Werfen Formation is only evidenced by bivalves, gastropods, one scaphopod genus, one crinoid genus, one ophiuroid genus, microconchids and trace fossils. The taxa that characterise the Werfen Formation, even in the Spathian, are mostly cosmopolitan and not endemic to the western Palaeotethys. The recovery of brachiopods, echinoids, holothuroids, sponges, bryozoans, corals, following the late Permian mass extinction in the western Palaeotethys took longer than five million years. Even those groups that initially recovered in the Early Triassic, i.e. bivalves and gastropods, were still recovering into the Middle Triassic (Erwin and Pan, 1996; Posenato, 2008b). The survival and recovery during the Werfen Formation was limited to the transitional zone between the proposed 'habitable zone' (Beatty et al., 2008) and anoxic conditions in the distal mid-shelf to the inner shelf, but also includes the shallow subtidal shelf in the late Spathian. Sluggish ocean circulation, sea-level changes, high sea surface temperatures, nutrient loading and high primary productivity may have limited benthic invertebrates to a reduced habitable space that would have affected their survival and recovery.

5. Eastern Lombardy, Italy

5.1 Stratigraphy

The biostratigraphy of the Servino Formation is not well constrained. Ammonoids are rare and although conodonts have been recorded, their precise stratigraphic occurrences have not been published. Other macro and microfauna that are used for biostratigraphy in other central European Lower Triassic successions are also rare. A review of the stratigraphical framework for the Servino Formation is given by Sciunnach et al. (1999). An improved stratigraphical framework is presented here based on: (i) the correlation with the Lower Triassic succession of the Balaton Highlands, Hungary, as these sediments are lithologically similar (personal observation); (ii) new finds of ammonoids, conodonts and bivalves made in this study; (iii) and the production of the first isotope curve for the entire formation.

Ca'San Marco Member

The Ca'San Marco Member comprises grey, laminated siltstones and bedded dolostones with a similar lithology to the Köveskál Dolomite Formation, Hungary (personal observation), which was deposited throughout the Induan (Figure 5.1). In the Orobic anticline Posenato et al. (1996) identified within it *Claraia intermedia,* and in the Val Fontanalle section of the Camuna anticline, *C. aurita* has been identified 15m above its base (Cassinis, 1990; Cassinis et al., 2007), indicating deposition during the Dienerian *C. aurita* s.s biozone (*sensu* Chapters 3-4).

Gastropod Oolite Member

The overlying Gastropod Oolite Member is made up of decimetre to metre thick beds of red oolitic grainstones that contain a high abundance of microgastropods (Sciunnach et al., 1999) and has been correlated to the Gastropod Oolite Member of the Werfen Formation (Cassinis, 1968, Assereto and Rizzini, 1975). The lack of zonal markers in

-149-

the Gastropod Oolite Member of Lombardy makes this correlation equivocal as the oolitic-bioclastic beds that characterise this member in the Werfen Formation are also common in the Siusi and Campil members (Chapter 4; Sciunnach et al., 1999; Posenato,
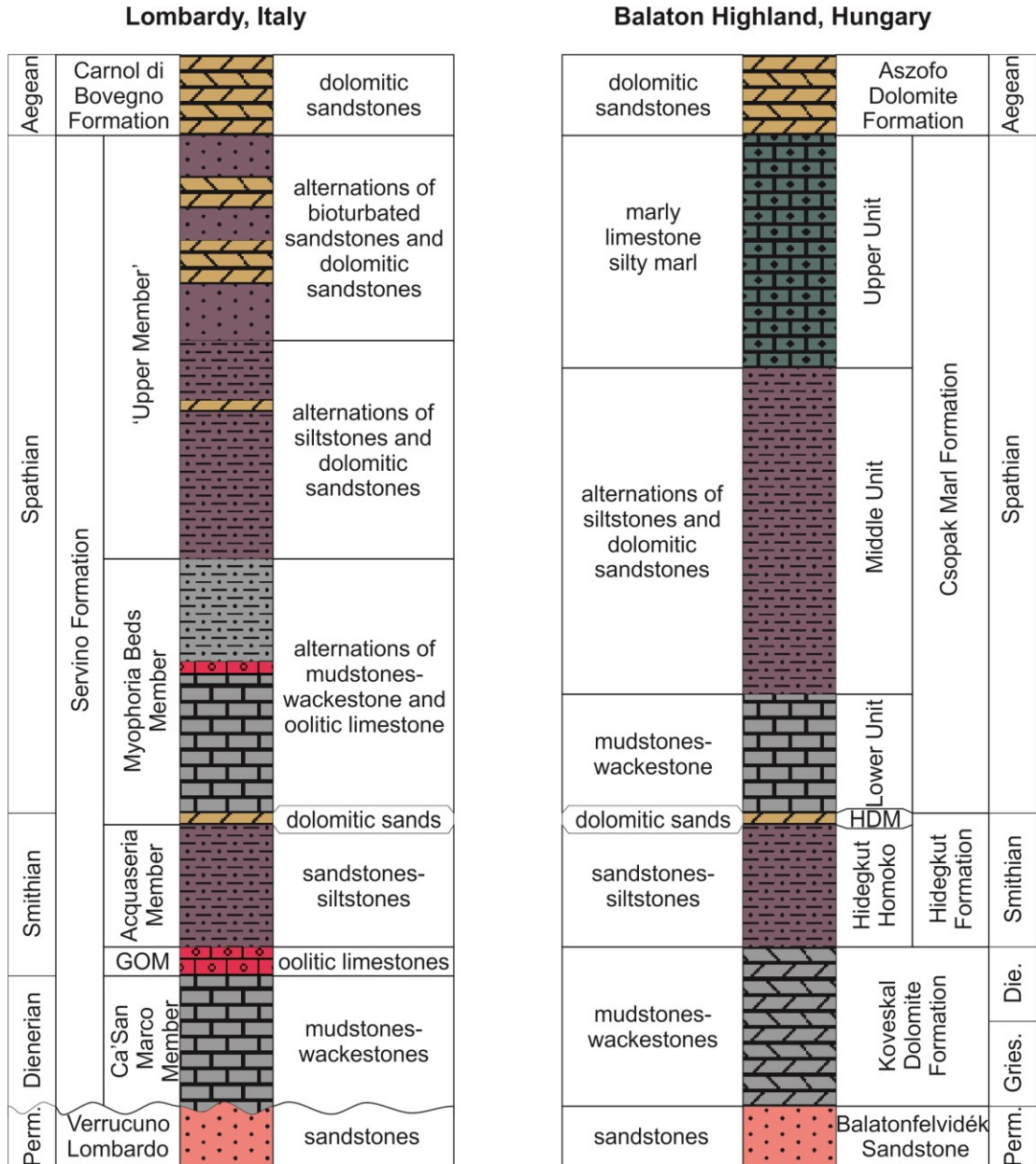
Figure 5.1: Lithological correlation between the Servino Formation, Italy, and the Lower Triassic succession of the Balaton Highland, Hungary. Lithostratigraphy of Hungary after Broglio Loriga et al. (1990). Vertical subdivision is thickness proportional (this study; Broglio Loriga et al., 1990). HDM = Hidegkút Dolomite Member. Perm. = Permian; Gries. = Griesbachian; Die. = Dienerian. GOM = Gastropod Oolite Member.

2008b), as well as in the younger "Myophoria Beds" Member of the Servino Formation. Conodonts recorded by Twitchett (2000) from the Gastropod Oolite Member suggest deposition during the *P. obliqua* zone which ranges from the Dienerian to Smithian.

Acquaseria Member

The Acquaseria Member consists of laminated siltstones and sandstones, and on the other hand, is lithologically similar to the Campil Member of the Werfen Formation (Chapter 4) that represents a local expression of the siliciclastic event that has been recognised across the Lower Triassic successions of Europe during most of the Smithian sub-stage (Twitchett, 1999). Conodonts recorded by Twitchett (2000) contain Pa elements belonging to the Smithian *Furnishius-Foliella* assemblage.

"Myophoria Beds" Member

Between the Acquaseria and "Myophoria Beds" members there is a ~10m peritidal unit comprising laminated, grey siltstones alternating with yellow, vuggy, sandy gypsum-bearing dolomite. This unit is lithologically similar to the Hidegkút Dolomite Member, Hidegkút Formation, Hungary (Figure 5.1), that was originally correlated with the supratidal-peritidal unit originally included within the Spathian Val Badia Member, Werfen Formation, by Broglio Loriga et al. (1990). This unit in the Werfen Formation, however, is now included in the uppermost part of the Smithian Campil Member, Werfen Formation (Posenato 2008b; Hofmann et al., 2015a). In the Path 424 section, analysed in this study, however, the member yields the gastropod *Natiria costata*, which is considered as being indicative of the Spathian (Neri and Posenato, 1985). Therefore, here this unit is included within the "Myophoria beds" Member and is interpreted as basal Spathian following the original interpretation by Broglio Loriga et al. (1990).

The remaining part of the "Myophoria Beds" Member can be correlated to Unit A of the Csopak Marl Formation, Hungary, and comprises bioturbated siltstones, oolitic-

bioclastic limestone and limestone beds. A diverse suite of fossils is reported from the Csopak Marl Formation, Hungary, and the "Myophoria Beds" Member also has a rich fauna including *Natiria costata, Werfenella rectostata, Neoschizodus ovatus, Costatoria costata, Eumorphotis telleri,* cf. *Tirolites cassianus, Dinarites* sp. and cf. *Holocrinus* (this study; Sciunnach et al., 1999). Its fauna and lithology are also similar to the lower Spathian Val Badia Member and to unit A of the Cencenighe Member of the Werfen Formation. Based on the occurrences of cf. *Tirolites cassianus* (this study) and *Dinarites* sp. the "Myophoria Beds" Member is correlated with the *Tirolites cassianus* Ammonoid Zone of Posenato (1992), i.e. lower Spathian.

"Upper Member"

The "Upper Member" can be divided into two parts. The lower part mostly comprises laminated red siltstones, whereas the upper part comprises bioturbated siltstones alternating with yellow, vuggy, sandy dolomite (Figure 5.1). These two parts correlate respectively to units B and C of the Csopak Marl Formation, Hungary. Fossils are rarely recorded from the "Upper Member" of the Servino Formation (Cassinis, 1968) making biostratigraphic correlations equivocal. *Meandrospira pusilla* was reported in the dolostone-rich facies of the "Upper Member" (Gaetani, 1982), but unfortunately this long-ranging taxon spans the Spathian to Anisian. The frequency and thickness of the yellow, sandy dolomite alternations increase going up section and the "Upper Member" grades into the Middle Triassic Carniola di Bovegno Formation (personal observation). The boundary between the Servino and Carniola di Bovegno formations, in this study, is interpreted at the top of the last bioturbated siltstones, and is tentatively correlated to the Lower/Middle Triassic boundary. The lower part of the "Upper Member" is therefore inferred to have been deposited coevally with the Middle Unit of the Csopak Marl Formation in the mid-Spathian and the upper part (bioturbated facies) is interpreted as

correlating with the Upper Unit of Csopak Marl, i.e. Upper Spathian (*T. carniolicus* ammonoid zone).

5.1.1 Conodonts

Conodonts from the Servino Formation were first investigated by Twitchett (2000) who recorded high abundances (>100 per kg) within the bioclastic tempestites of the Gastropod Oolite and Acquaseria members. In this study 12 samples were collected for
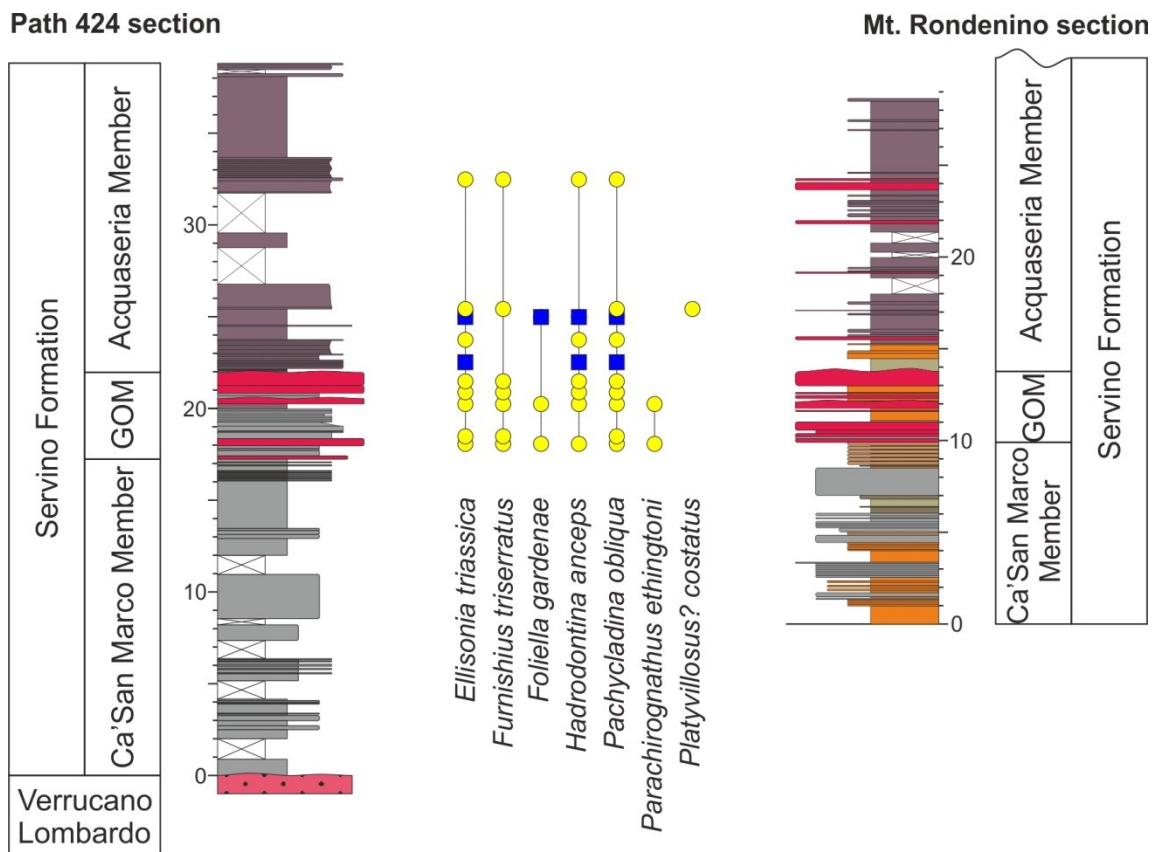
Figure 5.2: Stratigraphic ranges and occurrences of conodont elements from the Servino Formation. Conodont occurrences from the Path 424 section are indicated by yellow circles and from the Mt. Rondenino section by blue squares. Correlation between the sections is based on the large microgastropod-grainstone bed at the top of the Gastropod Oolite Member. GOM = Gastropod Oolite Member. Conodont data from the Mt. Rondenino section after Butler (2002), i.e. blue squares.

dissolution from the Gastropod Oolite, Acquaseria and "Myophoria Beds" members. Only seven of the samples yielded conodonts, five from the Gastropod Oolite Member and two from the Acquaseria Member. These data were combined with unpublished data from the Gastropod Oolite and Acquaseria members of the Path 424 section (Butler, 2002; Figure 5.2). *Pachycladina obliqua, Ellisonia triassica, Hadrodontina anceps, Foliella gardenae, Furnishius triserratus* and *Parachirognathus ethingtoni* all occur in the Gastropod Oolite and Acquaseria members and can be correlated to the Smithian *Parachirognathus-Furnishius* Conodont Zone of Sweet et al. (1971). Whereas, previously only the Acquaseria Member was included in this conodont zone. The occurrence of these conodont species in the basal beds of the Gastropod Oolite Member (Figure 5.2) suggests, for the first time using biostratigraphy, that the Gastropod Oolite Member was deposited during the Smithian.

5.1.2 Chemostratigraphy

A new isotope curve for the Servino Formation was produced from the Path 424 section (Figure 5.3). The carbonate content of the Ca'San Marco, Acquaseria and "Upper" members was low and fewer data were obtained from them. The Gastropod Oolite and "Myophoria Beds" members, however, have high carbonate content and most of the samples produced $\delta^{13}C$ data. The carbon isotope curve shows a large positive isotope excursion within the upper part of the Ca'San Marco Member, in the absence of a facies change (Figure 5.3).Values increase from -3.5‰ to +4.7‰ which corresponds to carbon isotope peak B in Horacek et al. (2007b) and correlates with the global event near the Induan/Olenekian boundary (Payne et al., 2004; Richoz, 2006; Horacek et al., 2007a). Although the isotope peak does not precisely indicate the Induan/Olenekian boundary, this boundary in the western Palaeotethys can be recognised at a sequence boundary within a few metres above (Posenato, 2008b). In this study, a sequence boundary was not recognised in the Path 424 section near this isotope peak, and so the facies change at
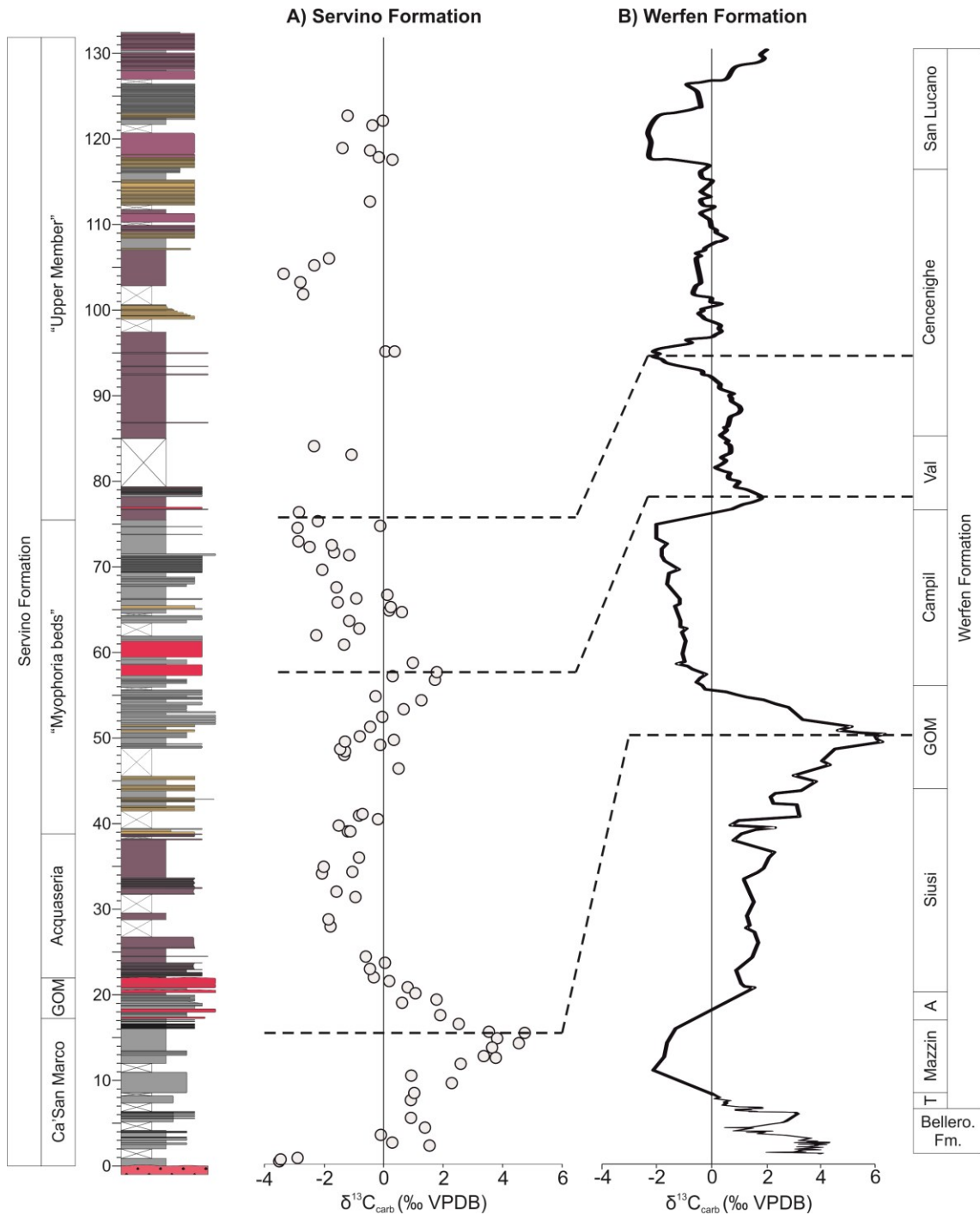
Figure 5.3: Carbon isotope profile from the Path 424 section and composite curve for the Werfen Formation, Italy (Chapter 4). Bellero = Bellerophon, GOM = Gastropod Oolite Member, T = Tesero Member, A = Andraz Member, Val = Val Badia Member. Colour in the lithology column refers to the rock colour observed in the field.

the base of the Gastropod Oolite Member, which occurs ~3m above the isotope peak, is interpreted as correlating with the Induan/Olenekian boundary.

Carbon isotope values decline to -2.0‰ in the middle part of the Acquaseria Member which confirms its lithological correlation with the Campil Member (*sensu* Horacek et al., 2007a). Carbon isotope values then rise to +1.72‰ at 18m above the base of the "Myophoria beds" Member, which corresponds to a similar peak recognised within the lower Val Badia Member, and correlates to a global event within the lower Spathian (Payne et al., 2004; Richoz, 2006; Sun et al., 2012). Values reach a minimum of -2.9‰ in the basal "Upper Member", which corresponds to a negative isotope peak recognised in the Unit B of the Cencenighe Member, Werfen Formation (Chapter 4; Figure 5.3).

The carbonate content in the samples collected from the "Upper Member" is low and only 16 samples yielded data making any correlation equivocal. These samples do appear to record a negative isotope peak of -3.4‰ at 105m, which may correlate with the negative isotope peak recognised in the San Lucano Member at Val Averta (Chapter 4; Figure 5.3). Within this isotope excursion, bioturbation increases from ii1 to ii5 in the "Upper member". Likewise, in the Val Averta section intense bioturbation is associated with the negative isotope excursion (Chapter 4). The carbon isotopes, therefore, provide some support for the correlation of the "Upper Member" with the San Lucano Member of the Werfen Formation.

5.2   Facies Analysis

In the Early Triassic, the Servino Formation was located on the proximal western edge of a broad shelf on the Palaeotethys margin (Csontos and Vörös, 2004). The lithology and facies of the mixed siliciclastic-carbonate succession from eastern Lombardy is similar to those recognised in the Balaton Highlands, Hungary (Haas and Budai, 1999; Koloszár, 1992; personal observation). The Servino Formation represents a more

proximal marine setting than the Werfen Formation and is represented by a 120-200m thick succession which is more condensed than the Werfen Formation (Sciunnach et al., 1996). The following facies analysis is based on the Path 424 and Mt. Rondenino sections (Figure 5.4; 5.5). Seven facies were recognised (Table 5.1), and their description follows the depth profile from shallow to deep (Figure 5.7).

Facies 1: gypsum-bearing dolomitic sands (peritidal).

Description: This facies is characterised by coarsening-upward successions ranging 1-2m in thickness. The base of the successions comprise grey planar laminated calcareous siltstones alternating with bedded (2-4cm) fine yellow vuggy (dolomitic) sandstones that transitionally increase in thickness from the base to the top of the sets. Grey decimetre-thick mudstones containing flat pebbles also occasionally intercalate. On the sandstone beds, convex-up bivalves occur at their bases and Twitchett (unpublished log) recognised nodular, chicken-wire structured, gypsum within these beds. Occasional *Skolithos* traces were also observed. This facies occurs at the base of the "Myophoria Beds" Member and in the "Upper Member".

Interpretation: The same lithologies and sedimentary structures were also recognised in the Hidegkút Dolomite Member, Hungary, which was interpreted as being deposited in the coastal part of a hypersaline lagoon (Haas and Budai, 1999). The nodular, chicken-wire, gypsum recorded in this facies is typical of gypsum-anhydrite precipitated in marine sabkha environments (Kinsman, 1969). The vugs were probably formed via dolomitisation (Naggy, 1999). The bedded dolomitic sandstones were deposited in a peritidal setting with the dolomite produced through evaporitic pumping in an arid/ semi-arid climate (Haas et al., 2012). Flat pebbles within the carbonate beds represent deposition on the marine sabkha during storms (Sepkoski, 1982).

Facies 2: bioturbated sandstones (shallow subtidal).

Description: highly bioturbated (ii3-5) purple fine sandstones and siltstones. Grey laminated siltstones occasionally intercalate. Beds are massive and range in thickness from 33-245cm. Occasionally, *Planolites* and *Rhizocorallium* burrows can be
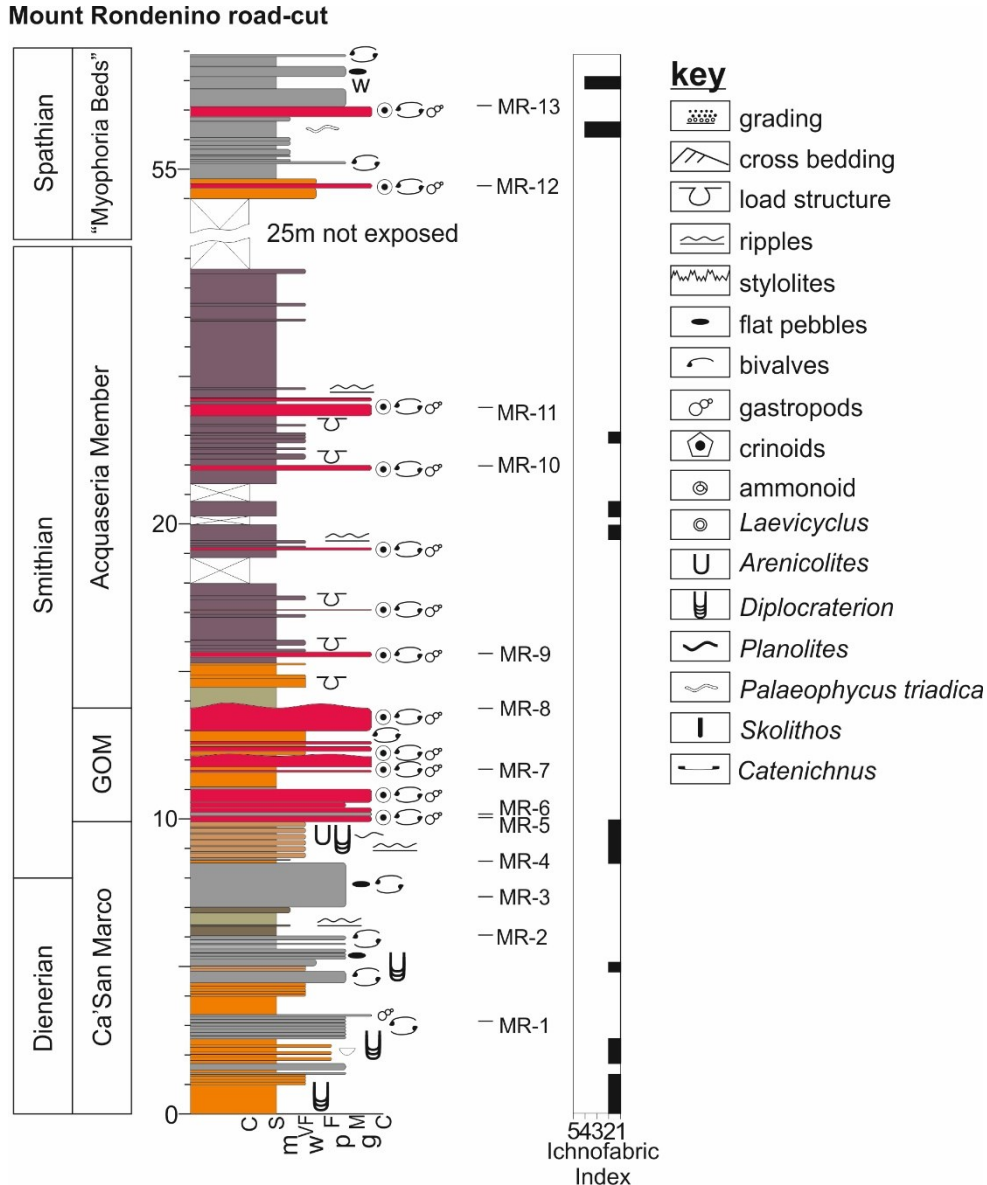
Figure 5.4: Log of the Mt. Rondenino road cut section with information on sedimentary structures, fossil content, collected samples (e.g. MR-1) and Ichnofabric index. Grain size scale: C = clay, S = siltstone, VF = very fine sand, F = fine sand, M = medium sand, m = mudstone, w = wackestone, p = packstone, g = grainstone.
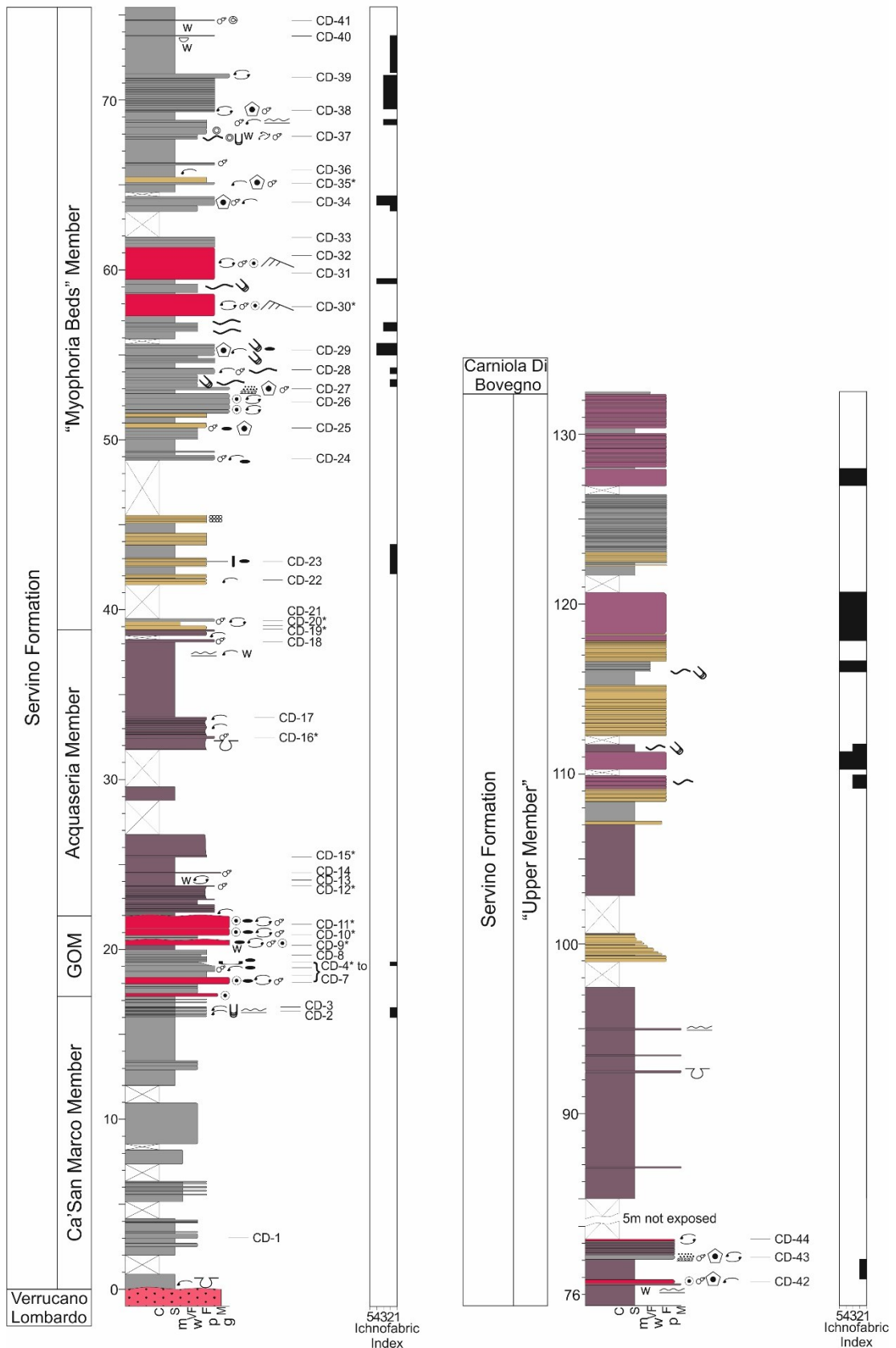
Figure 5.5: Log of the path 424 section with information on sedimentary structures, fossil content, collected samples (e.g. CD-1) and Ichnofabric index. Samples for also collected for acid dissolution are marked with *. Key in Figure 5.4.

recognised. The strong bioturbation means that other sedimentary structures are not preserved. This facies alternates with facies 1 in the upper part of the "Upper Member".

Interpretation: The intense bioturbation and lack of sedimentary structures makes the interpretation of this facies problematic. The dominance of coarse terrigenous material and the alternation with Facies 1 suggest that deposition took place in a shallow subtidal environment.

Facies 3: bedded mudstones and wackestones (shallow subtidal).

Description: This is characterised by planar laminated and cm-bedded grey silty mudstones and wackestones. The mudstones are often stylonodular or with small ball and pillow structures; beds with higher sand content preserve symmetrical ripples. Beds with higher siliciclastic content weather orange. In the topmost part of this facies the siliciclastic component becomes coarser (sand-size) and begins to alternate with thickening oolitic beds of facies 4. In addition, bioclastic beds and bioturbation occur in the topmost parts. This facies characterises the Ca'San Marco Member and the middle part of the "Myophoria Beds" Member, and can be divided into two subfacies based on the different fauna and degree of bioturbation observed in the two members.

Subfacies 3.1: In the Ca'San Marco Member ichnofabric indices range from ii1-2, bioturbation is represented by *Diplocraterion* and *Catenichnus,* and the shelly fauna are represented by microconchs, small (<1cm) gastropods and bivalves.

Subfacies 3.2: In the "Myophoria Beds" Member, the bioturbation ranges from ii1-4 and bioturbation is represented by *Rhizocorallium* and *Planolites*. The shelly fauna from the "Myophoria beds" is characterised by crinoids, ophiuroids, microconchs, larger (>1cm) gastropods and bivalves.

Table 5.1: Summary of facies described from the Servino Formation.

Facies	Lithology	Sedimentary structures	Depositional environment
1	Grey calcareous siltstones alternating with yellow dolomitic sandstones. Chicken-wire structured gypsum.	Parallel-laminated siltstones alternating with bedded sandstones. Flat pebbles. Bivalves occur convex-up at the base of sandstone beds. *Skolithos* and gastropods also occur.	Marine sabkha (supratidal to peritidal)
2	Fine- to medium-grained purple sandstones.	Moderate to strong bioturbation (ii3-5) overprinting sedimentary structures. *Planolites* and *Rhizocorallium*. In the absence of bioturbation, beds are planar-laminated.	Sand flat
3	Grey silty mudstones interbedded with very-fine sandstones.	The sandstones have rippled tops. The siltstones are laminated and occasionally with ball and pillow structures. Convex-up bivalves, *Diplocraterion*, *Rhizocorallium* and *Planolites* occur on bedding planes.	Inner shelf, subtidal intershoal (carbonate)
4	Purple siltstones and sandstones	Planar laminated. Wrinkle marks and symmetrical ripple marks on bedding surfaces.	Inner shelf, subtidal intershoal (siliciclastic)
5	Red-pink sandy oolitic limestones	Cross bedding in thicker beds and planar bedding in thinner beds. Hummocky tops, flat pebbles, rhomboidal dolomite.	Shoal
6	Grey marly limestones	Laminated siltstones, wrinkle marks, ripple marks, bivalves, gastropods and crinoids. Bioturbation (ii1-4), *Planolites*, *Laevicyclus* and *Diplocraterion*.	Mid-shelf
7	Grey siltstones interbedded with thin grey packstones.	Planar laminated, gutter casts, ammonoids, gastropods, bivalves and wrinkle marks.	Distal mid-shelf

Interpretation: This facies reflects an open or restricted shallow-subtidal lagoon environment deposited above fair-weather wave-base. The coarser intervals represent higher energy settings and improved oxygenation as inferred from the increase in bioturbation and the presence of benthic fauna. Sharp bases to limestone beds and randomly orientated bioclasts indicate storm reworking (Torok, 1998). The presence of stenohaline taxa in the "Myophoria Beds" also indicates a normal marine salinity. Coarsening-up and the increasing alternation of oolitic beds at the top of this facies are inferred to represent shallowing towards the oolitic and sand shoals of facies 5.

Facies 4: laminated purple siltstones and sandstones (shallow subtidal).

Description: This facies can be split into two subfacies.

Sub-facies 4.1: Planar laminated darker purple siltstones intercalated by thin beds of lighter fine purple well-sorted sandstones. The siltstone beds have wrinkle marks on bedding planes. The sandstone beds have symmetrically rippled tops and convex-up bivalves occur on the top of beds.

Sub-facies 4.2: Planar, cm-bedded, purple, well-sorted very-fine and fine sandstones alternating with thin beds of laminated purple siltstones. These beds are also occasionally intercalated by thin oolitic grainstones. Within the sandstone beds sparsely distributed, randomly orientated bivalves occur. The oolitic grainstones contain gastropods, ophiuroids, and microconchids. There are also a few bivalve fragments. The sandstone beds also contain small ball and pillow structures, and are also occasionally weakly bioturbated by *Planolites*. The facies occurs throughout the Acquaseria Member, within the Gastropod Oolite Member and lower part of the "Upper Member".

Interpretation: These rocks were deposited in shallow subtidal environments, within the intershoal areas of lagoons. Broadly, the grain-size of siliciclastic sediments reflects hydraulic energy of the depositional environment, with the sandstones likely to have

been deposited by currents, and the finer sediments being deposited during calmer conditions. The well-sorted sandstones indicate wave agitation and winnowing in a setting above fwwb. These deposits occur in the absence of any tidal structures and are therefore interpreted as subtidal. Subfacies 1 was probably deposited in calmer settings of an inner shelf lagoon. Subfacies 2, represents shallower conditions with a greater proximity to oolitic shoals, indicated by the increase abundance of oolitic tempestites.

Facies 5: Sandy, oolitic grainstones (shoal).

Description: Thin- to thick-bedded (16-189cm) red-pink, oolitic-sandy grainstones. The thinner oolitic beds are occasionally grey. The oolitic grainstones have hummocky tops, parallel-bedding, flat pebble intraclasts and marl-lined stylolites. Some of the thinner beds are graded and intercalate with facies 3 and 4. Rhomboidal dolomite grains with sub-rounded margins occur within bioclasts and the matrix cement. The ooids are either well preserved with observable elliptical layers or replaced by rhomboidal dolomite. The thickest beds (130-189cm) show cross-bedded stratification. This facies occurs in the Gastropod Oolite, Acquaseria and "Myophoria Beds" members and the fauna within the beds differs between these members. The fauna within the Gastropod Oolite Member comprises small gastropods, ostracods, lingulids, bivalves, and microconchids and in the Acquaseria Member ophiuroid ossicles are recorded. The fauna is similar in the "Myophoria Beds" Member but black, thick-shelled bivalves and crinoid ossicles also occur. There is a high abundance of shell fragments within these beds. In some beds sand grains fill bioclasts and are supported in a calcite matrix. In addition, large amounts of siderite have been reported from this facies (De Donatis and Falletti, 1999).

Interpretation: The presence of ooids and cross-bedding suggests sediments were produced and accumulated in wave-agitated zones. These beds are interpreted as being deposited on the distal inner ramp where waves broke reworking the ooids and fauna, forming lenticular masses that may have stood no more than a few metres above the

seafloor. The lack of cross-bedding and the sheet-like geometry of the thinner oolitic beds indicate that they represent redeposited amalgamated lobes of shoals (cf. Hips, 1998). The hummocky tops, erosive bases and grading of the beds in this facies suggest that deposition took place during waning conditions of storm events. The red colouration is likely due to high iron concentrations as in the Aggtelek Karst (Chapter 3) and the Werfen Formation (Chapter 4). Ferroan dolomite is likely to have been formed on the landward side of shoals with the ferroic coating grains occurring during the reworking of sediments on the more oxygenated external side of shoals (Assereto and Rizzini, 1975). Flat pebbles are probably extraclasts derived from more proximal settings (Wignall and Twitchett, 1999).

Facies 6: laminated and bedded marly limestones (mid-ramp).

<u>Description</u>: Grey, marly wackestones and packstones with sharp, planar bases, planar lamination or hummocky cross stratification. In the basal 4 metres of the "Upper Member" grey marly wackestones are replaced by purple siltstones. The packstones contain randomly orientated bivalves, crinoids and large gastropods. The mudstones are bioturbated (ii1-4), and contain *Planolites, Laevicyclus* and *Diplocraterion*. Wrinkle marks and convex-up bivalves occur on unbioturbated beds. The packstones contain pyrite, large and small gastropods, crinoids, ophiuroids and randomly orientated bivalves, and they also have rippled tops.

<u>Interpretation</u>: Low-energy conditions between storms are indicated by the accumulation of finer sediments. The packstone beds represent deposition during storm events and the ripples that occur may have been produced by storm-induced currents. Hummocky cross-stratification is typically associated with storm waves and deposition between fwwb and swwb in the outer shoreface (Tucker, 2011). This facies is, therefore, interpreted to have been deposited below fwwb but above storm weather-wave base, i.e. in the mid-ramp. The beds with preserved trace fossils were deposited in the mid-ramp

setting during fair-weather conditions in an oxygenated environment (Török, 1998). The alternations of bioturbated and laminated mudstones and presence of pyrite probably suggest alternations of oxic and anoxic conditions associated with the expansion of an oxygen minimum zone during fair-weather periods.

Facies 7: laminated grey calcareous siltstones (Outer ramp).

Description: Laminated grey calcareous siltstones rarely interbedded by <1cm silty packstones. The packstones are characterised by abundant large gastropods, ammonoids and bivalves. Small gutter casts are present on the bases of the silty packstones. Siltstone bedding surfaces display wrinkle structures.

Interpretation: Deposition of laminated siltstones occurred in a low-energy environment below mean storm weather wave base. The coarser beds were deposited by storm currents during storms below mean storm wave base. The restriction of shelly fauna to the coarser beds suggests that shelly fauna were transported to this environment during storm events.
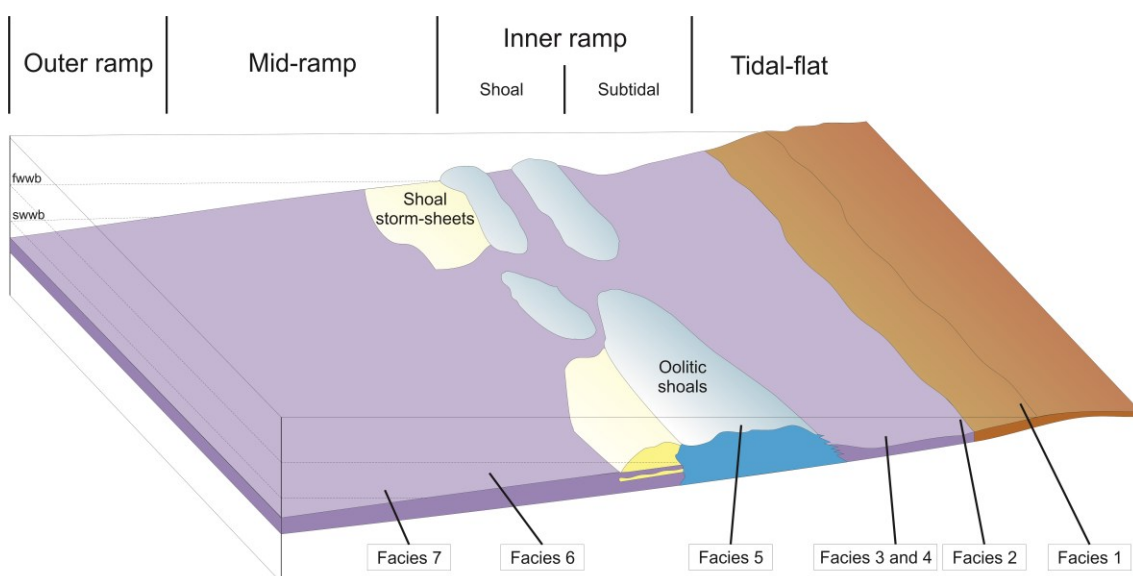
Figure 5.6: Schematic model of the Servino Formation shallow marine shelf. 1 – Marine sabkha, 2 – Sand flat, 3 – carbonate shallow subtidal, inner shelf, 4 – Siliciclastic shallow subtidal, inner shelf, 5 – Shoal, 6 – Mid-shelf, 7 – Distal mid-shelf.
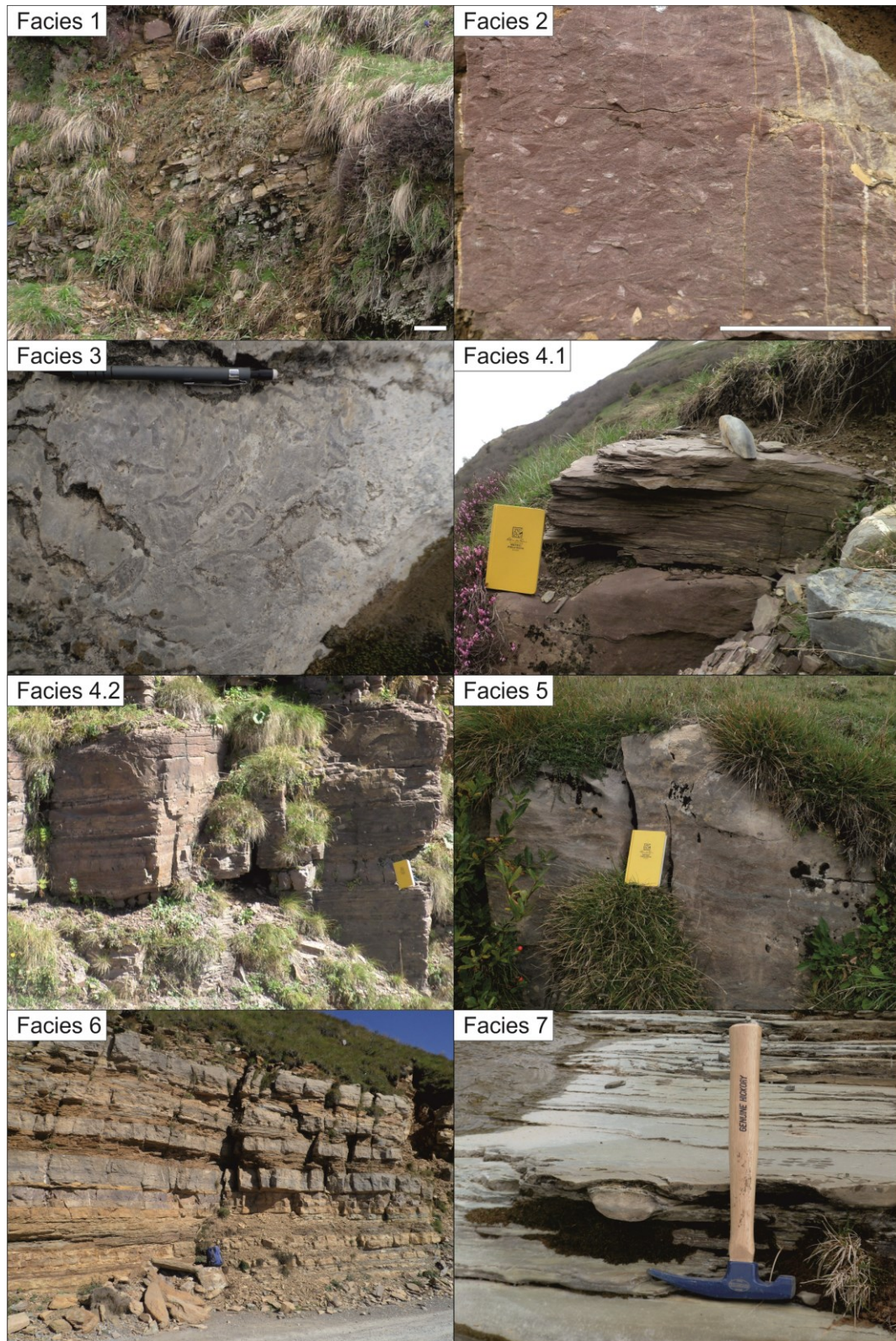
Figure 5.6 continued: Schematic model of the Servino Formation shallow marine shelf. 1 – Marine sabkha, 2 – Sand flat, 3 – carbonate shallow subtidal, inner shelf, 4 – Siliciclastic shallow subtidal, inner shelf, 5 – Shoal, 6 – Mid-shelf, 7 – Distal mid-shelf. Scale: field notebook = 19cm length, hammer = 27cm length, backpack = ~40cm , pencil and scale bar = 15cm.

5.2.1   Sea-level curve

Based on the facies analysis two overall sea-level transgressions can be identified: 1) at the base of the Servino Formation 2) at the base of the "Myophoria beds" (Figure 5.7). Complete Lower Triassic successions of the western Palaeotethys are characterised by four significant transgression-regression cycles (Hips, 1998; Posenato, 2008b). The Servino Formation in the studied sections starts with shallow marine deposition on top of a Permian alluvial plain that may correlate with the transgression observed at the base of the Dienerian elsewhere in the Palaeotethys (Broglio Loriga et al., 1990; Hips, 1998). The transition from the lagoonal facies of the Ca'San Marco Member into the shoal facies of the Gastropod Oolite Member reflects continual sea-level rise that correlates with a transgression identified around the Induan-Olenekian transition in the western Palaeotethys (De Zanche et al., 1993; Haas and Budai, 1999; Hips, 1998). This interpretation is supported by the bio-, litho- and chemostratigraphy of the Servino Formation (Figure 5.7). An overall regression then occurs throughout the Acquaseria Member, where this siliciclastic member is overlain by silty dolomites (base of the "Myophoria Beds" Member) that represent a peritidal environment and the Smithian-Spathian transition.

Another transgression-regression cycle began in the Spathian with deposition changing from the inner shelf to distal mid-ramp setting by the mid-Spathian (Figure 5.4). This transgressive event can also be correlated across the western Palaeotethys (De Zanche et al., 1993; Haas and Budai, 1999; Hips, 1998). Maximum flooding is marked by the abrupt appearance of ammonoids at the top of the "Myophoria Beds" Member. Deposition of the red siltstones then replaces grey laminated mudstones in the distal mid-ramp, followed by shallowing into an inner shelf environment in the lower part of the "Upper Member". The increasing alternation of the peritidal and subtidal facies at the top of the "Upper Member" indicates an overall regression.
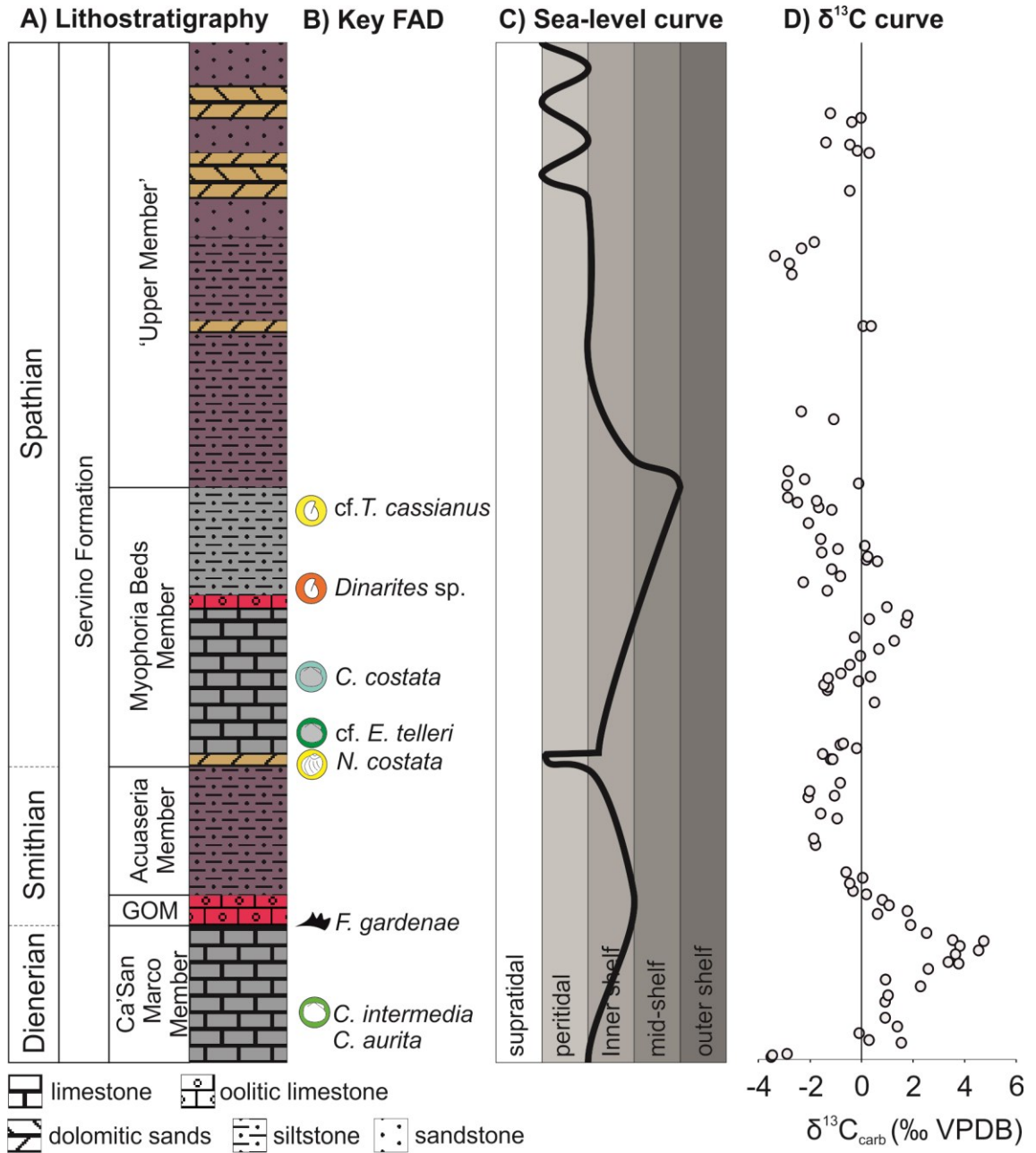
Figure 5.7: Summary stratigraphy of the Servino Formation. GOM = Gastropod Oolite Member. FAD = First appearance datums. Occurrences of *Claraia intermedia* after Posenato et al. (1996) and occurrences of *C. aurita* and *Dinarites* sp. after Cassinis et al. (2007). All other FAD's after this study.

5.3 Palaeoecological results

5.3.1 Alpha Diversity

A total of 10,234 MNI were identified in 58 samples from the Servino Formation and identified to the highest taxonomic level. These individuals represent 24 taxa of bivalves, gastropods, ophiuroids, crinoids, brachiopods, ostracods and microconchids (Figure 5.8-5.10; Table 5.2). The MNI per sample ranges from 1 to 1078, and 39 samples have a large enough abundance (i.e. >20 MNI) for quantitative analysis (Appendix 5.1).

The richness of samples ranges from 1 to 7 and the Simpson Diversity ranges from 1 to 4.3 (Figure 5.11). The most diverse sample, in terms of richness and Simpson diversity, comes from the 'Myophoria Beds' Member in shoal and mid-ramp sedimentary facies (Figure 5.11). The least diverse samples also come from the same member and sedimentary facies, as well as from the Acquaseria Member (Figure 5.11A). Sample richness and Simpson Diversity show very similar patterns (Figure 5.11). Differences in species richness between the different members are not significant ($p = 0.11$), but differences in the Simpson Diversity are, ($p = 0.02$) and the pairwise comparisons show that Simpson Diversity is significantly lower in the Acquaseria Member than the Ca'San Marco and "Myophoria Beds" Member (Table 5.3).

Changes in the alpha diversity of samples also appear to have an environmental aspect. Median richness is higher in the inner shelf, shoal and mid-shelf settings than the marine sabkha, siliciclastic inner shelf and distal mid-shelf environments. The differences, however, are not significant ($p = 0.39$), and the ranges of species richness values between the environments overlap (Figure 5.11B), suggesting that there is no significant environmental control. The median Simpson Diversity values, on the other
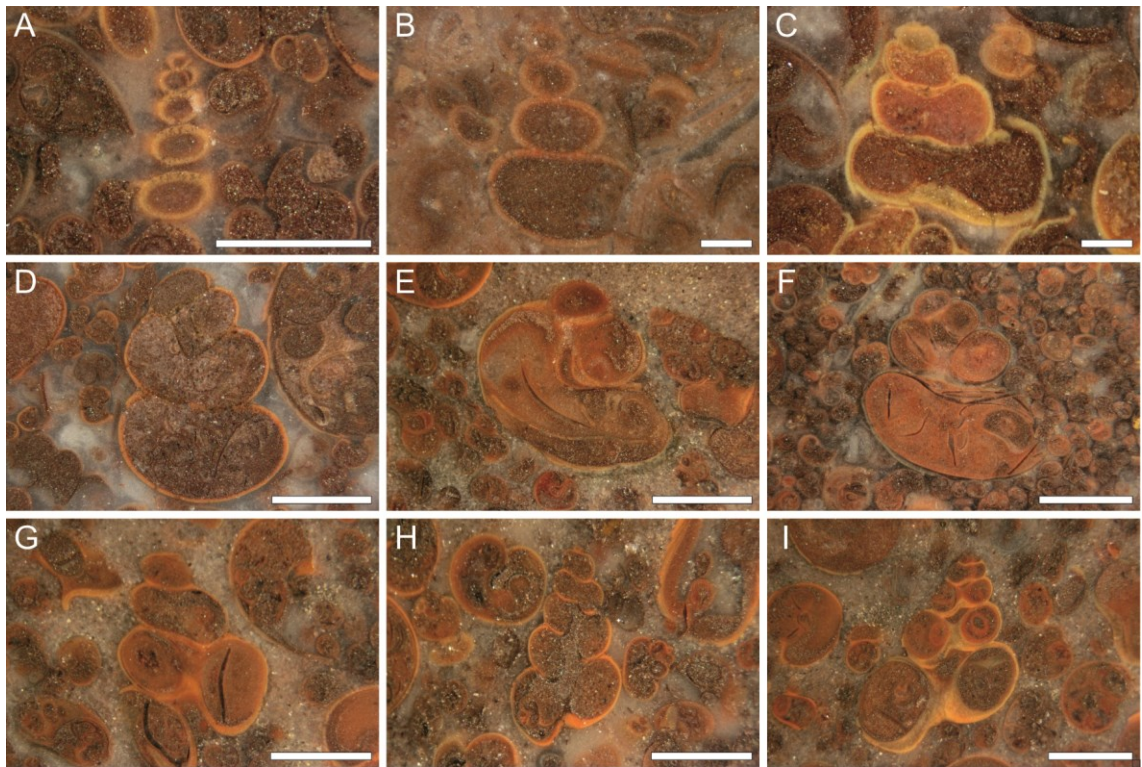
Figure 5.8: Selected serial sections of *Coelostylina werfensis* from the outer whorl to the central columella. A,D) CD-11. B) CD-10. C) MR-8. E, G-I) CD-12. F) MR-9. Scale bar = 1mm.

hand, are low, with highest values in the mid-shelf environment (Figure 5.11B), however, this difference is not significant ($p = 0.21$).

5.3.2 Alpha functional diversity

The Servino Formation taxa represent nine modes of life that mostly belong to suspension feeding lifestyles (Table 5.2). The functional richness of samples ranges from 1 to 6 and Simpson functional diversity ranges from 1 to 3.6 (Figure 5.12). As in alpha diversity the most functionally diverse samples are found in the "Myophoria Beds" Member, shoal and mid-shelf sedimentary facies. Trends in functional richness between the different members follow those of species richness (Figure 5.12A). The pairwise comparisons show that the Gastropod Oolite and Acquaseria members are significantly less functionally rich than the Ca'San Marco member (Table 5.4).
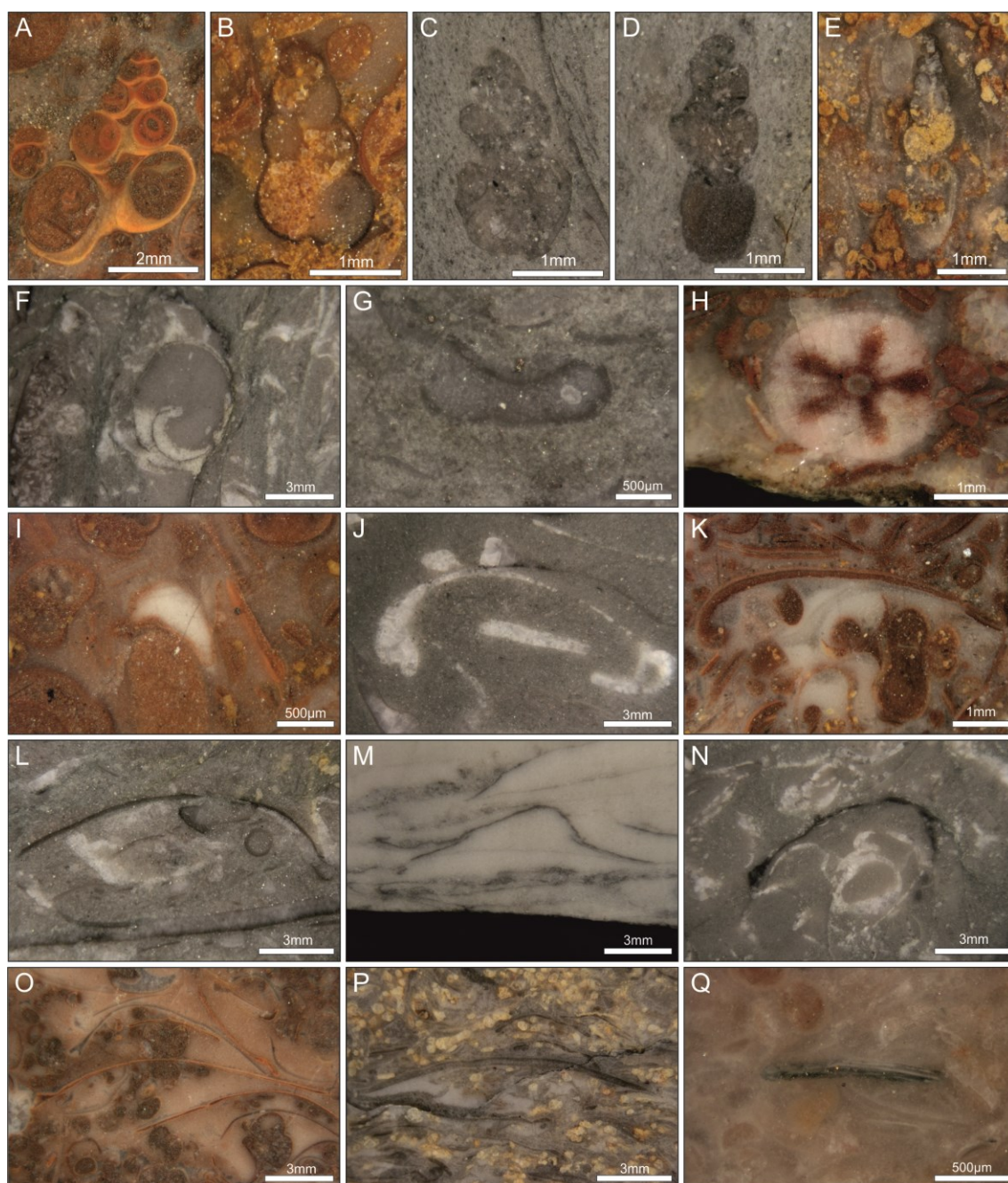
Figure 5.9: Macrofauna from Polished slabs of the Servino Formation. A) *Coelostylina werfensis*, Acquaseria Member, Path 424. B) *Polygrina* sp. A., Ca'San Marco Member, Mt. Rondenino. C-D) High-spired gastropod sp. A, Gastropod Oolite Member, Path 424. E) *Allcosmia* sp., "Myophoria Beds" Member, Path 424. F) *Natiria costata*, "Myophoria Beds" Member, Path 424. G) Microconch, Gastropod Oolite Member, Path 424. H) cf. *Holocrinus*, "Myophoria Beds" Member, Path 424. I) Ophiuroidea, Acquaseria Member, Path 424. J) *Neoschizodus laevigatus*, "Myophoria Beds" Member, Path 424. K) Bivalve indet sp. A, Gastropod Oolite Member, Path 424. L) *?Unionites*, "Myophoria Beds" Member, Path 424. M) cf. *Bakevellia*, Ca'San Marco Member, Path 424. N) *Costatoria costata*, "Myophoria Beds" Member, Path 424. O) cf. *Eumorphotis*, Gastropod Oolite Member, Path 424. P) cf. *Scythentolium*, "Myophoria Beds" Member, Path 424. Q) *Lingularia*, Gastropod Oolite Member, Path 424.
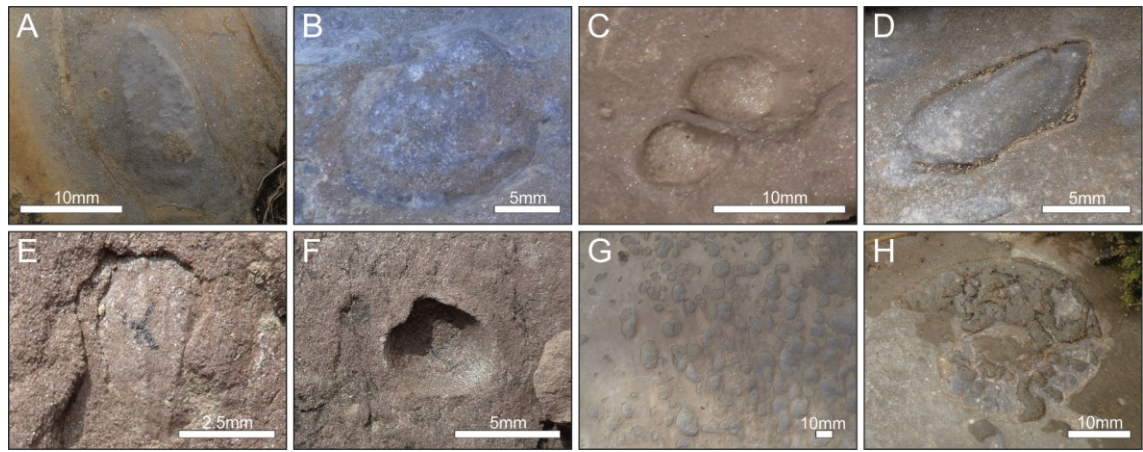
Figure 5.10: Macrofauna from bedding planes in the Servino Formation, Path 424 section. A) *Eumorphotis* cf. *telleri*, "Myophoria Beds" Member. B) *Neoschizodus laevigatus*, Ca'San Marco Member. C) cf. *Unionites fassaensis*, Acquaseria Member. D) cf. *Bakevellia albertii*. E) *Eumorphotis multiformis*, Acquaseria Member. E) cf. *Neoschizodus* sp., Acquaseria Member. G) *Natiria costata* assemblage, "Myophoria Beds" Member. H) cf. *Tirolites cassianus*, "Myophoria Beds" Member.

Table 5.2: List of all recorded taxa and their mode of life. Modes of life after Foster and Twitchett, (2014). T = Tiering: 2 = erect, 3 = epifaunal, 4 = semi-infaunal, 5 = shallow infaunal. M = Motility: 2 = slow, 4 = facultative, attached, 3 = facultative, unattached, 5 = unattached, 6 = attached. F = Feeding: 1 = suspension feeding, 2 = surface deposit feeding, 3 = miner, 4 = grazer, 5 = predator.

Species	Group	Mode of Life			Identification after
		T	M	F	
cf. *Bakevellia*	Bivalve	4	6	1	Neri and Posenato (1985)
Costatoria costata	Bivalve	5	3	1	Broglio Loriga and Posenato (1986)
cf. *Eumorphotis*	Bivalve	3	6	1	Broglio Loriga and Mirabella (1986)
Eumorphotis multiformis	Bivalve	3	6	1	Broglio Loriga and Mirabella (1986)
cf. *Eumorphotis telleri*	Bivalve	3	6	1	Broglio Loriga and Mirabella (1986)
Neoschizodus sp.	Bivalve	5	3	1	Neri and Posenato (1985)
Neoschizodus laevigatus	Bivalve	5	3	1	Neri and Posenato (1985)
Neoschizodus ovatus	Bivalve	5	3	1	Neri and Posenato (1985)
cf. *Scythentolium*	Bivalve	3	5	1	Neri and Posenato (1985)
cf. *Bakevellia albterii*	Bivalve	3	6	1	Neri and Posenato (1985)
?Unionites canalensis	Bivalve	5	3	1	Shigeta et al. (2009)
?Unionites fassaensis	Bivalve	5	3	1	Shigeta et al. (2009)
Bivalve sp. A	Bivalve	5	3	1	
Bivalve sp. B	Bivalve	3	6	1	
Coelostylina werfensis	Gastropod	3	3	1	Nützel and Schulbert (2005)
Polygyrina sp. A	Gastropod	3	3	1	Nützel and Schulbert (2005)
High-spired gastropod sp. A	Gastropod	3	3	1	
cf. *Allocosmia*	Gastropod	3	3	1	Posenato (1985)
Natiria costata	Gastropod	3	2	4	Neri and Posenato (1985)
Lingularia	Brachiopod	5	4	1	Posenato et al. (2014)
cf. *Holocrinus*	Crinoid	2	4	1	Kashiyama and Oji (2004)
Ophiuroidea	Ophiuroid	3	2	1/2	Glazek and Radwański (1968)
Ostracod	Ostracod	3	2	2	
Microconch	Microconchid	3	6	1	Zatoń et al. (2013)
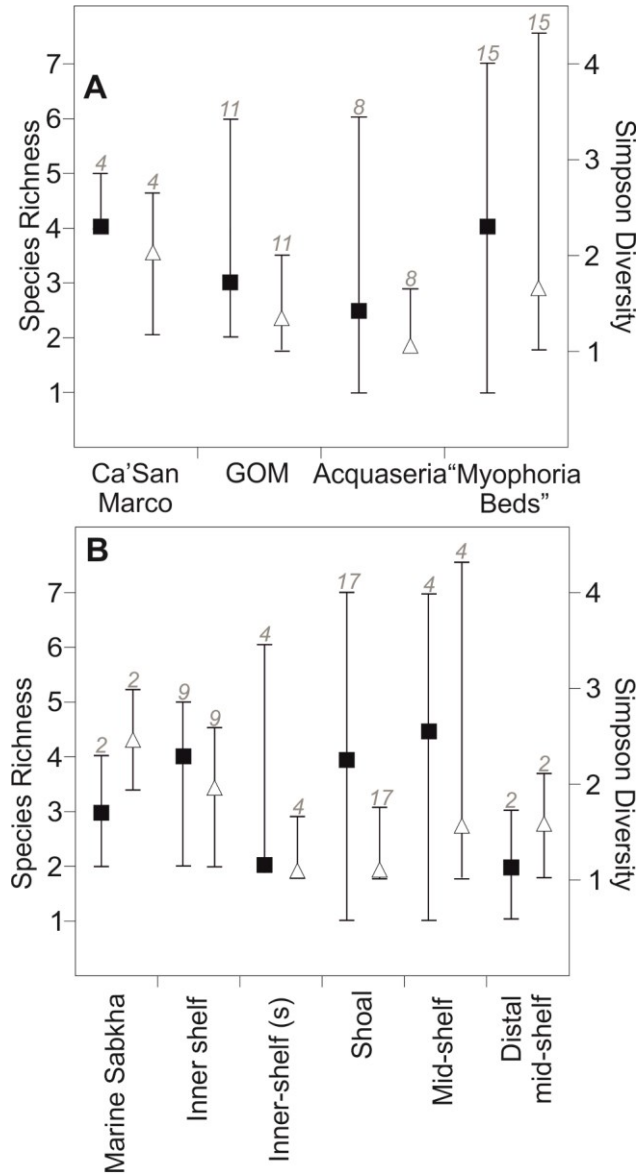
Figure 5.11: Alpha diversity of samples (A) for each member and (B) for each sedimentary facies of the Servino Formation. Median richness (black squares) and median Simpson Diversity (white triangles). (s) = siliciclastic facies.

Table 5.3: Mann-Whitney pairwise comparisons between (A) species richness and (B) Simpson Diversity of the Servino Formation members. Significant results are shown in bold.

A	Ca'San Marco	GOM	Acquaseria
Gastropod Oolite	0.08		
Acquaseria	0.08	0.52	
"Myophoria Beds"	0.92	0.12	0.10

B	Ca'San Marco	GOM	Acquaseria
Gastropod Oolite	0.06		
Acquaseria	**0.01**	0.20	
"Myophoria Beds"	0.52	0.18	**0.02**

Median functional richness and Simpson Functional Diversity increases from the inner shelf to mid-shelf environment before a decline into the outer shelf setting (Figure 5.12), but these differences are not significant ($p = 0.17$; $p = 0.22$, respectively). Simpson Functional Diversity in the inner and mid-shelf settings, have larger ranges than in the other sedimentary facies (Figure 5.12B) and the maximum Simpson Functional Diversity values are recorded in the "Myophoria Beds" Member.

5.3.3 Changes in taxonomic composition

Cluster and SIMPROF analysis show that 17 quantitative biofacies can be recognised (Figure 5.13, A-Q). The SIMPER analysis however shows that only six taxa dominate these assemblages: *?Unionites, Coelostylina werfensis,* microconchids, *Natiria costata, Neoschizodus ovatus* and cf. *Eumorphotis* (Appendix 5.2), which can be recognised as six groups at a lower similarity (Figure 5.13, 1-6). The SIMPER analysis made on these six groups shows that the samples within each group have an average similarity of 45-78% (Table 5.5). Six quantitative biofacies associations are, therefore, recognised in this study.

Samples prior to the Spathian are mostly characterised by the *Coelostylina werfensis* biofacies and are from inner shelf and shoal environments (Group 4: Figure 5.13). The *C. werfensis* biofacies is also restricted to pre-Spathian strata (Group 4: Figure 5.13). The cf. *Eumorphotis, Unionites* and microconch biofacies also mostly represent pre-Spathian samples (Figure 5.13, Groups 1, 3 and 6). The samples from the pre-Spathian
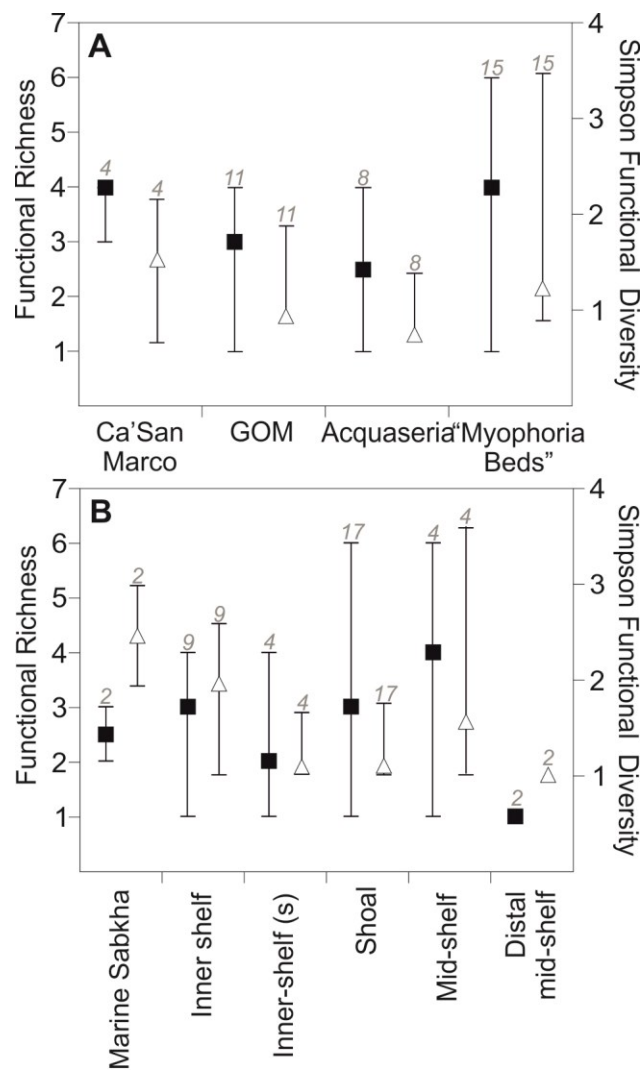
Figure 5.12: Alpha functional diversity of samples from (A) each member and (B) each sedimentary facies of the Servino Formation. Median richness (black squares) and median Simpson functional index (white triangles) with ranges

Table 5.4: Mann-Whitney pairwise comparisons between the species functional richness of the Servino Formation members. Significant results are shown in bold.

	Ca'San Marco	GOM	Acuaseria
GOM	**0.05**		
Acquaseria	**0.04**	0.76	
Strati a Myophoria	1.00	0.10	0.10
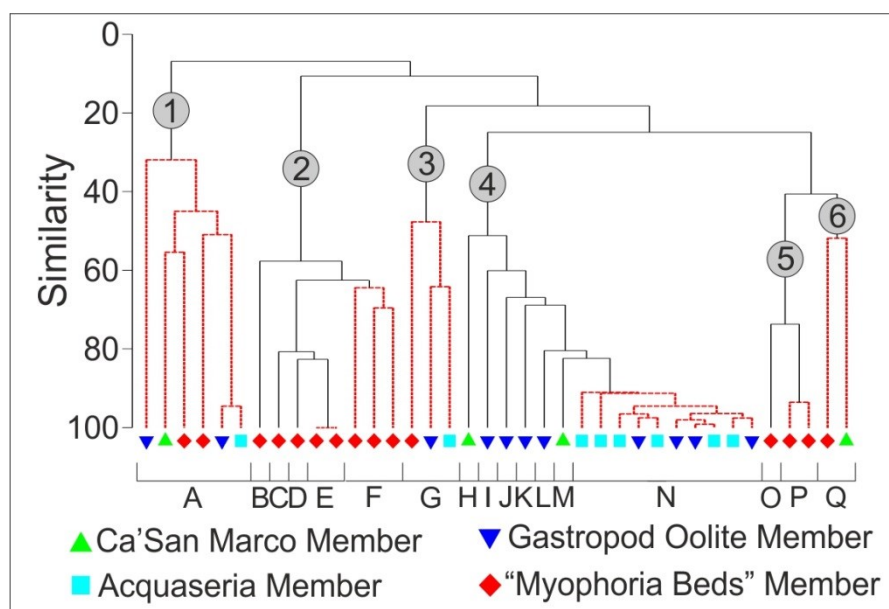
Figure 5.13: Dendrogram of the samples from the Servino Formation. Cluster analysis, together with the SIMPROF test, identified 17 groups that are significantly distinct (A-Q). These 17 groups are clustered into six biofacies associations (1-6). For biofacies see Table 5.5.

members are also distributed along an environmental gradient with inner ramp samples being dominated by both *Unionites* and microconchids but occasionally with a high *C. werfensis* component, whereas, the shoal environment is dominated mostly by *C. werfensis* (Figure 5.13C).

The nMDS plot (Figure 5.14A) shows that the samples from the "Myophoria Beds" Member mostly plot as a separate group with a small overlap to the pre-Spathian Servino Formation samples. The cluster analysis (Figure 5.13) and nMDS plots (Figure 5.14) show that this is due to the *Neoschizodus ovatus* and *Natiria costata* associations being restricted to the "Myophoria Beds" Member. Samples from the Spathian "Myophoria Beds" Member also record the *Unionites,* cf. *Eumorphotis* and microconch associations, which are not restricted to Spathian samples (Figure. 5.14). The results of the PERMANOVA show that the difference between the composition of samples from the Servino Formation members are significantly different ($p=0.001$). Pairwise
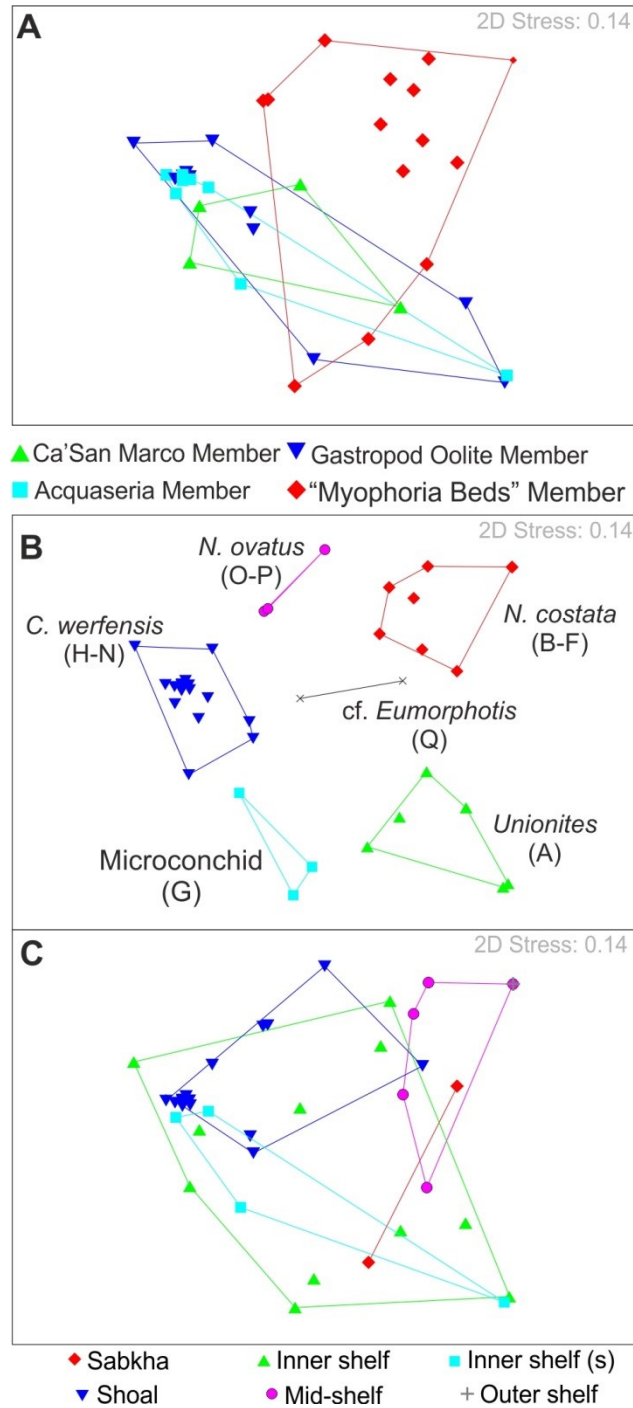
Figure 5.14: Non-metric multidimensional plots of samples from the Servino Formation. A) nMDS plot of samples according to different members of the Servino Formation. B) nMDS plots of samples according to biofacies associations. C) nMDS plot of samples according to sedimentary facies.

comparisons, however, show that the difference is only between the Spathian "Myophoria Beds" Member and pre-Spathian members (Appendix 5.3).

The nMDS plot (Figure 5.14A) shows that the samples from the "Myophoria Beds" Member mostly plot as a separate group with a small overlap to the pre-Spathian. The taxonomic composition of samples also shows composition differences between different environments: the *N. costata* biofacies occurs in marine sabkha to outer shelf environments; the *?Unionites* assemblage occurs in the marine sabkha and outer shelf settings; *N. ovatus* biofacies is restricted to the shoal; cf. *Eumorphotis* biofacies is restricted to the mid-ramp; and the microconchid biofacies is restricted to the inner shelf environment (Figure 5.14C). The PERMANOVA test shows that the differences in the taxonomic composition between the different sedimentary facies is significant (p=0.001) where the composition of samples from the inner shelf, shoal and mid-ramp are significantly different from one another (Appendix 5.3).

Table 5.5: Results of SIMPER analysis of the biofacies associations.

Species	Contribution (%)
Group 1 Average similarity: 45.45	
Unionites	90.36
Group 2 Average similarity: 68.58	
Natiria costata	92.16
Group 3 Average similarity: 53.21	
Microconch	100
Group 4 Average similarity: 77.04	
Coelostylina werfensis	93.76
Group 5 Average similarity: 80.31	
Neoschizodus ovatus	65.18
Coelostylina werfensis	19.62
Group 6 Average similarity: 51.88	
cf. *Eumorphotis*	42.77
Neoschizodus ovatus	37.59

5.3.4   Changes in ecological composition

The cluster analysis and SIMPROF test show 13 quantitative ecofacies (Figure 5.15, A-M). The SIMPER analysis shows that only four modes of life dominate these ecofacies: epifaunal, slow-moving grazers; semi-infaunal, facultatively motile, unattached, suspension feeders; epifaunal, stationary, attached, suspension feeders; and epifaunal, facultatively motile, unattached, suspension feeders (Appendix 5.4). At lower similarity levels these groups can be recognised in the cluster analysis (Figure 5.15, 1-4) and the SIMPER analysis shows that the samples within each group have an average similarity between 64.7-81.3% (Table 5.6) representing ecofacies associations.
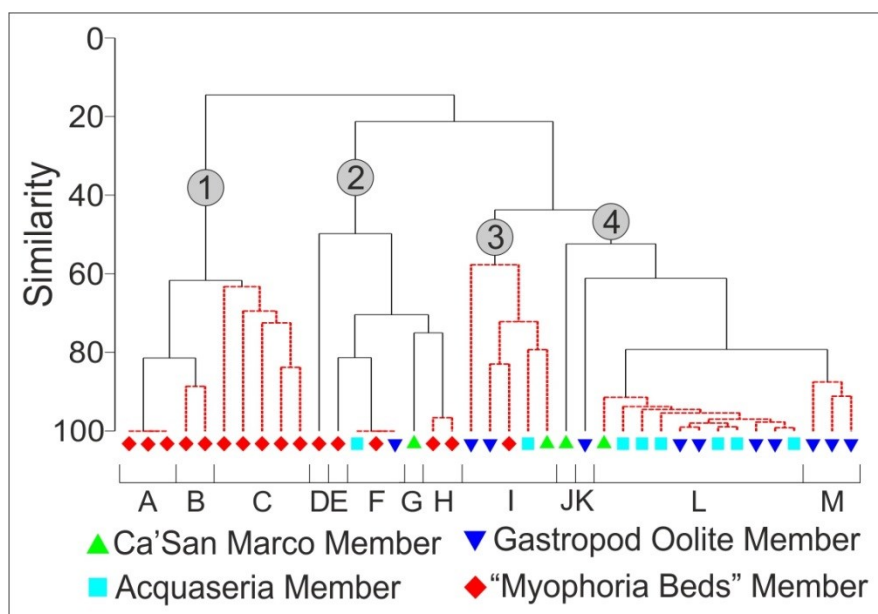
Figure 5.15: Dendrogram of the samples from the Servino Formation based on modes of life. Cluster analysis, together with the SIMPROF test, identified 13 groups that are significantly distinct (A-M). These 13 groups are clustered into four ecofacies associations and the SIMPER analysis (Table 5.5) has identified the taxa that constitute the nucleus of each ecofacies.

The first group (1 in Figure 5.15), dominated by epifaunal, slow-moving grazers, is restricted to the "Myophoria Beds" Member. The fourth group (4 in Figure 5.15) is dominated by epifaunal, facultatively motile, suspension feeders, and is restricted to the pre-Spathian Ca'San Marco, Gastropod Oolite and Acquaseria members. These two groups show a low similarity with one another (<20%; Figure 5.15) and plot separately in the nMDS plot. The stratigraphical restriction of these ecofacies is associated with the high abundance of high-spired gastropods in the pre-Spathian strata which is replaced by a high abundance of large gastropods in the Spathian. The shallow-infaunal, facultatively motile, unattached, suspension-feeding and epifaunal, stationary, attached, suspension-feeding ecofacies, on the other hand, occur in all of the sampled members and are not stratigraphically restricted (Figure 5.15).

The nMDS plot (Figure 5.16A) also shows that the pre-Spathian members are functionally similar and the pairwise comparisons of the PERMANOVA test shows that there is not a significant difference in the position of the centroids of the Ca'San Marco, Gastropod Oolite and Acquaseria members (Figure 5.16A; Appendix 5.5). The Spathian "Myophoria Beds" Member, however, does significantly differ from the pre-Spathian members (Appendix 5.5). The "Myophoria Beds" are also more heterogeneous, but the PERMDISP test shows that this result is not significant ($p =0.20$).

When the samples are grouped according to their sedimentary facies there is no obvious trend in the distribution of samples (Figure 5.16C), although the mid- and outer-shelf environments are characterised by epifaunal, slow-moving grazers. The PERMANOVA also recognised that the differences between the inner ramp and shoal environments with the mid- and outer-shelf environments is significant ($p=0.001$). Mid- and outer-shelf environments were, however, only sampled in the Spathian and so these differences may be due to the temporal aspect rather than an environmental gradient.
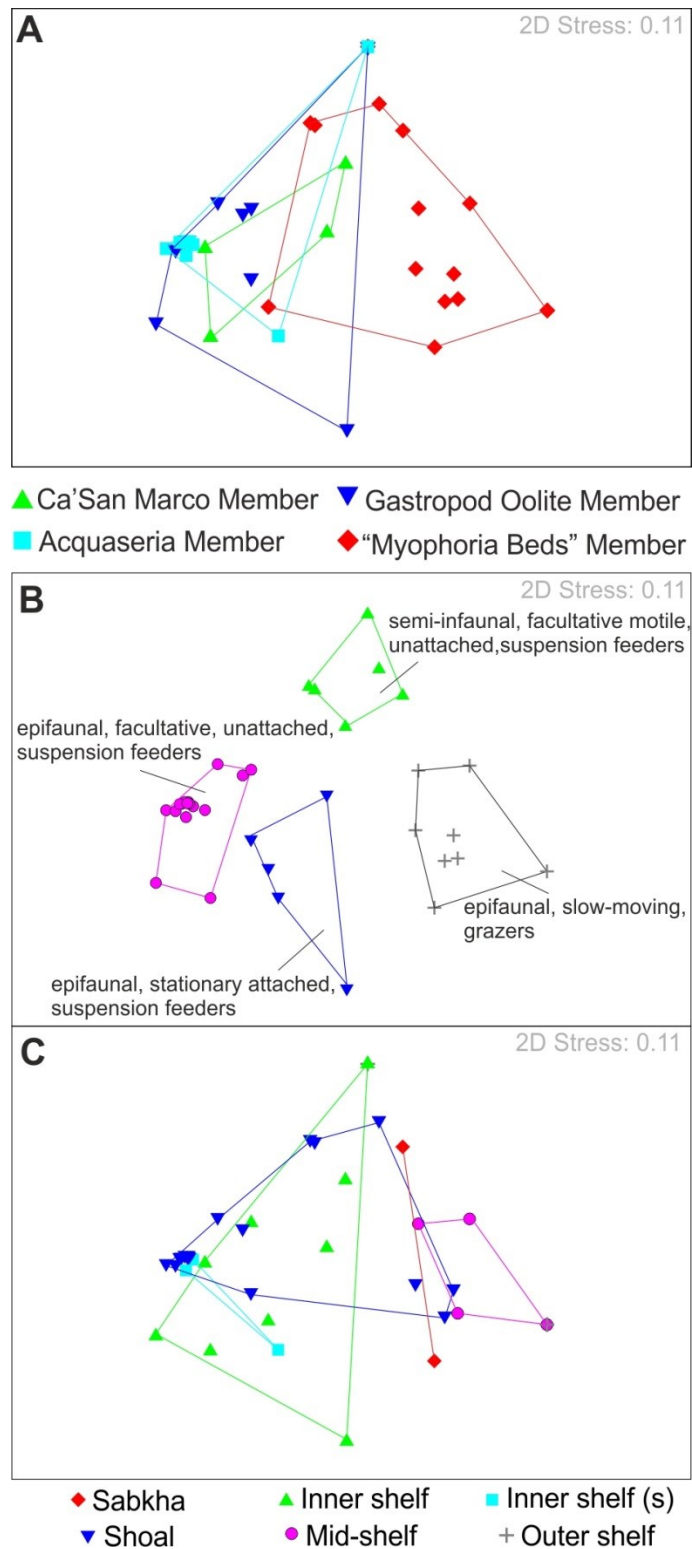
Figure 5.16: Non-metric multidimensional plots of samples from the Servino Formation based on modes of life. A) nMDS plot of samples according to different members of the Servino Formation. B) nMDS plots of samples according to biofacies associations. C) nMDS plot of samples according to sedimentary facies.

Table 5.6: Results of SIMPER analysis of the biofacies associations.

Species	Contribution (%)
Group 1 Average similarity: 70.1	
Epifaunal, slow-moving, grazers	86.6
Group 2 Average similarity: 64.7	
Semi-infaunal, facultative motile, unattached, suspension feeders.	91.5
Group 3 Average similarity: 68.2	
Epifaunal, stationary, attached, suspension feeders	70.8
Group 4 Average similarity: 81.3	
Epifaunal, facultative motile, unattached, suspension feeders	96.7

5.4 Discussion

Unlike the Werfen Formation, the Servino Formation has had relatively little palaeontological study. It is not as well exposed as the Werfen Formation, has fewer fossiliferous horizons (Twitchett and Barras, 2004; Posenato, 2008a), and as a consequence few taxa have previously been recorded. This study shows that the compositions of the Servino Formation fauna and ichnofauna are similar to those recognised in the Werfen Formation (Chapter 4; Twitchett and Wignall, 1996; Hofmann et al., 2011; Hofmann et al., 2015a) and the Lower Triassic succession of the Aggtelek Karst, Hungary (Chapter 3). The bulk diversity includes 23 benthic invertebrate taxa (i.e., bivalves, gastropods, microconchs, ophiuroids, crinoids, brachiopods and ostracods), ammonoids and seven conodont species. In common with most Lower Triassic successions, the fauna of the Servino Formation is represented by cosmopolitan opportunistic taxa that thrived in the aftermath of the late Permian mass extinction (Schubert and Bottjer, 1995; Hofmann et al., 2014; Pietsch and Bottjer, 2014; Hofmann et al., 2015a).

The age of the base of the Servino Formation is currently equivocal, however, the new isotope curve, identification of bivalves: *Claraia aurita* and *C. intermedia* in the Ca'San Marco Member allow a correlation with the upper Siusi Member of the Werfen Formation (Posenato et al., 1996; Sciunnach et al., 1999; Twitchett, 2000; Cassinis et al., 2007). The benthic assemblages from the Ca'San Marco Member are characterised by shallow tiering, absence of key taxa and ichnotaxa that represent advanced recovery, e.g. crinoids, *Thalassinoides* or *Rhizocorallium* (cf. Twitchett, 2006), small body sizes, low evenness, and indicate an initial recovery stage 1 to 2 as defined by Twitchett (2006).

A similar composition of benthic assemblages is recognised from the Gastropod Oolite and Acquaseria members. The composition of the benthic faunas from the pre-Spathian deposits is also comparable to other low latitude pre-Spathian faunas, e.g. Werfen Formation (Chapter 4; Hofmann et al., 2015), Sinbad Limestone Formation (Hofmann et al., 2014; Pietsch et al., 2014) and the Dinwoody Formation (Hofmann et al., 2013b). However, the species richness and evenness declines from the Ca'San Marco to Acquaseria Member (Figure 5.11A). In addition, there are relatively fewer trace fossils and bioturbation is confined to a few bedding planes with the absence of vertical domichnia suggesting a return to recovery stage 1 (Twitchett 2006) across the Dienerian/Smithian boundary. Furthermore, the Acquaseria Member is identified as the least species-rich sampled member of the Servino Formation (Figure 5.11A) as no skeletal remains were identified from the lithologically similar "Upper Member".

The Acquaseria and "Upper" members reflect periods when high siliciclastic loads were delivered to the Servino shelf. The linear sedimentation rates for the Smithian and Spathian of the Servino Formation (31 m/myr and 29 m/myr, respectively), however, are relatively low when compared to other lower Triassic formations (e.g. 243 m/myr and 46 m/myr for the same intervals in the Werfen Formation; Chapter 4), which is a

result of low subsidence rates in eastern Lombardy (Berra and Carminati, 2009). Even though the linear accumilation rate is low, the large siliciclastic loads that prevented carbonate mud accumulation in the Acquaseria and "Upper" members would have led to unfavourable living and preservational conditions for the benthos. The onset of increased sediment loads to the Servino ramp coincides with negative carbon isotope excursions (Figure 5.3). The onset of the negative carbon isotope excursions occur prior to the facies change, i.e. from carbonate to siliciclastic lithology, suggesting that the negative isotope excursion occurred independently from the lithological change. This in turn suggests that facies change cannot explain the excursions. An increase in sedimentation coinciding with a negative isotope excursions, however, would be an expected outcome as a result of climate change from a dry arid to a more humid environment (Haas and Budai, 1999). The Acquaseria and "Upper" member, therefore, are probably the result of relatively humid intervals.

The increase in terrigenous material during the Smithian and mid-Spathian also correspond to decreases in the carbon isotope values that have been correlated with increasing sea surface temperatures recognised in the eastern Palaeotethys (Sun et al., 2012) and Neotethys (Romano et al., 2012). In addition, the Servino shelf represents a proximal setting (Csontos and Vörös, 2004) and an increase in the riverine influx associated with a switch from a dry arid to more humid climate would be expected to also cause a negative isotope excursion (Kump and Arthur, 1999). In the outer ramp environment of the Boreal Ocean anoxic and euxinic conditions correlate with these carbon isotope excursions (Grasby et al, 2013), suggesting that climate warming in the Smithian and mid-Spathian resulted in sluggish ocean circulation, the expansion of the oxygen minimum zone and photic zone euxinia in shallower settings. The increase in terrigenous material during the deposition of the Acquaseria and "Upper" members also correlates with periods of increased weathering and primary productivity recognised in

the eastern Palaeotethys (Wei et al., 2015). The cause of these global environmental changes may have been from further pulses of volcanism from the Siberian Traps (Reichow et al., 2009; Chen and Benton, 2012). As a result of high siliciclastic loads, and the low energy environment for most of the Acquaseria and "Upper" members, it is probable that turbid and eutrophic conditions became established on the Servino shelf leading to seasonal hypoxia that would have supressed the activity of grazers (Graf et al., 1983; Algeo and Twitchett, 2010). Evidence for this comes from the lack of evidence for grazing activity in these units and the abundance of wrinkle marks, i.e. cyanobacterial mats (Fenchel, 1998).

The Acquaseria Member is characterised by small *Planolites* traces. This is similar to modern ecosystems, where, small infaunal deposit-feeding polychaetes dominate communities in environments affected by high sedimentation and low oxygen (Smith and Kukert, 1996). Ichnotaxa recorded from the Smithian of the western Palaeotethyan region also include *Diplocraterion, Arenicolites, Skolithos,* oblique *Rhizocorallium, Cochlichnus, Palaeophycus* and *Asteriacites* (Twitchett and Wignall, 1996; Twitchett and Barras, 2004; Šimo and Olšavskỳ, 2007; Chapter 3). Occurrences are generally restricted to a few bedding planes and burrows are never present in sufficient quantity to severely disrupt the sediment (ii1-2). Twitchett (1999) found that the Smithian strata of the Werfen Formation record reduced burrow depth and lower ichnofabric index compared to the older Siusi Member, suggesting that the sediment influx disrupted the recovery of benthic ecosystems.

Acquaseria Member samples also have lower median richness than those of the carbonate inner shelf settings. Even though the Smithian 'Campil event' can be traced across the Lower Triassic of central Europe (Twitchett, 1999; Kovacs et al., 2011) and records increased ecosystem stress, benthic species richness of the western Palaeotethyan margin increases (Figure 5.17). Most of these taxa, however, are bivalves

and almost all are suspension feeders (Appendix 5.6). Through the *T. cassianus* and *T. illyricus* zones, i.e. during the mid-Spathian event, there is no significant change in the species richness of western Palaeotethys. With the exception of a few gastropod taxa, the *T. illyricus* Zone fauna are also mostly suspension feeders. This probably reflects continuous high sediment loads that would have created turbid and eutrophic conditions that were habitable for opportunistic suspension feeding taxa and, therefore, environmental changes during the Smithian and mid-Spathian in the western Palaeotethys led to selective pressure on non-suspension feeders.

Spathian recovery of benthic ecosystems

The "Myophoria Beds" Member was found to have the most taxonomically and functionally rich samples in the Servino Formation (Figures 5.11; 5.12). They record the first occurrences of cf. *Holocrinus* and *Rhizocorallium* in the Servino Formation, which have been used as an indicator of advanced recovery (Twitchett, 2006), as well as increased bioturbation (ii1-4) and a taxonomic and functional turnover. This recovery coincides globally with cooler sea surface temperatures (Sun et al., 2012; Romano et al., 2012) and a retreat in the extent of the oxygen minimum zone (Grasby et al., 2013). Although diverse, fauna from outer shelf setting are restricted to tempestites which suggest that they were transported. During fair-weather conditions, the distal mid-shelf records low ichnofabric indices (ii1) and an absence of ichnofauna and skeletal material suggesting conditions were still unfavourable for the colonisation of the benthos in the more distal settings during the lower Spathian.

In the upper part of the "Upper Member", which based on carbon isotopes tentatively correlates to the base of the *Tirolites carniolicus* zone (Figure 5.3), bioturbation increases from ii 1 to 5 within one metre of rock and notably these changes occur in the absence of a facies change (Figure 5.5). The lack of shelly fauna makes this unit difficult to analyse in terms of alpha diversity. In addition, the diversity of shelly fauna

from the upper Spathian of the western Palaeotethyan region decreases from 56 to 35 (Figure 5.14). The extensive bioturbation and presence of key ichnotaxa recognised in upper Spathian western Palaetethyan formations, e.g. Szinpetri Limestone (Hips, 1998; Chapter 3) and Csopak Marl (Broglio Loriga et al., 1990), and members, e.g. Újmassa
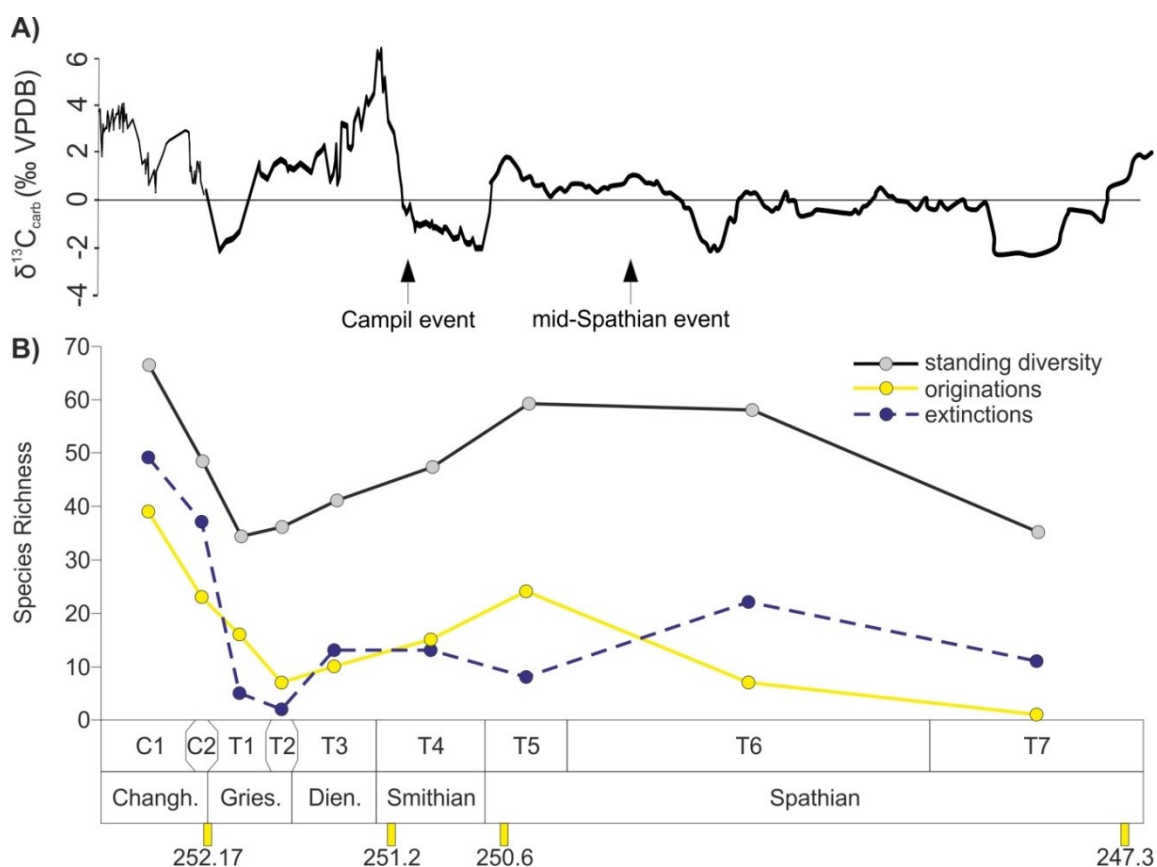
Figure 5.17: Composite isotope curve for the Changhsingian to Spathian (after Chapter 4) compared to changes in species richness of benthic invertebrates (excluding ostracods) in the western Palaeotethyan section. Radiometric ages after: Shen et al, (2011), Galfetti et al. (2007b), Ovtcharova et al. (2006), and Lehrmann et al. (2006). C1 = pre-*Hindeodus praeparvus z*one; C2 = *H. praeparvus* zone; T1 = *Claraia wangi-griesbachi* s.l. zone; T2 = *C. clarai z*one; T3 = *C. aurita* s.l. and *Eumorphotis multiforms* zones; T4 = *E. hinnitidea* zone; T5 = *E. kittli z*one; T6 = *E. telleri* zone; T7 = *Tirolites carniolicus* zone. Benthic invertebrate data after review of the literature and shown in Appendix 5.6 Note: ostracods were excluded due to absence of species-level investigations after T1.

Limestone (Hips and Pelikán, 2002) and San Lucano (Twitchett and Wignall, 1996; Chapter 4), suggests, however, that rather than being in crisis the health of benthic ecosystems was at its peak in the upper Spathian. In addition, the range of environments from peritidal to outer ramp settings represented by western Palaeotethyan sections suggest that the 'habitable zone' expanded both into shallower and deeper environments than previously during the Induan and Smithian. Therefore, models that suggest that peritidal and subtidal units of the upper Spathian were too shallow to support a diverse benthic community (e.g. Pietsch and Bottjer, 2014) can be rejected.

Shoal environments and microbialite reefs after the late Permian extinction

The oolitic shoal and oolitic tempestite beds from the Servino Formation contain a relatively diverse fauna that is compositionally very similar to the fauna from 'microbialite refuges' described by Forel et al. (2013b) and Yang et al. (2011). Quantitative reconstructions of the composition of microbialite faunas have not yet been made so a direct comparison is not possible. The two biofacies recognised in the oolitic shoal environments of the Servino Formation, i.e. *Coelostylina werfensis* and *Neoschizodus ovatus* biofacies, are temporally restricted to pre-Spathian and Spathian shoal environments, respectively. Likewise the metazoan communities of the microbial build-ups appear to have a temporal control with gastropod-ostracod-microconchid biofacies in Induan microbialites (Forel et al., 2013b; Kershaw et al., 2011; Yang et al., 2011) and a bivalve-gastropod-echinoderm-microconchid biofacies in the Olenekian (Lehrmann et al., 2001). The environmental setting of the oolitic shoals from Lombardy and the microbialites from Hungary, Italy and China are similar, i.e. wave-agitated environments around fair-weather wave-base (fwwb), which may be favourable for the colonisation of the macroinvertebrate groups. Alternatively, the environment may provide a favourable habitat for the microbial primary producers that form ooids or 'microbial reefs' (Diaz et al., 2014) which in turn create topographical highs on the

seafloor, albeit only a few metres high, favourable for the colonisation of primary and meso-consumers.

The lack of frame-builders on homoclinal ramp settings after the late Permian mass extinction and through into the Middle Triassic, has been described as a consequence of a high stress environment associated with ramp/shelf morphology, owing to the variable salinity and oxygenation as well as the high frequency of intense storms, preventing favourable conditions for the establishment of 'transient reefs' (Török, 1998). The input of large amounts of siliciclastic material during the Early Triassic in western Palaeotethys (Algeo and Twitchett, 2010), and the presence of oolitic shoals may provide an alternative obstacle to the formation of frame building microbialites. Migration of oolitic shoals may hinder the development of a stable substrate for the growth of the microbial biostromes, and high sedimentation rates would have outpaced the growth of microbialites (Ginsburg and Planavsky, 2008). The oolitic shoals of the Servino and Werfen formations, as well as the Aggtelek Karst are also characterised mostly by a facultatively motile fauna, which may be an adaptation to frequent substrate disturbances. During the Middle Triassic, a carbonate platform developed in eastern Lombardy which formed the oldest patch-reefs known from the western Palaeotethyan region (the Camorelli Limestone; Gaetani and Gorza, 1989). Additionally, tectonism during the Illyrian leading to the development of a carbonate platform from a ramp in Hungary, has been described as the process responsible for the formation of the oldest Mesozoic platform margin reef (Velledits et al., 2011) which would support the interpretation that homoclinal ramp/shelf morphology did not favour the establishment of reef ecosystems in the wake of late Permian mass extinction.

6 Spitsbergen, Svalbard

6.1 Stratigraphy

Detailed investigations of the stratigraphy of the Vikinghøgda Formation are given by Mørk et al. (1999), Nakrem et al. (2008), Hounslow et al. (2008), Nabbefeld et al. (2011), Mangerud and Mørk (2013) and Vigran et al. (2014), and of the Vardebukta Formation are given by Buchan et al. (1965), Worsley and Mørk (1978), Wignall et al. (1998) and Vigran et al. (2014). Here, new key finds of ammonoids and bivalves are incorporated to resolve better the Lower Triassic sub-stage boundaries.

			conodont zones	ammonoid zones	M	P	Lithostratigraphy	
	Anisian			*Karangatites evolutus*		L	**Bravaisberget Fm**	**Botneheia Fm.**
Lower Triassic	Olenekian	Spathian	*Neogondolella* ex. gr. *regalis*	*Keyserlingites subrobustus*	Vh8	S4	Kaosfjellet Member	Vendomdalen Member
				Parasibirites grambergi		S3		
				Bajarunja euomphala		S2		
		Smithian	*Scythogondolella mulleri*	*Anawasatchites tardus*			Iskletten Member	Lusitaniadalen Member
			Scythogondolella mosheri	*Euflemingites romunderi*	Vh7	N		
			Scythogondolella n. sp.		Vh6			
			Neospathodus waageni		Vh5			
	Induan	Die.	*Neospathodus pakistanensis*	*Vavilovites sverdrupi*	Vh4	O	Siksaken Member	Deltadalen Member
			Neospathodus dieneri			S1		
		Gries.		*Bukkenites rosenkrantzi*	Vh3		Selmaneset Member	
			Neogondolella carinata	*Otoceras boreale*	Vh2	P		
					Vh1			
	Permian					S-L	**Kapp Starostin Fm.**	

Figure 6.1: Stratigraphic subdivision of the Lower Triassic of Spitsbergen, Svalbard (vertical subdivision is proportional to thickness; after Mørk et al. (1999)). Conodont stratigraphy after Nakrem et al. (2008). Ammonoid stratigraphy after Dagys and Weitschat (1993). M = Magnetostratigraphy after Hounslow et al. (2008a). P = Palynology after Mørk et al. (1999). Gries. = Griesbachian, Die. = Dienerian.

Kapp Starostin Formation

The age of the Kapp Starostin Formation is poorly constrained as it lacks age-diagnostic ammonoids and conodonts. It is considered to span the Kungurian to Changhsingian (Blomeier et al., 2014; Bond et al., 2015), with Permian age determinations being undertaken by means of bryozoans, brachiopods, conodonts, corals and palynomorphs (Forbes et al., 1958; Gobbet, 1963; Szaniawski and Malkowski, 1979; Nakamura et al., 1987; Stemmerik, 1988; Nakazawa et al., 1990; Nakrem et al., 1992; Mangerud and Konieczny, 1993; Nakrem, 1994; Mørk et al., 1999; Chwieduk, 2007). The youngest age for the Kapp Starostin indicated by these fossils groups was Changhsingian (Mørk et al., 1999).

The boundary between the Kapp Starostin Formation, Vardebukta and Vikinghøgda formations is interpreted as a sequence boundary (Mørk et al., 1999). Below this sequence boundary chert nodules and bands are present within highly bioturbated sandstones or siltstones, whilst above no chert has been recorded (Figure 6.2-6.4; Mørk et al., 1999; Mørk and Worsley, 2006). Mørk et al. (1999) defined the Permian/Triassic boundary at this sequence boundary, but using magnetostratigraphy, ammonoids and conodonts Hounslow et al. (2008a) and Nakrem et al. (2008) placed the P/Tr boundary ~12m above the base of the Vikinghøgda Formation. In addition, Wignall et al. (1998) and Nabbefeld et al. (2010) interpret the late Permian mass extinction as occurring at the cessation of prolific bioturbation. In this study occurs: at 9.5m into the Vardebukta Formation at Festningen (Figure 6.4), 1.64m into the Vikinghøgda Formation at Lusitaniadalen, and 1.69m into the Vikinghøgda Formation at Deltadalen (Figures 6.2-6.3). Therefore, the Kapp Starostin Formation is interpreted to represent pre-extinction Permian deposits.
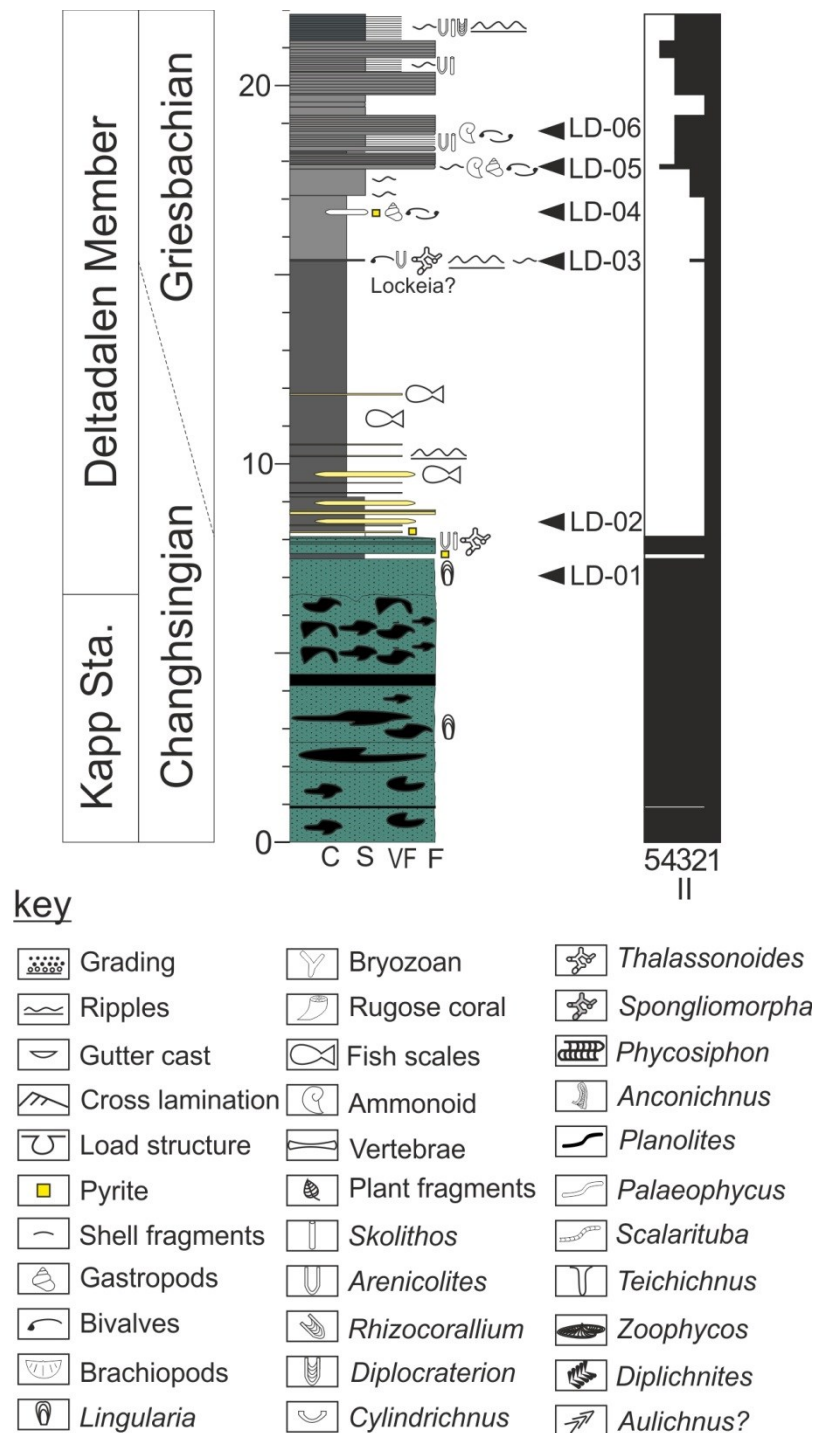
Figure 6.2: Stratigraphic section, position of samples and ichnofabric indices (II) at the Lusitaniadalen section. Stratigraphic log and ichnofabric indices modified from R.J. Twitchett's unpublished field notes (2006; 2007). Lithostratigraphy after Mørk et al. (1999). Kapp Sta. = Kapp Starostin Formation. Colour in the lithology column refers to the rock colour observed in the field.
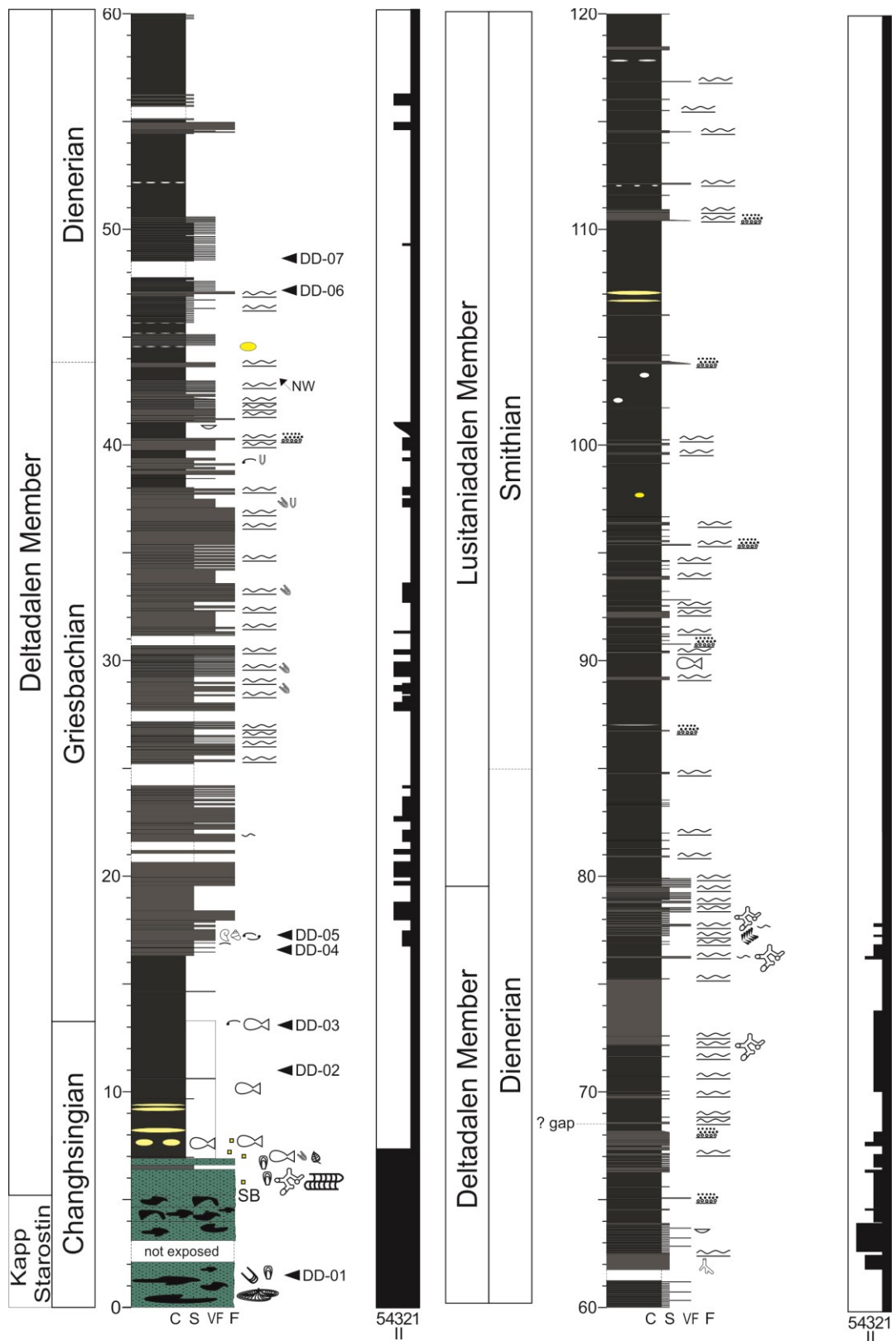
Figure 6.3: Stratigraphic section, position of samples and ichnofabric indices (II) at the Deltadalen section. Stratigraphic log and ichnofabric indices modified from R.J. Twitchett' s unpublished field notes (2006; 2007). Lithostratigraphy after Mørk et al. (1999).
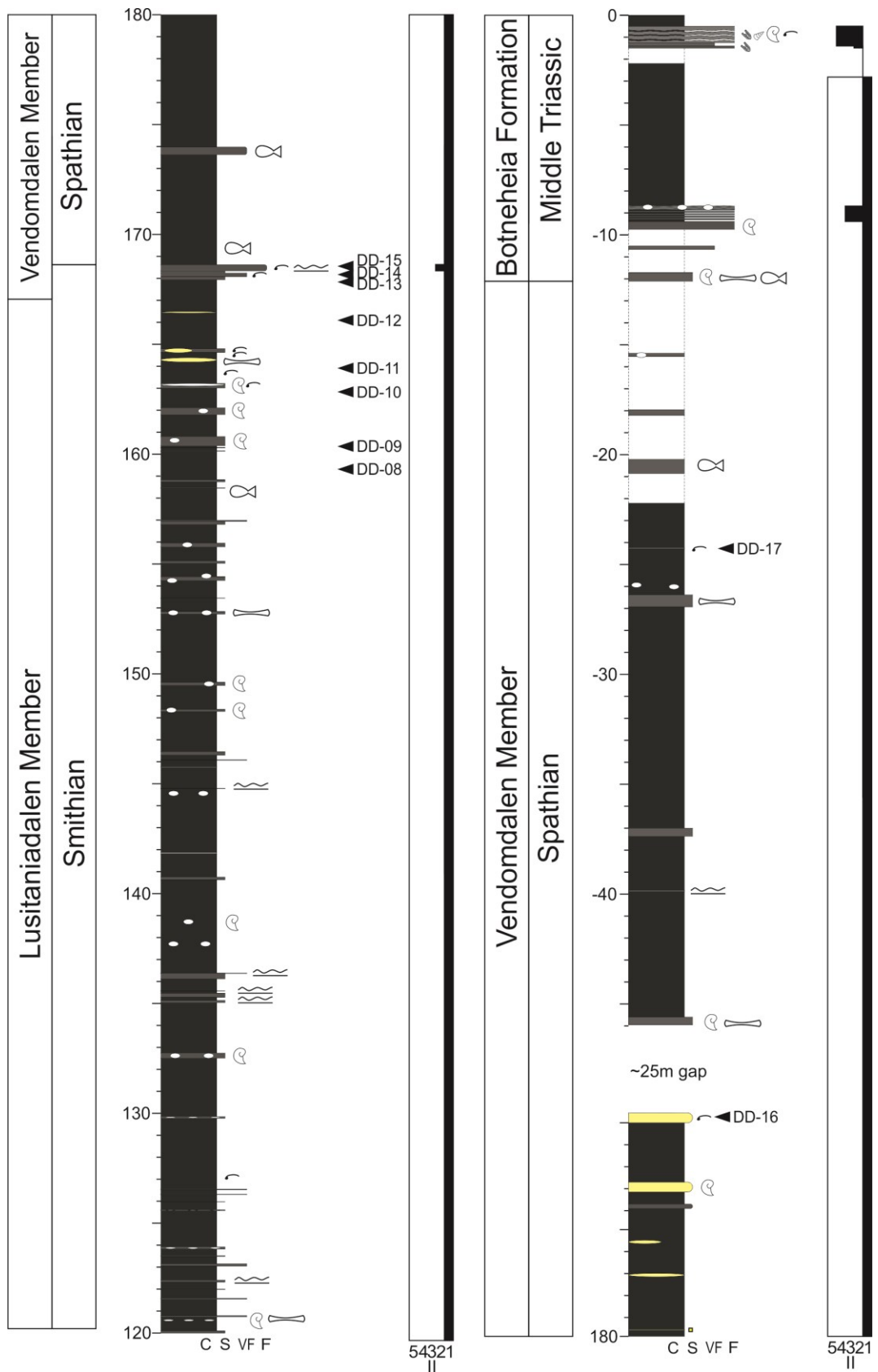
Figure 6.3: continued.
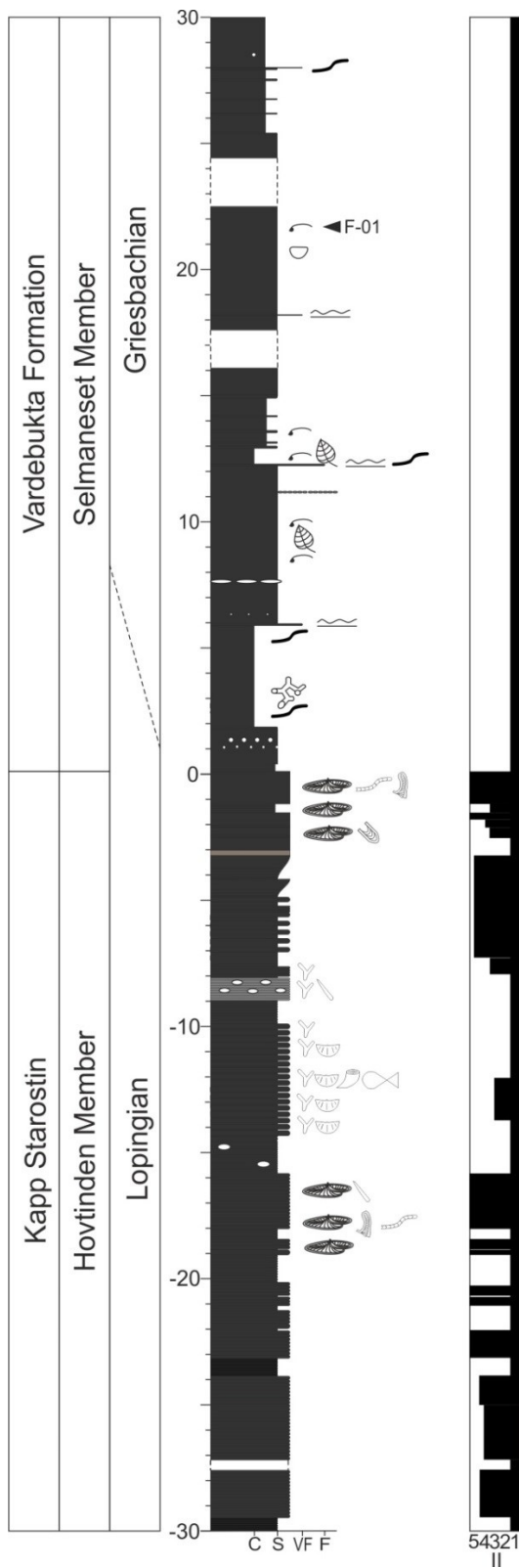
Figure 6.4: Stratigraphic section, position of samples and ichnofabric indices (II) at the Festningen section. Stratigraphic log and ichnofabric indices modified from R.J. Twitchett' s unpublished field notes (2006; 2007). Lithostratigraphy after Worsley and Mørk (2006).

Vardebukta Formation

The Vardebukta Formation has been divided into the Selmaneset and Siksaken members (Buchan et al., 1965). Conodonts have not been recorded from the Selmaneset Member, but the early Griesbachian ammonoid *Otoceras boreale* and the Permian/Triassic *Redaviasporites chalastus* assemblage Pollen Zone is reported by Vigran et al. (2014) occurring ~8m above the base of the Vardebukta Formation. In this study, ammonoids, were recorded in small concretions of the Selmaneset Member but not identified. This study also found that bivalves occur throughout the Selmaneset Member, and the Griesbachian bivalves *Claraia kilenensis, C.* cf. *clarai* and *C. stachei* are abundant in the silty mudstones of the Selmaneset Member with their first occurrence at 16m into the Vardebukta Formation, indicating deposition during the Triassic.

The $\delta^{13}C_{org}$ data of Wignall et al. (1998) show a 6‰ negative isotope excursion through the basal 8.5m of the Vardebukta Formation. This isotope excursion can be correlated with the large negative excursion reported worldwide in Permian/Triassic boundary sections (Thomas et al., 2004; Korte and Kozur, 2010). This excursion reaches a negative peak ~2m above the late Permian mass extinction in the Selmaneset Member. The Permian/Triassic boundary is therefore interpreted to occur at ~8m above the base of the Selmaneset Member.

Vikinghøgda Formation

The Vikinghøgda Formation has been divided into three members: the Deltadalen, Lusitaniadalen and Vendomdalen members. Its correlation has been constrained using magneto-, sequence and biostratigraphy (Dagis and Korcinskaja, 1987; Mørk et al., 1999; Hounslow et al., 2008a; 2008b; Nakrem et al., 2008).

Deltadalen Member

The Deltadalen member was deposited from the late Changhsingian to Dienerian (Hounslow et al., 2008a). The Permian/Triassic boundary, occurs within the basal ca. 10.5m. In a concretionary level ~5m above the base of the member, Mørk et al. (1999) reported *Neogondolella carinata, N.* cf. *meishanensis*, *N. houschkei, N.* cf. *orchard* and *N.* aff. *taylorae*. The presence of *N.* aff. *taylorae* led Nakrem et al. (2008) to correlate this level to the late Changhsingian *Clarkina praetaylorae* zone from the latest Permian of Iran. *Neogondolella taylorae*, however, ranges into the Griesbachian and so this concretionary level cannot be unequivocally assigned to the latest Permian. The conodont fauna from a concretionary level ~10.5m above the base of the Deltadalen Member includes of *N. carinata* which spans the Permian/Triassic boundary. The presence of the ammonoids *Otoceras boreale* and *Tompophioceras* cf. *gracile* suggest that this concretionary level is lower Griesbachian (Mørk et al., 1999; Nakrem et al., 2008). In this study the ammonoids *Otoceras boreale* were also identified from the same level indicating a lower Griesbachian age (Al McGowan, personal communication). On a siltstone bed ~8m above the base of the Deltadalen Member small cf. *Claraia griesbachi* were identified which indicate the Triassic. If the determination of *Ng.* cf. *meishanensis* is correct then the Permian/Triassic boundary occurs between ~5m and 8m above the base of the Deltadalen Member, although more specific level cannot be unequivocally determined.

From the Lusitaniadalen section Hounslow et al. (2008a) report the ammonoid *Bukkenites rosenkrantzi* ~37m above the base of the Deltadalen Member which is indicative of the upper Griesbachian. In addition, these authors record the Vh3/Vh4 megnetozone boundary 49m above the base of the Deltadalen Member which they correlate with the Griesbachian/Dienerian boundary in Abadeh, Iran. The Griesbachian-Dienerian transition is also marked globally by a transgression (Embry, 1997). The

transgression around the Vh3/Vh4 boundary (Mørk et al., 1999) would also support Hounslow et al's. (2008) interpretation. The upper Dienerian ammonoid *Koninckites* sp. is recorded from 52-57m above the base of the Deltadalen Member (Hounslow et al., 2008a), confirming a Dienerian age in its upper part.

Lusitaniadalen Member

The Vh4/Vh5 megnetozone boundary is described by Hounslow et al. (2008a) as indicating the Induan/Olenekian Boundary. This occurs ~5m above the base of the Lusitaniadalen Member. The Deltadalen/Lusitaniadalen Member boundary is marked by a 3rd order transgression (Mørk et al., 1999) which has also been used globally to indicate the Induan/Olenekian boundary (Embry, 1997; Orchard, 2007; Posenato, 2008b). The Dienerian conodont *Neospathodus* cf. *svalbardensis* is recorded ~1m above the base of the Lusitaniadalen Member (Mørk et al., 2008), suggesting that initial deposition of this member occurred during the upper Dienerian.

From the uppermost 2m of the Lusitaniadalen Member at the Milne Edwardsfjellet section the conodont *Neospathodus waageni* and the ammonoids *Xenoceltites subevolutus, Anawasatchites* sp. *Arctoprionites nodosus* and *Anasibirites* sp. indicate the Smithian *Anawasatchites tardus* Ammonoid Zone (Hounslow et al., 2008b). In addition, 7m below the top of the Lusitaniadalen Member at Botneheia Weitschat and Lehmann (1978) recorded the conodonts *Scythogondolella mulleri, S. moshri, Borinella* aff. *buurensis* and *Ns. waageni* that also correlate to the late Smithian *Anawasatchites tardus* Ammonoid Zone. The Lusitaniadalen Member was, therefore, deposited throughout most of the Smithian.

Vendomdalen Member

The base of the Vendomdalen Member spans the Smithian/Spathian boundary. At ~5m above the base of the Vendomdalen Member at the Dicksonfjellet section, Galfetti et al.

(2007c) record a $\delta^{13}C_{org}$ positive isotope peak which can be correlated to an isotope peak associated with the Smithian/Spathian boundary. This is also associated with a transgression which is also reported from the Smithian/Spathian boundary (Embry, 1997; Mørk et al., 1999; Orchard, 2007). The ammonoids from the Vendomdalen Marker bed (*Arctoprionites nodosus, Xenoceltites subevolutus, Anawasatchites tardus* and *Anasibirites* spp.), are indicative of the late Smithian *W. tardus* Ammonoid Zone. At ~20m above the base of the Vikinghøgda Formation Hounslow et al. (2008a) record the ammonoid *Bajarunia euomphala* which is indicative of the lowermost Spathian *Bajarunja euomphala* Ammonoid Zone. In addition, in a dolomitic bed 3m above this level, this study records the bivalve *Eumorphotis telleri* which is known from the lower Spathian in the Palaeotethys, thus supporting a Spathian age. In the nearby Milne Edwardsfjellet section *Bajarunia euomphala* is recorded at ~5m into the Vendomdalen Member. The Smithian/Spathian boundary is therefore inferred to have occurred between 5m and 20m above the base of the Vendomdalen Member.

In the upper part of the Vendomdalen Member Mørk et al. (1999) report the ammonoids *Keyserlingites subrobustus, Keyserlingites* sp., and *Popovites occidentalis,* and at the top of the Vendomdalen Member *Svalbardiceras spitzbergense*. The faunas indicate the mid- and late-Spathian *K. subrobustus* and *S. spitzbergense* ammonoid zones, respectively. In addition the conodont *C. timorensis*, which is used to indicate the Lower/Middle Triassic boundary (Lehrmann et al., 2005), is not recorded until 12m into the overlying Botneheia Formation (Hounslow et al., 2007). The upper part of the Vendomdalen Member was, therefore, deposited during the middle to late Spathian.

6.2   Sedimentology

Detailed descriptions of the sedimentology and shelf evolution of the Lower Triassic successions at Festningen, Lusitaniadalen and Deltadalen are given by Mørk et al. (1983), Wignall and Twitchett (1996), Wignall et al. (1998), Mørk et al. (1999),

Worsley and Mørk (2006). Using the unpublished field logs and data of Twitchett (2006; 2007) and field observations from this study the depositional environment for the investigated sections is described.

Kapp Starostin

Description: The Kapp Starostin Formation in the Deltadalen and Lusitaniadalen sections is characterised by bedded, fine to medium grained, well sorted, green glauconitic sandstones, which are highly bioturbated (ii5-6) by *Zoophycos, Thalassinoides, Arenicolites, Skolithos, Palaeophycus* and *Rhizocorallium* and contain light grey chert nodules. Occasionally, the chert is more persistent forming thin intercalations. These sandstone and chert beds have wavy-irregular tops and bases. The sandstones contain brachiopods (mostly lingulids) and abundant brachiopod shell and fish fragments.

At Festningen the upper 8m of the Vardebukta Formation is characterised by dark-grey, thin- to medium-bedded, silty mudstones. The silty mudstones are also intensely bioturbated (ii4-5) with abundant *Zoophycos, Rhizocorallium, Phycosiphon, Scalarituba* and back-filled cf. *Skolithos*. Maximum burrow depth is 30cm.

Interpretation:

The grain-size of sediments, in the broad sense, reflects the hydraulic energy of the environment (Tucker, 2001). The dominance of fine and medium grained sandstones and the well sorted nature of the sandstones suggest deposition was in an agitated environment, suggesting that deposition was not below wave base, as interpreted by Ehrenberg et al. (2001). The presence of glauconite is usually associated with an open-marine environment and slow sedimentation rates (Odin and Matter, 1981). The intense bioturbation and the lack of sedimentary structures, e.g. cross-bedding, suggest deposition took place in a well oxygenated environment (aerobic facies of Savrda and

Bottjer, 1991). The presence of chert is interpreted to be produced by upwelling of cold nutrient- and oxygen-rich waters (Baud and Beauchamp, 2002). Deposition, therefore, is interpreted to have occurred in a well-oxygenated open-marine setting above wave base.

The uppermost 8m of the Kapp Starostin Formation at Festningen has been interpreted as representing an outer shelf setting below wave base (Wignall et al., 1998). The predominance of fine grained silty mudstones and intense bioturbation suggests observed in this study supports deposition below wave base in a well oxygenated environment (Savrda and Bottjer, 1991).

Vardebukta Formation

Description: The Vardebukta Formation is characterised dominantly by dark grey silty mudstones with small concretions and occasionally thin silt- and fine sandstone beds. The beds are not disturbed by bioturbation (ii1) but on bedding planes of silty mudstones and siltstones small *Planolites* and *Thalassinoides* can be observed. Bivalves belonging to *Claraia* occur as impressions within the silty mudstones. The unpublished field notes of Twitchett (2006; 2007) show that the sandstone beds in the Vardebukta Formation have a higher proportion of bioturbation than the siltstones and silty mudstones (Figure 6.5).

Interpretation: After the extinction horizon the Vardebukta Formation is interpreted as representing an environment below wave base, as indicated by the dominance of fine grained rocks (Mørk et al., 1982; Worsley and Mørk, 2001). Interbedded siltstones and fine grained sandstones were deposited by storm-induced currents. As the sagittal planes of bivalves from the silty mudstones are always horizontally orientated and shells are always resting on their right valves, i.e. the normal life position of a paper pecten, the bivalves are assumed to be preserved in life position (Schatz, 2005). The

presence of laminated strata containing in situ epifaunal macroinvertebrates and small trace fossils is consistent with the exaerobic biofacies of Savrda and Bottjer (1991), i.e. an oxygen-restricted environment.

Vikinghøgda Formation

Deltadalen Member

Description: The basal 1.5m of the Deltadalen Member is characterised by bedded, fine to medium grained, well sorted, green glauconitic sandstones, which are highly bioturbated (ii5) by *Zoophycos, Thalassinoides, Arenicolites, Phycosiphon, Skolithos, Palaeophycus* and *Rhizocorallium*. Similar to the underlying Kapp Starostin facies, except for a lack of chert. The sandstone beds have wavy-irregular tops and bases. The sandstones contain brachiopods (mostly lingulids) and abundant brachiopod shell, plant debris and fish fragments. These beds alternate with a laminated 14-20cm dark grey-siltstone bed.
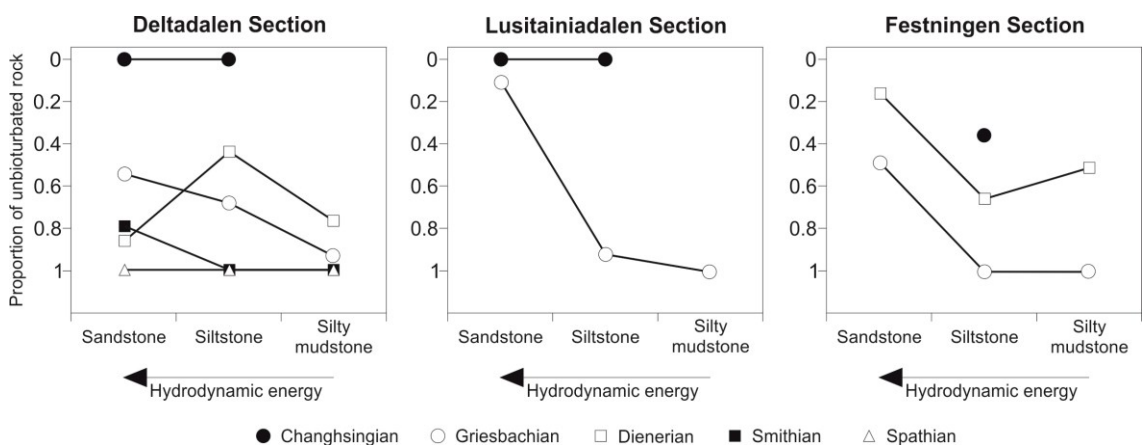
Figure 6.5: Proportion of unbioturbated sediment (ii1) between the different sub-stages of the Early Triassic. Ichnofabric indices of beds are from the unpublished field notes of Twitchett (2006; 2007).

Above the bioturbated sandstones the Deltadalen Member is characterised by laminated silty mudstones that contain pyritised tabular concretions and thin (2-6cm) silt- and sandstone beds. The tabular concretions are characterised by cross-laminations, and contain abundant fish scales and bivalve and lingulid shells. The thin silts- and sandstones contain convex-up bivalves and occasionally weakly bioturbated by small *Arenicolites, Planolites Thalassinoides* and *Lockeia*. They also occasionally have rippled surfaces. A concretion at ~10m above the base of the Deltadalen Member contains abundant bivalves, gastropods and inarticulate brachiopods (Mørk et al., 1999).

From 11m above the base of the Deltadalen Member through the remainder of the member, alternations of thin beds of light grey siltstones, very-fine, fine sandstones and dark grey silty mudstones occur, with sandstones making up a greater proportion in the middle of the member. The sandstone beds have rippled tops, cross laminations and are moderately bioturbated (ii1-3) by small *Rhizocorallium, Arenicolites, Planolites, Diplocraterion, Skolithos, Thalassinoides* and *Diplichnites*. Sandstone beds also occasionally contain poorly preserved convex-up bivalves. Some beds also have gutter casts at their base and are graded. The unpublished field notes of Twitchett (2006; 2007) show that the sandstone and siltstone beds in the Deltadalen member have a higher proportion of bioturbated sediment than the silty mudstones (Figure 6.5).

Interpretation: The dominance of fine and medium grained sandstones and the well sorted nature of the sandstones in the basal 1.5m of this member suggest deposition was in an agitated environment, above wave base. The presence of glauconite is usually associated with an open-marine environment and slow sedimentation rates (Odin and Matter, 1981). The intense bioturbation and the lack of sedimentary structures suggest deposition took place in a well oxygenated environment (Aerobic facies of Savrda and Bottjer, 1991). The alternation of a laminated siltstone bed is interpreted as the onset of the late Permian transgression (Nabbefeld et al., 2010). The lack of chert in this facies is

inferred to represent a cessation in the upwelling of oxygenated and nutrient-rich waters (Baud and Beauchamp, 2002).

The laminated silty mudstones and pyritised concretions represent deposition in an anoxic environment below storm wave base. Tabular concretions and tempestites with cross-laminations and rippled tops represent deposition during storm induced currents following intense storms.

The alternations of fine grained and coarser grained sediments suggest deposition in a mid-shelf environment. The finer deposits, i.e. silty mudstones, would have been deposited during fair-weather conditions, whereas, the coarser beds with rippled tops, cross-laminations, convex-up fauna and are bioturbated were deposited during storm events between fair-weather (fwwb) and storm-weather wave base (swwb). At the top of the Deltadalen Member the proportion of silty mudstones increases suggesting deepening near or just below swwb (Mørk et al., 1999).

Lusitaniadalen Member

Description: Characterised by alternations of up to 5m thick units of silty mudstones and thin bedded siltstones. The siltstone beds have rippled surfaces, show normal grading and are cross-laminated. The upper part of the Lusitaniadalen Member is characterised by an increasing frequency of concretionary siltstone beds that are either cross laminated or have rippled surfaces. The Lusitaniadalen/Vendomdalen Member boundary is also marked by bedded siltstones and sandstones which contain bivalve fragments within the bed and convex up bivalves on the surfaces. Concretions occur in both the silty mudstones and siltstone beds are increasingly common towards the top of the member. Some of the concretions contain pyrite. Large tabular septarian nodules also occur within the silty mudstones and form distinctive yellow marker horizons.

Ammonoid and vertebrates were recorded within the concretions. Bioturbation was not recorded in this member.

Interpretation: The laminated silty mudstones and the presence of pyrite suggest deposition in a low-energy anoxic setting below wave base. Siltstone tempestites with rippled tops and cross laminations and convex-up fauna would have been deposited by storm induced currents that reached the outer shelf during intense storms. The Lusitaniadalen Member contains thicker beds of silty mudstones and fewer siltstone tempestite intercalations than the Deltadalen Member. It is, therefore, interpreted to represent a deeper environment initially in the distal mid-shelf and then into the outer shelf below storm wave base. The increase in coarser sediments at the top of the Lusitaniadalen Member suggests increased storm-influence on the mid-shelf associated with shallowing around the Smithian/Spathian boundary (Embry, 1997; Mørk et al., 1999).

Vendomdalen Member

Description: The Vendomdalen is characterised by thicker units of silty mudstones (up to 10m) and fewer silt and sandstone intercalations, than the Lusitaniadalen Member. It also contains thick (35-45cm) dolomitic siltstones that are swaley and contain randomly orientated bivalves and weather yellow to form distinctive marker beds. There are also tabular septarian nodules and tabular concretions within the silty mudstones. The concretions often contain ammonoids, vertebrate remains and fish scales (Mørk et al., 1999; Figures 6.2-6.3). At the top of the Member the silty mudstones also contain abundant bivalves. The unpublished field notes of Twitchett (2006; 2007) show that slight bioturbation (ii2) was only recorded at the Vendomdalen Marker bed.

Interpretation:

The thick beds of laminated silty mudstones suggest deposition in a low-energy setting and the lack of tempestites suggests deposition on the distal outer shelf (Mork et al.,

1999). The dolomitic siltstones with a swaley structure and a decreasing laminae thickness, i.e. Bouma sequence, were deposited as low-density gravity flows on the outer shelf (Galfetti et al., 2008). As the sagittal planes of bivalves from the silty mudstones are always horizontally orientated and shells are always resting on their right valves, i.e. the normal life position of a paper pecten, the bivalves are assumed to be preserved in life position (Schatz, 2005). The lack of bioturbation is interpreted to represent an oxygen-restricted environment.

6.3   Systematic Palaeontology

The assemblages from most samples are preserved as internal and external moulds. Three samples, two from concretionary levels at the base of the Vikinghøgda Formation and one from a concretion in the upper Lusitaniadalen Member, however, contain a well-preserved silicified fauna and include specimens recovered from conodont residues. To avoid sampling bias these were not included in the palaeoecological analysis. Furthermore, the virtually complete removal of rock via acid dissolution means that for the first time the internal shell characteristics of bivalve shells were observed in Early Triassic specimens. This assemblage comprises twenty-four benthic invertebrate species, including three species of brachiopods, eighteen species of bivalves, four species of gastropods and one gastropod larval shell (Table 6.1).

Phylum **Brachiopoda** Duméril, 1805

Class **Lingulata** Goryansky and Popov, 1985

Order **Lingulida** Waagen, 1885

Family **Lingulidae** Menke, 1828

Genus *Lingularia* Bittner, 1901

Species *Lingularia freboldi* Gobbett, 1963

Figure 6.6, G-H.

1963   *Lingula freboldi*; Gobbett. p. 44. Plate 1, Figs 1-2.

Material. 29 specimens from the Kapp Starostin Formation at the Lusitaniadalen and Deltadalen sections (samples DD-01, LD-01).

Description. Shells sub-rectangular in outline, moderately convex, with slightly rounded umbo and margins. Equilateral. Flattened lateral and anterior margins. Lateral margins diverge slightly and the greatest width is near the ventral margin. Shell surface with numerous laminar growth lines, and strong laminar growth ridges.

Remarks. The specimens are assigned to *Lingularia* following the criteria of Posenato et al. (2014). These specimens are conspecific to *L. freboldi* described and figured by Gobbett (1963) and have only been described from the Permian.

Mode of Life. Shallow infaunal, facultatively motile, attached, suspension feeder (Zonneveld et al., 2007).

Species *Lingularia yini* (Peng and Shi, 2008)

Figure 6.6, I.

2008   *Sinolingularia yini*   Peng and Shi. p. 162, Fig. 7, A-H.

2014   *Lingularia yini*   Posenato et al. p. 376. Fig. 3, C-F.

Material. 35 specimens from the Deltadalen Member, Vikinghøgda Formation, Lusitaniadalen section (sample L-02).

Description. Shells elongate-oval in outline. Valves equilateral, slightly convex with rounded umbo and margins. Lateral margins subparallel with subrounded anterior and posterior margins. Shell surface generally smooth except for fine concentric growth lines.

Remarks. The specimens have a similar width/length ratio to *L. freboldi*, and other Early Triassic *Lingularia* species, therefore, this criterion cannot be used to distinguish between species. The small size, smooth ornamentation and oval outline of these specimens is similar to those assigned to *L. yini* in previous studies (e.g. Peng and Shi, 2008; Posenato et al., 2014).

Mode of Life. Shallow infaunal, facultatively motile, attached, suspension feeder (Zonneveld et al., 2007).
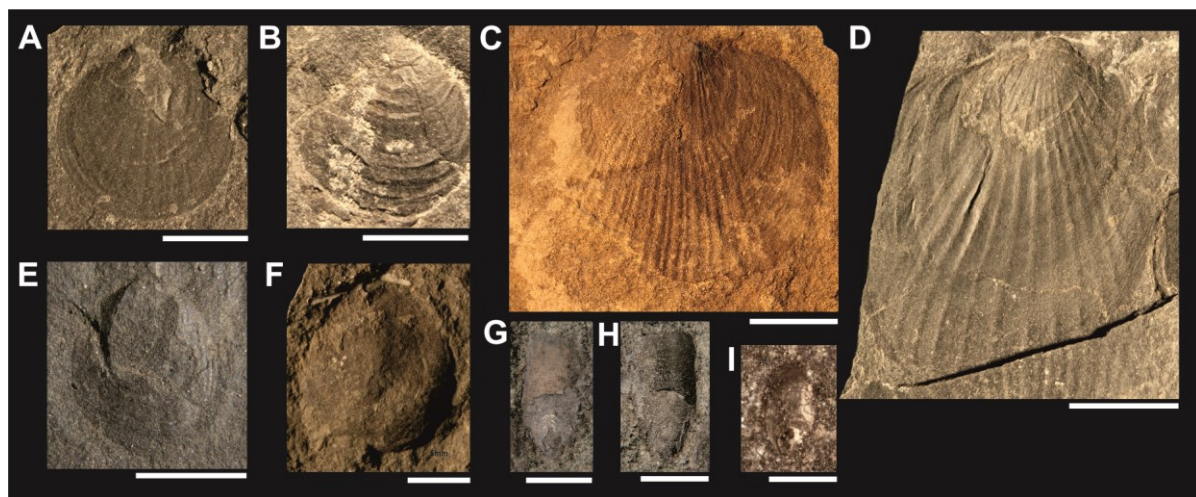
Figure 6.6: *Claraia* and *Lingularia* from Svalbard. A) *C. radialis*, left valve. Lusitaniadalen section, 17.8m. B) *C.* cf. *clarai*, left valve. Festningen section, 14.0m. C) *C. stachei*, Deltadalen section, 16.0m. D) *C. kilenensis*, left valve. Festningen section. 14.0m. E-F) cf. *C. griesbachi*, left valve. Deltadalen section, 13.0m. G-H) *Lingularia freboldi*. Lusitaniadalen section 5.8m. I) *Lingularia yini*, Lusitaniadalen section 7.8m. Scale bar = A-H) 5mm and I) 1mm.

Family: **Discinidae** Gray, 1840

Genus *Orbiculoidea* d'Orbigny, 1847

Species *Orbiculoidea winsnesi* Gobbet, 1963

Figure 6.7, C.

1963   *Orbiculoidea winsnesi* Gobbett, p 46. Plate 1, Figs. 4-5.

Material. Four specimens from the Deltadalen Member, Vikinghøgda Formation, Lusitaniadalen section (samples LD-04, LD-05).

Description. Shells sub-circular outline, pedicle moderately convex, valve inflated to apex, length slightly greater than width. The apex is located about a third of the diameter from the anterior margin. Ornamentation of fine concentric ridges which probably represent growth lamellae.

Remarks. Internal characters or pedicle valve not observed. One specimen attached to an ammonoid shell. Pedicle valve not observed. These specimens record all diagnostic characters with *Orbiculoidea winsnesi* as described by Gobbett (1963) from the Kapp Starostin Formation, Spitsbergen.

Figure 6.7: *Orbiculoidea winsnesi, Promyalina schamarae,* **cf.** *Austrotindaria canalensis.* A-B) *Promyalina schamarae,* articulated specimens. C) *Orbiculoidea winsnesi,* ventral valve. D) *?Austrotindaria canalensis.* exterior of left valve. Scale bar = 5mm.

Solitary discinids are sessile invertebrates attached by a sucker-like pedicle to hard surfaces and are probably facultatively motile (Mergl, 2010). Some recent discinids are infaunal, living attached on the underside of large boulders deeply embedded in coarse sand (Kato, 1996). Discinids have also been reported as attached to shelly fauna since the Ordovician (Mergl, 2010) and the attachment of one specimen to an ammonoid confirms an epifaunal mode of life. Discinids are suspension feeders and their co-occurrence with lingulids in laminated black shales has led some authors to infer a tolerance to low-oxygen conditions (Savoy, 1992; Hallam, 1995; Mergl, 2010).

Mode of Life. Surficial, stationary, attached, suspension feeder.

Phylum **Mollusca** Linnaeus, 1758

Class **Bivalvia** Linnaeus, 1758

Order **Pectinoida** Gray, 1854

Family **Asoellidae** Begg and Campbell, 1985

Genus *Leptochondria* Bittner, 1891

Species *Leptochondria occidanea* (Meek, 1877)

Figure 6.8, A-D.

1877	*Aviculopecten occidaneus*	Meek, p. 96, pl. 12
1889	*Halobia occidentalis*	Whiteaves, p.133, Pl. XVII, Fig. 5-6.
1961	*Pseudomonotis occidentalis*	Tozer, Plate XXVIII, Fig. 7-12.
1968	*'Pseudomonotis' occidentalis*	Tozer and Parker p. 543, Plate 25, Fig. C.
1978	*Pseudomonotis occidentalis*	Weitschat and Lehmann p. 92, Plate 14, Fig. 2.
1995	*Leptochondria occidaneus*	Newell and Boyd p. 70, Fig. 51.3-51.9.

Material. 554 specimens from the Lusitaniadalen and Vendomdalen members, Vikinghøgda Formation, Deltadalen section (samples DD-10, DD-11, DD-12, DD-14, DD-15).

Description. Shell small, equilateral, orbicular, slightly higher than long. Left valve feebly convex, with an orthogyrate umbo slightly projecting above a straight dorsal margin. Umbo located 40% anteriorly along the hinge line. Anterior auricle well demarcated from valve, with shallow auricular sinus. Posterior auricle not preserved. Valves covered with up to 50 radial ribs, as rounded ridges. Radial ornamentation is less defined towards the anterior and posterior margins, both auricles are also ornamented.

Remarks. Previous studies have assigned these specimens to *Pseudomonotis* however, the specimens from this study and previously described specimens from the Vikinghøgda Formation are not inequivalve and the umbo does not significantly protrude the hinge line, features that are diagnostic for *Pseudomonotis* (Newell and Boy, 1995). These specimens are similar to *Leptochondria occidanea*, and the diagnostic characteristics that were observed, i.e. hinge external, relatively small shell with most specimens <20mm, relatively short dorsal margin, posterior auricle small, left valve convex and ornamented with radial ribs, right valve less convex and mostly smooth (diagnosis after Newell and Boyd, 1995), which confirms this generic assignment. *Pseudomonotis occidentalis*, therefore, is considered a synonym of *L. occidanea*. The height of the largest specimen observed was 28.0mm, which is greater than the maximum 20mm diagnostic height for the genus as described by Newell and Boyd (1995). Size, however, is not a standard taxonomic criterion and these specimens are therefore assigned to *Leptochondria.*

Leptochondria was widespread in the Early Triassic, with six species described. These specimens agree well with the *L. occidanea* specimens figured by Newell and Boyd (1995) and Hofmann et al. (2014) from the Lower Triassic Thaynes Group, western

USA, by having a relatively pronounced anterior auricular sinus, a large posterior auricle and second-order ribs inserted by intercalation.

Mode of Life. Surficial, stationary, attached, suspension feeder (Hofmann et al. 2014).

Family **Deltopectinidae** Dickens, 1957

Genus *Crittendenia* Newell and Boyd, 1995

Species *Crittendenia kummeli* Newell and Boyd, 1995

Figure 6.8, E-F.

1978   *Posidonia mimer*   Weitschat and Lehmann. p 92. pl. 14, Fig. 3.

1995   *Crittendenia kummeli* Newell and Boyd. p.52. Fig. 38, 1-9.

2014   *?Crittendenia* sp.   Hofmann et al. p. 555. Fig. 11, N-O.

Material. 184 specimens from the Lusitaniadalen and Vendomdalen members, Vikinghøgda Formation, Deltadalen section (samples DD-10, DD-11, DD-12, DD-14, DD-15).

Description. Left valve suborbicular to slightly retrocrescent, slightly higher than long and distinctly inflated. Umbo prominent, prosogyrous, with beak projecting well beyond hinge line. Posterior auricle feebly demarcated. Left valves generally smooth except for faint commarginal growth lines.

Remarks. The left valve of *Crittendenia* is virtually indistinguishable from that of *Eobuchia*, but its right valve clearly differs in having a strongly prosogyrate umbo and a very wide byssal notch below the interior auricle (Wasmer et al., 2012). *Crittendenia kummeli* figured by Newell and Boyd (1995), *Crittendenia?* sp figured by Hofmann et al. (2014), *Posidonia mimer* figured by Weitschat and Lehmann (1978), and the specimens collected in this study, however, are more equilateral than *Eobuchia* and

other genera from the Buchiidae, and are their features in better agreement with the Deltopectinidae (as described by Newell and Boyd, 1995). The convex left valve, prominent umbo and mostly smooth characteristics of the shell are diagnostic for *C.*
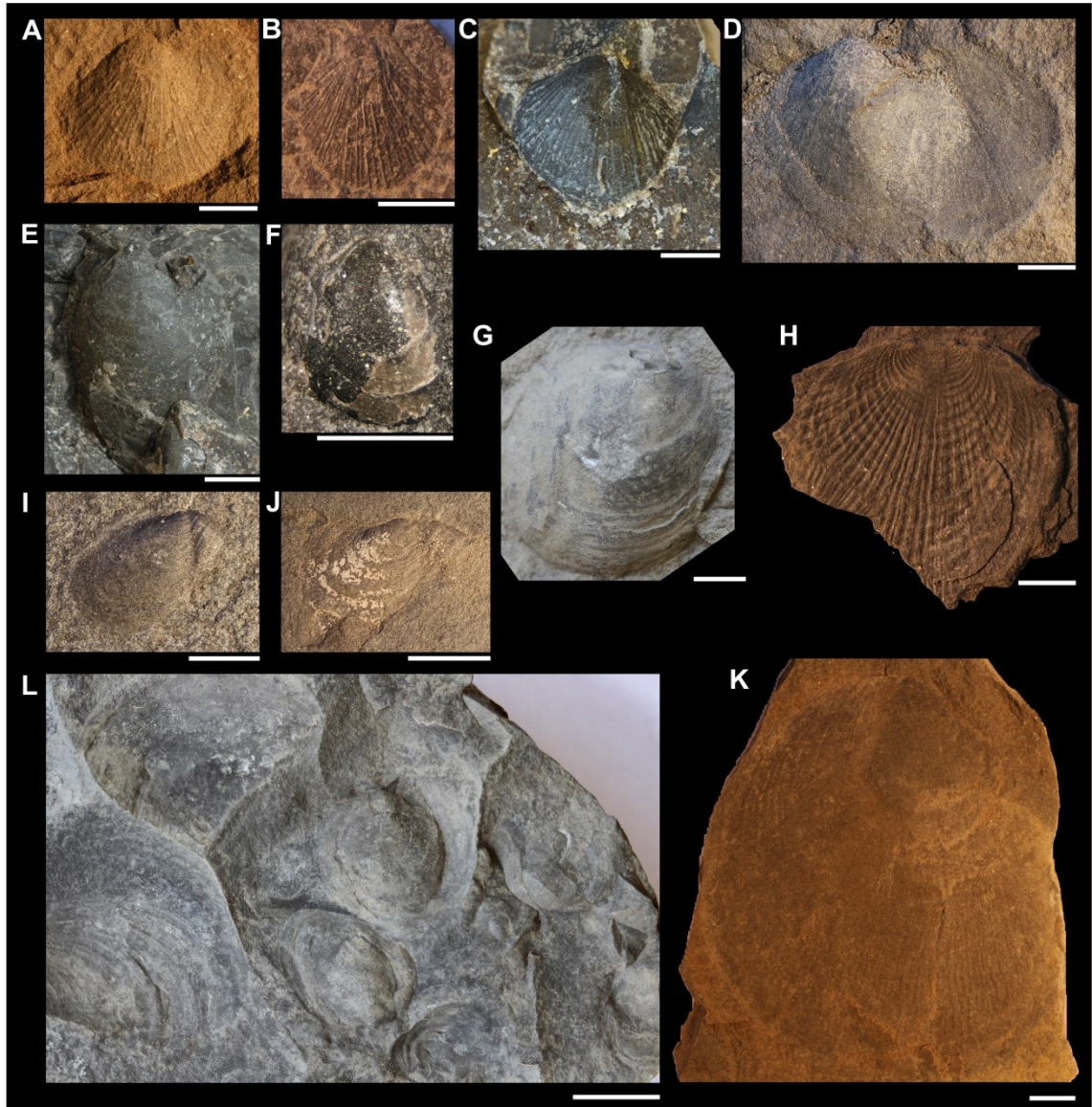
Figure 6.8: Bivalves from the Olenekian of the Deltadalen section, Svalbard. A-D) *Leptochondria occidanea*. A) Left valve, 165m. B) Left valve, 168m. C) Left valve, 162m. D) Left and right valve, 167m. E- F) *Crittendenia kummeli*. Left valve, 162m. G) *Eumorphotis telleri* Left valve, 185m. H) *Daonella* sp. Right valve, 225m. I-J) *Bakevellia costata*, left valve, 163m. K)?*Bositra* Left valve, 168m. L) *Eumorphotis telleri* assemblage, 185m. Scale bar = 5mm.

kummeli. *Posidonia mimer* figured by Tozer (1961), on the other hand, differ in having stronger concentric folds and densely packed, fine radial ribs.

Mode of Life. Surficial, stationary, attached, suspension feeder (Wasmer et al. 2012).

Family **Heteropectinidae** Beurlen, 1954

Genus *Eumorphotis* Bittner, 1901

Species **cf.** *Eumorphotis telleri* (Bittner, 1898)

Figure 6.8, G, L.

Material. 87 specimens from the Vendomdalen Member, Vikinghøgda Formation, Deltadalen section (sample DD-16).

Description. Outline orbicular to oval, equilateral, relatively large, inequivalve, with umbo protruding approximately 20% from the anterior margin. Conspicuously tumid, just below the umbonal area. Umbo, slightly prosogyrate, prominent, moderately broad, rounded and projecting above hinge margin. Shell ornamented with concentric folds marked by fine concentric lines and occasional faint widely spaced radial ribs.

Remarks. These specimens are similar to the *Eumorphotis telleri* specimens described from the Lower Triassic of northern Italy (Neri and Posenato, 1985; Broglio Loriga and Mirabella, 1986; Hofmann et al., 2015a; Chapter 5). The hinge line in these specimens, however, was not observed and it is not clear if the umbo of the left valve protrudes prominently beyond the hinge which is diagnostic of this genus and species, these specimens are therefore left in open nomenclature.

Mode of Life. Surficial, stationary, attached, suspension feeder (Ros-Franch et al., 2014).

Order **Pterioida** Newell, 1965

Family **Bakevelliidae** King, 1850

Genus *Bakevellia* King, 1848

Species *Bakevellia costata* (von Schlotheim, 1820)

Figure 6.8, I-J.

1820   *Mytulites costatus* von Schlotheim: p. 298

Material. 198 specimens from Lusitaniadalen member, Vikinghøgda Formation, Deltadalen section (samples DD-10, DD-11 and DD-12).

Description. Shell trapeziform, inequivalve. Right valve moderately convex. Commarginal, irregularly spaced, rectangular ribs with rounded edge that become more compact towards the anterior and posterior wings. Two thin secondary ribs on the gyros of primary ribs. Anterior wings separated by shallow sulcus from main body of shell. Posterior wing large.

Remarks. These specimens are poorly preserved as incomplete moulds and have a similar morphology to *Pteria, Confusionella* and *Bakevellia*. The absence of a straight hinge line and a pointed posterior auricle, however, suggest that they do not belong to *Pteria* (Shigeta et al., 2009). A diagnostic feature of *Confusionella* is a well-developed, narrow, posterior wing that extends far beyond the posterior end of the disc (Hofmann et al., 2015a) which was not observed in these specimens. The shape, commarginal ribs, and the presence of an anterior wing separated by a shallow sulcus from the main body and a large posterior wing is very similar to the specimens assigned to *Bakevellia costata* by Hautmann et al. (2013) and Hofmann et al. (2013a).

Mode of Life. Semi-infaunal, stationary attached, suspension feeder (Stanley, 1972).

Family **Myalinidae** Frech, 1891

Genus *Promyalina* Kittli, 1904

Species *Promyalina schamarae* (Bittner, 1899)

Figure 6.7, A-B.

1899   *Myalina schamarae*   Bittner. p.19, pl. 4, Figs 20-25.

2009   *Promyalina schamarae* Kumagae and Nakazawa. p. 157. Fig 144, 4-5.

Material. 12 specimens from the Deltadalen Member, Vikinghøgda Formation, Lusitaniadalen section (L-04 and L-05).

Description. Shell small, inequilateral, subquadrate or myaliniform, prosocline, higher than long, and moderately inflated. Umbo small, terminal, and prosogyrate. Posterior dorsal margin straight. Posterior margin slightly convex, forming a rounded posteroventral margin. Anterior margin long, nearly straight or weakly acute and partly depressed near the umbo.

Remarks. These specimens were preserved as articulated specimens so the internal characters and hinge in these specimens were not observed, but the external shells are very similar to *Promyalina schamarae* specimens described and figured from the Griesbachian Lazurnaya Bay Formation, Russia (Shigeta et al., 2009).

Mode of life. Surficial, stationary, attached, suspension feeder (Stanley, 1972; Hofmann et al., 2014).

Family **Halobiidae** Kittl, 1912

Genus *Daonella* Mojsisovics, 1874

Species *Daonella* **sp.**

Figure 6.8, H.

Material. 89 specimens from the Vendomdalen Member, Vikinghøgda Formation, Deltadalen section (sample DD-17).

Description. Broadly subovate shells with a central beak slightly towards the anterior margin. More than 40 radial ribs with flat tops that are organised in sets of threes with the middle rib in each set being narrower than the other two ribs. Commarginal folds generally prominent, especially near the umbo. Posterior margin with a triangular sector with broad flat costae.

Remarks. The oldest species of the Halobiidae family are currently reported from the Middle Triassic, these specimens therefore extend *Daonella* and the Halobiidae into the upper Spathian. These specimens differ from *Enteropleura* as they lack a clearly differentiated anterior triangular sector separated from the main disc (Hopkin and McRoberts, 2005). These specimens are similar to *D. dubia* but differ in that ribs are bundled in threes rather than pairs (Smith, 1914) and from *D. lindstromi* in its lack of convexity (Smith, 1914). The shape of the Halobiidae change noticeably during ontogeny, the relatively equal height/length ratio of the measured specimens in this study suggests a late growth stage (Schatz, 2004). Most of the external features described and figured by Drake and Lyttle (1981) for *D. rieberi* are indistinguishable from the specimens collected in this study. The position of the beak in our specimens, however, is more central then *D. rieberi* and the commarginal fold are more conspicuous and therefore considered a separate species.

The mode of life of halobiids is equivocal. They have been described as either semi-infaunal, epifaunal or pseudoplanktonic with different species having different modes of life (Ros-Franch et al., 2014). In terms of functional morphology *Daonella* is very similar to *Claraia* in that they are both thin-shelled and subcircular. Also, like *Claraia,* many of the *Daonella* species are described from facies that indicate a soft soupy substrate in an oxygen-deficient environment. Therefore, this study agrees with the

interpretation of Schatz (2005) who infers an epibenthic pleurothetic unattached mode of life on soft substrate especially adapted to low oxygen conditions.

Mode of Life. Surficial, facultatively motile, unattached, suspension feeder.

Family **Posidoniidae** Frech, 1909

Genus **cf. *Bositra*** de Gregorio, 1886

Species **cf. *Bositra aranea*** (Tozer, 1961)

Figure 6.8, K.

1961   *Posidonia aranea*   Tozer, p.102, pl XXVIII, No.12

Material. Four specimens from the Lusitaniadalen and Vendomdalen members, Vikinghøgda Formation, Deltadalen section (samples DD-11, DD-15).

Description. Medium size shell, with a diameter up to 88mm, and slightly inequilateral with the beak positioned about 40% of shell length from anterior. Shape generally obliquely oval, slightly longer than high with rounded anterior and posterior margins. Beak is slightly prosogyrous to orthogyrous, slightly inflated below umbonal margin. Ornamentation consists of fine commarginal ridges with rounded tops. More than 80 radial ribs evenly spaced every ~1mm along the shell margin. On the posterior side seven larger radial ribs are present.

Remarks. Early Triassic specimens belonging to the Posidoniidae are usually assigned to *Posidonia aranea*. Early Triassic *Posidonia* were included into the new genus *Peribositra* by Kurushin and Truschchelev (1989), however, Waller and Stanley (2005) considered *Peribositra* to be a junior synonym of *Bositra* as the distinguishing features described by Kurushin and Truschchelev (1989) could not be supported. The ligament structure is used for the discrimination between the genera of the Posidoniidae, i.e. duplivincular in *Posidonia* and alivincular in *Bositra* (Waller and Stanley, 2005), but

the ligament structure was not observed in this study. Therefore, a confident generic assignment cannot be made. Based on the more symmetrical nature of the specimens from this study the specimens better resemble *Bositra* than *Posidonia.* Waller and Stanley (2005) consider *Posidonia* to be a Palaeozoic genus, and *Bositra* to be confined to the Triassic and Jurassic, implying that the Early Triassic forms should be reassigned as *Bositra*.

Ecology. Waller and Stanley (2005) interpret a benthic reclining mode of life for *Bositra* probably retaining a facultative byssal attachment that is interpreted in *Posidonia*.

Mode of Life. Surficial, facultatively motile, attached, suspension feeder.

Family **Pterinopectinidae** Newell, 1938

Genus *Claraia* Bittner, 1901

Species *Claraia kilenensis* Spath, 1935

Figure 6.6, D.

1935   *Claraia kilenensis*   Spath   p73. Pl. XXII Fig. 1.

Material. Thirteen specimens from the Selmaneset Member, Vardebukta Formation, Festningen section (sample F-01).

Description. Oval outline, higher than long. Left valve convex with central, orthogyrate umbo projecting above dorsal margin. Left valve with ~20 thick radial ribs which are more irregularly and wider spaced in the central portion of the shell. Right valve flat and internal features not observed.

Remarks. *C. kilenensis* differs from *C. stachei* by having comparatively coarser and fewer (~20) radial ribs (Spath, 1935). The left valve is also more elongated than *C. stachei*.

Several modes of life have been interpreted for *Claraia* species ranging from benthic epibyssate to pseudoplanktonic and an occasional swimmer (Yang et al., 2001). These different interpretations are inferred from the different morphology of the byssal notch and shape of the auricle. He et al. (2007) interpret the shallower byssal notch described from Triassic *Claraia* species as representing increased motility and a facultatively motile mode of life.

Mode of Life. Surficial, facultatively motile, attached, suspension feeder (Ros-Franch et al., 2014).

Species *Claraia stachei* Bittner, 1901

Figure 6.6,

1901   *Pseudomonotis (Claraia) stachei*   Bittner. p. 587.

Material. 37 specimens from the Selmaneset Member, Vardebukta Formation, and Deltadalen Member, Vikinghøgda Formation (samples F-01, DD-05).

Description. Orbicular to oval outline, with similar height and length. Left valve weakly convex with central, orthogyrate umbo slightly projecting above dorsal margin. Approximately 30 primary and 30 secondary radial ribs. The concentric lines are thin and clearly visible but less pronounced than the radial ribs. Right valve not observed.

Mode of Life. Surficial, facultatively motile attached, suspension feeder (He et al., 2007).

Species *Claraia* cf. *clarai* Nakazawa 1977

Figure 6.6, B.

Material. Two specimens from the Selmaneset Member, Vardebukta Formation (sample F-01).

Description. Orbicular to oval outline. Left valve convex with weak radial ribs and 12 clear concentric folds. The hinge is not observed.

Remarks. These specimens have twice as many folds as *C. extrema*, and so according to Spath (1935) should therefore be included with *C. clarai.* These specimens, however, are more convex, smaller and also have more concentric folds than other *C. clarai* specimens described from the Lower Triassic (Nakazawa, 1977; Tozer, 1961). The byssal notch in these specimens was not observed and so it is difficult to confidently assign these specimens to a species.

Mode of Life. Surficial, facultatively motile attached, suspension feeder (He et al., 2007).

<div align="center">Species <i>Claraia radialis</i> Leonardi, 1935</div>

<div align="center">Figure 6.6, A.</div>

1935   *Claraia radialis*   Leonardi, p. 60, pl. 3, Fig 3-4.

2013   *Claraia radialis*   Pan et al. p.5, Fig. 3, A-K.

Material. Twelve specimens from Selmaneset Member, Vardebukta Formation (sample F-01).

Description. Orbicular outline, length similar to height, right valve faintly inflated. Greatest inflation of shell slightly anterior of the mid-line, just below the umbonal area and it becomes flat close to the ventral margin. Hinge line not observed. Ornamentation consisting of ~20 radial ribs with the strongest in the midline of the shell. Ribs are more pronounced than the concentric growth lines and the distance between them is greater than between growth lines.

Remarks. These specimens differ from *C. stachei* in having fewer ribs, and from *C. clarai* by having more pronounced ribs than concentric folds (Pan et al., 2013).

Mode of life. Surficial, facultatively motile attached, suspension feeder (see *C. kilenensis*).

Species *Claraia* **cf.** *griesbachi* (Bittner, 1899)

Figure 6.6, E-F.

1899   *Pseudomonotis griesbachi* Bittner, p. 2, pl. 1, Figs 1-4.

Material. Seven specimens from the Deltadalen Member, Vikinghøgda Formation, Deltadalen section (sample DD-02).

Description. Shell small and poorly preserved. Slightly higher than long. Left valve convex, and inflated just below the umbonal area. Surface covered with numerous fine commarginal growth lines. Right valve not observed.

Remarks. These specimens share the following diagnostic characters with *Claraia griesbachi*: subovate disc, slightly longer than high; several strong folds; numerous fine commarginal growth lines; and no radial ornamentation (Pan et al., 2014). *C. griesbachi* is, however, also diagnosed by characteristics of the hinge, which were not observed in this study. These specimens are not, therefore, clearly distinguishable from *C. aurita* and only a questionable assignment is made.

Mode of Life. Surficial, facultatively motile attached, suspension feeder (He et al., 2007).

Order **Solemyoida** Dall, 1889

Family **Nucinellidae** Vokes, 1956

Description. Shell nuculoid, obliquely oval, higher than long, monomyarian, only anterior abductor muscle present. Hinge with subumbonal taxodont teeth and single

elongate lateral tooth on the anterior dorsal margin. Ligament mostly opisthodetic, wholly external or in a sunken resilifer.

Remarks. Living nucinellids are often classified in the family Manzanellidae which extends back into the Permian. Oliver and Taylor (2012) show that, *Manzanella*, the type genus of Manzanellidae, differs in several key respects from nucinellids *Nucinella* and *Huxleyia*. *Manzanella* is dimyarian and subcircular, whereas *Nucinella* and *Huxleyia* are monomyarian and elliptical, and the taxodont teeth lie posterior to the beaks in *Manzanella*, but are largely anterior in *Nucinella* (Oliver and Taylor, 2012). These specimens are therefore assigned to the Nucinellidae.

Genus *Nucinella* Wood, 1851

Description. As for the family. Ligament prominent, external, does not invade the hinge plate.

Remarks. Only two taxa are described for the Nucinellidae, *Nucinella* and *Huxleyia*. The diagnosis for *Huxleyia* and *Nucinella* is as for the family; except that in *Huxleyia* the ligament is mostly internal and set in a sunken resilifer. In these specimens the ligament is opisthodetic, thus clearly not *Huxleyia* and are identified as *Nucinella*.

Species *Nucinella* sp.

Figure 6.9, A-J.

Material. 10 adult and 92 larval specimens from the Deltadalen Member, Vikinghøgda Formation, Lusitaniadalen section (samples LD-04, LD-05).

Description. Outline nuculoid, suboval, posterior dorsal margin distinct, slightly incurved; posterior margin long, almost straight. Inequilateral, beaks close to posterior margin. Shell small, thin and equivalve; H/L ~1.0. Umbo prominent. Smooth shell with growth lines. Monomyarian, posterior adductor muscle scar absent; anterior adductor large, oval. Three subumbonal pointed blade-like teeth plus two large anterior parallel

teeth. Ligament prominent, external and does not invade the hinge plate. Lateral tooth is very long. Left valve with a weak secondary ridge creating a shallow socket. In larval specimens ~3 subumbonal teeth plus ~12 anterior teeth which appear to be being replaced (undergoing metamorphosis).

Remarks. The majority of extant *Nucinella* range from intertidal to ca.500m water depth (la Perna, 2005), but some representatives have been described from water depths >3000m (Oliver and Taylor, 2012). In addition, a large *Nucinella* species has been described from a late Cretaceous cold-seep deposit (Amano et al., 2007), showing that this genus was adapted to a wide range of environmental settings. Bacterial symbiosis is now confirmed for *N. owenensis* and *H. habooba* and has been inferred for all species of the Nucinellidae (Oliver and Taylor, 2012). Currently the oldest known *Nucinella* is reported from the Jurassic (Clausen and Wignall, 1990) but these specimens from Svalbard now extend the range of *Nucinella* to the Early Triassic *H. parvus* Conodont Zone.

Mode of life. Shallow infaunal, facultatively motile, unattached, chemosymbiotic.
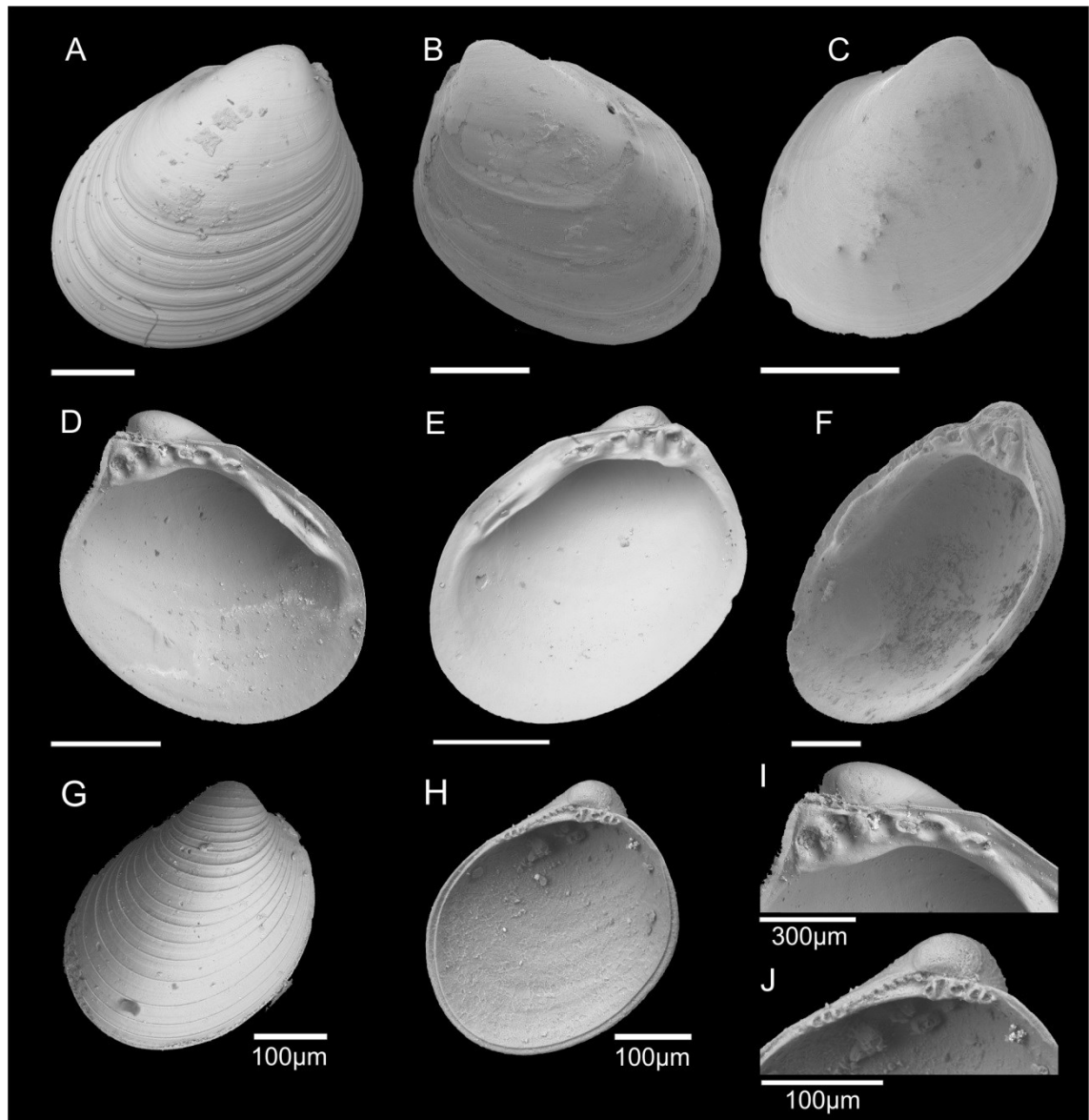
Figure 6.9: *Nucinella* **sp.** A) exterior of left valve. B) exterior of right valve. C) exterior of left valve. D) interior of left valve. E-F) interior of right valve. G) Exterior of left larval shell. H) Interior of right larval shell. I) Detail of hinge plate of an adult shell. J) Detail of hinge of a larval shell. Scale bar = 500μm.

Order **Nuculanoida** Carter et al., 2000

Family **Neilonellidae** Schileyko, 1989

Description. Hinge plate with taxodont teeth in two series; sometimes separated by narrow, plain area, without resilifer; ligament predominantly external, opisthodetic to amphidetic, and weak.

Remarks. The Neilonellidae are very similar to the Nuculanidae, but the lack of a resilifer in mature forms supports their separation (Coan and Valentich-Scott, 2012). The new specimens differ from the Malletiidae in lacking conspicuous gapes, and from the Tindariidae in having a short gap in the dentition below the beaks (Di Geronimo and La Perna, 1997). The family is currently known from the Jurassic to present in all oceans, especially in deep water and soft substrates (Coan and Valentich-Scott, 2012).

<div align="center">Genus Austrotindaria Fleming, 1948</div>

Description. Shell thin, equivalve, inequilateral, inflated; posterior end produced, poorly sculptured; ligament external, narrow, opisthodetic; no pallial line, sinus or muscle scars observed; small elongate pit below a short edentulous gap.

Remarks. There are three valid genera of the Neilonellidae: *Neilonella, Austrotindaria* and *Pseudoneilonella* (La Perna, 2007). The convex shape of the posterior margin in our specimens is in better agreement with *Austrotindaria* than *Neilonella* (see discussion in Di Geronimo and La Perna, 1997). *Austrotindaria* differs to *Neilonella* and *Pseudoneilonella* in having a delicate, almost smooth shell, which strongly contrasts with the sturdy sculptured shell of *Neilonella* and *Pseudoneilonella* (La Perna, 2007). *Austrotindaria* and *Pseudoneilonella* differ to *Neilonella* in having an opisthodetic rather than amphidetic ligament (La Perna, 2007). A small elongate pit between the posterior and anterior teeth has only been described from *Austrotindaria* (La Perna, 2007). This genus is currently known from the Miocene to Recent (La Perna, 2007; Coan and Valentich-Scott, 2012).

The type species of *Austrotindaria* is *A. wright* (Fleming, 1948). Diagnostic characters of *Austrotindaria* documented by Fleming (1948) are the absence of a resilifer; narrow, oblique, opisthodetic ligament; strong hinge-plate, separated into anterior and posterior parts by an edentulous gap; weak concentric sculpture; and no rostrum. Including the

type species, there are seven accepted species of this genus. The new specimens agree with the type species of *Austrotindaria*.

Species *Austrotindaria* **sp. A.**

Figure 6.10, A-I.

1930   *Nucula* sp. juv. ind   Spath. p53. Pl. XII, Fig 12.

1935   *Adontophora subovalis* Spath. p. 76, pl. XX, Fig.9.

1985   *Unionites fassaensis* var. *brevis* Neri and Posenato p 105, pl. 2. Fig 8.

2012   *Unionites? fassaensis* Hautmann et al. p 19. Fig. 7. L-M.

2013   *Unionites* cf. *borealis* Hautmann et al. p. 20. Fig. 7, X-Y.

2013   *Unionites fassaensis*   Hofmann et al. p 887. Fig. 8. 17-18.

2014   *Unionites fassaensis*   Hofmann et al. p 567. Fig. 13. C-D.

Material. 120 adult and 43 larval specimens from the Deltadalen member, Vikinghogda Formation (samples LD-04, LD-05, LD-06)

Description. Outline subtrigonal, equivalve, inequilateral with beaks lying approximately 40% of dorsal margin length from anterior; H/L ratio 0.6-1. Conspicuously tumid. Anterodorsal margin slightly rounded and gently sloping. Posterodorsal margin almost straight to slightly rounded and gently sloping. Slight angled junction with posterior margin. Ventral margin deeply rounded. Escutcheon short, relatively broad, elliptical; lunule narrow. Umbo orthogyrate, prominent, moderately broad, rounded, projecting above hinge margin. Shell ornamented with fine concentric growth lines; entire inner margin smooth. Protoconch smooth, broadly subovate.

Ligament, small, external with well-defined margin, opisthodetic, with a well-rounded triangular pit seated beneath the edentulous gap. Hinge plate with taxodont teeth in two series; sometimes separated by narrow, plain area, without resilifer, below the beak, broadening towards the anterior and posterior ends. Teeth robust, moderately long and

blunt, more posterior teeth than anterior separated by an edentulous gap. Smooth ventral margin. No pallial line, sinus or muscle scars. As the size of the shell increases the edentulous gap becomes proportionally smaller, more central and moves externally.

Remarks. The external morphology of these specimens is the same as most Early Triassic specimens identified as *Unionites fassaensis*, which is one of the most widespread bivalve species of the Early Triassic. Due to poor preservation, however, little is known about the internal morphology of the valves of Early Triassic which has created uncertainty about their systematic position (Hautmann et al., 2013).

The new Early Triassic specimens described herein are the first that preserve the internal characters. Internally, these specimens lack the following diagnostic characters of *Unionites*: a nymph extending nearly half of the posterior margin; an impressed adductor muscle scar; an overlap of anterior hinge; and a deeply impressed lunule and posterior keel (Geyer et al., 2005). These species, clearly do not belong to *Unionites*.

A distinguishing external feature that separates *Austrotindaria* sp. A and most *Unionites* species is the direction of the beak. In the specimens described here and most other *Austrotindaria* species the beak is orthogyrate to posteriorly opisthogyrate, whereas in *Unionites* it is prosogyrate. Based on this feature, most specimens previously assigned to *Unionites fassaensis* based solely on external morphology and possessing an orthogyrate beak are considered synonyms of *Austrotindaria* sp. A.

These specimens have a very similar shape, size and ornamentation to the type species of *Austrotindaria* (*A. wrighti* Flemming), however, they differ in possessing a small
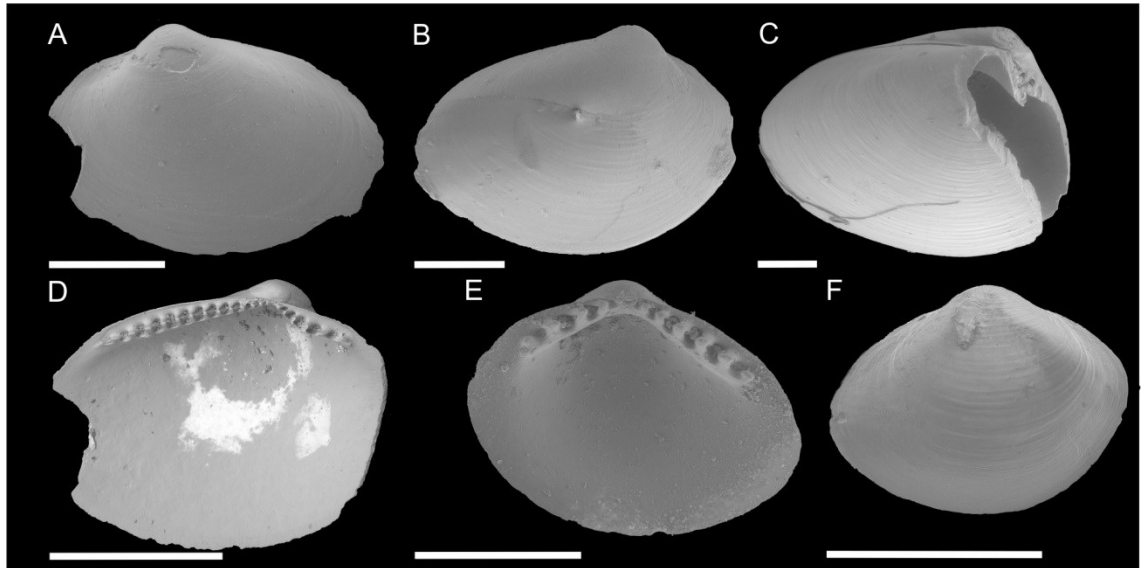
Figure 6.10: *Austrotindaria* **sp. A.** A) Exterior of right valve. B) Exterior of left valve. C) Articulated valves. D) Interior of right valve. E) Interior of left larval shell. F) Exterior of left valve. Scale bar = 1mm.

rounded triangular pit below the edentulous gap and differ from other species, e.g. *A. mawheraensis*, in lacking a weak posterior rostrum. They are, therefore, considered a separate species.

Mode of Life. Modern representatives of the Neilonellidae have palp proboscides that are used to sift through the sediment to retrieve buried food particles and a foot with papillated planar sole that is used for moving slowly through the sediment (Stasek, 1961). These are shallow infaunal, facultatively motile, unattached, miners.

Species *Austrotindaria* **sp. B.**

Figure 6.11, A-C.

1963   *Unionites fassaensis* Ciriacks. p81, pl 16, Fig. 13.

1963   *Unionites breviformis* Ciriacks. p 81, pl. 16, Figs 14-15

2009   *Unionites fassaensis*   Kumagae and Nakazawa p166. Fig 145. 5-9.

2012   *Unionites? fassaensis* Hautmann et al. p 19. Fig. 7. O.

2015   *Unionites fassaensis*   Hofmann et al. p.8. Fig. 4, K.

Material. Two specimens from the Deltadalen Member, Vikinghøgda Formation, Lusitaniadalen section (L-04, L-05).

Description. Outline subtrigonal, equivalve, inequilateral with beaks lying approximately 30% of dorsal margin length from posterior; H/L ratio 0.6-1. Conspicuously tumid. Anterodorsal margin slightly rounded gently sloping; posterodorsal margin almost straight to slightly rounded and gently sloping; slight angled junction with posterior margin. Ventral margin deeply rounded. Escutcheon short, relatively broad, elliptical; lunule narrow. Umbo, prosogyrate, prominent, moderately broad, rounded, projecting above hinge margin. Ornamented with fine concentric growth lines; entire inner margin smooth.

Ligament, small, external with well-defined margin, opisthodetic, with a well-rounded triangular pit seated beneath the edentulous gap. Hinge plate with taxodont teeth in two series; sometimes separated by narrow, plain area, without resilifer, narrow below the beak, broadening towards the anterior and posterior ends, without resilifer. Teeth, robust, moderately long and blunt, more than 50% fewer anterior than posterior teeth. Smooth ventral margin. No pallial line, sinus or muscle scars observed. As the size of the shell increases the proportional size of the edentulous gap becomes smaller, becomes more central and moves externally.
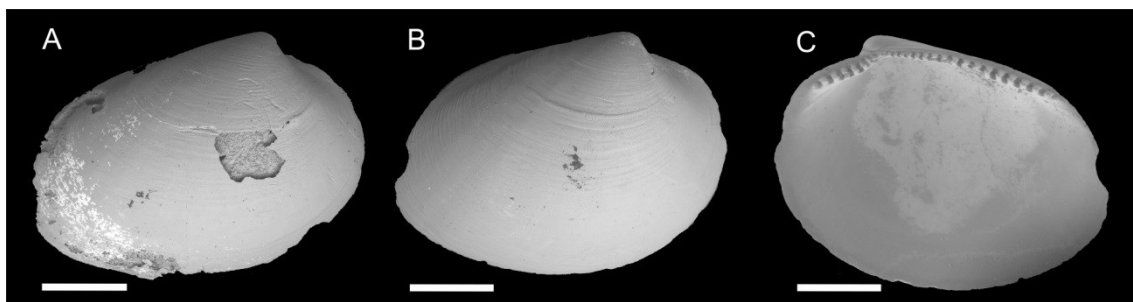
Figure 6.11: *Austrotindaria* sp. B. A-B) Exterior of right valve. C) Interior of right valve. Scale bar = 1mm.

Remarks. These specimens differ to *Austrotindaria* sp. A by having a less equal number of anterior to posterior teeth and with a more prosogyrous beak. The more prosogyrate beak in *Austrotindaria* sp. B means that externally these species have a similar morphology to Middle Triassic *Unionites* specimens. These specimens lack the diagnostic criteria of *Unionites*, except that they have a faint posterior keel. *Unionites* specimens described by Geyer et al. (2005) and from this study, however, have a strong posterior keel. Due to the lack of a posterior keel described in previous Lower Triassic specimens, this study considers previous *Unionites fassaensis* specimens with a prosogyrate beak and that lack a posterior keel, therefore, as *Austrotindaria* sp. B.

Species **cf. *Austrotindaria canalensis* nov. comb.** (Catullo 1846)

Figure 6.7, D.

1846   *Tellina canalensis*   Catullo p56, pl.4, Fig.4.

1859   *Tellina canalensis*   Schauroth p327, pl.2, Fig. 17.

1963   *Unionites canalensis*   Ciriacks p81, pl.16, Fig.11-12.

2009   *Unionites canalensis* Kumagae and Nakazawa p166. Fig 145. 1-4.

2012   *Unionites? canalensis* Hautmann et al. p. 20, Fig. 7, P-Y.

2015   *Unionites canalensis* Hofmann et al. p 8. Fig. 4.J.

Material. 22 specimens from the Deltadalen Member, Vikinghøgda Formation, Lusitaniadalen section (L-04, L-05, L-06).

Description. Outline sub-ovate to elongate, equivalve, inflated below the umbo; inequilateral with beak lying approximately 40% along the dorsal margin length from anterior margin; H/L ratio 0.4-0.7. Posterior margin elongated and almost straight, anterior margin narrowly rounded. Escutcheon and lunule indistinct. Umbo orthogyrate,

prominent, moderately broad, rounded, projecting above the hinge margin. Shell ornamented externally with fine concentric growth lines; entire inner margin smooth.

Remarks. The internal characters and hinge in these specimens were not observed, but the external shell is virtually identical to those that are typically assigned to *Unionites canalensis*, e.g. Hautmann et al. (2012). Ciriacks (1963) described the median position of the umbo as a diagnostic feature of *Unionites canalensis*, and this is present in these specimens and most Early Triassic specimens described as *Unionites canalensis*. *Unionites,* however, have a more anteriorly located umbone (Geyer et al., 2005). In addition, the beak in *Unionites* is prosogyrate rather than orthogyrate (Hautmann et al., 2012) as is in these and other Early Triassic specimens. Thus, clearly not *Unionites*.

The external features of these specimens are most similar to the Neilonellidae, e.g. *Nielonella ritteri* (Coan and Valentich-Scott, 2012). The posterior margin is more elongated than in *Austrotindaria* sp., and therefore interpreted to represent a separate species.

Mode of Life. These are shallow infaunal, facultatively motile, unattached, miners (see *Austrotindaria* sp.).

<div align="center">

Order **Unionoida** Stoliczka, 1871

Family **Anthracosiidae** Amalitsky, 1892

Genus *Unionites* Wissmann, 1841

Species *Unionites* **sp.**

Figure 6.12, A-F.

</div>

2009   *Triaphorus* aff. *multiformis* Kumagae and Nakazawa p.171, Fig. 145, 18-25.

Material. Three specimens from the Deltadalen Member, Vikinghøgda Formation, Lusitaniadalen section (L-04, L-5, L-06).

Description. Outline suboval to elongate-elliptical or rectangular to trapeziform. Shell equivalved, inflated below the umbo; inequilateral with beaks lying approximately 15% of dorsal margin length from anterior margin. Lower part of anterior dorsal margin slightly projecting beyond plane of commissure, posterodorsal margin almost straight to slightly round and gently sloping. Escutcheon long and narrow, lunule deeply impressed. Umbo prosogyrate and rising above hinge margin. Body well demarcated from the anterior auricle. Ornamented with fine concentric growth lines; entire inner margin smooth. Protoconch smooth, orbicular.

Small subumbonal grove limits the shell projection posteriorly. Posterior lateral tooth below posterior dorsal margin of left valve. Hinge of left valve with anterior platform that bears depression for corresponding anterior hinge margin of right valve, followed posteriorly by small, tuberculiform subumbonal tooth fitting above posterior lateral tooth of right valve. Ligament fixed to a nymph, which extends about half-length of posterior dorsal margin. Muscle scars isomyarian with the anterior adductor muscle scar deeply impressed.

Remarks. Insufficient knowledge of the internal morphology of Early Triassic *Unionites* has created uncertainty about their systematic position. Based on the external morphology alone these specimens would have been assigned to *Triaphorus* aff. *multiformis* (Shigeta et al., 2009). These specimens have the following diagnostic internal characters: an overlap of the anterior hinge margin of the right valve over that of the left; the presence of a nymph extending nearly half the length of the posterior hinge margin; an impressed anterior adductor muscle scar; a deeply impressed lunule; and a long and narrow escutcheon, which is diagnostic of the genus *Unionites*. There are around 50 nominal species of *Unionites* and without an investigation of each of these a more specific assignment of these specimens cannot be made.
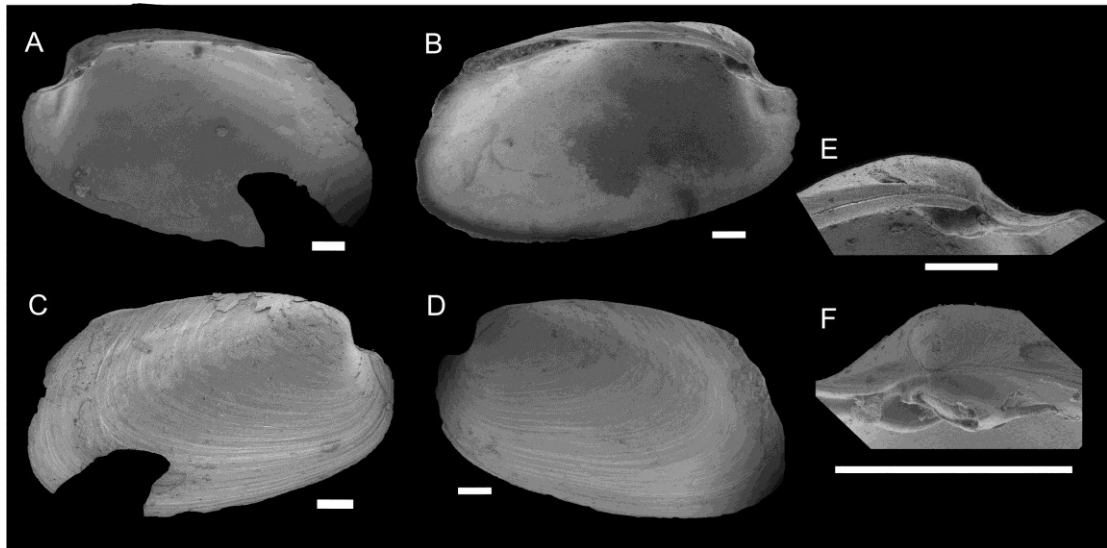
Figure 6.12: *Unionites* **sp.** A) Interior of right valve. B) interior of left valve. C) exterior of right valve. D) exterior of left valve. E) Detail of subumbonal tooth pit. F) Detail of subumbonal tooth. Scale bar = 500μm.

Mode of Life. Shallow infaunal, facultative, unattached, suspension feeder (Hautmann et al., 2012).

Order **Trigoniida** Dall, 1889

Family **Myophoriidae** Bronn, 1849

Genus *Neoschizodus* Gieberl, 1855

Species *Neoschizodus laevigatus* (Ziethen, 1830)

Figure 6.13, A-E.

1830   *Trigonia laevigata*   Ziethen, p. 94, pl. 71, Figs 2, 6.

Material. Five adult and 81 larval specimens from the Deltadalen Member, Vikinghøgda Formation, Lusitaniadalen section (samples L-04, L-05).

Description. Outline trigonally subovate, equivalve, inflated, and slightly inequilateral, H/L ~1, slightly higher than long, umbo small and orthogyrate, umbonal ridge elevated and subangular to rounded. Anterodorsal margin recurvate, passing to widely arched

ventral margin, lunule narrow, posterodorsal margin straight, posterior margin is slightly concave, entire inner margin smooth. Faint concentric growth lines.

Larval shells have a similar external morphology, hinge short and subumbonal, with narrow short nymphs running down the anterior and posterior margins. Some shape as protoconch observed on mature specimen. Protoconch smooth with fine concentric lines probably reflecting growth lines.

Remarks. These specimens have most of the required diagnostic criteria for assignment to *Neoschizodus*: an orthogyrous to moderately prosogyrous shell with an incurved beak; obliquely truncate and pointed respiratory margin; and a posterior ridge angular to subangular in transverse. The nymph, teeth and umbonal platform were not observed in these specimens so it is not known if these specimens have a myophorian hinge that is also diagnostic of this genus. These specimens do, however, have a similar external morphology to other described *Neoschizodus laevigatus* specimens from the Lower and Middle Triassic and are thus assigned to *N. laevigatus.*
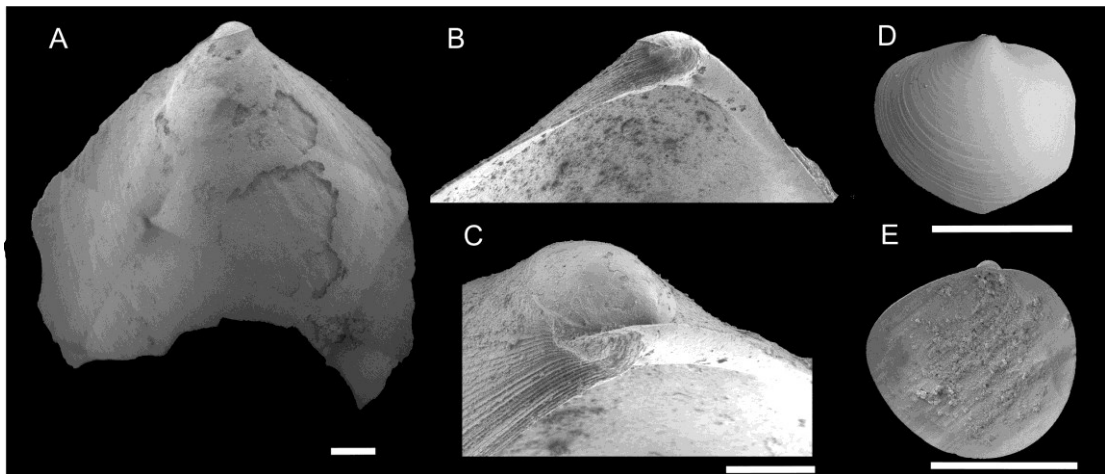
Figure 6.13: *Neoschizodus laevigatus* A) exterior of right valve. B-C) detail of hinge and protoconch in right valve. D) exterior of right valve, Juvenile specimen. E) interior of left valve, juvenile specimen. Scale bar = 200μm.

A protoconch was recorded in this study on an adult specimen and other were found as individuals in the conodont residues. These are the first protoconchs described for this genus. The hinge plate was not observed to be myophorian, but it is not known how a myophorian hinge plate develops through ontogeny (Newell and Boyd, 1975). Hautmann and Nützel (2005) suggest that a small prodissoconch I and a relatively large prodissoconch II in bivalves suggests a planktotrophic larvae stage and therefore a planktotrophic larvae stage is interpreted for *N. laevigatus.*

Mode of Life. Shallow infaunal, facultatively, unattached, suspension feeder.

Class **Gastropoda** Cuvier, 1798

Order **Amphigastropoda** Simroth, 1906

Family **Euphemitidae** Knight, 1956

Genus ***Warthia*** Waagen, 1880

Species ***Warthia zakharovi*** Kaim, 2009

Figure 6.14, A-C.

2009   *Warthia zakharovi*   Kaim, p. 141, Fig. 132-134.

Material. 308 specimens from the Deltadalen member, Lusitaniadalen section (L-04, L-05).

Description. Shell globular, almost as long as wide. Slit short and broad at base of U-shaped sinus. In well preserved specimens thin ribs perpendicular to the growth direction are present, which may represent growth lamellae.

Remarks. Kaim (2009) describe *Warthia zakharovi* as being smooth with no ornamentation. The ornamentation in these specimens from Svalbard probably reflects growth lines and is visible due to their exceptional preservation. Some of these

specimens will also likely include protoconchs, however, as *Warthia* develop they reabsorb previous whorls, therefore, making developmental stage difficult to interpret.

Mode of Life. Surficial, fully motile, slow, surface deposit feeder (Linsley, 1977).

Order **Vetigastropoda** Salvini-Plawen, 1980

Family **Eotomariidae** Wenz, 1938

Genus ***Wannerispira*** Kaim and Nützel, 2010

Species ***Wannerispira shangganensis*** Kaim and Nützel, 2010

Figure 6.16, A-D.

2010   *Wannerispira shangganensis* Kaim and Nutzel, p. 124, Fig. 3.

Material. 19 specimens from the Deltadalen Member, Lusitaniadalen section (samples L-04, L-05).

Description. Shell trochoidal, relatively high spired. The earliest whorls are rounded and smooth. The selenizone is concave between a pair of spiral ribs with a lower rib on shell periphery. Demarcation between the lateral flank and base is slightly angulated with weak spiral ribs. The base is ornamented with conspicuous spiral ribs. Growth
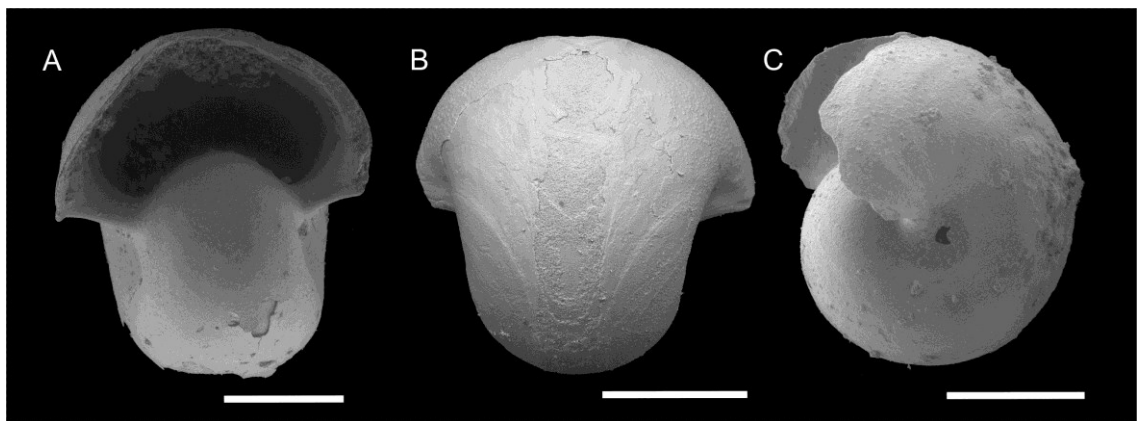
Figure 6.14: ***Warthia zakharovi.*** A) Dorsoaperatural view, B-C) dorsal views. Scale bar = 1mm.

lines visible at intersection of spiral ribs, otherwise no axial ornamentation recorded. Aperture is D-shaped; peristome uninterrupted and inner lip has columellar fold; selenizone gives a U-shaped depression to the outer lip. Coiling dextral. Protoconch I openly coiled; smooth. Protoconch II has is slightly more than one whorl and strongly ornamented with spiral threads.

Remarks. These specimens are conspecific with *Wannerispira shangganensis* described by Kaim and Nützel (2010), however, the specimens figured by Kaim and Nützel (2010) appear to be more slender than the specimens from this study, and therefore may be considered to represent a separate subspecies.

Vetigastropoda have a diverse range of living habits as part of wood-fall communities (Kiel et al., 2008). The specimens in this study occurred in association with wood fragments, however, no direct relationship was observed. Specimens of the Eotomariidae from the Zechstein Reef are described as motile algal grazers that were
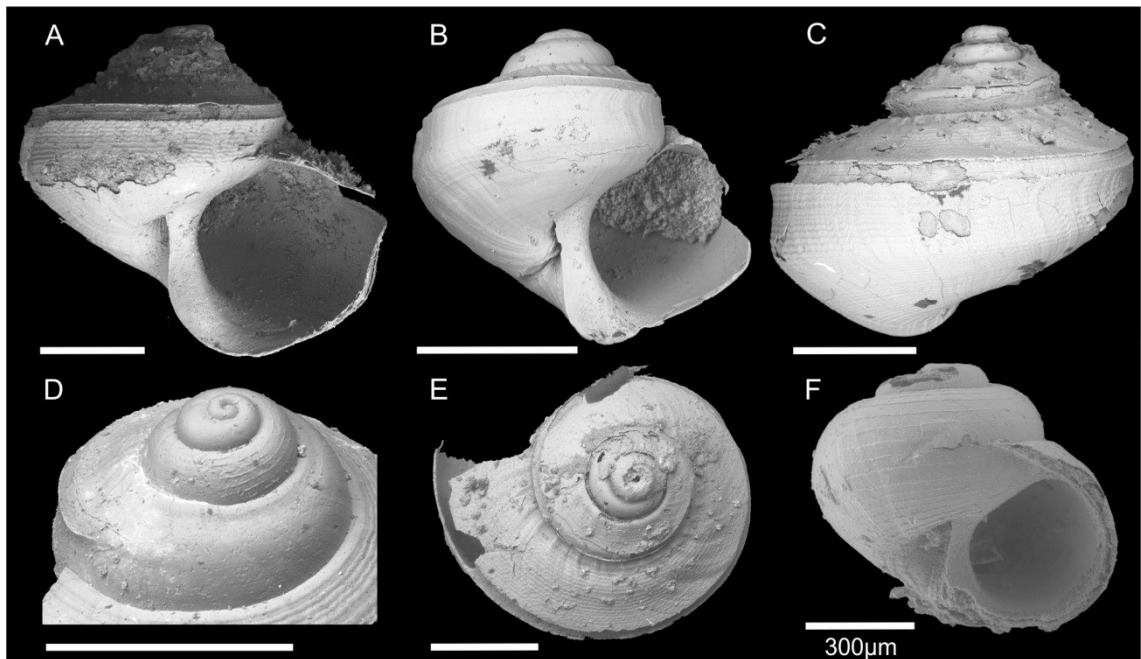
Figure 6.15: *Wannerispira shangganensis.* A-B) apertural view, C) lateral view, D), side view of initial whorls, E) apical view, F) apertural view of a larval shell. Scale bar = 500µm.

probably confined to a hard substrate (Hollingworth and Pettigrew, 1988). The lack of a hard substrate in this study, however, suggests that these specimens probably had a similar life habit to deep-sea vetigastropods that typically consume sediment (Hickmann et al., 1988).

Mode of Life. Surficial, fully motile, slow, surface deposit feeder.

<div align="center">

Order **Architectibranchia** Haszprunar, 1985

Family **Tubiferidae** Cossmann, 1895

Genus ***Sinuarbullina*** Gründel, 1997

Species ***Sinuarbullina yangouensis* comb. nov.** (Pan et al., 2003)

Figure 6.15.

</div>

2003   *Jiangxispira yangouensis* Pan et al. p. 44, Fig. 3, 1-7.

2005   *Soleniscus?*   Wheeley and Twitchett, p.40. Fig. 2, L-M.

Material. Four specimens from the Deltadalen Member, Vikinghøgda Formation, Lusitaniadalen section (LD-05).

Description. The shell is egg-shaped with a distinctly elevated spire. The teleoconch whorls have a subsutural ramp. The ramp from the outer whorl face is rounded with a rib on the shell periphery. The whorls are smooth in most cases both growth lines are visible and prosocyrt on the outer whorl face but strongly curving in an apertural direction and opisthocyrt at the ramp. The surface of the shell shows simple colour stripes around the ramp. The aperture is an elongated tear-drop shape; the inner lip has a columnellar fold. Protoconch is heterostrophic, sinistral, nearly discoidal with lightly elevated spire 30° offset from the shell axis; protoconch has 1-2 round whorls.
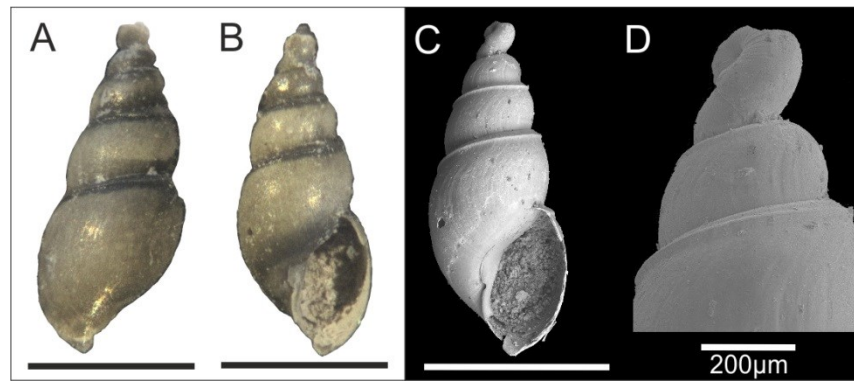
Figure 6.16: *Sinuarbullina yangouensis.* A) lateral view, B-C) apertural view, D) protoconch. Scale Bar = 1mm, except D.

Remarks. Pan et al. (2003) described *Jiangxispira* as a new genus but the diagnostic features are within the diagnostic criteria of the genus *Sinuarbullina* described by Gründel (1997), i.e. 1) shell egg-shaped with an elevated spire; 2) teleoconch whorls have a subsutural ramp, with a rounded or angular transition from the ramp to the outer whorl; 3) whorls are smooth, may have faint spiral furrows; 4) aperture is tear-drop shaped without columnellar folds; and 6) protoconch is heterostrophic. *Jiangxispira* is, therefore, considered a junior synonym of *Sinuarbullina*.

Seven species are included in *Sinuarbullina*, and *S. convexa* (=*Cylindribullina convexa*) are the only accepted Early Triassic species (Gründel and Nützel, 2012). The new specimens, however, are more slender (H/L 2.4-2.7) than those described from the Sinbad Limestone by Batten and Stokes (1986), and are conspecific of *Jiangxispira yangouensis* specimens from the Griesbachian Dayie Formation.

The shell morphology is similar to *Meekospira* that has been interpreted as a slow moving shell dragger (Hughes, 1986). *Meekospira*, however, could have also have been a burrower (Hollingworth and Pettigrew, 1988). The ancestral condition in high-spired gastropods is presumably an algal grazer over hard substrates (Declerck, 1995) but possibly a detritus feeder in soft substrates.

Mode of Life. Surficial, fully motile, slow, surface deposit feeder.

Order **Ptenoglossa** Gray, 1853

Family **Pseudozygopleuridae** Knight, 1930

Figure 6.17, A-C.

Material. Three specimens from the Deltadalen Member, Lusitaniadalen section (L-04, L-05).

Description. Teleoconch not observed. Protoconch is elongate conical shape and is composed of five whorls. The initial whorl is smooth and has a diameter of 0.08mm. Collabral ornamentation is initiated on the second whorl and continues to the base of the protoconch. The collabral ornamentation consists of narrow costellae which intersect at or just below the mid-whorl. Costallae in the upper part of the whorls are 40° to the shell axis and slightly curved and in the lower part of the whorls are 200° to the shell axis. Growth lines are visible between the costallae as faint collabral ribs perpendicular to the costallae. Aperture is circular, with a small columnellar fold. Five whorls were observed in these specimens.

Remarks. Hoare and Sturgeon (1978) describe the protoconchs from the Pseudozygopleuridae and show that there is a remarkable consistency within the family, and that they can be readily differentiated from Zygopleuridae and Loxonematidae. The protoconchs of the Pseudozygopleuridae are elongate, conical in shape with 3-5 whorls; initial whorl smooth; collaberal ornamentation from second whorl; narrow opisthocline to sigmoidal transverse costallae that extend up and below from the suture and curve uniformly to the mid-whorl; at this juncture the costallae are equally spaced; and a protoconch sculpture gives way to younger ornamentation during the development of the teleoconch. The ornamentation of the protoconchs of the Zygopleuridae differs by having smooth whorls, and fine riblets at the sutures (Nützel and Mapes, 2001).

Pseudozygopleuridae protoconchs are similar to the Ladinulidae, but their costallae are opisthocline not vertical (Bandel, 2006). These specimens are therefore assigned to the Pseudozygopleuridae. No teleoconch is apparently present these specimens as the sculpture of the prodissoconch is uninterrupted.

The only Mesozoic representative of the Pseudozygopleuridae has been reported from the Jurassic of Poland (Kaim, 2004). Those specimens possess protoconchs that lack the pseudozygopleurid ornamentation as diagnosed by Hoare and Sturgeon (1978) and so may represent a separate family. The specimens from this study, on the other hand, provide the first unequivocal evidence that the diverse late Palaeozoic Pseudozygolpleuridae survived the late Permian mass extinction.

Ecology. Nützel (1998) used the diameter of the first whorl and the number of protoconch whorls to separate planktotrophic pseudozygopluerid species from non-planktotrophic species. The small size of the specimens recorded in this study probably reflects a planktotrophic juvenile lifestyle. The absence of teleoconch in any of the specimens, i.e. no metamorphosis, may indicate that adults were unable to live in this environment.
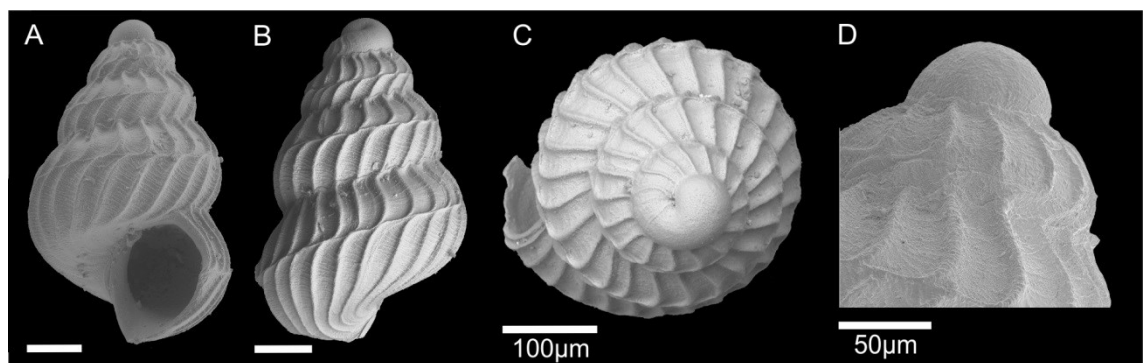
Figure 6.17: Pseudozygopleuridae larval shells. A) Apertural view. B) lateral view. C) apical view. D) lateral vies of P1 protoconch. Scale bar in A and B = 200μm.

6.4   Palaeoecological results

6.4.1   Alpha Diversity

No genera and only one species become extinct across the late Permian extinction horizon in this study. Two samples were collected from the bioturbated glauconitic sandstones at the top of the Kapp Starostin Formation and the base of the Vikinghøgda Formation, prior to the late Permian mass extinction (DD-01, LD-01; Figures 6.2-6.3). These samples only consist of the inarticulate brachiopod *Lingularia freboldi*. In the first concretionary sample of the Vikinghøgda Formation, i.e. after the extinction horizon (Figure 6.2, LD-02), the fauna comprises the same genus *Lingularia*, but only the smaller species *L. yini*. In addition, the median geometric size of *Lingularia* significantly declines ($p = <0.01$) by 47% (4.7mm to 2.2mm) between the Kapp Starostin and Vikinghøgda formations, and by 59% (2.2mm to 1.3mm) across the extinction horizon (Figure 6.18).

A further six samples, with >20 MNI, were collected from the lowermost Triassic at Deltadalen, Lusitaniadalen and Festningen (Figures 6.2-6.4). The samples from the siltstone tempestites and silty mudstones at the base of the Deltadalen Member, are characterised by a single genus (*Claraia*) and one, two or three species. Two samples from concretions at 10m and 11.5m above the base of the Deltadalen Member (LD-04, LD-05 ; Figure 6.2), show an increase in species richness (S = 7-11) and Simpson Diversity (2.0-2.2).
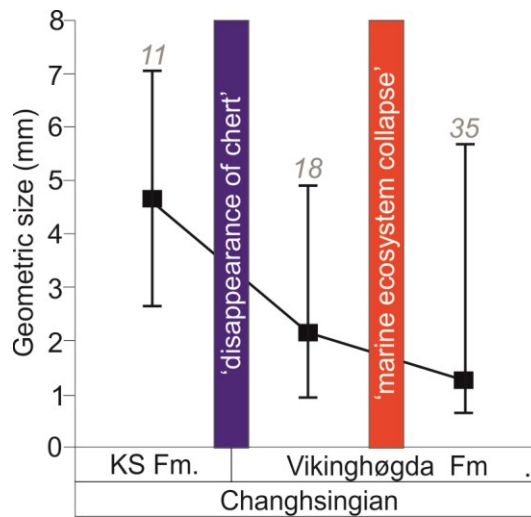
Figure 6.18: Size change of *Lingularia* through the Kapp Starostin-Vikinghøgda Formation transition. Marine ecosystem collapse is interpreted at the top of the last intensely bioturbated sandstone bed (after Nabbefeld et al., 2010). KS = Kapp Starostin Formation.

On siltstone tempestites in the uppermost part of the Lusitaniadalen Member and in the Vendomdalen Marker bed only bivalves were recorded. This consists of five monotypic genera (Table 6.1), and the species richness of the samples ($S = 1$-4) is lower than those recognised from the concretions in the lower part of the Deltadalen Member. Even in the concretionary sample (DD-10) from the upper Lusitaniadalen Member, which contains a silicified fauna, species richness is lower than in the sampled Deltadalen concretions.

Two samples were collected from the Spathian strata, one from a turbidite bed (DD-10, Figure 6.3) which consists only of the first occurrence of cf. *Eumorphotis telleri*, and the second from silty mudstones (DD-17, Figure 6.3) which consist solely of *Daonella* sp.

Table 6.1: Absolute abundance of benthic invertebrates from bulk samples from the Permian-Triassic transition in Svalbard (this study). Only samples with >20 MNI are included. Samples are ordered into stratigraphic order.

Genus	Species	DD-01	LD-01	LD-02	F-1	LD-04	LD-05	DD-05	DD-08	DD-10	DD-11	DD-12	DD-14	DD-15	DD-16	DD-17
Lingularia	*freboldi*	215	99	-	-	-	-	-	-	-	-	-	-	-	-	-
	yini	-	-	82	-	-	-	-	-	-	-	-	-	-	-	-
Orbiculoidea	*winsnesi*	-	-	-	-	1	1	-	-	-	-	-	-	-	-	-
Claraia	cf. *clarai*	-	-	-	1	-	-	-	-	-	-	-	-	-	-	-
	kilensis	-	-	-	13	-	-	-	-	-	-	-	-	-	-	-
	stachei	-	-	-	10	-	-	24	-	-	-	-	-	-	-	-
cf. *Eumorphotis*	*telleri*	-	-	-	-	-	-	-	-	-	-	-	-	-	87	-
Daonella	sp.	-	-	-	-	-	-	-	-	-	-	-	-	-	-	89
cf. *Bositra*	*aranea*	-	-	-	-	-	-	-	-	-	2	-	-	2	-	-
Crittendenia	*kummeli*	-	-	-	-	-	-	-	49	99	4	2	20	10	-	-
Bakevellia	*costata*	-	-	-	-	-	-	-	-	24	90	80	-	-	-	-
Leptochondria	*occidanea*	-	-	-	-	-	-	-	157	168	5	3	19	120	-	-
Promyalina	*schamarae*	-	-	-	-	4	8	-	-	-	-	-	-	-	-	-
Neoschizodus	*laevigatus*	-	-	-	-	2	-	-	-	-	-	-	-	-	-	-
Unionites	*canalensis*	-	-	-	-	2	-	-	-	-	-	-	-	-	-	-
Nucinella	sp.	-	-	-	-	2	6	-	-	-	-	-	-	-	-	-
Austrotindaria	sp. A	-	-	-	-	49	62	-	-	-	-	-	-	-	-	-
Austrotindaria	sp. B	-	-	-	-	1	2	-	-	-	-	-	-	-	-	-
cf. *Austrotindaria*	*canalensis*	-	-	-	-	10	-	-	-	-	-	-	-	-	-	-
Sinuarbullina	*yangouensis*	-	-	-	-	4	-	-	-	-	-	-	-	-	-	-
Wannerispira	*shaggenensis*	-	-	-	-	16	8	-	-	-	-	-	-	-	-	-
Warthia	*zakharovi*	-	-	-	-	151	157	-	-	-	-	-	-	-	-	-
Species richness	S	1	1	1	3	11	7	1	2	3	4	3	2	3	1	1
Individuals	N	215	99	82	24	241	242	24	206	291	101	85	39	132	87	89
Simpson Diversity	Δ	1.0	1.0	1.0	2.2	2.3	2.1	1.0	1.6	2.2	1.3	1.1	2.1	1.2	1.0	1.0

6.4.2 Alpha Functional diversity

The two pre-extinction samples (LD-01, DD-01), i.e. from the Kapp Starostin Formation and basal Deltadalen member, and the first concretionary level immediately overlying the extinction horizon are only represented by shallow infaunal, facultatively motile, attached, suspension feeding lingulids. Samples from the silty mudstones of the lowermost Deltadalen Member only contain *Claraia*, so only one mode of life is recorded (epifaunal, facultatively motile, attached, suspension feeders). The concretionary samples (LD-04, DD-05) from the Deltadalen Member with the silicified fauna, however, have an increased functional diversity with six modes of life and elevated sample functional richness ($S = 5$-6).

The four bivalve species from the uppermost Lusitaniadalen Member and Vendomdalen Marker Bed represent three modes of life: epifaunal, facultatively attached, suspension feeder; epifaunal, stationary, attached, suspension feeder; and semi-infaunal, stationary attached, suspension feeder. The functional richness of samples ranges between 1-3 (Table 6.4). The samples from the Spathian strata only represent one mode of life. In the turbidite bed (DD-22K) the fauna represent epifaunal, stationary, suspension feeders, whereas, in the silty mudstones the fauna have an epifaunal, stationary, unattached, mode of life.

6.4.3 Changes in taxonomic composition

The cluster analysis and SIMPROF test recognises eight biofacies. The SIMPER analysis shows that the pre-extinction faunas are dominated by *Lingularia freboldi* and the composition changes across the extinction horizon to *Lingularia yini* biofacies in the concretionary sample at the base of the Vikinghøgda Formation and *Claraia stachei*
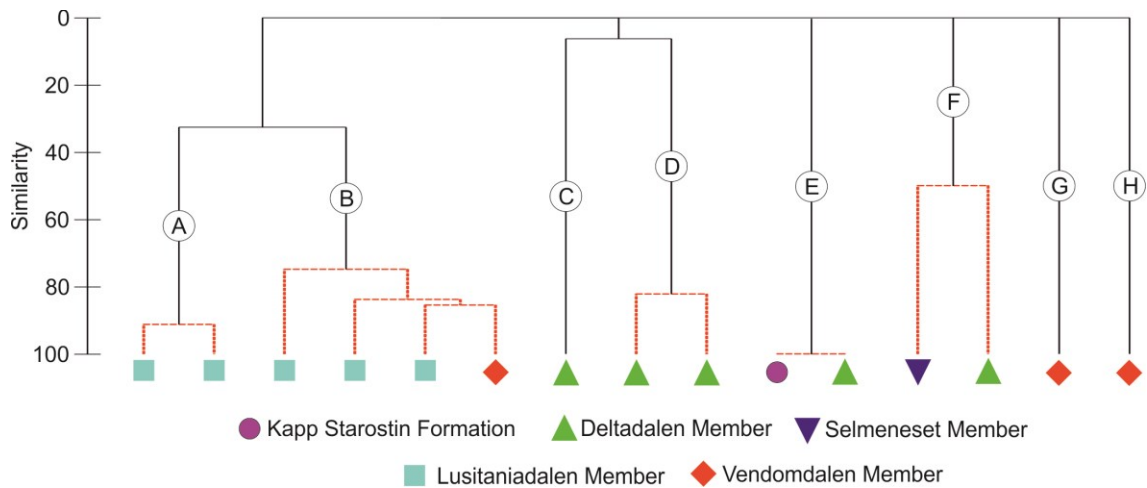
Figure 6.19: Cluster analysis of the samples from the Lower Triassic successions of the Svalbard. The cluster analysis together with the SIMPROF test identified 8 groups of samples which are statistically distinct (A-H). The 8 groups have been interpreted as different benthic biofacies.

Table 6.2: SIMPER analysis on biofacies recognised by the SIMPROF test. Biofacies letters correspond to Figure 6.12.

Species	Cumulative (%)
Biofacies A	
Bakevellia costata	73
Leptochondria occidanea	88
Biofacies B	
Leptochondria occidanea	66
Crittendenia kummeli	100
Biofacies C	
Lingularia yini	99
Biofacies D	
Warthia zakharovi	45
Austrotindaria sp. B	70
Wannerispira shangganensis	79
Promyalina schamarae	86
Biofacies E	
Lingularia freboldi	100
Biofacies F	
Claraia stachei	68
Biofacies G	
Daonella sp.	100
Biofacies H	
cf. *Eumorphotis telleri*	100

biofacies in the silty mudstones. The well preserved faunas from samples LD-04, LD-05 are dominated by *Warthia zakharovi* and *Austrotindaria* sp. (Figure 6.19; Table 6.2).

The cluster analysis (Figure 6.19) shows that two quantitative biofacies can be recognised in the beds from the upper Lusitaniadalen Member and Vendomdalen Member marker bed, and the SIMPROF test together with the Simper analysis show that the samples are either dominated by *Leptochondria occidanea* and *Crittendenia kummeli* or *Bakevellia costata* and *Leptochondria occidanea*. The Spathian samples are each dominated by a single taxon that only occurs once in this study and, therefore, represent individual biofacies.

6.4.4 Changes in functional composition

The cluster analysis and SMPROF test (Figure 6.20) show six functional compositions. The SIMPER analysis shows that Changhsingian samples are characterised by shallow infaunal, facultatively motile, attached, suspension feeders that span across the Kapp Starostin and Vikinghøgda formational boundary and the extinction horizon. The late Changhsingian samples from the silty mudstone at the base of the Vikinghøgda Formation, however, are characterised by surficial, facultatively motile, attached, suspension feeders. The concretionary samples (LD-04, LD-05) from the base of the Vikinghøgda Formation represent a separate functional community characterised by surficial, slow-moving, surface deposit-feeders and shallow infaunal, facultatively motile, unattached, deposit feeders.

The cluster analysis shows that the samples from siltstone tempestites in the Lusitaniadalen Member and the Vendomdalen Member can be divided into two functional compositions, one characterised by epifaunal, stationary, attached, suspension feeders and the other by: semi-infaunal and epifaunal, stationary, attached,
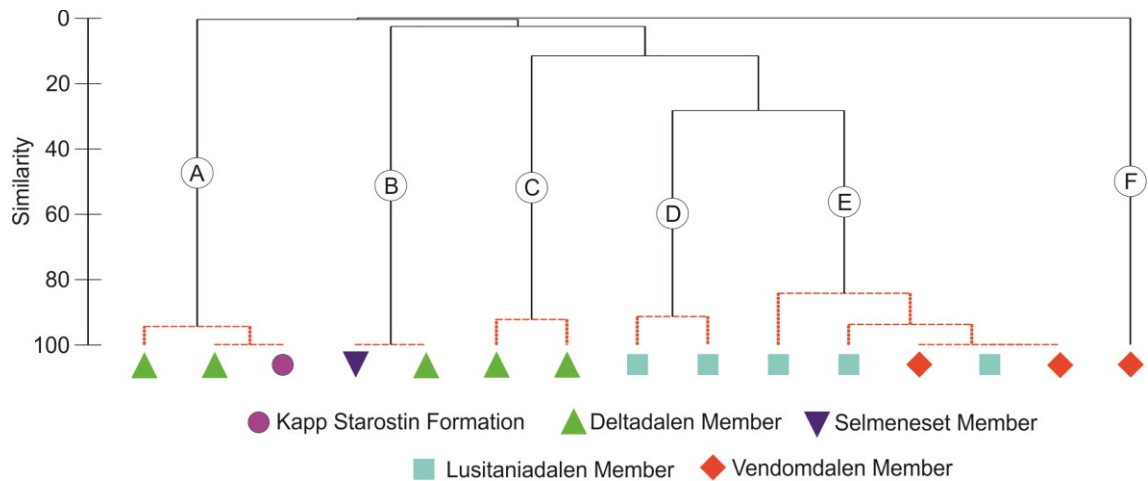
Figure 6.20: Cluster analysis of the samples according to modes of life from the Lower Triassic successions of the Svalbard. The cluster analysis together with the SIMPROF test, identified 6 groups of samples which are statistically distinct (A-H). The 8 groups have been interpreted as different benthic ecofacies.

Table 6.3: SIMPER analysis on ecofacies recognised by the SIMPROF test. Ecofacies letters correspond to Figure 6.20.

Species	Cumulative (%)
Ecofacies A	
Shallow infaunal, facultatively motile, attached, suspension feeder	100
Ecofacies B	
Epifaunal, facultatively motile, attached, suspension feeder	100
Ecofacies C	
Epifaunal, slow-moving, surface deposit-feeder	50
Shallow infaunal, facultatively motile, unattached, miner	80
Ecofacies D	
Shallow-infaunal, stationary, attached, suspension feeder	80
Ecofacies E	
Epifaunal, stationary, attached, suspension feeder	100
Ecofacies F	
Epifaunal, stationary, unattached, suspension feeder	100

suspension feeders. The sample DD-17, from the silty mudstones, however, is characterised by epifaunal, facultatively, motile, unattached, suspension feeders.

6.5   Discussion

Late Permian mass extinction event

No taxonomic or functional loss due to the late Permian mass extinction event was recorded in this study, and only one species disappears across the extinction event (Table 6.2). The pre-extinction glauconitic sandstone facies sampled in this study only yielded a low diversity of inarticulate brachiopods (this study; Gobbett, 1963). The upper part of the Hovtinden Member elsewhere in Spitsbergen is often described as unfossilifereous (Gobbett, 1963; Wignall et al., 1998), although 16 bivalve (Nakazawa, 1999; Bond et al., 2015) and nine brachiopod (Shen et al., 2005; Bond et al., 2015) species have previously been described. In addition, unpublished logs of Twitchett (2006) record bryozoans and rugose corals (Figure. 6.4). None of the species from the upper Hovtinden Member, however, are known from the Triassic, which suggests that the late Permian mass extinction caused a major local taxonomic and ecological turnover in benthic invertebrate communities, as already recorded for the ichnofauna (Wignall et al., 1998; Nabbefeld et al., 2010).

The environmental changes associated with the late Permian extinction affected the size of the benthic fauna that survived, and the size of taxa that originated in the aftermath (Twitchett, 2007). Even though *Lingularia* is characterised as a disaster taxon that thrived in the extinction aftermath (Rodland and Bottjer, 2001), in western Palaeotethys it significantly reduced its size due to the stressed environment in the wake of the late Permian mass extinction, i.e. it records a Lilliput effect (Metcalfe et al., 2011; Posenato et al., 2014). This study shows that *Lingularia* also reduced its size in the Boreal Ocean to a median size comparable to the western Palaeotethys (1-1.5mm geometric size).

Although fewer specimens were counted in this study, the maximum geometric size of *Lingularia* in the immediate wake of the extinction event was similar to that recoded in the Werfen Formation (6mm; Figure 6.18; Metcalfe et al., 2011; Posenato et al., 2014). In addition, previous authors (Twitchett, 2001; Fraiser and Bottjer, 2004; Twitchett et al., 2005; Twitchett, 2007; Metcalfe et al., 2011; Fraiser et al., 2011) found that taxa that originated in the extinction aftermath, especially in the first two conodont zones of the Triassic, also have significantly smaller sizes than in stratigraphically younger strata. A similar trend is evidenced in this study by the silicified fauna being dominantly made up of microscopic individuals, with the largest specimen having a geometric size of only 17mm (*Austrotindaria* sp.) in the *H. parvus* zone compared to 44mm (cf. *Bositra aranea*) from the uppermost Lusitaniadalen Member and 47mm (cf. *Eumorphotis telleri*) in the Spathian.

Stunting in benthic invertebrates is associated with multiple environmental factors and palaeoenvironmental studies from Svalbard have shown that locally the late Permian mass extinction event is associated with blooms of phytoplankton, anoxia, euxinia and habitat loss (Wignall and Twitchett, 1996; Nabbefeld et al., 2010; Dustira et al., 2013). Anoxia and extremely high temperatures are known to increase the metabolic rate and decrease the aerobic capacity of marine invertebrates (Cossins, 1987; Pörtner, 2010) and because metabolic rates are inversely correlated with body size (Schmidt-Nielsen, 1984) temperature, decreasing O_2 and the other environmental changes could act synergistically to explain the observed size change of benthic invertebrates across the late Permian mass extinction event and stunting of invertebrates during the Early Triassic (Twitchett, 2007). The observed size change, however, may have been caused by a decrease in life expectancy. Growth line analysis of *Lingularia* by Metcalfe et al. (2011) shows that these small specimens had 100 closely spaced (~100μm) growth lines

which suggests that the small size of *Lingularia* in the Early Triassic is due to stunting, rather than a reduced life expectancy.

Facies at the base of the Vikinghøgda Formation are similar to those from the top of the Kapp Starostin Formation in central Svalbard, but lack chert that is otherwise persistent throughout the Kapp Starostin Formation. The size of *Lingularia freboldi* significantly decreases into this chert-free unit (Figure 6.181) suggesting an increase in environmental stress prior to the late Permian mass extinction. The production of chert during the Permian of the Boreal Ocean has been attributed to the upwelling of nutrient- and oxygen-rich cold waters and its cessation, consequently, has been interpreted as resulting from a breakdown of these conditions and the establishment of warm and sluggish oceanic conditions prior to the late Permian extinction (Beauchamp and Baud, 2002; Grasby and Beauchamp, 2009). The cessation in chert production in the Boreal Realm also correlates with the cessation of chert in the Panthalassa Ocean (Isozaki, 1997) suggesting that initial global warming and environmental deterioration occurred prior to the late Permian extinction. Additionally, the initial decline of carbon isotope values prior to the late Permian extinction has been associated with the onset of Siberian Trap volcanism (Racki, 1999; Korte et al., 2010), increasing sea surface temperatures (Joachimski et al., 2012) and initial establishment of upper Changhsingian anoxic conditions in the Boreal Ocean (Grasby and Beauchamp, 2009; Grasby et al., 2013; Dustira et al., 2013). Initial volcanism prior to the late Permian extinction (Reichow et al., 2009), appear to have had profound effects on the functioning of marine ecosystems preceding the main volcanism event that led to the late Permian mass extinction.

Distribution of fauna

The silicified benthic fauna from the *H. parvus* Conodont Zone, i.e. earliest Griesbachian, represents the most ecologically advanced benthic fauna known from

coeval deposits worldwide. It is also the only benthic fauna to show advanced recovery (*sensu* Twitchett, 2006) by the first conodont zone of the Triassic. In addition, bioturbation of the sediments in the *H. parvus* Zone by *Thalassinoides* and *Rhizocorallium*, also suggest an advanced recovery stage comparable with ichnofaunas recorded from the northwest Pangaean coast (Beatty et al, 2008; Zonneveld et al., 2010a; Figures 6.2-6.3

A high proportion of the bioturbated sediment in this study was observed in the coarser deposits associated with high-energy, well oxygenated setting by wave activity (Figure 6.5), consistent with other advanced recovery faunas (Twitchett et al., 2004; Shigeta et al., 2009; Hautmann et al., 2011) and the habitable zone hypothesis (Beatty et al., 2008). The concretionary fauna from 10m above the base of the Deltadalen Member (L-04; Figure 6.2), however, occurs within laminated silty mudstones which suggests deposition in an oxygen-depleted environment. Furthermore, chemosymbiosis has been inferred for the Nucinellidae and, therefore, the high abundance of *Nucinella* sp. in the conodont residues suggests an adaptation to sulfidic conditions (Oliver and Taylor, 2009), that have been inferred from biomarkers in the same facies at the base of the Deltadalen Member (Nabbefeld et al., 2010). A *Nucinella* biofacies has also been reported from a similar anoxic-euxinic environmental setting in the Toarcian (Danise et al., 2013) and around the oxygen-minimum zone in the modern ocean (Oliver and Taylor, 2009). Oliver and Taylor (2009) also found that in modern seas the bivalve fauna associated with nucinellids in oxygen-restricted settings include *Nucula*, which morphologically and ecologically are very similar to the *Austrotindaria* identified in this study. Even though the concretionary samples are more diverse, seven of the species (*Warthia zakharovi, Neoschizodus laevigatus, Austrotindaria* sp. A*, Austrotindaria* sp. B, *Austrotindaria canalensis*, *Unionites* sp. and *Promyalina schamarae*) are

opportunistic and flourished in the wake of the late Permian mass extinction (Fraiser, 2011). The diverse fauna from this study, therefore, represent a fauna adapted to an oxygen-restricted environment around the oxygen-minimum zone just below wave base.

The silty mudstones, that are interpreted to have been deposited below wave base, contain a low diversity, high abundance paper pecten fauna in life position (Schatz, 2005) with palaeoecological characteristics that are consistent with limited post-Permian recovery and persistent environmental stress (Twitchett, 2006). In the Induan these comprise *Claraia* species, and in the Spathian *Daonella* sp. Worldwide, *Claraia* has been reported from laminated silty mudstone settings below wave base in the Induan (Kapoor, 1996; Nakazawa et al. 1975; Wignall et al., 1996; Twitchett et al., 2001; Heydari et al., 2003; Bjerager et al., 2005; Komatsu and Huyen, 2007; Komatsu et al., 2008; Shigeta et al., 2009; Komatsu et al., 2014). *Claraia* and *Daonella* generally occur as monospecific shell beds, suggesting that these taxa are autochthonous and represent short-term colonisation of an otherwise inhospitable sea floor, i.e. representing an exaerobic biofacies (*sensu* Savrda and Bottjer, 1991). Palaeoecological evidence suggests that the silty mudstones in the Induan and Spathian were deposited under anoxic-dysoxic conditions (Wignall and Twitchett, 2002b) that characterised the outer shelf and limited recovery even into the Spathian.

The fauna recorded from the upper Lusitaniadalen Member and Vendomdalen Member boundary, on the other hand, are only characterised by bivalves and includes taxa also known from eastern Panthalassa (Hofmann et al., 2014). In addition, the *Leptochondria occidanea* biofacies recorded in this study and by Hofmann et al. (2014) spans the Smithian/Spathian boundary in a distal mid-shelf environment and in both studies sampled from cross-laminated siltstones and silty-limestones. Silty mudstones that alternate with the *Leptochondria occidanea* biofacies beds represent deposition in more

distal environments and lack conspicuous benthic faunas, suggesting that even around the Smithian/Spathian boundary benthic faunas were restricted to environments influence by wave activity, i.e. the habitable zone (Beatty et al., 2008).

The *Leptochondria occidanea* biofacies fauna is restricted to within a few centimetres of the sediment, has a low species and functional richness, and represents recovery stage 2 of Twitchett's (2006) recovery model. This indicates a reversal in the ecological state of benthic communities between the Griesbachian and upper Smithian. In addition, a well-preserved fauna from a concretionary sample from the upper Lusitaniadalen Member (DD-22K; Figure 6.2) with the same biofacies as identified in the siltstone tempestites, suggests that these difference are not due to changes in preservation. The lack of stratigraphically continuous fossiliferous beds in the Vikinghøgda Formation, however, makes it difficult to investigate the timing and magnitude of subsequent biotic crisis.

Implications for the Early Mesozoic Diversification event

The silicified fauna from this study comprises gastropod and bivalve taxa not recognised previously from the Early Triassic, and have important implications for the diversification of several bivalve and gastropod lineages.

The gastropods comprise a mixture of Palaeozoic holdover taxa and a newly originated lineage. Three of the four Palaeozoic families identified in this study could be described as "dead clades walking" (*sensu* Jablonski, 2002). *Warthia* and *Wannerispira* have previously been recognised from the Griesbachian and have previously been interpreted in this way (Kaim and Nützel, 2011; Kaim et al., 2010). The presence of larval shells of the Pseudozygopleuridae (Figure 6.17) represents the youngest occurrence of this family and shows that it too survived the late Permian mass extinction event only to

subsequently go extinct. The remaining Palaeozoic family recorded in this study is the Naticopsidae, which diversified during the Early and Middle Triassic and played an important role in the recovery (Nützel, 2005).

The gastropod *Sinuarbullina yangouensis* also identified in this study represents the oldest occurrence of the architectibranchs (*sensu* Gründel and Nützel, 2012), a group that rapidly diversified in the late Triassic and Jurassic. Architectibranchs have been recorded from the Carboniferous (Gründel and Nutzel, 2012), but Knight (1941) suggests that these Carboniferous specimens have a heterostrophic protoconch and thus they are not architectibranchs. The first unequivocal occurrence of the architectibranchs, evidently occurs in the first conodont zone of the Triassic (this study; Pan et al., 2003), but, as hypothesised for other benthic invertebrate groups, such as, crinoids (Baumiller et al., 2010; Oji and Twitchett, 2015), their origin may have been in the Palaeozoic.

The silicified bivalves belong to three lineages: Pteriomorpha, Protobranchia and Palaeoheterodonta. The genera *Nucinella* and *Austrotindaria* belong to the Protobranchia and represent the oldest occurrences of the Nucinellidae and Nuculanida, respectively. Recent analyses show that the protobranchs rapidly diversified in the late Triassic and Jurassic (Bieler et al., 2014), but these new occurrences demonstrate initial diversification of the Nucinellidae and the Neilonellidae in the basal Triassic, supporting the interpretation of Sharma et al. (2013) who found that the late Permian mass extinction caused an upturn in the diversification of the protobranchs.

This study found that some Early Triassic specimens previously identified as *Unionites fassaensis* and *U. canalensis* (Palaeoheterodonta) are misidentifications of the protobranch *Austrotindaria*. Some specimens from this study, however, are definitely identified as *Unionites*, and together with *Neoschizodus* represent two Palaeoheterodonta lineages that diversified in the wake of the late Permian extinction

event and subsequently rapidly diversified during the Triassic (Newell and Boyd, 1975; Geyer et al., 2005; Ros et al., 2011; Ros and Echevarria, 2011). This study supports the findings of Sharma et al. (2013) and Bieler et al. (2014) that the Palaeoheterodonta diversified in the Early Triassic and show a signature of the late Permian extinction event.

Accelerated diversification rates after the late Permian mass extinction reported by Sharma et al. (2013) is reflected in the Early Triassic by the diversification of five new and one surviving lineage of bivalves and gastropods (this study), Archiheterodonta (Hautmann and Nützel, 2005) and crinoids (Rouse et al., 2013; Oji and Twitchett, 2015). Previous studies have identified the middle and upper Triassic (e.g. Rouse et al., 2013) as being key intervals for the radiation of extant groups, but the previous absence of well-preserved faunas from the Lower Triassic may have resulted in the importance of the late Permian mass extinction event being underestimated.

Planktotrophic larval development

The exceptional preservation of bivalve and gastropod protoconchs in this study provides valuable insights into the early ontogeny of these taxa. Valentine and Jablonski (1983; 1986) had suggested that benthic invertebrates with a planktotrophic larval stage were selected against by the late Permian extinction. On the other hand, planktotrophic larval shell development has already been inferred for many Early Triassic gastropods (Nützel and Erwin, 2002; Pan et al., 2003; Nützel and Schulbert, 2005) and the Pseudozygopleuridae (Nützel and Mopes, 2001). Furthermore, a small prodissoconch I and relatively large prodissoconch II in the bivalves *Nucinella, Austrotindaria, Unionites* and *Neoschizodus*, also suggests planktotrophic larval development (cf. Hautmann and Nützel, 2005). Thus, it seems that a planktotrophic larval lifestyle was a particular advantage in the mid-outer shelf depositional environment of the Lower

Triassic, as observed in similar depositional environments during the Palaeozoic (e.g. Nützel and Mapes, 2001; Frýda, 2001; Bandel et al., 2002).

One possible advantage of a planktotrophic larval development is protection from benthic predation (Nützel and Frýda, 2003), however, benthic predators are rarely recorded from the Early Triassic benthic assemblages (e.g. Schubert and Bottjer, 1995; Hofmann et al., 2013a; 2013b; 2014; 2015a) and were not recorded in this study. An alternative advantage of a planktotrophic larval stage is more effective dispersal which allows a wide distribution and an effective gene flow (Goldson et al., 2001). This adaptation may explain some of the apparent selectivity of the late Permian mass extinction, as those groups that suffered large taxonomic losses, e.g. Rhynchonellid brachiopods, are inferred to have lecithotrophic larval development and do not disperse long distances (Altenburger and Wanninger, 2009; Posenato et al., 2014). The cosmopolitan opportunists that thrived in the wake of the late Permian mass extinction, including *Austrotindaria* (=*Unionites*), *Lingularia* and *Claraia*, all have an inferred planktotrophic larval stage (Hammond and Poiner, 1984; Yang et al., 2001; this study). The effective dispersal and wide distribution of the Early Triassic benthos may explain how benthic invertebrates rapidly colonised the vacated seafloor once harsh environmental condition had ameliorated, and may explain why there was a lack of available ecospace for novel body plans to evolve into (e.g. Erwin et al., 1987; Foster and Twitchett, 2014).

Chapter 7 Functional diversity of marine ecosystems following the late Permian mass extinction event

Note: An earlier version of this chapter was published as Foster, W.J. and Twitchett, R.J. 2014. *Nature Geoscience* 7, 233-238. Here, I present the results from an updated database (last updated 05/02/2015). These new data have resulted in some changes to the results and analysis, which have been highlighted (Appendix 7.5), but the broad patterns and conclusions are unaffected.

7.1. Introduction

Palaeoecological studies of the Late Permian mass extinction and other events do not use taxonomic data alone (e.g. Twitchett and Barras, 2004; McGhee *et al.,* 2012), as they are insufficient for discerning ecological patterns (Fraiser and Bottjer, 2005). The ecological impact of past extinctions is, however, difficult to quantify and is arguably poorly understood (Webb and Leighton, 2011). However, recent work has established ordinal measurement scales to categorise extinction events (McGhee *et al.,* 2004) as well as the subsequent recoveries (Twitchett, 2006). Changes in life habits (specifically; tiering, motility and feeding) have been quantified by Bambach et al. (2007) using a three-dimensional model. Initial studies using their model have concentrated on key radiations (e.g. the Ediacaran and Cambrian explosion). Similar models (e.g. Novack-Gottshall, 2007) investigating the same questions have also focused on these events (e.g. Villéger et al., 2011). Fewer studies, however, have considered the role of extinction in reducing the functional diversity of marine ecosystems prior to the subsequent re-filling of ecospace during the recovery (*sensu* Bush and Novack-Gottshall, 2011).

Here, the ecospace model of Bambach et al. (2007) is used to provide the first quantitative analysis of the autecology of all known Permian-Triassic benthic marine genera. This approach has not been used previously to quantify ecological change during extinction events. Our analyses show that the Late Permian extinction event caused almost no loss of overall functional diversity at the global scale, but did result in

significant ecological shifts in benthic marine communities from particular depositional settings, palaeolatitudes and regions.

7.2.   Methods

Two complementary databases were constructed and analysed (Appendix 7.1; 7.2). Firstly, a database of all known marine invertebrate genus-level occurrences from the Late Permian to the Middle Triassic, compiled from the Paleobiology Database <www.paleobiodb.org> (PaleoDB; Appendix 7.1), supplemented by additional published data (including Chapters 3-6), along with locational, stratigraphic, lithological and environmental data. This database comprises 27,592 recorded occurrences of 1490 genera, an additional 5329 occurrences and 70 genera compared to Foster and Twitchett (2014). Occurrence data do not capture Lazarus taxa, however, especially those that range-through, but do not occur within, the study interval, and therefore underestimate the total number of genera known to have existed in any particular time interval. Therefore, a second database comprising range-through data of 1835 genera, compared with 1770 genera by Foster and Twitchett (2014), was compiled by ranging-through the occurrence database, and supplementing these data with additional data from the PaleoDB and Sepkoski (2002) (Appendix 7.2).

The occurrences were binned into 12 unequal-duration time intervals equivalent to Permian ages and Triassic sub-ages. Vetting of the data followed (Miller and Foote, 2009; see Appendix 7.3). Modes of life were inferred by using data from extant relatives, previous publications and functional morphology, and each genus was assigned to a bin in the ecospace model of Bambach et al. (2007) based on its tiering, motility and feeding habits (Appendix 7.4). Occurrences with sufficient geological information were assigned one of five broad depositional settings along an onshore-offshore gradient: Inner Shelf (i.e. above fair weather wave base), Middle Shelf (between fair and storm weather wave base), Outer Shelf (between storm weather wave

base and the shelf edge), Slope and Basin (beyond the shelf edge), and Reefs (including build ups and bioherms). All occurrences were assigned to one of the following palaeolatitudinal zones: Tropics (within 30° of the palaeoequator), northern (>30° north) and southern (>30° south). Finally, all occurrences were assigned to one of four regions: Panthalassa, Boreal Ocean, Palaeotethys and Neotethys.

Aggregation of data within these bins was quantified using Green's coefficient of dispersion (Green, 1966). High Green coefficient values indicate dominance by one or two categories within a particular stratigraphic bin, with values >0.5 are considered to represent a significant bias (Clapham et al., 2009). In order to take into account variations in sampling intensity within and between the different time bins and categories we applied the subsampling routine of Miller and Foote (1996) using a modified R script of Lloyd et al. (2008) to standardise the functional richness based on the number of occurrences. Subsampling quotas were set at 750 occurrences per bin for the global analysis and 100 occurrences for the smaller scale analyses of palaeolatitude, region or depositional setting. In each case, time bins with less than the specified quota of occurrences were excluded from subsampling. This compromise avoids the degradation that may occur if the quality of the poorest bin is used as the subsampling quota (Lloyd et al., 2008), but recognise that higher subsampling levels could reveal additional variability.

7.3.   Global-scale changes in functional diversity

Global genus-level extinction is estimated at 62% (using range-through data) or 78% (using occurrence data). There are often considerable differences between the range-through and occurrence data, with the former providing lower extinction estimates for most modes of life (Figure 7.1). This difference is an unsurprising consequence of the poor quality Early Triassic fossil record, which is due to a variety of factors including

rock record biases, incomplete sampling and poor preservation. Thus, while occurrence

data indicate that as many as nine modes of life completely disappeared across the P/Tr

boundary (Figure 7.2), six of these are recorded by the range-through data, implying
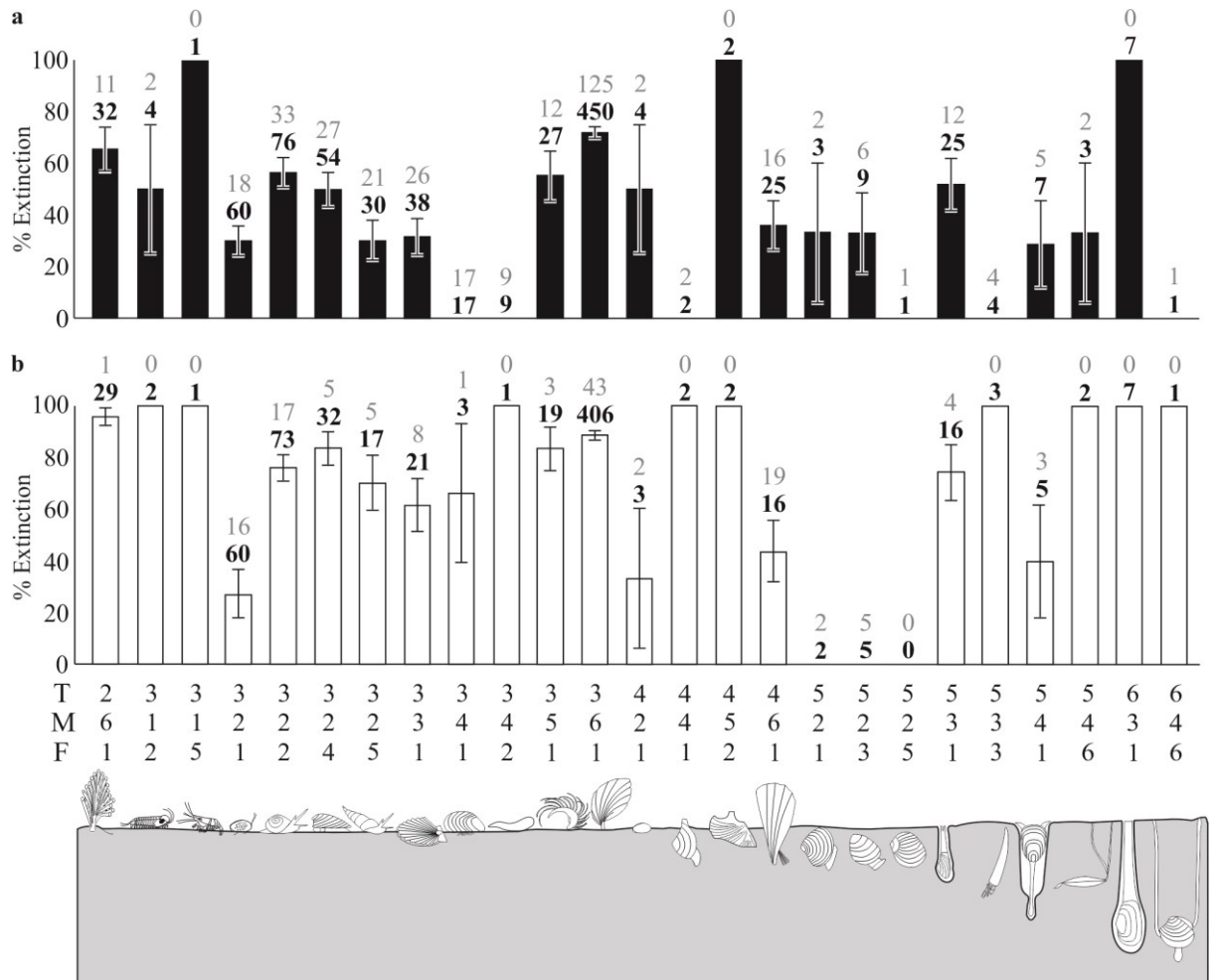
Figure 7.1: The percentage of genera that became extinct during the late Permian mass extinction in each individual mode of life, for (a) range-through and (b) occurrence data. The numbers of genera recorded in the Changhsingian (bold) and surviving into the Griesbachian (grey) are reported above each respective bar. Error bars represent one standard error in each direction (Appendix 7.3). T = Tiering: 2 = erect, 3 = surficial, 4 = semi-infaunal, 5 = shallow infaunal, 6 = deep infaunal; M = Motility: 1 = fast fully motile, 2 = slow fully motile, 3 = facultatively motile unattached, 4 = facultatively motile attached, 5 = stationary unattached, 6 = stationary attached; F = Feeding: 1 = suspension feeding, 2 = surface deposit feeder, 3 = miner, 4 = grazer, 5 = predator, 6 = other.

that genera exhibiting those particular modes of life have either been overlooked, were present but at abundances that were too low to be recorded by the fossil record, or existed at locations other than those that have been sampled to date. Thus, at most, only three modes of life disappeared across the P/Tr boundary: surficial, fast moving predators; semi-infaunal, stationary, unattached deposit feeders; and deep infaunal, facultatively motile, unattached suspension feeders (Figure. 7.1).

Range-through data at the taxonomic resolution of families and superfamilies, which have longer ranges than their constituent genera and may span an interval of time from which no constituent genera have been recorded, show, however, that even this is an over-estimate (Figure 7.2a). The boundary-crossing family Erymidae demonstrates that at least one genus of surficial, fast moving, predator must have been present somewhere. Likewise, deep infaunal, facultatively motile, unattached, suspension feeders must have survived the extinction event, as demonstrated by the boundary-crossing superfamily Pholadomyoidea. Thus, it would appear that the greatest mass extinction event of the past 500 million years led to the loss of just a single mode of life – that of semi-infaunal, stationary, unattached deposit feeders; a consequence of the extinction of the rostroconchs. Subsampling to standardise the global occurrence data also supports a small change in functional diversity across the P/Tr boundary, despite the significant drop in generic richness (Figure 7.2b). Therefore, overly simplistic models suggesting that Early Triassic marine ecosystems functioned for millions of years with primary producers only and no higher trophic levels (e.g. Chen and Benton, 2012) can be rejected.

The resistance of functional groups to global extinction, even those with few constituent genera, is further demonstrated by the upward trajectory of functional diversity since the start of the Phanerozoic (Bambach et al., 2007; Novack-Gottshall, 2007; Villéger et al., 2011; Bush et al., 2007). Even though functional diversity was reduced locally and

regionally, for example in the tropics, because the Late Permian extinction did not reduce functional diversity at the global scale an ecologically diverse group of marine metazoan survivors were able to refill this vacant ecospace once conditions ameliorated (Valentine, 1980; Erwin et al., 1987; Erwin, 1994). This explains why relatively few classes, orders, or phyla originated in the early Mesozoic, despite a return to levels of taxonomic diversity that were similar to the early Palaeozoic (Alroy et al., 2008). This may also explain why just one novel mode of life originated in the Early Triassic, namely the erect, facultatively motile, attached suspension feeders, which appeared with the evolution of motile crinoids in the Smithian (Baumiller et al., 2010; Bush and Bambach, 2011; Figure 7.2a). Globally, the Early Triassic benthic ecosystem functioned much like a ship manned by a skeleton crew; each post was occupied, but by only a few individual taxa.
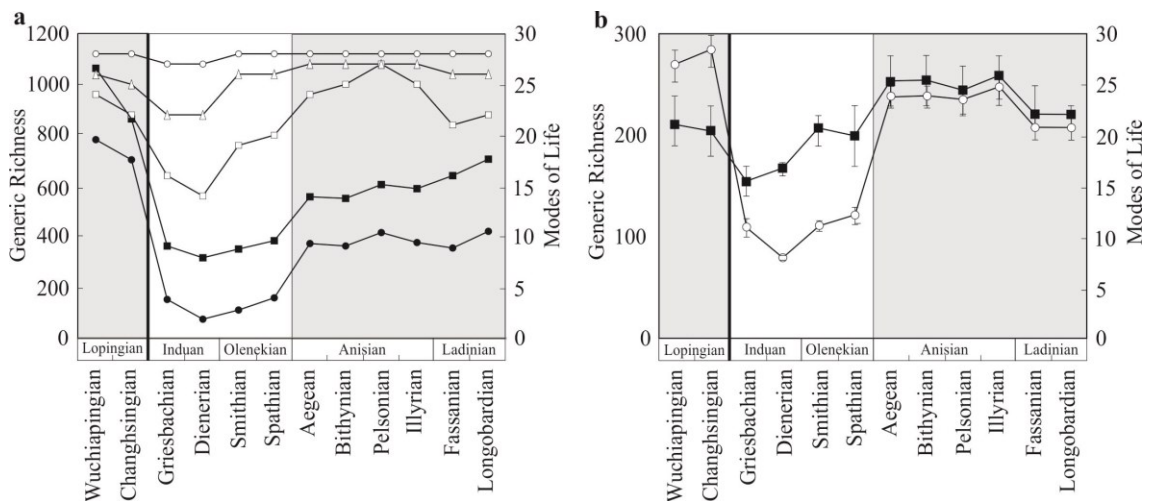
Figure 7.2: Diversity curves for generic and functional richness across the studied interval. (a) Generic richness of raw range-through data (filled squares) and occurrence data (filled circles); and number of modes of life occupied using generic range-through (open triangles), generic occurrence data (open squares), and range-through data for higher taxonomic levels (open circles). (b) Subsampled generic and functional richness using occurrence data. Median generic richness (open circles) and median number of modes of life occupied (filled squares). Error bars represent 5th and 95th percentiles. The Lopingian and Middle Triassic epochs are shaded, bold vertical line shows the Permian/Triassic boundary.

The Late Permian extinction event was highly selective (Figure 7.3; Knoll et al., 2007), with the erect and surficial, stationary, attached suspension feeders comprising 61% of the genera that disappeared. Selection against these formally dominant groups led to increases in the relative abundance at the global scale of most other groups during the Induan (Figure 7.3). Despite slightly increasing in relative abundance in the Olenekian, sessile epifaunal suspension feeders never returned to the same level of dominance that characterised the Lopingian. Instead, the appearance of motile crinoids (Baumiller et al., 2010) and the radiation of the 'modern biota', including motile and infaunal bivalves (Stanley, 1968), predatory arthropods (Signor and Brett, 1984), and grazing gastropods (Vermeij, 1977), increasingly filled a diverse suite of lifestyles during the early Mesozoic (Figure 7.3). By the Middle Triassic, functional evenness at the global scale had increased, due especially to a radiation of the mobile grazing epifauna. Beginning even before the Late Permian extinction event, surficial, slow moving grazers underwent a gradual, uninterrupted increase in relative abundance through the entire study interval (Figure 7.3). Apart from those groups that originated after the extinction, this represents the most important change to the functional landscape of benthic marine ecosystems during the earliest stages of the Mesozoic Marine Revolution.

7.4. Latitudinal trends and regional biases

Although the Late Permian extinction event eliminated just a single mode of life at the global scale, at smaller scales functional diversity loss was more pronounced. Prior to the extinction event, equatorial palaeolatitudes, as expected, housed the greatest ecological and functional diversity (Figure 7.4a). Following extinction, however, raw and subsampled data record similar levels of functional diversity in tropical and northern palaeolatitudes during the Induan, and especially in the Dienerian (Figure 7.4a). This low gradient of functional diversity between the tropics and northern belt during the Induan may reflect the cosmopolitan nature of Induan benthic faunas (Chen
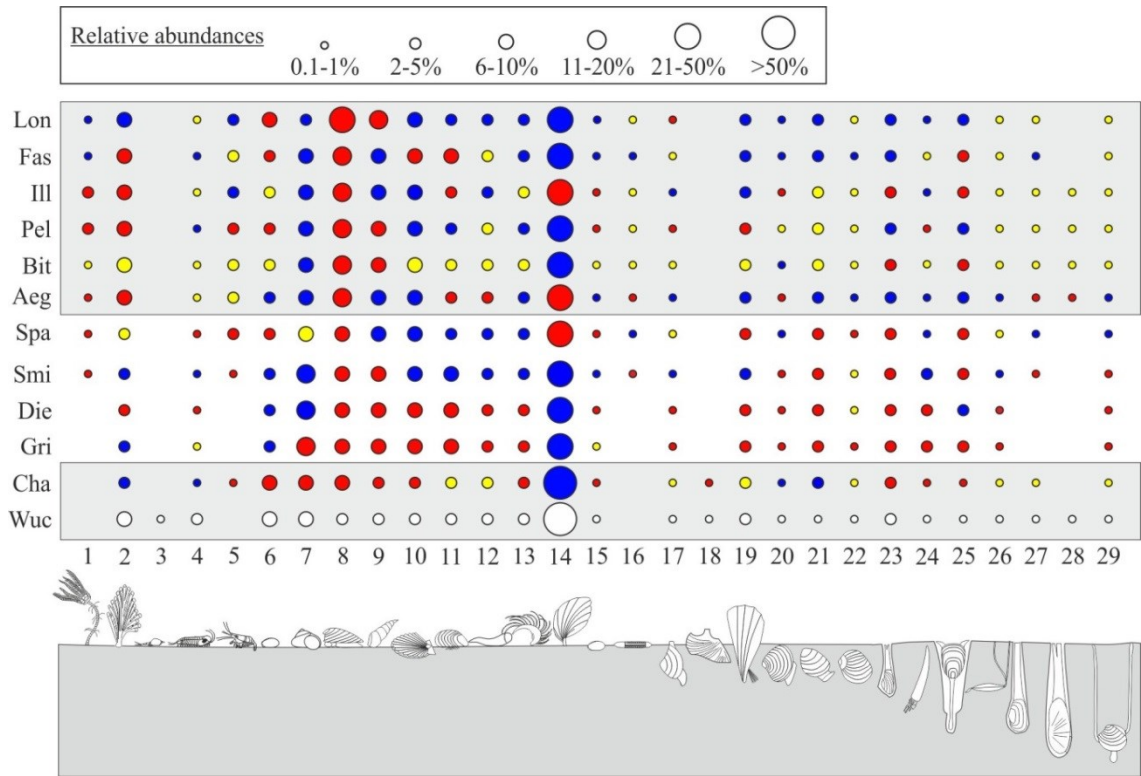
Figure 7.3: Relative abundance of genera in each mode of life across the studied interval.
Colours indicate changes in abundance of >0.1%: increases (red), decreases (blue) and no change (yellow) from the previous time bin. Wuchiapingian abundances are unshaded. 1 = erect, facultatively motile, attached suspension feeder. 2 = erect, stationary, attached suspension feeder; 3= surficial, fast-moving suspension feeder; 4 = surficial, fast-moving deposit feeder; 5 = surficial, fast-moving predator; 6 = surficial, slow-moving suspension feeder; 7 = surficial, slow moving deposit feeder; 8 = surficial, slow-moving grazer; 9 = surficial, slow-moving predator; 10 = surficial, facultatively motile, unattached suspension feeder; 11 = surficial, facultatively motile, attached suspension feeder; 12 = surficial, facultatively motile, attached deposit feeder; 13 = surficial, stationary, unattached suspension feeder; 14 = surficial, stationary, attached suspension feeder; 15 = semi-infaunal, slow-moving suspension feeder; 16 = semi-infaunal, facultatively motile, unattached predator; 17 = semi-infaunal, facultatively motile, attached suspension feeder; 18 = semi-infaunal, stationary, unattached deposit feeder; 19 = semi-infaunal, stationary, attached suspension feeder; 20 = shallow infaunal, slow-moving suspension feeder; 21 = shallow infaunal, slow-moving miner; 22 = shallow infaunal, slow-moving predator; 23 = shallow infaunal, facultatively motile, unattached suspension feeder; 24 = shallow infaunal, facultatively motile, unattached miner; 25 = shallow infaunal, facultatively motile, attached suspension feeder; 26 = shallow infaunal, facultatively motile, attached other; 27 = deep infaunal, facultatively motile, unattached suspension feeder; 28 = deep infaunal, facultatively motile, unattached suspension feeder; 29 = deep infaunal, facultatively motile, attached other. Images of fauna are not to scale.

and Benton, 2012) and implies relatively greater ecological impact in the tropics. Greater ecological impact in the tropics may be a consequence of climate warming, including concomitant factors such as expansion of hypoxic dead zones, reduced circulation, reduced nutrient cycling, and temperature rise itself, as well as the loss of reef ecosystems.

By the Anisian, raw and subsampled data show that tropical functional diversity had exceeded that recorded at low palaeolatitudes during the Lopingian, and a steep functional gradient between the tropics and higher latitudes had been re-established (Figure 7.4a). Greater tropical functional diversity during the Middle Triassic is probably due to migration from higher latitudes of taxa with lifestyles that were not previously recorded in the tropics. In many time bins, however, occurrences are not distributed evenly between palaeolatitudes, but are biased towards the tropics (Green coefficients > 0.5; Figure 7.4a). The Anisian records the greatest such bias, being dominated by well-studied sections from Europe and South China (Allison and Briggs, 1993), and the 'global' record of Spathian-Anisian recovery is therefore really a 'tropical' record.

Raw functional diversity decreases from the Changhsingian to the Griesbachian in all regions except the Boreal Ocean, which records an earlier decline, with minima being recorded at different times within the Early Triassic (Figure 7.4b). Results of subsampling suggest, however, that except for Panthalassa these trends may be an artefact of sampling biases (Figure 7.4b). The timing and patterns of recovery of functional diversity also apparently vary between regions, although there are too few post-Griesbachian occurrences in Neotethys and the Boreal Ocean for robust subsampling. A return to greater functional diversity occurred sooner in Panthalassa than in Palaeotethys, although relative differences during the Middle Triassic may be due to sampling problems because the regional occurrence data are strongly biased towards Palaeotethys during the Anisian (Green coefficients >0.5; Figure 7.4b). Indeed,

the widely held view that post-extinction recovery did not occur until the Anisian (e.g. Chen and Benton, 2012) is likely due to this regional bias and the 'global' signal is evidently just a Palaeotethyan signal.

7.5   Functional diversity in reefs and shelf settings

Although most Early Triassic occurrences are from the inner shelf, there is no major sampling bias between depositional settings through most of the study interval (Green coefficients <0.5 except for Pelsonian; Figure 7.4c). It is well known that reefs disappeared during the earliest Triassic (e.g. Flügel, 2002), but our raw and subsampled data demonstrate for the first time that the major loss of functional diversity in reef ecosystems occurred significantly before the late Changhsingian mass extinction horizon (Figure 7.4c). During the Wuchiapingian, metazoan reefs were globally the most important habitat in terms of functional richness, recording 19 of the 23 known modes of life (i.e. 83%), from 74 localities in UK, Russia, Germany, Greece, China, Greenland, Lithuania and Pakistan. Only five modes of life are, however, recorded in Changhsingian reefs, from a total of 36 localities from China, Russia, Tajikistan, Greece and Thailand. These data imply that reef ecosystems underwent precipitous collapse, and/or a major contraction, prior to climate warming in the latest Changhsingian. This may have been due to Lopingian sea-level fall or to a currently unknown episode of climatic or oceanographic change, possibly related to the earliest phases of Siberian Trap volcanism (Reichow et al., 2009). The subsequent rebuilding of reefs began locally in the Smithian (Brayard et al., 2011; Hofmann et al., 2015b) and Spathian, involving organisms such as sponges (Brayard et al., 2011), cementing bivalves (Pruss et al., 2007) and *Tubiphytes* (Payne et al., 2006b). Metazoan reefs of the Anisian were as functionally rich as their Wuchiapingian predecessors (Figure 7.4c), although reefs were not common until after the Illyrian following the appearance and radiation of the Scleractinia (Velledits et al., 2011).

During the Early Triassic 'reef gap', basin and slope settings gradually lost functional richness, whereas shelf seas, especially the inner and outer shelf, were functionally the most diverse settings (Figure 7.4c). By the Middle Triassic, inner shelf settings housed greater functional richness than the re-emerging reefs. The 'habitable zone' hypothesis
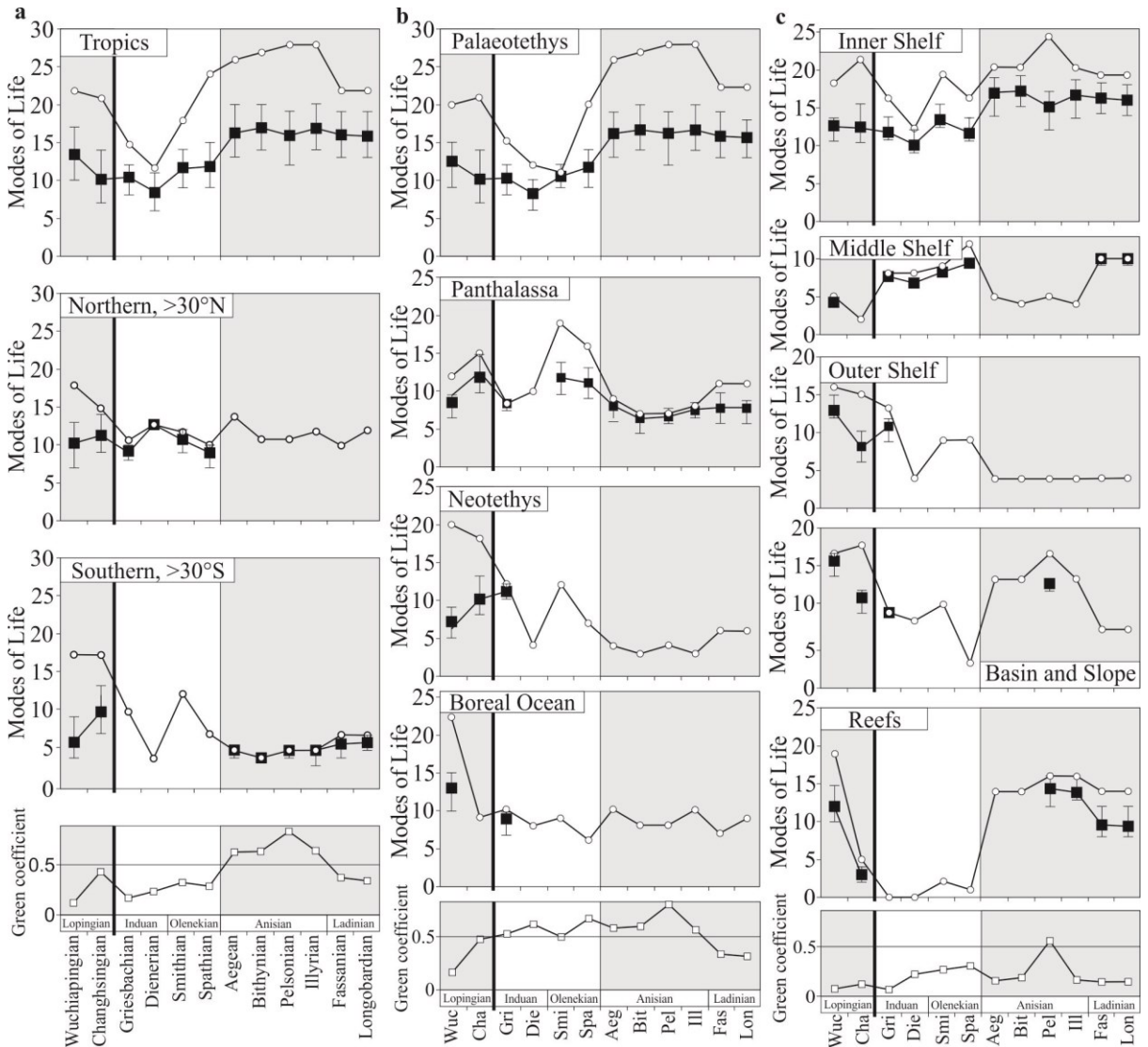
Figure 7.4. Permian-Triassic functional richness in different (a) palaeolatitudes, (b) regions, and (c) environments. Raw data (open circles) and subsampled medians (filled squares). Error bars represent 5th and 95th percentiles. Green coefficient values >0.5 indicate bias in the data within that time bin. The Lopingian and Middle Triassic epochs are shaded. The Permian/ Triassic boundary is marked with a thick line.

(Beatty et al., 2008) predicts that nearshore, wave-aerated settings should house greater diversity in the earliest Triassic and although our inner shelf data support this hypothesis, the outer shelf data imply that even if deeper settings were taxonomically depauperate functional diversity was still maintained, at least in the Griesbachian (Figure 7.4c).

7.6   Size change

Even though Early Triassic shelf settings were functionally diverse, the loss of erect and deep infaunal taxa led to a reduction in occupied tiers. This restriction of benthic animals to within a few centimetres above and below the sediment-water interface is the most dramatic such shift of the entire Phanerozoic (Ausich and Bottjer, 2001), and characterises the immediate extinction aftermath worldwide (Twitchett and Barras, 2004; Twitchett, 2006). It would have significantly impacted nutrient cycling and secondary production, with bioturbation depths in most ecosystems returning to levels not recorded globally since the Cambrian. Genera identified as being 'deep infaunal' reappear first in the Griesbachian and again in the Smithian of eastern Panthalassa, but are represented by small-sized taxa such as *Nucinella* sp. nov. (Chapter 6) and *Sinbadiella pygmaea* (Hautmann and Nützel, 2005), which probably could not burrow that deeply. Full ecosystem functioning would not have been restored until larger bioturbators reappeared. The earliest reappearances of the erect tier in shelf settings are also represented by relatively small-sized animals: in a mid-shelf setting of a seamount by crinoids in the Griesbachian (Oji and Twitchett, 2015), in the inner shelf by bryozoans in the Dienerian (Baud et al., 2008); and in slope and basin settings by the crinoid *Holocrinus* in the Smithian (Shigeta et al., 2009).

Despite the significant worldwide loss of species richness, the late Permian extinction event did not significantly reduce functional diversity of benthic marine ecosystems at the global scale. Where, only one mode of life, associated with the extinction

rostroconchs, disappeared after the late Permian mass extinction. As a consequence, few higher taxa and only one new mode of life originated in the extinction aftermath, associated with the evolution of motile crinoids. The extinction, however, was highly selective where epifaunal, stationary, attached, suspension feeders comprising 61% of the taxa that disappeared. This led to an increase in motility, predation and infaunalisation in the extinction aftermath.

At smaller scales, however, significant changes in functional diversity, both positive and negative, did occur in particular regions and depositional settings. The homogenous nature of shelly faunas around the world is reflected by a reduction in the number of modes of life occupied between northern and tropical latitudes. In addition, reef and basinal environments suffered major losses in functional diversity. Unexpectedly, however, although outer ramp settings were taxonomically depauperate, functional diversity was still maintained and comparable to inner shelf settings. Ecological changes during this critical time in Earth history are more complex than simple models have hitherto suggested, and supposed 'global' patterns may reflect biases in regional data, especially in the post-extinction recovery interval.

Chapter 8   Modified recovery model and hypothesis testing

Novel and quantitative palaeoecological and geochemical data were collected from the Aggtelek Karst, Hungary (Chapter 3), eastern Lombardy, Italy (Chapter 4), the Dolomites, Italy (Chapter 5), and Svalbard (Chapter 6) to investigate the magnitude and pattern of benthic marine recovery following the late Permian mass extinction event and to test the 'habitable zone' hypothesis, whether carbon isotope excursions during the Lower Triassic coincide with biotic crises, and whether recovery was faster at higher latitudes hypotheses.

In order to test these hypotheses it is important to quantify the recovery of benthic invertebrate communities. Although there are several models for measuring recovery (e.g. Harries et al., 1996; Twitchett, 2006; Chen and Benton, 2012; Pietsch and Bottjer, 2014) the empirical model described by Twitchett (2006) is the most widely cited in the literature. This model is based on the stepwise recovery of the marine benthic communities from the initial post-extinction aftermath to the final recovery of the benthic fauna (Twitchett, 2006), based on empirical data from the Werfen Formation, Italy. Recent findings, however, have found that this model is too coarse to characterise the difference in the pace of recovery between different geographical settings (e.g. Hofmann et al., 2011; Pietsch and Bottjer, 2014). Using the novel palaeoecological data collected in this study, therefore, the model of Twitchett (2006) is modified to quantify better the recovery of benthic invertebrates following the late Permian mass extinction.

8.1   Revised recovery model

Taxonomic analysis of well-preserved fauna from Svalbard suggests that most previous studies of the Early Triassic misidentified the nuculanoid bivalve *Austrotindaria* as *Unionites*. This has important implications for Permian-Triassic changes in the functional compositions of benthic communities because *Austrotindaria* has a significantly different mode of life from *Unionites*. Early Triassic benthic communities

dominated by *Austrotindaria* (=*Unionites* for previous authors), therefore, represent infaunal deposit-feeding communities rather than infaunal suspension-feeding communities. This new finding that oxygen-restricted environments in the Early Triassic are dominated by infaunal deposit-feeding taxa is also consistent with the functional composition of oxygen-restricted environments described from the Jurassic (Aberhan, 1994). In addition, it has been reported that infaunal deposit-feeding communities of the Silurian, Early Triassic and modern are associated with high sedimentation rates (Algeo and Twitchett, 2010; Levinton and Bambach, 1975). The *Austrotindaria* assemblages of the Early Triassic, therefore, represent communities adapted to oxygen-restriction and high sedimentation rates associated with climate warming during the late Permian. Similar dominance of deposit-feeding infauna is also recorded by the ichnofaunal record with the proliferation of *Planolites* (Twitchett and Wignall, 1996; Twitchett, 1999; 2006; Twitchett and Barras, 2004; Algeo and Twitchett, 2010).

The ichnological record appears to change to a new state in the upper Spathian, marked by a significant increase in the proportion of bioturbated rock, i.e. ichnofabric indices 4-5 (Chapters 3-5; Twitchett and Barras, 2004), and increased burrow diameter (Twitchett, 1999; Chen et al., 2011b). Body and trace fossils are, however, still small when compared to the Middle Triassic (Twitchett, 1999; Zonneveld et al., 2001; Hagdorn and Velledits, 2006; Twitchett, 2007; Zonneveld et al., 2010), suggesting that final recovery in the Middle Triassic still represents a separate recovery stage. Establishing quantitative values for species richness and evenness into the recovery model (as done by Pietsch and Bottjer, 2014), however, is not credible as assemblages with low diversities and high dominance are still present into the Spathian sub-stage, which otherwise shows a marked recovery. With the novel observations of the western Palaeotethys made in this study, the empirical recovery model of Twitchett (2006) can

be modified to reflect better the recovery of benthic communities following the late Permian mass extinction (Figure 8.1).

The four recovery stages of Twitchett (2006) are clearly defined by changes in infaunal and epifaunal tiering. Recovery Stage 1 is characterised by the dominance of infaunal, deposit-feeding body or trace fossils, e.g. *Austrotindaria* and *Planolites*, limited to within a few centimetres of the sediment-water interface. Small *Lingularia*, bellerophontids, microconchids and *Claraia* are also associated with this fauna and characteristic of this stage.

Recovery Stage 2 is marked by an expansion of the infaunal tier, but the epifaunal tier is still restricted to within a few centimetres of the sediment. This stage can be divided into two: 2a is defined by an increase of infaunal tiering by the return of suspension feeding domichnia, e.g. *Diplocraterion*, with burrow depths up to 12cm, and an initial
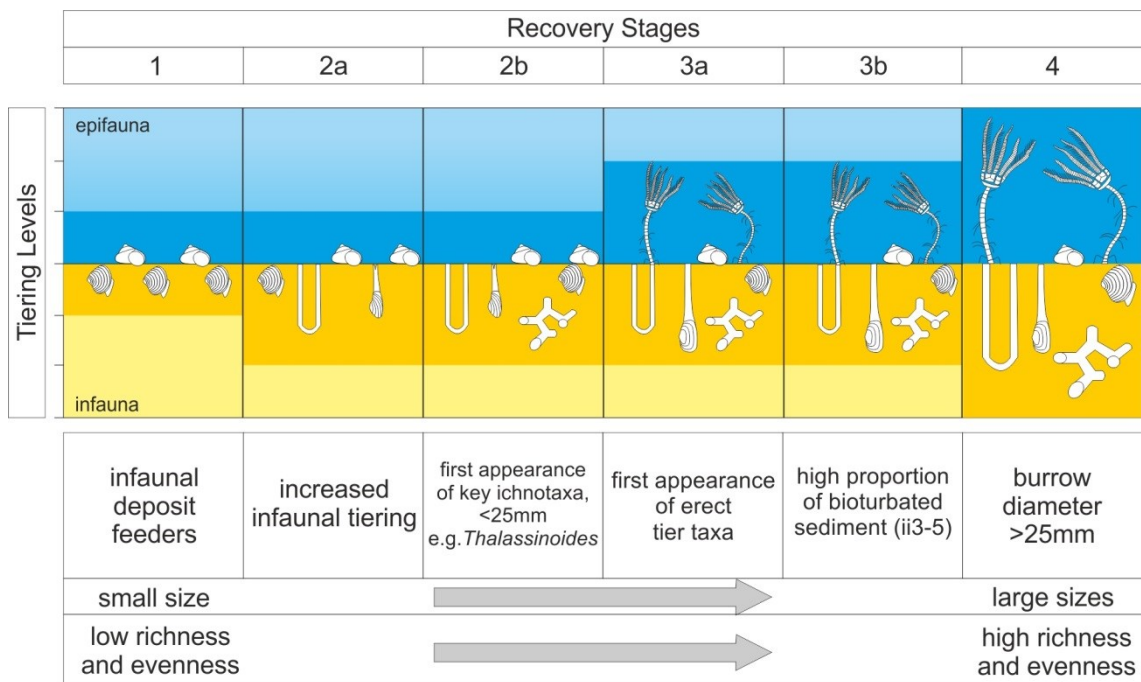
Figure 8.1: Revised palaeoecological recovery model for the recovery of benthic ecosystems in the aftermath of the late Permian mass extinction. Modified after Twitchett (2006), see text for further details.

increase in the size of fossils; 2b is defined by the first appearance of key ichnotaxa attributable to the activity of crustaceans, e.g. *Thalassinoides* and *Rhizocorallium*, with burrow diameters typically <25mm. Previously, the return of *Rhizocorallium* and *Thalassinoides* was used to indicate recovery stage 3 (Twitchett, 2006), however because they occur prior to the return of the erect tier and in the absence of further changes in the depth of infaunal tiering (Hofmann et al., 2011) they are included as a subdivision of recovery stage 2. In addition, the body fossil record shows the first appearance of deep infaunal taxa, e.g. *Pleuromya* (Fraiser and Bottjer, 2007) and *Sinbadiella* (Hautmann and Nützel, 2005) that are of a reduced size and unlikely to burrow more than 12cm into the sediment.

Recovery stage 3a is defined by an expansion of the erect tier signified by the return of crinoids, sponges and/or bryozoans. The upper Spathian, also shows a further recovery signal indicated by persistent bioturbation, e.g. high proportion of rock with ichnofabric indices between 3 and 5, with burrow diameters typically <25mm. Changes in tiering, however, do not significantly differ from stage 3a and are therefore considered a separate subdivision of recovery stage 3, i.e. 3b. The increased proportion of bioturbated sediment, however, may be a response to changes in sedimentation rates. In addition, in some environments, i.e. the swash zone, the preservation potential of bioturbation is significantly reduced due to the constant reworking of sediment. Records of an increase in bioturbation, however, have been recorded from peritidal/shallow subtidal to outer shelf settings below wave base (e.g. "Upper Member", Lombardy; San Lucano Member, Dolomites; Szinpetri Limestone, Aggtelek Karst; Tvillingodden Formation, Svalbard (Chapters 3-6; Worsley and Mørk, 2006)) and in settings with high sedimentation rates (e.g. Szinpetri Limestone, Chapter 3). This subdivision, therefore, appears to be a recognisable biological signal.

Full recovery was not observed in this study, but previous studies show that the Middle Triassic faunas typical of full recovery, i.e. Recovery stage 4, are characterised by increased burrow size, typically >25mm (Twitchett, 2006; Zonneveld et al., 2010), increased size of body fossils (Hagdorn and Velledits, 2006; Twitchett, 2007) leading to increased tiering into the water column and depth of infaunal tiering. Species richness, functional richness and evenness values cannot be quantified into different recovery stages, but, generally these parameters increase between the different stages with the highest values recorded in the Middle Triassic (Chapters 3-6; Twitchett et al., 2004; Posenato, 2008a; Komatsu et al., 2010; Stiller, 2001).

8.2   'Habitable zone' hypothesis

The first objective of this study was to test the 'habitable zone' hypothesis of Beatty et al. (2008) that diverse benthic communities were restricted to settings aerated by wave activity between the upper shoreface and offshore transition, and limited to higher palaeolatitudinal settings.

Benthic invertebrate faunas from the shoal and mid-ramp/shelf deposits of the western Palaeotethys and Boreal Ocean show high taxonomic and ichnological species richness, high functional richness, high heterogeneity, high evenness (Chapters 3-6; Figure 8.2; Twitchett and Wignall, 1996; Hofmann et al., 2011). In outer ramp/shelf environments distal to these, however, benthic faunas become sparse over the Permian/Triassic boundary and are characterised by low richness, low evenness faunas characterised by paper pectens, e.g. *Claraia* and *Daonella*, and unbioturbated sediment. This is consistent with the 'habitable zone' hypothesis. Similarly quantitative studies of Lower Triassic successions from the western US also report diverse benthic faunas from mid-ramp and shoal settings whilst more distal settings lack benthic faunas and bioturbated rock (Mata and Bottjer, 2011; Hofmann et al., 2013a; Hofmann et al., 2013b; Hofmann et al., 2014; Pietsch et al., 2014).
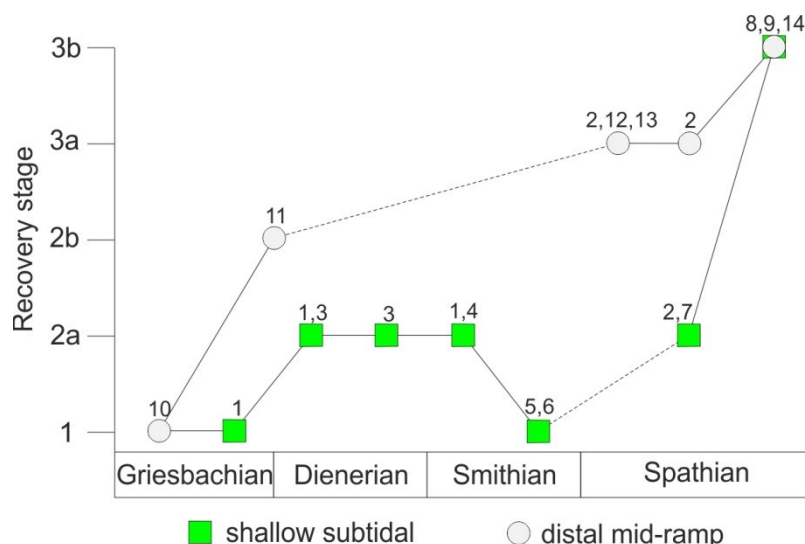
Figure 8.2: Recovery between different facies of the western Palaeotethys using the modified recovery model. 1 = Bódvaszilas Sandstone Formation 2 = Szin Marl Formation, 3 = mid-Siusi Member, 4 = Gastropod Oolite Member, 5 = Campil Member, 6 = Acquaseria Member, 7 = Cencenighe Member, 8 = San Lucano Member and 9 = "Upper" Member, 10 = Mazzin Member, 11 = lower-Siusi Member, 12 = Val Badia Member, 13 = "Myophoria Beds" Member and 14 = Szinpetri Limestone Formation (Chapters 3-5; Twitchett, 1999; Twitchett and Barras, 2004; Hofmann et al., 2011).

Benthic invertebrate assemblages from more proximal settings of the shoal environments of the western Palaeotethyan sections (e.g. Aggtelek Karst, Lombardy and the Dolomites) are characterised by lower richness, lower evenness and exclusively represented by low tier opportunistic taxa until the *Tirolites carniolicus* Zone (Chapters 3-5; Figure 8.2). Their palaeoecological characteristics are consistent with limited post-Permian recovery and persistent environmental stress. The absence of grazers and stenohaline taxa, and the abundance of wrinkle marks in these proximal settings suggest that large salinity fluctuations, high sedimentation rates, eutrophication and related oxygen-stress were the main control on the fauna in this environment (Chapter 3-5). The faunas from the western Palaeotethys, therefore, show that although diverse benthic faunas were restricted to the 'habitable zone', persistent environmental stress in proximal nearshore environments excluded diverse benthic communities.

The presence of a 'habitable zone' in the western Palaeotethys contradicts the conclusions of Beatty et al. (2008) that the habitable zone was limited to higher palaeolatitudinal settings. In addition, the distribution of Early Triassic skeletal and trace fossil communities that show increased infaunal tiering, richness, size and a return
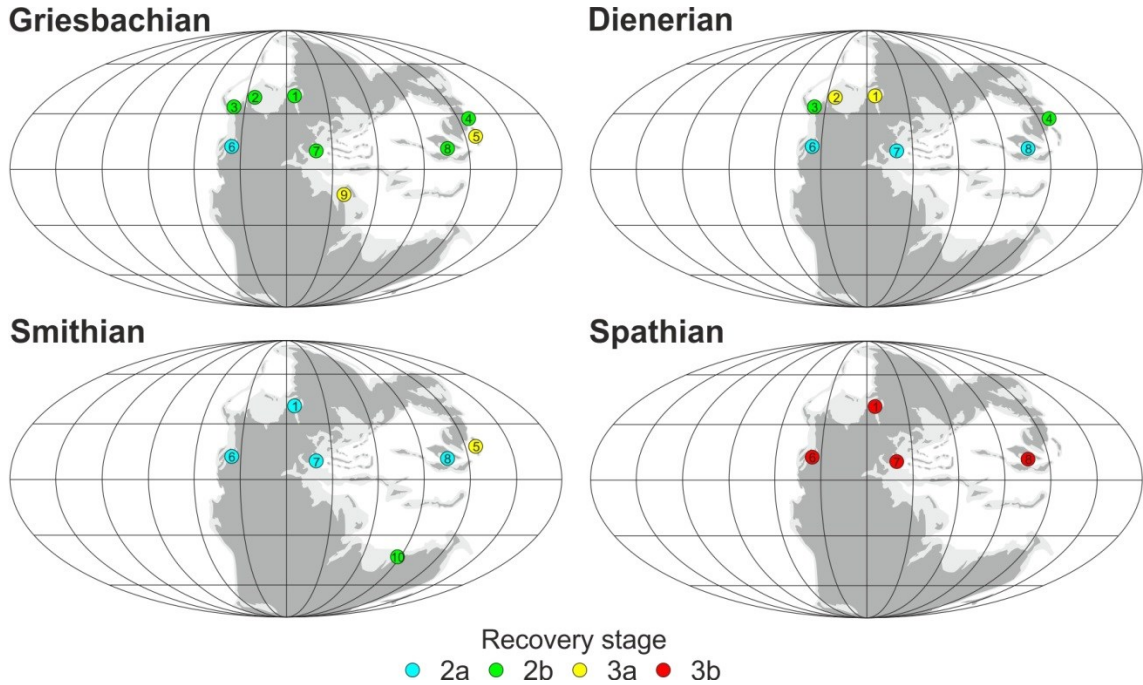
Figure 8.3: Distribution of skeletal and trace fossil communities that reflect recovery, i.e. at least recovery stage 2a. 1: Svalbard, (this study; Wignall et al., 1998; Nakrem and Mørk, 1991), 2: Nunavut, (Beatty et al., 2008), 3: British Columbia, (Zonneveld et al., 2010c), 4: Primorye, (Shigeta et al., 2009), 5: Japan, (Sano and Nakishima, 1997; Kashiyama and Oji, 2004; personal observation), 6: western US, (Fraiser and Bottjer, 2009; Mata and Bottjer, 2011; Brayard et al., 2011; Hofmann et al., 2013a; Hofmann et al., 2013b; Hofmann et al., 2014; Pietsch et al., 2014), 7: Italy, Hungary and Slovenia, (this study; Twitchett and Wignall, 1996; Hofmann et al., 2011; Kolar-Jurkovšek et al., 2013; Hofmann et al., 2015), 8: south China, (Hautmann et al., 2011; Chen et al., 2010b; Chen et al., 2011; He et al., 2015), 9: Oman and Persian Gulf, (Twitchett et al., 2004; Knaust, 2010a; Jacobsen et al., 2011; Oji and Twitchett, 2015), 10: Australia, (Chen et al., 2012; Luo and Chen, 2013). Palaeogeographic reconstruction after Blakey (2011).

of domichnia (e.g. *Diplocraterion*), i.e. palaeoecological characteristics consistent with Recovery stage 2a, all occur in settings influenced by the activity of waves, suggesting that the distribution of the habitable zone was global and not restricted to particular regions or latitudes (Figure 8.3).

The distal setting of the Szinpetri Limestone, Aggtelek Karst, i.e. below wave base, and the mid-shelf setting of the *Keyserlingites subrobustus* Zone of the Tvillingodden and Botneheia formations (cf. Mørk et al., 1999; Worsley and Mørk, 2001; Hounslow et al., 2008) record increased sample richness, proportion of bioturbated sediment and ichnotaxa associated with the activity of crustaceans, e.g. *Thalassinoides* and *Rhizocorallium*, suggesting a retreat of the oxygen minimum zone during the *T. carniolicus* Zone (Chapter 3; Worsley and Mork, 2001). Furthermore, in the nearshore proximal settings of the San Lucano Member, Dolomites (Twitchett and Wignall, 1996; Chapter 4); the upper part of the "Upper Member", east Lombardy (Chapter 5); the Nanlinghu Formation, China (Chen et al., 2011b); and in the western US (Hofmann et al., 2013a; Hofmann et al., 2014) an increase in bioturbation and ichnodiversity are recorded, suggesting the waning of previously harsh environmental conditions restricting benthic fauna. Globally, this recovery signal is associated with climate cooling (Sun et al., 2012), subsequent reestablishment of strong latitudinal temperature gradients (Brayard et al., 2006), the re-establishment of ocean circulation (Isozaki, 1997; Grasby et al., 2013) and retreat of the oxygen minimum zone creating an expanded habitable area that was rapidly filled by shallow water taxa (Chapters 3 and 7).

8.3   Subsequent biotic crises

The second objective of this study was to test the hypothesis that carbon isotope variations represent subsequent biotic crises that directly delayed the recovery of benthic invertebrates (cf. Payne et al., 2004).

In the Werfen Formation, Italy, elevated extinction rates are recorded at the Permian/Triassic boundary, in the late Dienerian, at the Smithian/Spathian boundary and in the late Spathian which are all contemporaneous with negative and positive carbon isotope excursions (Figure 4.15). Origination rates are elevated in the Griesbachian and Spathian following carbon isotope excursions, whereas at the Induan/Olenekian boundary, where there are a cluster of isotope excursions, extinction and origination rates are low (Figure 4.15). The same trends are also observed in the regional data for the western Palaeotethys, except the Smithian which also shows elevated origination rates (Figure 5.17). Between the Griesbachian, Dienerian and Smithian, however, no significant changes in the composition of the benthic communities was observed in east Lombardy, Dolomites or the Aggtelek Karst (Chapters 3-5). After the late Dienerian event, however, there is a reduced heterogeneity in assemblages due to the extinctions of *Claraia* and bellerophontids (Chapter 4).

The elevated extinction rates in the late Dienerian and the subsequent low origination rates suggest that the cluster of carbon isotopes from the Dienerian-Smithian interval (Figure 4.3; 4.15) either reflects a biotic crisis/crises or persistent harsh conditions that delayed the recovery following the late Permian mass extinction. The lack of a significant change in the composition of benthic communities, however, suggests that, prior to these carbon isotope fluctuations, recovery was slow.

The ichnological record from the Smithian Campil Member records a decrease in burrow size, ichnodiversity and reduced infaunal tiering (Twitchett and Wignall, 1996; Twitchett, 1999). When the post-extinction recovery for the Werfen Formation is categorised using the modified recovery model (Figure 8.4), the restriction of benthic fauna to within a few centimetres of the sediment in the Smithian suggests a reversal in the recovery of marine ecosystems. This is associated with a warming event (Sun et al., 2012; Romano et al., 2012). The dominance of low-richness, low-evenness

Austrotindaria (=*Unionites*) assemblages in siliciclastic beds (Hofmann et al., 2015a; Chapter 5) and high-richness, high-evenness assemblages in carbonate beds (Chapter 4) in the Smithian suggests that stress was greater in settings affected by increased sedimentation and that facies in less stressed mid-shelf settings may not record a reversal in benthic recovery. These changes are associated with increased influx of terrigenous material and a switch from relatively dry to wet conditions that can be recognised across western Palaeotethys localities: Aggtelek Karst (Hips 1998), Lombardy (Twitchett, 2000), Balaton Highlands (Kovacs et al., 2011; Haas et al.,
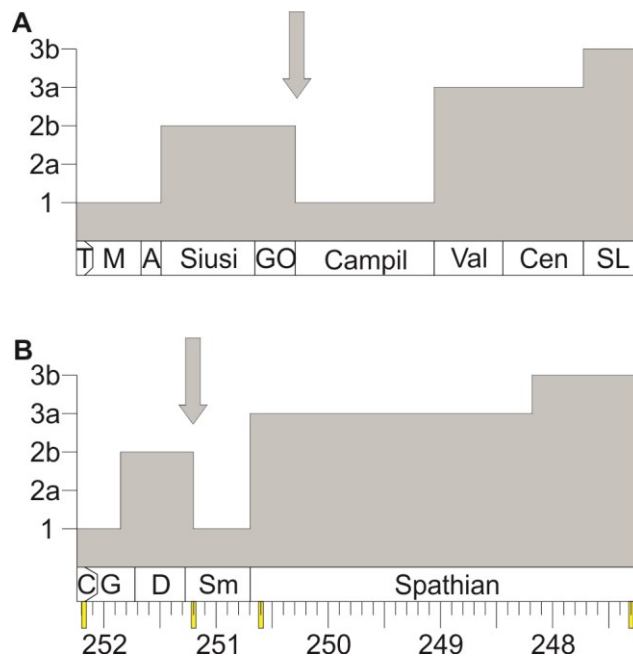
Figure 8.4: Post-extinction recovery in the Werfen Formation. A) x-axis proportional to thickness of the Werfen Formation and B) x-axis proportional to Early Triassic radiometric ages. Based on benthic community data from: Twitchett and Wignall, 1996; Twitchett, 1999; Twitchett and Barras, 2004; Hofmann et al., 2011; this study. Arrow indicates a reversal in recovery. T = Tesero Member, M = Mazzin Member, A = Andraz Member, GO = Gastropod Oolite Member, Val = Val Badia Member, Cen = Cencenighe Member, SL = San Lucano Member. C = post-extinction Changhsingian, G = Griesbachian, D = Dienerian, Sm = Smithian.

2012), Bükk Mountains (Hips and Pelikán, 2002), Southern Croatia and Western Bosnia and Herzegovina (Aljinović, 1995), Slovenia (Twitchett, 1999) and Austria (Mostler and Rossner, 1984).

In the western Palaeotethyan sections there is a significant change in the composition of benthic communities between the Smithian and Spathian as well as increased species richness, increased heterogeneity, stenohaline taxa and the first appearance of deeper infaunal and erect epifaunal tiers, associated with a more stable carbon isotope record during the Spathian (Neri and Posenato, 1985; Twitchett, 1999; Hofmann et al., 2015a; Chapter 3-5). In addition, an increase in beta diversity has been used as a measure of advanced recovery by Hautmann et al. (2011) and Hofmann et al. (2014), and such an increase is only recorded in the western Palaeotethys (Chapters 3-5) and eastern Panthalassa (Hofmann et al., 2014) in the Spathian, as this was the only sub-stage showing different faunal compositions between different environmental settings. These data, suggest that Spathian faunas record a more advanced recovery state than those of the Griesbachian-Smithian interval.

This Spathian recovery signal coincides with amelioration of extreme hothouse conditions of the Griesbachian-Smithian sub-stages (Romano et al., 2012; Zhang et al., 2015), reduced sedimentation rates (Algeo and Twitchett, 2010; Chapter 4) and a more stable carbon isotope record (Chapter 4: Figure 4.3). Therefore, rapid carbon isotope excursions during the Griesbachian-Smithian reflect persistent environmental stress with limited recovery and further biotic crises.

8.4   Faster recovery at higher latitudes

The third objective of this study was to test the hypothesis that recovery was faster at higher latitudes (cf. Twitchett and Barras, 2004).

The recovery of benthic ecosystems has more recently been described as globally synchronous (Knaust, 2010; Hofmann et al., 2011), as the reappearance of key ichnotaxa, e.g. *Thalassinoides, Rhizocorallium* and *Diplichnites*, associated with the activity of crustaceans and diverse mollusc communities are recorded from the Griesbachian from a range of latitudes and regions (Hofmann et al., 2011; Twitchett and Barras, 2004; Beatty et al., 2008; Zonneveld et al., 2010c). The diverse benthic fauna recovered from the *H. parvus* Zone in Svalbard (Chapter 6) and the Sverdrup Basin (Beatty et al., 2008; Zonneveld et al., 2010), however, shows more advanced recovery than recorded elsewhere during this conodont zone, except the mid-latitude setting of eastern Panthalassa (Beatty et al., 2008), suggesting that recovery may have occurred at a faster pace in the mid-palaeolatitudinal settings (Figure 8.5). Knaust (2010) suggests that the diverse benthic ichnofauna recorded from the *H. parvus* Zone in a low latitude Neotethyan locality represents comparable recovery to the Boreal Realm, but in fact the faunas lack key ichnotaxa, e.g. *Thalassinoides*, and represent a less advanced stage of recovery. In addition, within the same region, i.e. eastern Panthalassa, low latitude settings recorded limited post-extinction recovery (stage 2a) by the late Griesbachian, whereas, the higher palaeolatitudinal setting of the Alberta and British Columbia show more advanced recovery (stage 2b) within the Griesbachian demonstrating a latitudinal aspect to the recovery of benthic faunas.

The fauna from Oman, albeit a conodont zone younger than that from Svalbard, is ecologically more advanced than the fauna from Svalbard, as it contains representatives of the erect tier. The sizes of gastropod specimens reported from Oman (max length: >20mm; Wheeley and Twitchett, 2005) are also larger than observed in this study (max length: 3.6mm, max width: 4.6mm), suggesting a more advanced state of recovery. Comparable faunas from the *Isarcicella isarcica* and *I. carinata* Conodont Zones from Svalbard were not recorded in this study and have not been recorded from
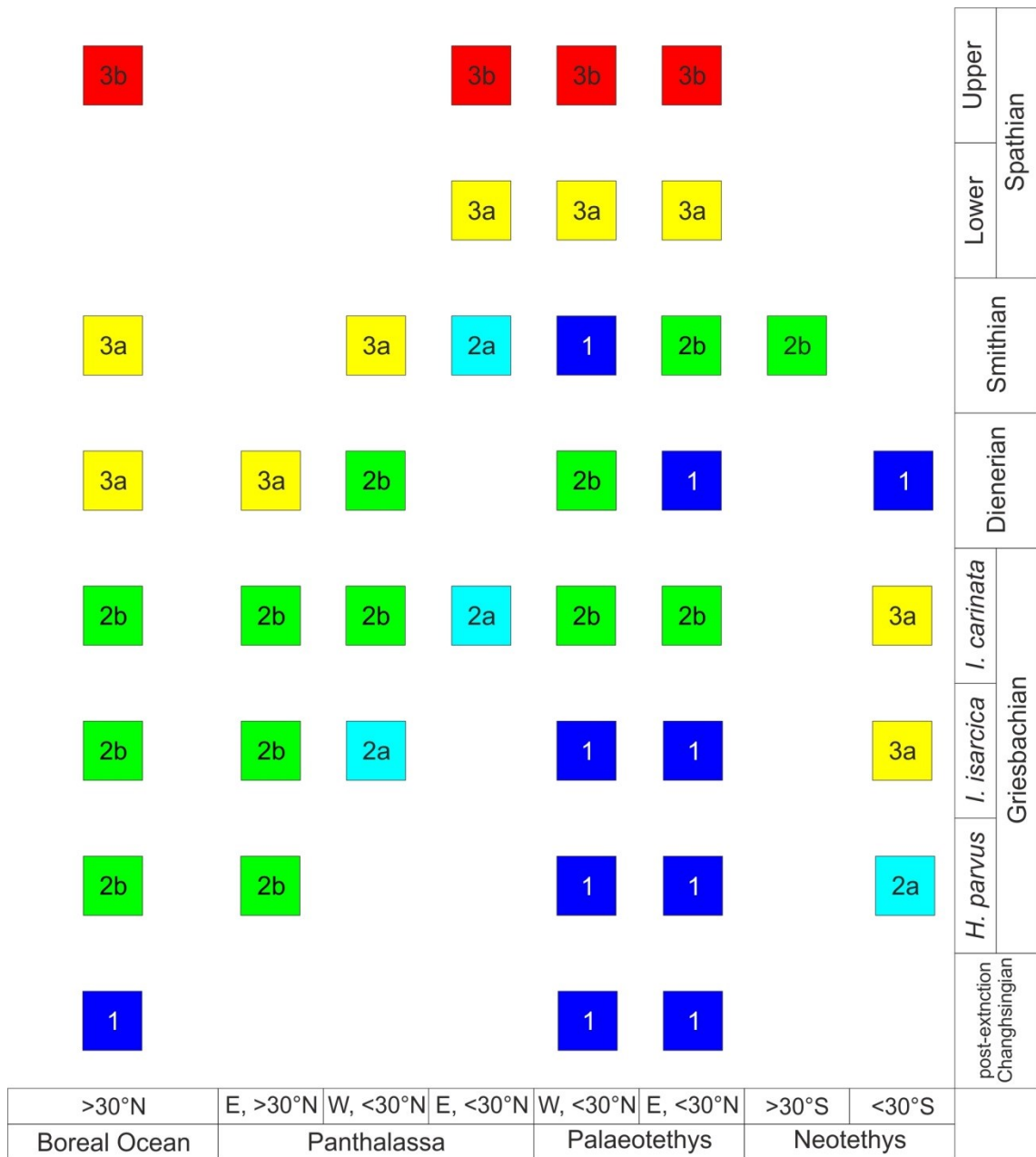
Figure 8.5: Post-extinction recovery of benthic marine communities between different regions. Western Palaeotethys (this study; Twitchett and Wignall, 1996; Twitchett and Barras, 2004; Hofmann et al., 2011; Metcalfe et al., 2011; Kolar-Jurkovšek et al., 2013; Hofmann et al., 2015), eastern Palaeotethys (Lehrmann et al., 2006; Chen et al., 2010b; Yang et al., 2011; Hautmann et al., 2011; Chen et al., 2011), Neotethys <30°S (Twitchett et al., 2004; Jacobsen et al., 2011; Knaust, 2010; Oji and Twitchett, 2015), Neotethys >30°S (Chen et al., 2012) eastern Panthalassa (Kashiyama and Oji, 2004; Shigeta et al., 2009; personal observation), western Panthalassa <30°N (Fraiser and Bottjer, 2009; Mata and Bottjer, 2011; Brayard et al., 2011; Hofmann et al., 2013a; Hofmann et al., 2013b; Hofmann et al., 2014; Pietsch et al., 2014), western Panthalassa >30°N (Beatty et al., 2008; Zonneveld et al., 2010), Boreal Ocean (this study, Wignall et al., 1998; Nakrem and Mørk, 1991; Beatty et al., 2008).

the Boreal Ocean. The occurrence of erect bryozoans, articulate brachiopods, a species rich fauna, extensive bioturbation and a diverse ichnofauna from the Vikinghøgda and Vardebukta formations in the Dienerian (Wignall et al., 1998; Mørk et al., 1999; this study), however, suggests an advanced recovery fauna comparable to that described in Oman. Furthermore, the composition of the faunas from Oman and Svalbard appear to be comparable, i.e. gastropod-bivalve dominated assemblages (Jacobsen et al., 2011).

Further recovery beyond stage 3a is not recorded until the upper Spathian, and appears to be synchronous, globally, which coincides with climate cooling (Sun et al., 2012), the reestablishment of a latitudinal temperature gradient (Brayard et al., 2006) and the subsequent reignition of ocean circulation (Isozaki, 1997). Initial recovery, therefore appears to occur at a faster pace in the mid-latitudinal settings, however, advanced recovery (stage 3b) appears to occur synchronously in the upper Spathian.

8.5   Wider implications

The restriction of benthic faunas to a 'habitable zone' and the impact of subsequent biotic crises during the Induan and Olenekian are the reasons that benthic faunas investigated in this study and previously (Twitchett, 2006; Posenato et al., 2008a; Chen and Benton, 2012) do not reach full recovery within the Early Triassic. Locally, full recovery has not been recorded until the Pelsonian or Illyrian sub-stages of the Middle Triassic, associated with the recovery of reef ecosystems (Gaetani and Gorza, 1989; Senowbari-Daryan et al., 1993; Velledits et al., 2011), Lazarus taxa (Erwin and Pan, 1996), a marked increase in the diversity of bivalves (Posenato, 2008a) and other groups (Payne et al., 2006a), burrow size (Zonneveld et al., 2010a; Knaust 2010c) and reappearance of stenotopic hard-bottom dwellers (Posenato, 2002), amongst others. Future studies investigating the recovery following the late Permian mass extinction, therefore, should also investigate the Middle Triassic.

Chapter 9   Conclusions

Novel quantitative palaeoecological analyses of benthic communities from the Aggtelek Karst, Hungary, Lombardy and the Dolomites, Italy, and Svalbard have shown that:

- Fossil assemblages of the Induan (Griesbachian and Dienerian) and lower Olenekian (Smithian) of the Aggtelek Karst, which were deposited in nearshore, proximal ramp settings, have low diversity and low evenness and are exclusively represented by low tier, opportunistic, euryhaline taxa. Their palaeoecological characteristics are consistent with limited post-Permian recovery and persistent environmental stress. Skeletal assemblages were not recorded in similar settings of the Spathian and lack of bioturbation suggests ongoing environmental stress.

- The Spathian Szin Marl Formation, Aggtelek Karst, records increased species richness, changes in taxonomic composition, increased heterogeneity, stenohaline taxa and the appearance of deeper infaunal and erect epifaunal tiers. This is consistent with advanced ecological recovery, but is at least partly driven by an increased range of sampled facies and environments.

- In the Szinpetri Limestone Formation, Aggtelek Karst, sample richness and bioturbation increase to levels not recorded in Griesbachian to mid-Spathian rocks. Globally, this is associated with climate cooling, the re-establishment of ocean circulation and retreat of the oxygen minimum zone, in the *Tirolites carniolicus* Zone, creating an expanded habitable zone which was rapidly filled by shallow water taxa.

- In the Dolomites, elevated extinction rates were recorded around the Permian/Triassic boundary, associated with a negative isotope excursion. In the subsequent Mazzin and Siusi members there were also elevated origination rates.

- Elevated extinction rates in the Werfen Formation are also recorded around the Smithian/Spathian boundary associated with a positive isotope excursion and subsequent high origination rates in the Val Badia and Cencenighe members. With ecological recovery reaching a more advanced state than in the older members of the Werfen Formation.

- The elevated extinction rates in the upper Dienerian of the Werfen Formation on the other hand are followed by no new originations and a subsequent decline in the standing species and functional diversity. This is associated with three rapid carbon isotope excursions, and increased sedimentation in the Smithian led to a reversal in the recovery of benthic marine communities.

- In the Werfen Formation a significant change in the taxonomic composition of benthic assemblages was only recorded across the Campil/Val Badia member boundary (i.e. Smithian/Spathian boundary), with the *Austrotindaria* (=*Unionites*), microconchid and *Coelostylina* biofacies replaced by *Natiria costata* and *Neoschizodus ovatus* biofacies. In addition, the Spathian records increased species richness, increased heterogeneity, the appearance of stenohaline taxa, and deeper infaunal and erect epifaunal tiers.

- Further recovery is recorded in the subtidal facies of the San Lucano Member, as evidenced by more extensive bioturbation than is recorded in the underlying members of the Werfen Formation.

- The Smithian Acquaseria Member, Servino Formation, records a decline in bioturbation, species and functional richness. This is associated with a negative isotope excursion and environmental deterioration that correlates with evidence of increased sedimentation rates and further warming during the Smithian, i.e. the 'Campil Event'.

- The Mid-Spathian lower part of the "Upper Member", Servino Formation records a decline in bioturbation that correlates with increased sedimentation associated with climate warming during the mid-Spathian.

- The "Myophoria Beds" Member, Servino Formation, records an increase in species richness, functional richness, changes in taxonomic composition, increased heterogeneity and the appearance of stenohaline erect taxa, and is the most diverse member of the Servino Formation, reflecting a lower Spathian recovery pulse.

- The upper part of the "Upper Member" records a shallow subtidal environment with more extensive bioturbation than recorded in older members of the Servino Formation. This correlates with an upper Spathian recovery pulse identified in the Aggtelek Karst and Dolomites suggesting a regional recovery pulse in the *T. carniolicus* Zone.

- *Lingularia* species significantly declined in size across the Kapp Starostin/Vikinghøgda Formation boundary and subsequently across the late Permian mass extinction event associated with deteriorating environmental conditions during the late Changhsingian.

- The oldest silicified fauna of the Triassic was identified 10m above the base of the Vikinghogda Formation, Lusitaniadalen. It records unusually high taxonomic and functional richness during the *H. parvus* Zone and a more advanced ecological state than contemporaneous benthic assemblages reported in other regions.

- The silicified fauna from the *H. parvus* Zone in Svalbard demonstrate that the aftermath of the late Permian mass extinction was a key interval for the diversification of the Architectibranchs, Protobranchia and Palaeoheterodonta.

- Only one mode of life (semi-infaunal, stationary, unattached, deposit feeders) disappears during the late Permian mass extinction, due to the extinction of rostroconchs, and only one new mode of life (erect, facultatively, motile, attached, suspension feeders) originated in the extinction aftermath, associated with the evolution of motile crinoids.

- At smaller scales, significant changes, positive and negative, in functional diversity occur in particular regions and depositional environments. These include a decline in the functional diversity of reef ecosystems which show a precipitous collapse before the onset of climate warming in the late Changhsingian.

- Occurrences are not evenly distributed between palaeolatitudes or regions throughout the study interval, but are biased towards the tropics and the Palaeotethys, being dominated by well-studied sections from Europe and South China, and therefore the "global" record is actually a tropical, Palaeotethyan record.

- The restriction of benthic communities that show signs of recovery to wave-aerated settings of shoal and mid-ramp/shelf environments in this study are consistent with the habitable zone hypothesis.

- The presence of a habitable zone in the low-palaeolatitude setting of the western Palaeotethys throughout the Early Triassic suggests that the habitable zone is not restricted to mid-palaeolatitudes as previously hypothesised.

- Subsequent biotic crises (elevated extinction rates) during the Early Triassic correlate with carbon isotope excursions in the western Palaeotethys. The restriction of benthic communities to within a few centimetres of the sediment-water interface in the Smithian suggests a reversal in the recovery associated with subsequent climate warming and increased sedimentation rates.

- The benthic fauna recovered from Svalbard in the *H. parvus* Zone shows that initial recovery was faster in the mid-palaeolatitudinal setting of the Boreal Ocean than in other regions, but, further recovery indicated by the occurrence of persistent bioturbation appears to be globally synchronous in the late Spathian.

References

Aberhan, M. 1994. Guild-Structure and evolution of Mesozoic benthic shelf communities. *Palaios* 9, 516-545.

Aberhan, M., Kiessling, W. and Fürsich, F.T. 2006. Testing the role of biological interactions in the evolution of mid-Mesozoic marine benthic ecosystems. *Paleobiology* 32, 259-277.

Algeo, T.J., Hannigan, R., Rowe, H., Brookfield, M., Baud, A., Krystyn, L. and Ellwood, B.B. 2007. Sequencing events across the Permian-Triassic boundary, Guryul Ravine (Kashmir, India). *Palaeogeography, Palaeoclimatology, Palaeoecology* 252, 328-346.

Algeo, T.J. and Twitchett, R.J. 2010. Anomalous Early Triassic sediment fluxes due to elevated weathering rates and their biological consequences. *Geology* 38, 1023-1026.

Algeo, T.J., Hinnov, L., Moser, J., Maynard, J.B., Elswick, E., Kuwahara, K. and Sano, H. 2010. Changes in productivity and redox conditions in the Panthalassic Ocean during the latest Permian. *Geology* 38, 187-190.

Algeo, T.J., Chen, Z-Q., Fraiser, M.L. and Twitchett, R.J. 2011. Terrestrial-marine teleconnections in the collapse and rebuilding of Early Triassic marine ecosystems. *Palaeogeography, Palaeoclimatology, Palaeoecology* 308, 1-11.

Algeo, T.J., Henderson, C.M., Ellwood, B., Rowe, H., Elswick, E., Bates, S., Lyons, T., Hower, J.C., Smith, C., Maynard, B., Hays, L.E., Summons, R.E., Fulton, J. and Freeman, H. 2012. Evidence for a diachronous late Permian marine crisis from the Canadian Arctic region. *Geological Society of America Bulletin* 124, 1424-1448.

Aljinović, D. 1995. Storm influenced shelf sedimentation – An example from the Lower Triassic (Scythian) siliciclastic and carbonate succession near Knin (southern Croatia and western Bosnia and Herzegovina). *Geologia Croatica* 48, 17-32.

Allison, P.A. and Briggs, D.E.G. 1993. Paleolatitudinal sampling bias, Phanerozoic species diversity, and the end-Permian extinction. *Geology* 21, 65-68.

Alroy, J., Aberhan, M., Bottjer, D.J., Foote, M., Fürsich, F.T., Harries, P.J., Hendy A.J., Holland S.M., Ivany L.C., Kiessling W., Kosnik M.A., Marshall C.R., McGowan A.J., Miller A.I., Olszewski T.D., Patzkowsky M.E., Peters S.E., Villier L., Wagner P.J., Bonuso N., Borkow P.S., Brenneis B., Clapham M.E., Fall L.M., Ferguson C.A., Hanson V.L., Krug A.Z., Layou K.M., Leckey E.H., Nürnberg S., Powers C.M., Sessa J.A., Simpson C., Tomašových, A and Visaggi, C. C. 2008. Phanerozoic trends in the global diversity of marine invertebrates. *Science* 321, 97-100.

Altenburger, A. and Wanninger, A. 2009. Comparative larval myogenesis and adult myoanatomy of the rhynchonelliform (articulate) brachiopods *Argyrotheca cordata*, *A. cistellula,* and *Terebratalia transversa*. *Frontiers in Zoology* 6, 1-14.

Amano, K., Jenkins, R.G. and Hikida, Y. 2007. A new gigantic *Nucinella* (Bivalvia: Solemyoida) from the Cretaceou cold-seep deposit in Hokkaido, northern Japan.*Veliger* 49, 8-90.

Anderson, M.J. 2001. A new method for non-parametric multivariate analysis of varience. *Austral Ecology* 26, 32-46.

Anderson, M.J., Gorley, R.N. and Clarke, K.R. 2008. *PEMANOVA+ for PRIMER: Guide to software and statistical methods.* PRIMER-E, Plymouth.

Asserto, R.L., Bosellini, A., Sestini, N.F. and Sweet, W.C. 1973. The Permian-Triassic boundary in the Southern Alps (Italy). In: 2. *Canadian Society of Petroleum Geologists Memoir*, Calgary, Canada. 176-199.

Assereto, R.L. and Rizzini, A. 1975. Reworked ferron dolomite grains in the Triassic "Oolite a Gasteropodi" of Camoniche Alps (Italy) as indicators of early diagenesis. *Neues Jahrbuch für Geologie und Paläontologie* 148, 215-232.

Ausich, W.I. and Bottjer, D.J. 2001. Sessile Invertebrates. In: D.E.G. Briggs and Crowther, P.R. (eds). *Palaeobiology II*. Blackwell Science Ltd, Oxford. 384-385.

Bambach, R.K., Bush, A.M and Erwin, D.H. 2007. Autecology and the filling of ecospace: key metazoan radiations. *Palaeontology* 50, 1-22.

Bandel, K. 2006. Families of the Cerithioidea and related superfamilies (Palaeo-Caenogastropoda; Mollusca) from the Triassic to the recent characterized by protoconch morphology-including the description of new taxa. *Freiberger Forschungshefte C* 511, 59-138.

Bandel, K. Nützel, A. and Yancey, T.E. 2002. Larval shells and shell microstructures of exceptionally well=preserved late Carboniferous gastropods from the Buckhorn Asphalt deposit (Oklahoma, USA). *Senckenbergiana lethaea* 82, 639-689.

Batten, R.L. and Stokes, W.L. 1986. Early triassic gastropods from the Sinbad member of the Moenkopi Formation, San Rafael Swell, Utah. *American Museums Novitates* 2864, 1-33.

Baud, A., Nakrem, H.A., Beauchamp, B., Beatty, T.W., Embry, A.F and Henderson, C.M. 2008. Lower Triassic bryozoan beds from Ellesmere Island, High Arctic, Canada. *Polar Research* 27, 428-440.

Baumiller, T.K. 2001. Experimental and biostratinomic disarticulation of crinoids; taphonomic implications. In: Féral, J-P and David, B (eds*). Echinoderm Research*. Swets and Zeitlinger Lisse, Netherlands. 243-248.

Baumiller, T.K., Salamon, M.A., Gorzelak, P., Mooi, R., Messing, C.G and Gahn, F.J. 2010. Post-Paleozoic crinoid radiation in response to benthic predation preceded the Mesozoic marine revolution. *Proceedings of the Natural Academy of Sciences* 107, 5893-5896.

Beatty, T.W., Zonneveld, J-P and Henderson, C.M. 2008. Anomalously diverse Early Triassic ichnofossil assemblages in northwest Pangea: A case for a shallow-marine habitable zone. *Geology* 36, 771-774.

Beauchamp, B. and Baud, A. 2002. Growth and demise of Permian biogenic chert along northwest Pangea: evidence for end-Permian collapse of thermohaline circulation. *Palaeogeography, Palaeoclimatolgy, Palaeoecology* 184, 37-63.

Becker, L., Poreda, R.J., Hunt, A.G., Bunch, T.E. and Rampino, M. 2001. Impact event at the Permian-Triassic boundary: Evidence from extraterrestrial noble gases in fullerenes. *Science* 291, 1530-1533.

Becker, L., Poreda, R.J., Basu, A.R., Pope, K.O., Harrison, T.M., Nicholson, C. and Iasky, R. 2004. Bedout: A possible end-Permian impact crater offshore of Northwestern Australia. *Science* 304, 1469-1476.

Beerling, D.J., Harfoot, M., Lomax, B. and Pyle, J.A. 2007. The stability of the stratospheric ozone layer during the end-Permian eruption of the Siberian Traps. *Philosophical Transactions of the Royal Society A* 365, 1843-1866.

Benton, M.J. and Twitchett, R.J. 2003. How to kill (almost) all life: the end-Permian extinction event. *TRENDS in Ecology and Evolution* 18, 358-365.

Berner, R.A. 2005. The carbon and sulfur cycles and atmospheric oxygen from middle Permian to middle Triassic. *Geochemica et Cosmochimica Acta* 69, 3211-3217.

Berra, F. and Carminati, E. 2010. Subsidence history from a backstripping analysis of the Permo-Mesozoic succession of the Central Southern Alps (Northern Italy). *Basin Research* 22, 952-975.

Bhattachraya, H.N. and Bhattachraya, B. 2011. Sole marks in storm beds from a glacially influenced Late Palaeozoic shallow sea, Talchir Formation, Talchir Basin, India. *Indian Journal of Geosciences* 65, 175-188.

Bieler, R., Mikkelsen, P.M., Collins, T.M., Glover, E.A., Gonzalez, V.L., Graf, D.L., Harper, E.M., Healy, J., Kawauchi, G.Y., Sharma, P.P., Staubach, S., Strong, E.E., Taylor, J.D., Temkin, I., Zardus, J.D., Clark, ., Guzman, A., McIntyre, E., Sharp, P. and Giribet, G. 2014. Investigating the bivalve tree of life – an exampler-based approach combing molecular and novel morphological characters. *Invertebrate Systematics* 28, 32-115.

Black, B.A., Lamarque, J-F., Shields, C.A. Elkins-Tanton, L.T. and Kiehl, J.T. 2014. Acid rain and ozone depletion from pulsed Siberian Traps magmatism. *Geology* 42, 67-70.

Blakey, R. 2011. Global Paleogeography. http://www2.nau.edu/rcb7/globaltext2.html (2011).

Blomeier, D., Dustira, A.M., Forke, H. and Scheibner, C. 2014. Facies analysis and depositional environments of a storm-dominated, temperate to cold, mixed siliceous-

carbonate ramp: the Permian Kapp Starostin Formation in NE Svalbard. *Norwegian Journal of Geology* 93, 75-94.

Bond, D.P.G. and Wignall, P.B. 2010. Pyrite framboid study of marine Permian-Triassic boundary sections: A complex anoxic event and its relationship to contemporaneous mass extinction. *Geological Society of America Bulletin* 122, 1265-1279.

Bond, D.P.G., Wignall, P.B., Joachimski, M.M., Sun, Y., Savov, I., Grasby, S.E., Beauchamp, B. and Blomeier, D.P.G. 2015. An abrupt extinction in the Middle Permian (Capitanian) of the Boreal Realm (Spitsbergen) and its link to anoxia and acidification. *Geological Society of America Bulletin* doi: 10.1130/B31216.1.

Bonsdorff, E., Blomqvist, E.M., Mattila, J. and Norkko, A. 1997. Coastal eutrophication: causes, consequences and perspectives in the Archipelago areas of the northern Baltic Sea. *Estuarine, Coastal and Shelf Science* 44, 63-72.

Bosellini, A. and Hardie, L.A. 1973. Depositional theme of a marginal marine evaporate. *Sedimentology* 20, 5-27.

Brack, P., Rieber, H., Nicora, A. and Mundil, R. 2005. The Global boundary Stratotype Section and Point (GSSP) of the Ladinian Stage (Middle Triassic) at Bagolino (Southern Alps, northern Italy) and its implications for the Triassic time scale. *28*, 233-244.

Brayard, A., Bucher, H., Escarguel, G., Fluteau, F., Bourquin, S and Galfetti, T. 2006. The Early Triassic ammonoid recovery: Paleoclimatic significance of diversity gradients. *Palaeogeography, Palaeoclimatology, Palaeoecology* 239, 374-395.

Brayard, A., Nützel, A., Stephen, D.A., Bylund, K.G., Jenks, J. and Bucher, H. 2010. Gastropod evidence against the Early Triassic Lilliput effect. *Geology* 38, 147-150.

Brayard, A., Vennin, E., Olivier, N., Bylund, K.G., Jenks, J., Stephen, D.A., Bucher, H., Hofmann, R., Goudemand, N. and Escarguel, G. 2011.Transient metazoan reefs in the aftermath of the end-Permian mass extinction. *Nature Geoscience* 4, 693-697.

Broglio Loriga, C. and Mirabella, S. 1986. Il genre *Eumorphotis* Bittner, 1901 nella biostratigrafia dello Scitico, Formazione di Werfen (Dolomiti). *Memorie di Scienze Geologiche* 38, 245-281.

Broglio Loriga, C., Masetti, D. and Neri, C. 1983. La formazione di Werfen (Scitico) delle Dolomiti occidental: sedimentologia e biostratigrafia. *Rivista Italiana di Paleontologia e Stratigrafia* 88, 45-50.

Broglio Loriga, C., Neri, C., Posenato, R. 1986a. The Lower Triassic of the Dolomites and Cadore. In: Permian and Permian-Triassic boundary in the South-Alpine segment of western Tethys. IGCP 203, Brescia, Excursion Guidebook, 29-34.

Broglio Loriga, C., Neri, C., Posenato, R. 1986b. The Werfen Formation (Lower Triassic) in the Costabella Mt., Uomo section. In: Permian and Permian-Triassic

Boundary in the South-Alpine Segment of western Tethys. IGCP 203, Brescia, Excursion Guidebook, 116-133.

Broglio Loriga, C., Góczán, F., Haas, J., Lenner, K., Neri, C., Oravecz-Scheffer, A., Posenato, R., Szabo, I., and Tóth-Makk, A. 1990. The Lower Triassic sequence of the Dolomites (Italy) and Transdanubian mid-mountains (Hungary) and their correlation. *Memorie di Scienze Geologiche*, *Padova*, 42, 41-103

Buchan, S.H., Challinor, A., Harland, W.B. and Parker, J.R. 1965. *The Triassic stratigraphy of Svalbard*. Norsk Polarinstitutt Skrifter Nr. 135, Oslo.

Burgess, S.D., Bowring, S. and Shen, S-Z. 2014. High-precision timeline for Earth's most severe extinction. *PNAS* 111, 3316-3321.

Bush, A.M., Bambach, R.K and Daley, G.M. 2007. Changes in theoretical ecospace utilization in marine fossil assemblage between the mid-Paleozoic and late Cenozoic. *Paleobiology* 33, 76-97.

Bush, A.M. and Bambach, R.K. 2011. Paleoecologic megatrends in marine Metazoa. *Annual Review of Earth and Planetary Sciences* 39, 241-269.

Bush, A.M. and Novack-Gottshall, P.M. 2011. Modelling the ecological-functional diversification of marine Metazoa on geological time scales. *Biology Letters* 8, 151-155.

Butler, R.J. 2002. *The taxonomy and taphonomy of conodont elements from the Servino Formation (Lower Triassic) of eastern Lombardy*. Master Thesis, University of Bristol.

Cai, W-J., Hu, W., Huang, W-J., Murrell, M.C., Lehrter, J.C., Lohrenz, S.E., Chou, W-C., Zhai, W., Hollibaugh, J.T., Wang, Y., Zhao, P., Guo, X., Gundersen, K., Dai, M. and Gong, G-C. 2011. Acidification of subsurface coastal waters enhanced by eutrophication. *Nature Geoscience* 4, 766-770.

Cao, C., Love, G.D., Hays, L.E., Wang, W., Shen, S. and Summons, R.E. 2009. Biogeochemical evidence for euxinic oceans and ecological disturbance presaging the end-Permian mass extinction event. *Earth and Planetary Science Letters* 281, 188-201.

Carmichael, R.H., Shriver, A.C., Valiela, I. 2012. Bivalve response to estuarine eutrophication: The balance between enhanced food supply and habitat alterations. *Journal of Shellfish Research* 31, 1-11.

Cassinis, G. 1968. Studio stratigrafico del "Servino" di Passo Valdì (Trias inferiore dell'Alta Val Caffaro). *Atti dell'Istituto di Geologia dell'Università Pavia* 19, 15-39.

Cassinis, G. 1990. Itinerario n° 3 – Val Trompia. In: M.B. Bianca, R. Gelati, A. Gregnanin (eds): *Alpi e Prealpi Lombarde, Guide Geologiche Regionali*, BE-MA Editrice, Milano. 291.

Cassinis, G. and Perotti, C.R. 2007. A stratigraphic and tectonic review of the Italian southern alpine Permian. *Palaeoworld* 16, 140-172.

Cassinis, G., Durand, M. and Ronchi, A. 2007. Remarks on the Permian-Triassic transition in central and eastern Lombardy (Southern Alps, Italy). *Journal of Iberian Geology* 33, 143-162.

Chen, Z-Q. and Benton, M.J. 2012. The timing and pattern of biotic recovery following the end-Permian mass extinction. *Nature Geoscience* 5, 375-383.

Chen, Z-Q., Shi, G.R. and Kaiho, K. 2004. New ophiuroids from the Permian/Triassic boundary beds of south China. *Palaeontology* 47, 1301-1312.

Chen, Z-Q., Kaiho, K., George, A.D. and Tong, J. 2006b. Survival brachiopod faunas of the end-Permian mass extinction from the southern Alps (Italy) and South China. *Geological Magazine* 143, 301–327.

Chen, Z-Q., Tong, J., Kaiho, K and Kawahata, H. 2007. Onset of biotic and environmental recovery from the end-Permian mass extinction within 1-2 Million Years: a case study of the Lower Triassic of the Meishan section, South China. *Palaeogeography, Palaeoclimatology, Palaeoecology* 252, 176-187.

Chen, Z.Q., Tong, J., Zhang, K., Yang, H,. Liao, Z., Song, H. and Chen, J. 2009. Environmental and biotic turnover across the Permian-Triassic boundary on a shallow carbonate platform in western Zhejiang, South China. *Australian Journal of Earth Sciences: An International Geoscience Journal of the Geological Society of Australia* 56, 775-797.

Chen, Z-Q., Tong, J., Liao, Z-T. and Chen, J. 2010b. Structural changes of marine communities over the Permian-Triassic transition: Ecologically assessing the end-Permian mass extinction and its aftermath. *Global and Planetary Change* 73, 123-140.

Chen, J., Chen, Z-Q. and Tong, J. 2011a. Environmental determinants and ecologic selectivity of benthic faunas from nearshore to bathyal zones in the end-Permian mass extinction: Brachiopod evidence from South China. *Palaeogeography, Palaeoclimatology, Palaeoecology* 308, 84-97.

Chen, Z-Q., Tong, J. and Fraiser, M.L. 2011b. Trace fossil evidence for restoration of marine ecosystems following the end-Permian mass extinction in the Lower Yangtze region, South China. *Palaeogeography, Palaeoclimatology, Palaeoecology* 299, 449-474.

Chen, Z-Q., Fraiser, M.L. and Bolton, C. 2012. Early Triassic trace fossils from Gondwana Interior Sea: Implication for ecosystem recovery following the end-Permian mass extinction in south high-latitude region. *Gondwana Research* 22, 238-255.

Chen, Y., Twitchett, R.J., Jiang, H., Richoz, S., Lai, X., Sun, Y., Liu, X. and Wang, L. 2013. Size variation of conodonts during the Smithian-Spathian (Early Triassic) global warming event. *Geology* 41, 823-826.

Chwieduk, E. 2007. Middle Permian rugose corals from the Kapp Starostin Formation, south Spitsbergen (Treskelen peninsula). *Acta Geologica Polonica* 57, 281-304.

Ciriacks, K.W. 1963. Permian and Eotriassic bivalves of the Middle Rockies. *Bulletin of the American Museum of Natural History* 125, 1-98.

Clapham, M.E., Shen, S. and Bottjer, D.J. 2009. The double mass extinction revisited: reassessing the severity, selectivity, and causes of the end-Guadalupian biotic crisis (Late Permian). *Paleobiology* 35, 32-50.

Clapham, M.E., Fraiser, M.L., Marenco, P.J. and Shen, S-Z. 2013. Taxonomic composition and environmental distribution of post-extinction rhynchonelliform brachiopod faunas: Constraints on short-term survival and the role of anoxia in the end-Permian mass extinction. *Palaeogeography, Palaeoclimatology, Palaeoecology* 374, 284-292.

Clarke, K.R. 1993. Non-parametric multivariate analyses of changes in community structure. *Australian Journal of Ecology* 18, 117-143.

Clarke, K.R. and Gorley, R.N. 2006. *PRIMER v6: User Manual/Tutorial*. PIMER-E Ltd.

Clarke, K.R. and Warwick, R.M. 2001. *Change in marine communities*: *An approach to statistical analysis and interpretation (2nd Edition)*. PRIMER-E: Plymouth.

Clarkson, M.O., Kasemann, S.A., Wood, R.A., Lenton, T.M., Daines, S.J., Richoz, S., Ohnemueller, F., Meixner, A., Poulton, S.W. and Tipper, E.T. 2015. Ocean acidification and the Permo-Triassic mass extinction. *Science* 348, 229-232.

Clausen, C.K. and Wignall, P.B. 1990. Early Kimmeridgian bivalves of southern England. *Mesozoic Research* 2, 97-149.

Coan, E.V. and Valentich-Scott, .P. 2012. Bivalve seashells of tropical West America. Marine bivalve mollusks from Baja California to northern Peru. *Santa Barbara Museum of Natural History Monographs* 6.

Corsetti, F.A., Baud, A., Marenco, P.J. and Richoz, S. 2005. Summary of Early Triassic carbon isotope records. *Comptes Rendus Palevol* 4, 473-486.

Cossins, A.R. and Bowler, K. 1987. Rate compensations and capacity adaptations. In: *Temperature biology of animals* Springer, Netherlands. 155-203.

Crasquin, S., Perri, M.C., Nicora, A. and De Wever, P. 2008. Ostracods across the Permian-Triassic boundary in western Tethys: the Bulla parastratotype (Southern Alps, Italy). *Rivista Italiana di Paleontologia e Stratigrafia* 114, 233-262.

Csontos, L., Vörös, A. 2004. Mesozoic plate tectonic reconstruction of the Carpathian region. *Palaeogeography, Palaeoclimatology, Palaeoecology* 210, 1-56.

Cubasch, U., Hasselmann, K., Hock, H., Maier-Reimer, E., Mikolajewicz, U., Santer, B.D. and Sausen, R. 1992. Time-dependent greenhouse warming computations with a coupled ocean-atmosphere model. *Climate Dynamics* 8, 55-69.

Dagys, A.S. and Korčinskaja, M. 1987. The first discoveries of conodonts in the Otoceras beds of Svalbard. *Trudy Instituta Geolog I Geofiziki* 689, 110-113.

Dagys, A.S. and Weitschat, W. 1993. Correlation of the Boreal Triassic. *Mitteilungen Geologisch-Paläontologisches Institut Universität Hamburg* 75, 249–256.

Danise, S., Twitchett, R.J., Little, C.T.S., Clemence, M-E. 2013. The impact of global warming and anoxia on marine benthic community dynamics: an example from the Toarcian (Early Jurassic). *Plos one* 8, 1-14.

De Zanche, V. and Farabegoli, E. 1982. Scythian-Anisian lithostratigraphic units in the southern Alps. *Geol. Paläont. Mitt. Innsbruck* 11, 299-308.

De Zanche, V., Gianolla, P., Mietto, P., Siorpaes, C and Vail, P.R. 1993. Triassic sequence stratigraphy in the Dolomites (Italy). *Memorie di Scienze Geologiche, Padova* 45, 1-27.

Declerck, C.H. 1995. The evolution of suspension feeding in gastropods. *Biological Reviews* 70, 549-569.

Di Geronimo, I. and La Perna, R. 1997. Pleistocene bathyal molluscan assemblages from southern Italy. *Rivista Italiana di Paleontologia e Stratigrafia* 103, 1-10.

Diaz, R.J. and Rosenberg, R. 2008. Spreading Dead Zones and consequences for marine ecosystems. *Science* 321, 926-929.

Diaz, M.R., Van Norstrand, J.D., Eberli, G.P., Piggot, A.M., Zhou, J. and Klaus, J.S. 2014. Functional gene diversity of oolitic sands from Great Bahama Bank. *Geobiology* 12, 221-249.

Dickens, G.R. 2003. Rethinking the global carbon cycle with a large, dynamic and microbially mediated gas hydrate capacitor. *Earth and Planetary Science Letters* 213, 169-183.

Dineen, A.A., Fraiser, M.L. and Sheehan, P.M. 2014. Quantifying functional diversity in pre-and post-extinction paleocommunities: A test of ecological restructuring after the end-Permian mass extinction. *Earth-Science Reviews* 136, 339-349.

Drake, A.A. and Lyttle, P.T. 1981. *The Accotink schist, Lake Barcroft metasandstone, and Popes Head Formation – Keys to an understanding of the tectonic evolution of the northern Virginia Piedmont* (No. 1205). U.S. Geological Survey, Washington.

Droser, M.L. and Bottjer, D.J. 1993. Trends and patterns of Phanerozoic ichnofabrics. *Annual Review of Earth and Planetary Sciences* 21, 205-225.

Dustira, A.M., Wignall, P.B., Joachimski, M., Blomeier, D., Hartkopf-Fröder, C. and Bond, D. 2013. Gradual onset of anoxia across the Permian-Triassic boundary in Svalbard, Norway. *Palaeogeography, Palaeoclimatology, Palaeoecology* 374, 303-313.

Ehrenberg, S.N., Pickard, N.A.H.,henriksen, L.B., Svana, T.A., Gutteridge, P. and Macdonald, D. 2001. A depositional and sequence stratigraphic model for cold-water, spiculitic strata based on the Kapp Starostin Formation (Permian) of Spitsbergen and equivalent deposits from the Barents Sea. *AAPG Bulletin* 12, 2061-2087.

Ellis, R.J. 2010 Tackling unintelligent design. *Nature* 463, 164-165.

Elrick, M. 1995. Cyclostratigraphy of Middle Devonian carbonates of the eastern Great basin. *Journal of Sedimentary Research* 65, 61-79.

Embry, A. 1997. Global sequence boundaries of the Triassic and their identification in the Western Canada sedimentary basin. *Canadian Society of Petroleum Geologists Bulletin* 45, 415-433.

Erwin, D.H. 1993. *The great Paleozoic crisis: life and death in the Permian*. Columbia University Press.

Erwin, D.H. 1994. Early introduction of major morphological innovations. *Acta Palaeontologica Polonica* 38, 281-294.

Erwin, D.H. and Pan, H-Z. 1996. Recoveries and radiations: gastropods after the Permo-Triassic mass extinction. In: Hart, M.B. (ed).*Biotic recovery from ma extinction events*. Geological Society Special Publication No.102, 223-229.

Erwin, D.H., Valentine, J.W. and Sepkoski, J.J. 1987. A comparative study of diversification events; The early Paleozoic versus the Mesozoic. *Evolution* 41, 1177-1186.

Farabegoli, E., Perri, C. and Posenato, R. 2007. Environmental and biotic changes across the Permian-Triassic boundary in western Tethys: The Bulla parastratotype, Italy. *Global and Planetary Change* 55, 109-135.

Farabegoli, E. and Perri, M.C. 2012. Millennial physical events and the end-Permian mass mortality in the western Palaeotethys; timing and primary causes. In: J.A. Talent (ed). *Earth and Life*. Springer.

Farley, K.A., Ward, P., Garrison, G. and Mukhopadhyay, S. 2005. Absence of extraterrestrial [3]He in Permian-Triassic age sedimentary rocks. *Earth and Planetary Science Letters* 240, 265-275.

Fenton, S., Grice, K., Twitchett, R.J., Böttcher, M.E., Looy, C.V. and Nabbefeld, B. 2007. Changes in biomarker abundances and sulfur isotopes of pyrite across the Permian-Triassic (P/Tr) Schuchert Dal section (East Greenland). *Earth and Planetary Science Letters* 262, 230-239.

Fisher, R.A., Corbet, A.S. and Williams, C.B. 1943. The relation between the number of species and the number of individuals in a random sample of an animal population. *Journal of Animal Ecology* 12, 42-58.

Fleming, C.A. 1948. New species and genera of marine Mollusca from the Southland fiords. *Transactions of the Royal Society of new Zealand* 77, 72-92.

Flemming, B.W. 2012. Siliciclastic back-barrier tidal-flat. In: Davis, R.A. Dalrymple, R.W (eds). *Principles of Tidal Sedimentology*. Springer, Dordrecht. 231-267.

Flügel, E. 2002. Patterns of Phanerozoic reef crises. In: Kiessling, W., Flügel, E. and Golonka, J (eds) *Phanerozoic Reef Patterns*. SEPM Special Publications, 391-463.

Forbes, C.L., Harland, W.B. and Hughes, N.F. 1958. Palaeontological evidence for the age of the Carboniferous and Permian rocks of central Vestspitsbergen. *Geological magazine* 95, 463-490.

Forel, M-B., Crasquin, S., Kershaw, S. and Collin, P-Y. 2013b. In the aftermath of the end-Permian extinction: the microbialite refuge? *Terra Nova* 25, 137-143.

Foster, W.J. and Twitchett, R.J. 2014. Functional diversity of marine ecosystems after the late Permian mass extinction event. *Nature Geoscience* 7, 233-238.

Fraiser, M.L. 2011. Paleoecology of secondary tierers from Western Pangean tropical marine environments during the aftermath of the end-Permian mass extinction. *Palaeogeography, Palaeoclimatology, Palaeoecology* 308, 181-189.

Fraiser, M.L. and Bottjer, D.J. 2004. The non-actualistic Early Triassic gastropod fauna: A case study of the Lower Triassic Sinbad Limestone member. *Palaios* 19, 259-275.

Fraiser, M.L. and Bottjer, D.J. 2005. Restructuring in benthic level-bottom shallow marine communities due to prolonged environmental stress following the end-Permian mass extinction. *Comptes Rendus Palevol* 4, 583-591.

Fraiser, M.L. and Bottjer, D.J. 2007a. When bivalves took over the world. *Paleobiology* 33, 397-413.

Fraiser, M.L. and Bottjer, D.J. 2007b. Elevated atmospheric CO_2 and the delayed biotic recovery from the end-Permian mass extinction. *Palaeogeography, Palaeoclimatology, Palaeoecology* 252, 164–175.

Fraiser, M.L. and Bottjer, D.J. 2009. Opportunistic behaviour of invertebrate marine tracemakers during the Early Triassic aftermath of the end-Permian mass extinction. *Australian Journal of Earth Sciences* 56, 841-857.

Fraiser, M.L. and Twitchett, R.J. and Bottjer, D.J. 2005. Unique microgastropod biofacies in the Early Triassic: Indicator of long-term biotic stress and the pattern of biotic recovery after the end-Permian mass extinction. *Comptes Rendus Palevol* 4, 543-552.

Fraiser, M.L., Twitchett, R.J., Frederickson, J.A., Metcalfe, B. and Bottjer, D.J. 2011. Gastropod evidence against the Early Triassic Lilliput effect: comment. *Geology* 39, 232.

Frýda, J. 2001. Discovery of a larval shell in Middle Paleozoic subulitoidean gastropods with description of two new species from the Early Devonian of Bohemia. *Bulletin of the Czech Geological Survey* 76, 29-37.

Gaetani, M. 1982. Elementi statigrafici e strutturali della galleria Bellano-Varenna (Nuova S.S. 36) (Como). *Rivista Italiana di Paleontologia e Stratigrafia* 88, 1-10.

Gaetani, M. and Gorza, M. 1989. The Anisian (middle Triassic) carbonate bnk of Camorelli (Lombardy, southern Alps). *Facies* 21, 41-56.

Galfetti, T., Bucher, H., Brayard, A., Hochuli, P.A., Weissert, H., Guodun, K., Atudorei, V. and Guex, J. 2007a. Late Early Triassic climate change: insights from carbonate carbon isotopes, sedimentary evolution and ammonoid paleobiogeography. *Palaeogeography, Palaeoclimatology, Palaeoecology* 243, 394-411.

Galfetti, T., Bucher, H., Ovtcharova, M., Schaltegger, U., Brayard, A., Brühwiler, T., Goudemand, N., Weissert, H., Hochuli, P.A., Cordey, F. and Guodun, K. 2007b. Timing of the Early Triassic carbon cycle perturbations inferred from new U-Pb ages and ammonoid biochronozones. *Earth and Planetary Science Letters* 258, 593-604.

Galfetti, T., Hochuli, P.A., Brayard, A., Bucher, H., Weissert, H. and Vigran, J.O. 2007c. Smithian-Spathian boundary event: evidence for global climatic change in the wake of the end-Permian biotic crisis. *Geology* 35, 291-294.

Galfetti, T., Bucher, H., Martini, R., Hochuli, P.A., Weissert, H., Crasquin-Soleau, S., Brayard, A., Goudemand, N., Brühwiler, T. and Guodun, K. 2008. Evolution of Early Triassic outer platform Palaeoenvironments in the Nanpanjiang Basin (South China) and their significance for the biotic recovery. *Sedimentary Geology* 204, 36-60.

Gallet, Y., Krystyn, L., Besse, J., Saidi, A. and Ricou, L.E. 2000. New constraints on the Upper Permian and Lower Triassic geomagnetic polarity timescale from the Abadeh section (central Iran). *Journal of Geophysical Research: Solid Earth* 105, 2805-2815.

Geyer, G., Hautmann, M., Hagdorn, H., Ockert, W., Streng, M. 2005. Well-preserved mollusks from the Lower Keuper (Ladinian) of Hohenlohe (Southwest Germany). *Paläontogische Zeitschrift* 79,429-460.

Ginsburg, R.N. and Planavsky, N.J. 2008. Diversity of Bahamian microbialite substrates. In: Dilek, Y., Furnes, H. and Muehlenbachs, K (eds). *Links between geological processes, Microbial Activities and Evolution of Life*. Springer, Netherlands.

Glazek, J. and Radwansk, A. 1968. Determination of brittle star vertebrae in thin sections. *Bulletin de l Academie polonaise des sciences-serie des sciences geologicques et geographiques* 16, 91.

Graf, G., Schulz, R., Peinert, R. and Meyer-Reil, L.A. 1983.Benthic response to sedimentation events during autumn to spring at a shallow-water station in the Western Kiel Bight. *Marine Biology* 77, 235-246.

Gobbett, D.J. 1963. Carboniferous and Permian brachiopods of Svalbard. *Norsk Polarinstitutt Skrifter Nr.127*, Oslo.

Goldson, A.J., Hughes, R.N. and Gliddon, C.J. 2001. Population genetic consequences of larval dispersal made and hydrography: a case study with bryozoans. *Marine Biology* 138, 1037-1042.

Grall, J. and Chauvaud, L. 2002. Marine eutrophication and benthos: the need for new approaches and concepts. *Global Change Biology* 8, 813-830.

Grard, A., François, L.M., Dessert, C., Dupŕe, B. and Goddéris, Y. 2005. Basaltic volcanism and mass extinction at the Permo-Triassic boundary: environmental impact and modelling of the global carbon cycle. *Earth and Planetary Science Letters* 234, 207-221.

Grasby, S.E. and Beauchamp, B. 2009. Latest Permian to Early Triassic basin-to-shelf anoxia in the Sverdrup Basin, Arctic Canada. *Chemical Geology* 264, 232-246.

Grasby, S.E., Beauchamp, B., Embry, A. and Sanei, H. 2013. Recurrent Early Triassic ocean anoxia. *Geology* 41, 175-178.

Green, R.H. 1966. Measurement of non-randomness in spatial distributions. *Res. Population Ecol.* 8, 1-7.

Grice, K., Cao, C., Love, G.D., Böttcher, M.E., Twitchett, R.J., Grosjean, E., Summons, R.E., Turgeon, S.C., Dunning, W. and Jin, Y. 2005. Photic zone euxinia during the Permian-Triassic superanoxic event. *Science* 307, 706-709.

Groves, J.R., Rettori, R., Payne, J.L., Boyce, M.D. and Altiner, D. 2007. End-Permian mass extinction of Lagenide foraminifers in the Southern Alps (Northern Italy). *Journal of Paleontology* 81, 415-434.

Gründel, J. 1997. Heterostropha (Gastropoda) aus dem Dogger Norddeutschlands und Nordpolens. III. Opisthobranchia. *Berliner geowissenschatliche Abhandlungen* 25, 177-223.

Gründel, J. and Nützel, A. 2012. On the early evolution (Late Triassic to Late Jurassic) of the Architectibranchia (Gastropoda: Hetereobranchia), with a provisional classification. *Neues Jahrbuch für Geologie und palaontologie-Abhandlungen* 264, 31-59.

Haas, J. and Budai, T. 1999. Triassic sequence stratigraphy of the Transdanubian range (Hungary). *Geologica Carpathica* 50, 459-475.

Haas, J., Budai, T. and Raucsik, B 2012. Climatic controls n sedimentary environments in the Triassic of the Transdanubian Range (Western Hungary). *Palaeogeography, Palaeoclimatology, Palaeoecology* 353-355, 31-44.

Hagdorn, H. and Bottjer, D.J. 1997. Wrinkle structures: Microbially mediated sedimentary structures common in subtidal siliciclastic settings at the Proterozoic-Phanerozoic transition. *Geology* 25, 1047-1050.

Hagdorn, H. and Velledits, F. 2006. Middle Triassic crinoid remains from the Aggtelek platform (NE Hungary). *Neues Jahrbuch für Geologie und palaontologie-Abhandlungen* 240, 373-404.

Hallam, A. 1991. Why was there a delayed radiation after the end-Palaeozoic extinctions? *Historical Biology* 5, 257-262.

Hallam, A. 1995. Oxygen-restricted facies of the basal Jurassic of North West Europe. *Historical Biology* 10, 247-257.

Hallam, A. and Wignall, P.B. 1997. *Mass extinctions and their aftermath*. Oxford University Press, Oxford.

Hammer, O., Harper, D.A.T. and Ryan, P.D. 2001. PAST: Paleontological Statistics software package for education and data analysis. *Palaeontologica Electronica* 4, 1-9.

Hammond, L. and Poiner, I.R. 1984. Genetic structure of three populations of the 'living fossil' brachiopod *Lingula* from Queensland, Australia. *Lethaia* 17, 139-143.

Hanehan, M.J., Rae, J.W., Foster, G.L., Erez, J., Prentice, K.C., Kucera, M., Bostock, H.C. and Elliot, T. 2013. Calibration of the boron isotope proxy in the planktonic foraminifera *Globigerinoides ruber* for use in palaeo-CO_2 reconstruction. *Earth and Planetary Science Letters* 364, 11-122.

Harfoot, M.B., Pyle, J.A. and Beerling, D.J. 2008. End-Permian ozone shield unaffected by oceanic hydrogen sulphide and methane releases. *Nature Letters* 1, 247-252.

Harland, W.B. 1997. The Geology of Svalbard. Geological Society memoir No.17, The Geological Society, London.

Harries, P.J., Kauffman, E.G. and Hansen, T.A. 1996. Models for biotic suvival following mass extinction. In: Hart, M.B. (ed).*Biotic recovery from ma extinction events*. Geological Society Special Publication No.102, 41-60.

Hausmann, I.M. and Nützel,A. 2015. Diveristy and palaeoecology of a highly diverse Late Triassic marine biota from the Cassian Formation of north Italy. *Lethaia* 48, 235-255.

Hautmann, M. and Nützel, A. 2005. First record of a Heterodont bivalve (Mollusca) from the Early Triassic: palaeoecological significance and implications for the 'Lazarus Problem'. *Palaeontology* 48, 1131-1138.

Hautmann, M., Bucher, H., Brühwiler, T., Goudemand, N., Kaim, A. and Nützel, A. 2011. An unusually diverse mollusc fauna from the earliest Triassic of South China and its implications for benthic recovery after the end-Permian biotic crisis. *Geobios* 44, 71-85.

Hautmann, M., Smith, A.B., McGowan, A.J. and Bucher, H. 2013. Bivalves from the Olenekian (Early Triassic) of south-western Utah: systematics and evolutionary significance. *Journal of Systematic Palaeontology* 11, 263-293.

Hays, L.E., Beatty, T., Henderson, C.M., Love, G.D. and Summons, R.E. 2007. Evidence for photic zone euxinia through the end-Permian mass extinction in the Panthalassic Ocean (Peace River Basin, Western Canada). *Palaeoworld* 16, 39-50.

Hays, L.E., Grice, K., Foster, C.B. and Summons, R.E. 2012. Biomarker and isotopic trends in a Permian-Triassic sedimentary section at Kap Stosch, Greenland. *Organic Geochemistry* 43, 67-82.

He, W., Feng, Q., Weldon, E.A., Gu, S., Meng, Y., Zhang, F. and Wu, S. 2007. A late Permian to Early Triassic bivalve fauna from the Dongpan section, southern Guangxi, south China. *Journal of Paleontology* 81, 1009-1019.

He, W., Shi, G.R., Feng, Q., Campi, M.J., Gu, S., Bu, J., Peng, Y. and Meng, Y. 2007. Brachiopod miniaturization and its possible causes during the Permian-Triassic crisis in deep water environments, South China. *Palaeogeography, Palaeoclimatology, Palaeoecology* 252, 145-163.

He, W., Shi, G.R., Twitchett, R.J., Zhang, Y., Zhang, K-X., Song, H-J., Yue, M-L., Wu, S-B., Yang, T-L. and Xiao, Y-F. 2015. Late Permian marine ecosystem collapse began in deeper waters: evidence from brachiopod diversity and body size changes. *Geobiology* 13, 123-138.

Hermann, E., Hochuli, P.A., Méhay, S., Bucher, H., Brühwiler, T., Ware, D., Hautmann, M., Roohi, G., ur-Rehman, K. and Yaseen, A. 2011. Organic matter and palaeoenvironmental signals during the Early Triassic biotic recovery: The Salt Range and Surghar Range records. *Sedimentary Geology* 234, 19-41.

Hips, K. 1990. Az aggteleki-hegységi és a balaton-felvidéki also-triász kifejlődések lito- és biosztratigráfiai összehasonlitása – Szakdolgozat, MTA Geol. Kut. Csop., kézirat.

Hips, K. 1996a. The biostratigraphic significance of the *Cyclogyra-Rectocornuspira* Association (Foraminifera; Early Triassic): Data from the Aggtelek Mountains (Northeastern Hungary). *Neues Jahrbuch für Geologie und Paläontologie, Monatshefte* 7, 439-451.

Hips, K. 1996b. Stratigraphic and facies evaluation of the Lower Triassic formations in the Aggtelek-Rudabánya Mountains, NE Hungary. *Acta Geologica Hungarica* 39, 369-411.

Hips, K. 1998. Lower Triassic storm-dominated ramp sequence in northern Hungary: an example of evolution from homoclinal through distally steepened ramp to Middle Triassic flat-topped platform. In: Wright V.P. and Burchette T.P. (eds). *Carbonate Ramps*. Geological Society, London, Special Publications, 149, 315-338.

Hips, K. 2001. The Structural setting of Lower Triassic Formations in the Aggtelek-Rudabánya Mountain (Northeastern Hungary) as revealed by geological mapping. *Geologica Carpathica* 52, 287-299.

Hips, K. 2003. Gutensteini formáció a Szilicei takaró Aggteleki fáciesében. *Földtani Közlöny* 133, 445-468.

Hips, K. 2007. Facies pattern of western Tethyan Middle Triassic black carbonates: The example of Gutenstein Formation in Silica Nappe, Carpathians, Hungary, and its correlation to formations of adjoining areas. *Sedimentary Geology* 194, 99-114.

Hips, K. and Pelikán, P. 2002. Lower Triassic shallow marine succession in the Bükk Mountains, NE Hungary. *Geologica Carpathica* 53, 351-367.

Hoare, R.D. and Sturgeon, M.T. 1978. The Pennsylvanian a gastropod genera *Cyclozyga* and *Helminthozyga* and the classification of the Pseudozygopleuridae. *Journal of Paleontology* 52, 850-858.

Hoegh-Guldberg, O. and Bruno, J.F. 2010. The impact of climate change on the world's marine ecosystems. *Science* 328, 1523-1528.

Hofmann, R., Goudemand, N., Wasmer, M., Bucher, H. and Hautmann, M. 2011. New trace fossil evidence for an early recovery signal in the aftermath of the end-Permian mass extinction. *Palaeogeography, Palaeoclimatology, Palaeoecology* 310, 216-226.

Hofmann, R., Hautmann, M., Wasmer, M. and Bucher, H. 2013a. Palaeoecology of the Spathian Virgin Formation (Utah, USA) and its implications for the Early Triassic recovery. *Acta Palaeontologica Polonica* 58 , 149-173.

Hofmann, R., Hautmann, M. and Bucher, H. 2013b. A new paleoecological look at the Dinwoody Formation (Lower Triassic, western USA): Intrinsic versus extrinsic controls on ecosystem recovery after the end-Permian mass extinction. *Journal of Paleontology* 87, 854-880.

Hofmann, R., Hautmann, M., Brayard, A., Nützel, A., Bylund, K.G, Jenks, J.F., Vennin, E., Olivier, N. and Bucher, H. 2014 Recovery of benthic marine communities from the end-Permian mass extinction at the low latitudes of eastern Panthalassa. *Palaeontology* 57, 547-589.

Hofmann, R, Hautmann, M. and Bucher, H. 2015a. Recovery dynamics of benthic marine communities from the Lower Triassic Werfen Formation, northern Italy. *Lethaia* DOI: 10.1111/let.12121.

Hofmann, R., Buatois, L.A., MacNaughton. and Mángano, M.G. 2015b. Loss of the sedimentary mixed layer as a result of the end-Permian extinction. *Palaeogeography, Palaeoclimatology, Palaeoecology* 428, 1-11.

Holland, S. 2010. Additive diversity partitioning in palaeobiology: revisiting Sepkoski's question. *Palaeontology* 53, 1237-1254.

Holland, S.M. and Patzkowsky, M.E. 2004. Ecosystem structure and stability: middle upper Ordovician of central Kentucky, USA. *Palaios* 19, 316-331.

Hollingworth, N. and Pettigrew, T. 1988. Zechstein reef fossils and their palaeoecology. *The Palaeontological Association Field Guides to fossils* 3, 1-72.

Hopkin, E.K. and McRoberts, C. 2005. A new Middle Triassic flat clam (Pterioida: Halobiidae) from the Middle Anisian of north-central Nevada, USA. *Journal of Paleontology* 74, 796-800.

Horacek, M., Brandner, R. and Abart, R. 2007a. Carbon isotope record of the P/T boundary and the Lower Triassic in the Southern Alps: Evidence for rapid changes in storage of organic carbon. *Palaeogeography, Palaeoclimatology, Palaeoecology* 252, 347-354.

Horacek, M., Povoden, E., Richoz, S. and Brandner, R. 2010a. High-resolution carbon isotope changes, litho- and magnetostratigraphy across Permian-Triassic Boundary sections in the Dolomites, N-Italy. New constraints for global correlation. *Palaeogeography, Palaeoclimatology, Palaeoecology* 290, 58-64.

Horacek, M., Brandner, R., Richoz, S. and Povoden-Karadeniz, E. 2010b. Lower Triassic sulphur isotope curve of marine sulphates from the Dolomites, N-Italy. *Palaeogeography, Palaeoclimatology, Palaeoecology* 290, 65-70.

Hounslow, M.W., Szurlies, M., Muttoni, G. and Nawrocki, J. 2007. The magnetostratigraphy of the Olenekian-Anisian boundary and a proposal to define the base of the Anisian using a magnetozone datum. *Albertiana* 36, 72-77.

Hounslow, M.W., Peters, C., Mørk, A., Weitschat, W and Vigran, J.O. 2008a. Biomagnetostratigraphy of the Vikinghøgda Formation, Svalbard (Arctic Norway), and the geomagnetic polarity timescale for the lower Triassic. *Geological Society of America Bulletin* 120, 1305-1325.

Hounslow, M.W., Hu, M., Mørk, A., Weitschat, W., Vigran, J.O., Karloukovski, V. and Orchard, M.J. 2008b. Intercalibration of Boreal and Tethyan timescales: the magneto-biostratigraphy of the Middle Triassic and the latest Early Triassic from Spitsbergen (Arctic Norway). *Polar Research* 27, 469-490.

Huggett, J.M. and Gale, A.S. 1997. Petrology and palaeoenvironmental significance of glauconite in the Eocene succession at Whitecliff Bay, Hampshire basin, UK. *Journal of the Geological Society* 154, 897-912.

Hughes, R.N. 1986. *A functional biology of marine gastropods*. Springer.

Isozaki, Y. 1997. Permo-Triassic boundary superanoxia and stratified superocean: Records from lost deep sea. *Science* 276, 235-238.

Jacobsen, N.D., Twitchett, R.J and Krystyn, L. 2011. Palaeoecological methods for assessing marine ecosystem recovery following the Late Permian mass extinction event. *Palaeogeography, Palaeoclimatology, Palaeoecology* 308, 200-212.

Jeppsson, L. and Anehus, R. 1995. A buffered formic acid technique for conodont extraction. *Journal of Paleontology* 69, 790-794.

Jeppsson, L., Anehus, R. and Fredholm, D. 1999. The optimal acetate buffered Acetic acid technique for extracting phosphatic fossils. *Journal of Paleontology* 73, 964-972.

Jin, Y.G., Wang, Y., Wang, W., Shang, Q.H., Cao, C.Q. and Erwin, D.H. 2000. Pattern of marine mass extinction near the Permian-Triassic boundary in South China. *Science* 289, 432-436.

Joachimski, M.M., Lai, X., Shen, S., Jiang, H., Luo, G., Chen, B., Chen, J. and Sun, Y. 2012. Climate warming in the latest Permian and the Permian-Triassic mass extinction. *Geology* 40, 195-198.

Jost, L. 2006. Entropy and diversity. *OIKOS* 113, 363-375.

Jost, L. 2007. Partitioning diversity into independent alpha and beta components. *Ecology* 80, 2427-2439.

Jouzel, J., Koster, R.D., Suozzo, R.J. and Russell, G.L. 1994. Stable water isotope behaviour during the last glacial maximum: A general circulation model analysis. *Journal of Geophysical Research* 99, 791-801.

Kaiho, K., Kajiwara, Y., Nakano, T., Miura, Y., Kawahata, H., Tazaki, K., Ueshima, M., Chen, Z-Q. and Shi, G.R. 2001. End-Permian catastrophe by a bolide impact: evidence of a gigantic release of sulfur from the mantle. *Geology* 235, 33-47.

Kaim, A. 2004. The evolution of conch ontogeny in Mesozoic open sea gastropods. *Acta Palaeontologica Polonica* 62, 3-183.

Kaim, A. and Nützel, A. 2011. Dead bellerophontids walking – The short Mesozoic history of the Bellerophontoidea (Gastropoda). *Palaeogeography, Palaeoclimatology, Palaeoecology* 308, 190-199.

Kaim, A., Nützel, A., Bucher, H., Brühwiler, T. and Goudemand, N. 2010. Early Triassic (Late Griesbachian) gastropods from south China (Shanggan, Guangxi). *Swiss Journal of Geosciences* 103, 121-128.

Kamo, S.L., Czamanske, G.K., Amelin, Y., Fedorenko, V.A., Davis, D.W. and Trofimov, V.R. 2003. Rapid eruption of Siberian flood-volcanic rocks and evidence for coincidence with the Permian-Triassic boundary and mass extinction at 251 Ma. *Earth and Planetary Science Letters* 214, 75-91.

Kapoor, H.M. 1996. The Guryul Ravine section, candidate of the Global Stratotype Section and Point of the Permo-Triassic boundary. *The Palaeozoic-Mesozoic boundary candidates of global stratotype section (GSSP) and point of the Permian-Triassic boundary*, 99-10.

Kashiyama, Y. and Oji, T. 2004. Low-diversity shallow marine benthic fauna from the Smithian of northeast Japan: Paleoecologic and paleobiogeographic implications. *Paleontological Research* 8, 199-218.

Kato, M. 1996. The unique intertidal subterranean habitat and filtering system of a limpet-like brachiopod. *Discinisca sparselineata. Canadian Journal of Zoology* 74, 1983-1988.

Kearsey, T., Twitchett, R.J., Price, G.D. and Grimes, S.T. 2009. Isotope excursions and palaeotemperature estimates from the Permian/Triassic boundary in the Southern Alps (Italy). *Palaeogeography, Palaeoclimatology, Palaeoecology* 279, 29-40.

Kershaw, S., Zhang, T. and Lan, G. 1999. A ?microbialite carbonate crust at the Permian-Triassic boundary in South China, and its palaeoenvironmental significance. *Palaeogeography, Palaeoclimatology, Palaeoecology* 146, 1-18.

Kershaw, S., Crasquin, S., Forel, M-B., Randon, C., Collin, P-Y., Kosun, E., Richoz, S. and Baud, A. 2011. Earliest Triassic microbialites in Çürük Dag, southern Turkey: composition, sequences and controls on formation. *Sedimentology* 58, 739-755.

Kiel, S., Amano, K. and Jenkins, R.G. 2008. Bivalves from Cretaceous cold-seep deposits on Hokkaido, Japan. *Acta Palaeontologica Polonica* 53, 525-537.

Kinsman, D.J. 1969. Modes of formation, sedimentary associations, and diagnostic features of shallow-water and supratidal evaporites. *AAPG Bulletin* 53, 830-840.

Knaust, D. 1998. Trace fossils and ichnofabrics on the Lower Muschelkalk carbonate ramp (Triassic) of Germany: tool for high-resolution sequence stratigraphy. *Geologische Rundschau* 87,21-31.

Knaust, D. 2007. Invertebrate trace fossils and ichnodiversity in shallow-marine carbonates of the German Middle Triassic (Muschelkalk). *SEPM Special Publication No. 88*, 221-238.

Knaust, D. 2010. The end-Permian mass extinction and its aftermath on an equatorial carbonate platform: insights from ichnology. *Terra Nova* 22, 195-202.

Knies, J., Grasby, S.E., Beauchamp, B. and Schubert, C.J. 2012. Water mass denitrification during the latest Permian extinction in the Sverdrup Basin, Arctic Canada. *Geology* 41, 167-170.

Knoll, A.H., Bambach, R.K., Payne, J.L., Pruss, S. and Fischer, W.W. 2007. Paleophysiology and end-Permian mass extinction. *Earth and Planetary Science Letters* 256, 295-313.

Kolar-Jurkovšek, T., Vuks, V.J., Aljinović, D., Hautmann, M., Kaim, A. and Jurkovšek, B. 2013. Olenekian (Early Triassic) fossil assemblage from eastern Julian Alps (Slovenia). *Annales Societatis Geologorum Poloniae* 83, 213-227.

Koloszár, L. 1992. Lombardiai (Olaszország) és Balaton-felvidéki also-triász szelvények litosztratigráfiai összehasonlitása. *Általános Földtani Szemle* 26, 311-317.

Komatsu, T., Naruse, H., Shigeta, Y., Takashima, R., Maekawa, T., Dang, H.T., Dinh, T.C., Nguyen, P.D., Nguyen, H.H., Tanaka, G. and Sone, M. 2014. Lower Triassic mixed carbonate and siliciclastic setting with Smithian-Spathian anoxic to dysoxic facies, An Chau basin, northeastern Vietnam. *Sedimentary Geology* 300, 28-48.

Korte, C., Kozur, H.W., Bruckschen, P. and Veizer, J. 2003. Strontium isotope evolution of Late Permian and Triassic seawater. *Geochemica et Cosmochimica Acta* 67, 47-62.

Korte, C. and Kozur, W.H. 2005. Carbon isotope stratigraphyacross the Permian/Triassic boundary at Jolfa (NW-Iran), Peitlerkofel (Sas de Pütia, Sass de Putia), Pufels (Bula, Bulla), Tesero (all three southern Alps, Italy) and Gerennavár (Bükk Mts., Hungary). *Journal of Alpine Geology* 47, 119-135.

Korte, C. and Kozur, H.W. 2010. Carbon-isotope stratigraphy across the Permian-Triassic boundary: A review. *Journal of Asian Earth Sciences* 39, 215-235.

Korte, C., Pande, P., Kalia, P., Kozur, H.W., Joachimski, M.M. and Oberhänsli, H. 2010. Massive volcanism at the Permian-Triassic boundary and its impact on the isotopic composition of the ocean and atmosphere. *Journal of Asian Earth Sciences* 37, 293-311.

Kovács, S. and Haas, J. 2010. Displaced south Alpine and Dinaridic elements in the mid-Hungarian zone. *Central European Geology* 53, 135-164.

Kovács, S., Less, G.Y., Piros, O., Reti, Z. and Róth, L. 1989. Triassic formations of the Aggtelek-Rudabánya Mountains (Northeastern Hungary). *Acta Geologica Hungarica* 32, 31-63.

Kovács, S., Sudar, M., Gradinaru, E., Gawlick, H-J., Kamata, S., Haas, J., Pero, C., Gaetani, M., Mello, J., Polak, M., Aljinovic, D., Ogorelec, B., Kolar-Jurkovšek, T., Jurkovšek, B. and Buser, S. 2011. Triassic evolution of the tectonostatigraphic units of the Circum-Pannonian Region. *Jahrbuch der Geologischen Bundesanstalt* 151, 199-280.

Kozur, H. 1996. The conodonts *Hindeodus, Isarcicella* and *Sweetohindeodus* in the Uppermost Permian and Lowermost Triassic. *Geologia Croatica* 49, 81-115.

Kraus, S.H., Siegert, S., Mette, W., Struck, U. and Korte, C. 2009. Stratigraphic significance of carbon isotope variations in the shallow-marine Seis/Siusi Permian-Triassic boundary section (Southern Alps, Italy). *Fossil Record* 12, 197-205.

Krystyn, L. 1974. Die Tirolites-Fauna (Ammonoidea) der untertriadischen Werfener Schichten Europas und ihre stratigraphische Bedeutung. *Sitzungsber. Öster. Akad. Wiss., Math.-Naturwiss. Kl., Abt. I* 183, 1-3.

Kump, L.R. and Arthur, M.A. 1999. Interpreting carbon-isotope excursions: carbonates and organic matter. *Chemical Geology* 161, 181-198.

Kump, L.R., Pavlov, A. and Arthur, M.A. 2005. Massive release of hydrogen sulphide to the surface ocean and atmosphere during intervals of oceanic anoxia. *Geology* 33, 397-400.

Kurushin, N.I., and Truschchelev, A.M. 1989. *Posidonia* from the Triassic sediments of Siberia and the Far East. In: Dagys, A.S. and Dubatolov, V.N (eds). *Upper Paleozoic and Triassic of Siberia*. Academy of Sciences of the USSR, Siberian Department, Transactions of the Institute of geology and geophysics, 172, 57-171.

La Perna, R. 2005. A gigantic deep-sea Nucinellidae from the tropical West Pacific (Bivalvia: Protobranchia) *Zootaxa* 88, 1-10.

La Perna, R. 2007. Taxonomy of the family Neilonellidae (Bivalvia, Protobranchia): Miocene and Plio-Pliestocene species of *Pseudoneilonella* Laghi, 1986 from Italy. *Veliger* 49, 196-208.

Labat, D., Goddéris, Y., Probst, J. L. and Guyot, J.L. 2004. Evidence for global runoff increase related to climate warming. *Advances in Water Resources* 27, 631-642.

Lai, X., Wang, W., Wignall, P.B., Bond, D.P.G., Jiang, H., Ali, J.R., John, E.H. and Sun, Y. 2008. Palaeoenvironmental change during the end-Guadalupian (Permian) mass extinction in Sichuan, China. *Palaeogeography, Palaeoclimatology, Palaeoecology* 269, 78-93.

Lazutkina, O.F. 1963. Discovery of a bryozoan of the Paleozoic genus *Batostomella* in the Triassic. *Paleontologiskii Zhurnal* 4, 126-128.

Lehrmann, D.J., Wan, Y., Wei, J., Yu, Y. and Xiao, J. 2001. Lower Triassic peritidal cyclic limestone: an example of anachronistic carbonate facies from the Great Bank of Guizhou, Nanpanjiang Basin, Guizhou province, south China. *Palaeogeography, Palaeoclimatology, palaeoecology* 173, 103-123.

Lehrmann, D.J., Payne, J.L., Felix, S.V., Dillett, P.M., Wang, H., Yu, Y. and Wei, J. 2003. Permian-Triassic boundary sections from shallow-marine carbonate platforms of the Nanpanjiang Basin, South China; implications for Oceanic conditions associated with the end-Permian extinction and its aftermath. *Palaios* 18, 138-152.

Lehrmann, D.J., Ramezani, J., Bowring, S.A., Martin, M.W., Montgomery, P., Enos, P., Payne, J.L., Orchard, M.J., Hongmei, W. and Jiayong, W. 2006b. Timing of recovery from the end-Permian extinction: Geochronologic and biostratigraphic constraints from south China. *Geology* 34, 1053-1056.

Leonardi, P., 1935. Il Trias inferiore delle Tre Venezie. *Mem. Inst. Geol. Univ. Padove* 11, 1-136.

Levinton, J.S. and Bambach, R.K. 1975. A comparative study of Silurian and recent deposit-feeding bivalve communities. *Paleobiology* 1, 97-124.

Lloyd, G.T., Davis, K.E., Pisani, D., Tarver, J.E., Ruta, M., Sakamoto, M., Hone, D.W.E., Jennings, R. and Benton, M.J. 2008. Dinosaurs and the Cetaceous Terrestrial Revolution. *Proceedings of the Royal Society B* 275, 2483-2490.

Loo, L-O. and Rosenberg, R. Bivalve suspension-feeding dynamics and benthic-pelagic coupling in an eutrophicated marine bay. *Journal of Experimental Marine Biology and Ecology* 130, 253-276.

Looy, C.V., Brugman, W.A., Dilcher, D.L. and Visscher, H. 1999. The delayed resurgence of equatorial forests after the Permian-Triassic ecologic crisis. *PNAS* 96, 13857-13862.

Lowe, D. 1975. Water escape structures in course-grained sediments. *Sedimentology* 22, 157-204.

Ludvigsen, R. Westrop, S.R., Pratt, B.R. Tuffnell, P.A. and Young, G.A. 1986. Dual biostratigraphy: zones and biofacies. *Geoscience Canada* 13, 139-154.

Luo, M. and Chen, Z-Q. 2013. New arthropod traces from the Lower Triassic Kockatea Shale Formation, northern Perth Basin, Western Australia: ichnology, taphonomy and palaeoecology. *Geological Journal* 29, 111-220.

Luo, G., Kump, L.R., Wang, Y., Tong, J., Arthur, M.A., Yang, H., Huang, J., Yin, H. and Xie, S. 2010. Isotopic evidence for an anomalously low oceanic sulphate concentration following end-Permian mass extinction. *Earth and Planetary Science Letters* 300, 101-111.

Magaritz, M., Bär, R., Baud, A. and Holser, W.T. 1988. The carbon-isotope shift at the Permian/Triassic boundary in the southern Alps is gradual. *Nature* 331, 337-339.

Magaritz, M. and Holser, W.T. 1991. The Permian-Triassic of the Gartnerkofel-1 Core (Carnic Alps, Austria): Carbon and Oxygen isotope variation. *Abh. Geol. B-A* 45, 149-163.

Mangerud, G. and Mørk, A. 2013. Bio and palynostratigraphy at the Permian – Triassic transition in Svalbard and the Barents Sea area. *The Permian Strata of Svalbard Abstracts and Proceedings,* 22.

Mangerud, G. and Konieczny, R.M. 1993. Palynology of the Permian succession of Spitsbergen, Svalbard. *Polar Research* 12, 65-93.

Manly, B.F.J. 2006. *Randomization, bootstrap and Monte Carlo methods in biology, 3rd Edition.* Chapman and Hall, London.

Marriott, S.B., Hillier, D. and Morrissey, L.B. 2013. Enigmatic sedimentary structures in the Lower Old Red Sandstone, south Wales, UK: possible microbial influence on surface processes and early terrestrial food webs. *Geological magazine* 150, 396-411.

Massari, F., Neri, C., Pittau, P., Fontana, D and Stefani, C. 1994. Sedimentology, palynostratigraphy and sequence stratigraphy of a continental to shallow-marine rift-

related succession: Upper Permian of the Eastern Southern Alps (Italy). *Memorie di Scienze Geologiche, Padova* 46, 119-243.

Mata, S.A. and Bottjer, D.J. 2011. Origin of Lower Triassic microbialites in mixed carbonate-siliciclastic successions: Ichnology, applied stratigraphy, and the end-Permian mass extinction. *Palaeogeography, Palaeoclimatology, Palaeoecology* 300, 158-178.

McGhee, G.R., Sheehan, P.M., Bottjer, D.J. and Droser, M.L. 2004. Ecological ranking of Phanerozoic biodiversity crises: Ecological and taxonomic severities are decoupled. *Palaeogeography, Palaeoclimatology, Palaeoecology* 211, 289-297.

McGhee, G.R., Sheehan, P.M., Bottjer, D.J. and Droser, M.L. 2012. Ecological ranking of Phanerozoic biodiversity crises: The Serpukhovian (early Carboniferous) crisis had a greater ecological impact than the end-Ordovician. *Geology* 40, 147-150.

McGhee, G.R., Clapham, M.E., Sheehan, P.M., Bottjer, D.J. and Droser, M.L. 2013. A new ecological-severity ranking of major Phanerozoic biodiversity crises. *Palaeogeography, Palaeoclimatology, Palaeoecology* 370, 260-270.

McGowan A. J., Smith, A.B and Taylor, P.D. 2009. Faunal diversity, heterogeneity and body size in the Early Triassic: testing post-extinction paradigms in the Virgin Limestone of Utah, USA∗, *Australian Journal of Earth Sciences* 56, 859-872.

McKenzie, J.A. and Vasconcelos, C. 2009. Dolomite Mountains and the origin of the dolomite rock which they mainly consist; historical developments and new perspectives. *Sedimentology* 56, 205-219.

Mergl, M. 2010 Discinid brachiopod life assemblages: Fossil and extant. *Bulletin of Geosciences*, 85, 27-38.

Metcalfe, B., Twitchett, R.J. and Price-Lloyd, N. 2011. Changes in size and growth rate of 'Lilliput' animals in the earliest Triassic. *Palaeogeography, Palaeoclimatology, Palaeoecology* 308, 171-180.

Mette, W. and Roozbahani, P. 2012. Late Permian (Changhsingian) ostracods of the Bellerophon Formation at Seis (Siusi)(Dolomites, Italy). *Journal of Micropalaeontology* 31, 73-87.

Meyer, K.M., Kump, L.R. Ridgwell, A. 2008. Biogeochemical controls on photic-zone euxinia during the end-Permian mass extinction. *Geology* 36, 747-750.

Meyer, K.M., Yu, M., Jost, A.B., Kelley, B.M. and Payne, J.L. 2011. $\Delta^{13}C$ evidence that high primary productivity delayed recovery from end-Permian mass extinction. *Earth and Planetary Science Letters* 302, 378-384.

Miller, A.I. and Foote, M. 1996. Calibrating the Ordovician radiation of marine life: implications for Phanerozoic diversity trends. *Paleobiology* 22, 304-309.

Miller, A.I. and Foote, M. 2009. Epicontinental seas versus open-ocean settings: the kenetics of mass extinction and origination. *Science* 326, 1106-1109.

Mitchell, J.S. and Heckert, A.B. 2010. The setup, use and efficacy of sodium polytungstate separation methodology with respect to microvertebrate remains. *Journal of Paleontological techniques* 7, 1-12.

Mørk, A., Vigran, J.O and Hochuli, P.A. 1990. Geology and palynology of the Triassic succession of Bjørnøya. *Polar Research* 8, 141-163.

Mørk, A. and Worsley, S. 2006. The Festningen Section. *NGF Abstracts and Proceedings* 3, 31-35.

Mørk, A., Knarud, R. and Worsley, D. 1983. Depositional and diagenetic environments of the Triassic and Lower Jurassic succession of Svalbard. *Calgary Canadian Society of Petroleum Geologists* 8, 371-398.

Mørk, A, Elvebakk, G., Forsberg, A. W., Hounslow, M. W., Nakrem, H. A., Vigran, J. 0. and Weitschat, W. 1999. The type section of the Vikinghogda Formation: a new Lower Triassic unit in central and eastern Svalbard. *Polar Research* 18, 51-82.

Mort, H.P., Adatte, T., Föllmi, K.B., Keller, G., Steinmann, P., Matera, V., Berner, Z. and Stüben, D. 2007. Phosphorous and the roles of productivity and nutrient recycling during oceanic anoxic event 2. *Geology* 35, 483-486.

Mostler, H. and Rossner, P.D.R. 1984. Mikrofazies und Palökologie der höheren Werfener Schichten (Untertrias) der Nördlichen Kalkalpen. *Facies*, 10, 87-143.

Müller, R.D., Goncharov, A., Kritski, A. 2005. Geophysical evaluation of the enigmatic Bedout basement high, offshore northwestern Australia. *Earth and Planetary Science Letters* 237, 264-284.

Mundil, R., Ludwig, K.R., Metcalfe, I. and Renne, P.R. 2004. Age and timing of the Permian mass extinction: U/Pb dating of closed-system zircons. *Science* 305, 1760-1763.

Nabbefeld, B., Grice, K., Twitchett, R.J., Summons, R.E., Hays, L., Böttcher, M.E and Asif, M. 2010. An integrated biomarker, isotopic and palaeoenvironmental study through the late Permian event at Lusitaniadalen, Spitsbergen. *Earth and Planetary Science Letters* 291, 84-96.

Nagy, Z.R. 1999. Platform-basin transition and depositional models for the Upper Triassic (Carnian) Séndorhegy Limestone, Balaton Highland. *Acta Geologica Hungarica* 42, 267-299.

Nakamura, K., Kimura, G. and Winsnes, T.S. 1987. Brachiopod zonation and age of the Permian Kapp Starostin Formation (Central Spitsbergen). *Polar Research* 5, 207-219.

Nakazawa, K. 1977. On *Claraia* of Kashmir and Iran. *Journal of the Palaeontological Society of India* 20, 191-204.

Nakazawa, K. 1999. Permian bivalves from West Spitsbergen, Svalbard Islands, Norway. *Paleontological Research* 3, 1-17.

Nakazawa, K., Suzuki, H., Kumon, F. and Winsnes, T.S. 1990. Scientific results of the japanese geological expedition to Svalbard 1986. In: T. Tatsumi (ed.). *The Japanese Scientific expedition to Svalbard 1983-1986*, Tokyo, 179-214.

Nakrem, H.A. 1994. Bryozoans from the lower Permian Vøringen Member (kapp Staostin Formation), Spitsbergen, Svalbard. *Norsk Polarinstitutt Skifter* 196, 1-93.

Nakrem, H.A. and Mørk, A. 1991. New early Triassic Bryozoa (Trepostomata) from Spitsbergen, with some remarks on the stratigraphy of the investigated horizons. *Geological Magazine* 128, 129-140.

Nakrem, H.A., Nilsson, I. and Mangerud, G. 1992. Permian biostratigraphy of Svalbard (Arctic Norway) – a review. *International Geology Review* 34, 933-959.

Nakrem, H.A., Orchard, M.J., Weitschat, W., Hounslow, M.W., Beatty, T.W. and Mørk, A. 2008. Triassic conodonts from Svalbard and their Boreal correlations. *Polar Research* 27, 523-539.

Neri, C. and Posenato, R. 1985. New biostratigraphical data on uppermost Werfen Formation of western Dolomites (Trento, Italy). *Geol. Paläont. Mitt. Innsbruck* 14, 83-107.

Nesbitt, E.A. and Campbell, K.A. 2006. The Paleoenvironmental significance of *Psilonichnus*. *Palaios* 21, 187-196.

Newell, N.D. and Boyd, D.W. 1975. Parallel evolution in early Trigoniacean bivalves. *Bulletin of the American museum of Natural history* 154, 1-158.

Nicora, A. and Perri, M.C. 1999. Bio- and chronostratigraphy: Conodonts. In: G. Cassinis, L. Cortesogno, L. Gaggero, F. Massari, C. Neri, U. Nicosia, and P. Pittau (eds.). *Stratigraphy and Facies of the Permian Deposits Between Eastern Lombardy and the Western Dolomites. International Field Conference on ''The Continental Permian of the Southern Alps and Sardinia (Italy).* Regional Reports and General Correlations,'' 15–25 September, 1999, Brescia, Italy. Earth Science Department, Pavia University. p. 97–100

Noé, S.U. 1987. Facies and Paleogeography of the Marine Upper Permian and f the Permian-Triassic boundary in the southern Alps (Bellerophon Formation, Tesero Horizon). *Facies* 16, 89-142.

Novack-Gottshall, P.M. 2007. Using a theoretical ecospace to quantify the ecological diversity of Paleozoic and modern marine biotas. *Paleobiology* 33, 273-294.

Nützel, A. 1998. Über die Stammesgeschichte der Ptenoglossa (Gastropoda). *Berliner Geowissenschaafliche Abhandlungen, Reihe E* 26, 1-229.

Nützel, A. 2005. A new Early Triassic gastropod genus and the recovery of gastropods from the Permian/Triassic extinction. *Acta Palaeontologica Polonica* 50, 19-24.

Nützel, A. and Erwin, D.H. 2002. *Battenizyga*, a new Early Triassic gastropod genus with a discussion of the caenogastropod evolution at the Permian/Triassic boundary. *Paläontologische Zeitschrift* 76, 21-27,

Nützel, A. and Frýda, J. 2003. Paleozoic plankton revolution: evidence from early gastropod ontogeny. *Geology* 31, 829-831.

Nützel, A and Schulbert, C. 2005. Facies of two important Early Triassic gastropod lagerstätten: implications for diversity patterns in the aftermath of the end-Permian mass extinction. *Facies* 51, 480-500.

Nützel, A. and Mapes, R.H. 2001. Larval and juvenile gastropods from a Carboniferous black shale: palaeoecology and implications for the evolution of the Gastropoda. *Lethaia* 34, 143-162.

Odin, G.S. and Matter, A. 1981. Origin of glauconites. *Sedimentology* 28, 611-641.

Oji, T. and Twitchett, R.J. 2015. The oldest post-Palaeozoic crinoid and Permian-Triassic origins of the Articulata (Echinodermata). *Zoological Science* 32, 211-215.

Oliver, P.G. and Taylor, J.D. 2012. Bacterial symbiosis in the Nucinellidae (Bivalvia: Solemyida) with descriptions of two species. *Journal of Molluscan Studies* 78, 81-91.

Olszewski, T.D. 2004. A unified mathematical framework for the measurement of richness and evenness within and among multiple communities. *OIKOS* 104, 377-387.

Orchard, M.J. 2007. Conodont diversity and evolution through the latest Permian and Early Triassic upheavals. *Palaeogeography, Palaeoclimatology, Palaeoecology* 252, 93-117.

Ovtcharova, M., Bucher, H., Schaltegger, U., Galfetti, T., Brayard, A. and Guex, J. 2006. New Early to Middle Triassic U-Pb ages from South China: Calibration with ammonoid biochronozones and implications for the timing of the Triassic biotic recovery. *Earth and Planetary Science Letters* 243, 463-475.

Pálfy, J., Parrish, R.R., David, K. and Vörös, A. 2003. Mid-Triassic integrated U-Pb geochronology and ammonoid biochronology from the Balaton Highland (Hungary). *Journal of the Geological Society* 160, 271-284.

Pan, H-Z., Erwin, D.H., Nützel, A. and Xiang-Shui, Z. 2003. *Jiangxispira,* a new gastropod genus from the Early Triassic of China with remarks on the phylogeny of the heterostropha at the Permian/Triassic boundary. *Journal of Paleontology* 77, 44-49.

Pan, Y-H., Hu, S-X., Sha, J-G., Zhang, Q-Y., Wang, Y-Q., Zhou, C-Y., Wen, W., Huang, J-Y. and Xie, T. 2014. Early Triassic bivalves from the Feixianguan Formation in Xingyi, Guizhou and the Ximatang Formation in Qiubei, Yunnan (southern China). *Palaeoworld* 23, 143-154.

Patzkowsky, M. E. and Holland, S. M. 2012. *Stratigraphic Paleobiology: Understanding the distribution of fossil taxa in time and space*. The University of Chicago Press, Chicago.

Payne, J.L. 2005. Evolutionary dynamics of gastropod size across the end-Permian extinction and through the Triassic recovery interval. *Paleobiology* 31, 269-290.

Payne, J.L. and Clapham, M.E. 2012. End-Permian mass extinction in the oceans: an ancient analog for the twenty-first Century? *Annual Review of Earth and Planetary Sciences* 40, 89-111.

Payne, J.L. and Kump, L.R. 2007. Evidence for recurrent Early Triassic massive volcanism from quantitative interpretation of carbon isotope fluctuations. *Earth and Planetary Science Letters* 256, 264-277.

Payne, J.L., Lehrmann, D.J., Wei, J., Orchard, M.J., Schrag, D.P. and Knoll, A.H. 2004. Large perturbations of the carbon cycle during recovery from the end-Permian extinction. *Science* 305, 506-509.

Payne, J.L. Lehrmann, D.J., Wei, J. and Knoll, A.H. 2006a. The pattern and timing of biotic recovery from the end-Permian extinction on the Great Bank of Guizhou, Guizhou Province, China. *Palaios* 21, 63-85.

Payne, J.L., Lehrmann, D.J., Christensen, S., Wei, J and Koll, A.H. 2006b. Environmental and biological controls on the initiation and growth of a Middle Triassic (Anisian) reef complex on the Great Bank of Guizhou, Guizhou Province, China. *Palaios* 21, 325-343.

Payne, J.L., Turchyn, A.V., Paytan, A., DePaolo, D.J., Lehrmann, D.J., Yu, M. and Wei, J. 2010. Calcium isotope constraints on the end-Permian mass extinction. *PNAS* 107, 8543-8548.

Peizhen, Z., Molnar, P. and Downs, W.R. 2001. Increased sedimentation rates and grain sizes 2-4 Myr ago due to the influence of climate change on erosion rates. *Nature* 410, 891-897.

Perri, M.C. 1991. Conodont biostratigraphy of the Werfen Formation (Lower Triassic), Southern Alps, Italy. *Bollettino della Societa Paleontoloica Italiana* 30, 23-46.

Perri, M.C. and Andraghetti, M. 1987. Permian–Triassic boundary and Early Triassic conodonts from the Southern Alps. Italy. *Rivista Italiana di Paleontologia e Stratigrafia* 93, 291–328.

Perri, M.C. and Farabegoli, E. 2003. Conodonts across the Permian–Triassic boundary in the Southern Alps. *Courier Forschungsinstitut Senckenberg* 245, 281–313.

Petes, L.E., Menge, B.A. and Murphy, G.D. 2007. Environmental stress decreases survival, growth, and reproduction in New Zealand mussels. *Journal of Experimental Marine Biology and Ecology* 351, 83-91.

Pietsch, C. and Bottjer, D.J. 2014. The importance of oxygen for the disparate recovery patterns of the benthic macrofauna in Early Triassic. *Earth-Science Reviews* 137, 65-84.

Pietsch, C., Mata, S.A. and Bottjer, D.J. 2014. High temperature and low oxygen perturbations drive contrasting benthic recovery dynamics following the end-Permian mass extinction. *Palaeogeography, Palaeoclimatology, Palaeoecology* 399, 98-113.

Pihl, L., Svenson, A., Moksnes, P-O, and Wennhage, H. 1999. Distribution of green algal mats throughout shallow soft bottoms of the Swedish Skagerrak archipelago in relation to nutrient sources and wave exposure. *Journal of Sea Research* 41,281-294.

Pöppelreiter, M. 2002. Facies, cyclicity and reservoir properties of the Lower Muschelkalk (Middle Triassic) in the NE Netherlands. *Facies* 46, 119-132.

Posenato, R. 1985. Un'Associazione oligotipica a *Neoschizodus ovatus* (GULDFUSS) della formazione di Werfen (Triassico inf-Dolomiti). *Atti 3° Simposio di Ecologia e Paleoecologia delle Comunitá bentoniche*, 141-153.

Posenato, R. 1992. Tirolites (Ammonoidea) from the Dolomites, Bakony and Dalmatia : Taxonomy and biostratigraphy. *Ecologae Geologicae Helvetiae* 85, 893-929.

Posenato, R. 2002. Bivalves and other macrobenthic fauna from the Ladinian "Muschelkalk" of Punta del Lavatoio (Alghero, SW Sardinia). *Rendiconti della Societá Paleontologica Italiana* 1, 185-196.

Posenato, R. 2008a. Patterns of bivalve biodiversity from Early to Middle Triassic in the Southern Alps (Italy): Regional vs. global events. *Palaeogeography, Palaeoclimatology, Palaeoecology* 261, 145-159.

Posenato, R. 2008b. Global correlations of mid Early Triassic events: The Induan/Olenekian boundary in the Dolomites (Italy). *Earth-Science Reviews* 91, 93-105.

Posenato, R., Sciunnach., D. and Garzanti,E. 1996. First report of *Claraia* (Bivalvia) in the Servino Formation (Lower Triassic) of the western Orobic Alps, Italy. *Rivista Italiana di Paleontologia e Stratigrafia* 102, 201-210.

Posenato, R. 2009. Survival patterns of macrobenthic marine assemblages during the end-Permian mass extinction in the western Tethys (Dolomites, Italy). *Palaeogeography, Palaeoclimatology, Palaeoecology* 280, 150-167.

Posenato, R. 2010. Marine biotic events in the Lopingian succession and latest Permian extinction in the Southern Alps (Italy). *Geological Journal* 45, 195-215.

Posenato, R., Holmer, L.E. and Prinoth, H. 2014. Adaptive strategies and environmental significance of lingulid brachiopods across the late Permian extinction. *Palaeogeography, Palaeoclimatology, Palaeoecology* 399, 373–384.

Powers, C.M and Pachut, J.F. 2008. Diversity and distribution of Triassic bryozoans in the aftermath of the end-Permian mass extinction. *Journal of Paleontology* 82, 362-371.

Pruss, S.B. and Bottjer, D.J. 2004a. Early Triassic trace fossils of the western United States and their implications for prolonged environmental stress from the end-Permian mass extinction. *Palaios* 19, 551-564.

Pruss, S.B. ad Bottjer, D.J. 2004b. Late Early Triassic microbial reefs of the western United States: a description and model for their deposition in the aftermath of the end-Permian mass extinction. *Palaeogeography, Palaeoclimatology, Palaeoecology* 211, 127-137.

Pruss, S.B., Payne, J.L. and Bottjer, D.J. 2007. *Placunopsis* bioherms: the first metazoan buildups following the end-Permian mass extinction. *Palaios* 22, 17-23.

Racki, G. 1999. Silica-secreting biota and mass extinctions: survival patterns and processes. *Palaeogeography, Palaeoclimatology, Palaeoecology* 154, 107-132.

Rampino, M.R. and Caldeira, K. 2005. Major perturbation of ocean chemistry and a 'Strangelove Ocean' after the end-Permian mass extinction. *Terra Nova* 17, 554-559.

Raup, D.M. 1993. Extinction from a paleontological perspective. *European Review* 1, 207-216.

Raup, D.M. and Sepkoski, J.J. 1982. Mass extinctions in the marine fossil record. *Science* **215**, 1501-1503.

Reading, H. and Collinson, J.D. 1996. Clastic coasts. In: Reading, H (eds). *Sedimentary Environments: Processes, Facies, Stratigraphy (3rd Edition)*. Wiley-Blackwell, UK.

Rees, P.M. Land-plant diversity and the end-Permian mass extinction. *Geology* 30, 827-830.

Reichow, M.K., Pringle, M.S., Al'Mukhamedov, A.I., Allen, M.B., Andreichev, V.I., Buslov, M.M., Davies, C.E., Fedoseev, G.S., Fitton, J.G., Inger, S., Medvedev, A.Y., Mitchell, C., Puchkov, V.N., Safonova, I.Y., Scott, R.A. and Saunders, A.D. 2009. The timing and extent of the eruption of the Siberian Traps large igneous province: Implications for the end-Permian environmental crisis. *Earth and Planetary Science Letters* 277, 9-20.

Renne, P.R. and Basu, A.R. 1991. Rapid eruption of the Siberian Taps flood basalts at the Permo-Triassic boundary. *Science* 253, 176-179.

Renne, P.R., Zichao, Z., Richards, M.A., Black, M.T. and Basu, A.R. 1995. Synchrony and causal relations between Permian-Triassic boundary crises and Siberian flood volcanism. *Science* 269, 1413-1416.

Retallack, G.J. 1999. Postapocalyptic greenhouse paleoclimate revealed by earliest Triassic paleosols in the Sydney Basin, Australia. *Geological Society of American Bulletin* 111, 52-70.

Richoz, S. 2006. Stratigraphie et variations isotopiques du carbone dans le Permien supérieur et le Trias inférieur de quelques localités de la Néotéthys (Turquie, Oman et Iran). *Mémoire de Géologie de Lausanne* 46, 275.

Rodland, D.L. and Bottjer, D.J. 2001. Biotic recovery from the end-Permian mass extinction: Behavior of the inarticulate brachiopod *Lingula* as a disaster taxon. *PALAIOS* 16, 95-101.

Romano, C., Goudemand, N., Vennemann, T.W., Ware, D., Schneebeli-Hermann, E., Hochuli, P.A., Brühwiler, T., Brinkmann, W. and Bucher, H. 2012. Climatic and biotic upheavals following the end-Permian mass extinction. *Nature Geoscience* 6, 57-60.

Ros, S. And Echevarria, J. 2011. Bivalves and evolutionary resileience: old skills and new strategies to recover from the P/T and T/J extinction events. *Historical Biology: An International Journal of Paleobiology* 23, 411-429.

Ros, S., De Renzi, M., Damborenea, S.E. and Márquez-Aliaga, A.2011. Coping between crises: early Triassic-early Jurassic bivalve diversity dynamics. *Palaeogeography, Palaeoclimatology, Palaeoecology* 311, 184-199.

Ros-Franch, S., Márquez-Aliaga, A. and Damborenea, S.E. 2014. Comprehensive database of Induan (Lower Triassic) to Sinemurian (Lower Jurassic) marine bivalve genera and their paleobiogeographic record. *Paleontological Contributions* 8, 1-219.

Rouse, G.W., Jermiin, L.S., Wilson, N.G., Eeckhaut, I., Lanterbecq, D., Oji, T., Youn, C.M., browning, T., Cisternas, P., Helgen, L.E., Stuckey, M. and messing, C.G. 2013. Fixed, free, and fixed: the fikle phylogeny of extant Crinoidea (Echinodermata) and their Permian-Triassic origin. *Molecular Phylogenetics and Evolution* 66, 161-181.

Savoy, L.E. 1992. Environmental record of Devonian-Mississippian carbonate and low-oxygen facies trnasitions, southernmost Canadain Rocky Mountains and northwesternmost Montana. *Geological Society of America Bulletin* 104, 1412-1432.

Savrda, C.E. and Bottjer, D.J. 1991. Oxygen-related biofacies in marine strata: an overview and update. In: Tyson, R.V. and Pearson, T.H. (eds). *Modern and Ancient Continental Shelf Anoxia*. Geological Society Special Publication No.58, 201-219.

Schatz, W. 2004. Revision of the subgenus *Daonella* (*Arzella*) (Halobiidae: Middle Triassic). *Journal of Paleontology* 78, 300-316.

Schatz, W. 2005. Palaeoecology of the Triassic black shale bivalve *Daonella* – new insights into an old controversy. *Palaeogeography, Palaeoclimatology, Palaeoecology* 216, 189-201.

Scheyer, T.M., Romano, C., Jenks, J. And Bucher, H. 2014. Early Triassic marine biotic recovery: the predators' perspective. *PLOS one* 9, 88987.

Schmidt-Nielsen, K. 1984. *Scaling: why is animal size so important?* Cambridge University Press, Cambridge.

Schobben, M., Joachimski, M.M., Kon, D., Leda, L.and Korte, C. 2014. Palaeotethys seawater temperature rise and intensified hydrological cycle following the end-Permian extinction. *Gondwana Research* 26, 675-683.

Scholger, R., Mauritsch, H.J. and Brandner, R. 2000. Permian-Triassic boundary magnetostratigraphy from the southen Alps (Italy). *Earth and Planetary science Letters* 176, 495-508.

Schubert, J.K. and Bottjer, D.J. 1995. Aftermath of the Permian-Triassic mass extinction event: paleoecology of Lower Triassic carbonates in the western USA. *Palaeogeography, Palaeoclimatology, Palaeoecology* 116, 1-39.

Schubert, J.K., Bottjer, D.J. and Simms, M.J. 1992. Paleobiology of the oldest known articulate crinoid. *Lethaia* 25, 97-110.

Sciunnach, D., Garzanti, E., Posenato, R and Rodeghiero, F. 1999. Stratigraphy of the Servino Formation (Lombardy, Southern Alps): towards a refined correlation with the Werfen Formation of the Dolomites. *Memorie di Scienze Geologiche* 51, 103-118.

Senowbari-Daryan, B., Zühlke, R., Bechstädt, T. and Flügel, E. 1993. Anisian (Middle Triassic) Buildups of the northern Dolomites (Italy): the recovery of reef communities after the Permian/Triassic crisis. *Facies* 28, 181-256.

Sepkoski, J.J. 1982. Flat-pebble conglomerates, storm deposits, and the Cambrian bottom fauna. In: Einsele, G. and Seilacher, A. (eds). *Cyclic and Event Stratification.* 371-385.

Sepkoski, J.J. 1984. A kinetic model of Phanerozoic taxonomic diversity. III. Post-Paleozoic families and mass extinctions. *Paleobiology* 10, 246-267.

Sepkoski, J.J. 1996. Patterns of Phanerozoic extinction: a perspective from global databases. In: Walliser, O.H. (ed), *Global Events and Event Stratigraphy*. Springer, Berlin. 35–51.

Sepkoski, J.J. 2002. A compendium of fossil marine animal genera. *Bulletins of American Paleontology*. 362, 1-560.

Sharma, P.P., Zardus, J.D., Boyle, E.E., Gonzalez, V.L., Jennings, R.M., McIntyre, E., Wheeler, W.C., Etter, R.J. and Giribet, G. 2013. Into the deep: A phylogenetic approach to the bivalve subclass Protobranchia. *Molecular Phylogenetics and Evolution* 69, 188-204.

Sheldon, N.D. 2006. Abrupt chemical weathering increase across the Permian-Triassic boundary. *Palaeogeography, Palaeoclimatology, Palaeoecology* 231, 315-321.

Shen, S-Z., Tazawa, J-I. and Shi, G.R. 2005. Carboniferous and Permian Rugosochonetidae (Brachiopoda) from West Spitsbergen. *Alcheringa*: *An Australian Journal of Palaeontology* 29, 241-256.

Shen, S-Z., Crowley, J.L., Wang, Y., Bowring, S.A., Erwin, D.H., Sadler, P.M., Cao, C-Q., Rothman, D.H., Henderson, C., Ramezani, J., Zhang, H., Shen, Y., Wang, X-D., Wang, W., Mu, L., Li, W-Z., Tang, Y-G., Liu, X-L., Liu, L-J., Zeng, Y., Jiang, Y-F. and Jin, Y-G. 2011. Calibrating the end-Permian mass extinction. *Science* 334, 1367-1372.

Shen, J., Schoepfer, S.D., Feng, Q., Zhou, L., Yu, J., Song, H., Wei, H. and Algeo, T.J. 2014. Marine productivity changes during the end-Permian crisis and Early Triassic recovery. *Earth-Science Reviews* doi:10.1016/j.earscirev.2014.11.002.

Shepard, F.P. 1967. *The Earth beneath the Sea*. John Hopkins University Press, Baltimore.

Shigeta, Y., Zakharov, Y.D., Maeda, H. and Popov, A.M. (eds). 2009. *The lower Triassic system in the Abrek Bay area, South Primorye, Russia*. National Museum of Nature and Science Monographs No.38, Tokyo.

Siegert, S., Kraus, S.H., Mette, W., Struck, U. and Korte, C. 2011. Organic carbon isotope values from the Late Permian Seis/Siusi succession (Dolomites, Italy): Implications for palaeoenvironmental changes. *Fossil Record* 14, 207-217.

Signor, P.W. and Brett, C.E. 1984. The mid-Paleozoic precursor to the Mesozoic marine revolution. *Paleobiology* 10, 245-258.

Šimo, V and Olšavský, M. 2007. *Diplocraterion parallelum* Torell, 1870, and other trace fossils from the Lower Triassic succession of the Drienok Nappe in the Western Carpathians, Slovakia. *Bulletin of Geosciences* 82, 165-173.

Simpson, E.H. 1949. Measurement of diversity. *Nature* 163, 688.

Smith, J.P. 1914. *The Middle Triassic marine invertebrate faunas of North America*. US Geological Survey, Washington.

Smith, C.R. and Kukert, H. 1996. Macrobenthic community structure, secondary production, and rates of bioturbation and sedimentation at the Kane'ohe Bay Lagoon floor. *Prac. Sci.* 50, 211-229.

Song, H., Tong, J. and Chen, Z-Q. 2011. Evolutionary dynamics of the Permian-Triassic foraminifer size: Evidence for Lilliput effect in the end-Permian mass extinction and its aftermath. *Palaeogeography, Palaeoclimatology, Palaeoecology* 308, 98-110.

Song, H., Wignall, P.B., Tong, J. and Yin, H. 2013. Two pulses of extinction during the Permian-Triassic crisis. *Nature Geoscience* 6, 52-56.

Song, H., Wignall, P.B., Chu, D., Tong, J., Sun, Y., Song, H., He, W. and Tian, L. 2014. Anoxia/ high temperature double whammy during the Permian-Triassic marine crisis and its aftermath. *Scientific Reports* 4, 4132-4139.

Spath, L.F. 1930. The Eotriassic invertebrate fauna of east Greenland. *Meddelelser Om Grønland* 83, 1-89.

Spath, L.F. 1935. Additions to the Eo-Triassic invertebrate fauna of east Greenland. *Meddelelser Om Grønland* 98, 1-114.

Stanley, S.M. 1968. Post-Paleozoic adaptive radiation of infaunal bivalve molluscs: a consequence of mantle fusion and siphon formation. *Journal of Paleontology* 42, 214-229.

Stanley, S.M. 1972. Functional morphology and Evolution of bysally attached bivalve mollusks. *Journal of Paleontology* 46, 165-212.

Stanley, S.M. 2007. An analysis of the history of marine animal diversity. *Paleobiology* 33, 1-55.

Stanley, S.M. 2009. Evidence from ammonoids and conodonts for multiple Early Triassic mass extinctions. *Proceedings of the Natural Academy of Sciences* 106, 1564-1567.

Stasek, C.R. 1961. The ciliation and function of the labial palps of *Acila castrensis* (protobranchia, Nuculidae), with an evaluation of the role of the protobanch organs of feeding in the evolution of the Bivalvia. *Proceedings of the Zoological Society of London* 137, 511-538.

Steckbauer, A., Duarte, C.M., Carstensen, J. Vaquer-Sunyer, R. and Conley, D.J. 2011. Ecosystem impacts of hypoxia: thresholds of hypoxia and pathways to recovery. *Environmental research Letters* 6, 1-12.

Stemmerik, L. 1998. Discussion. Brachiopod zonation and age of the Permian Kapp Starostin Formation (Central Spitsbergen). *Polar Research* 6, 179-180.

Stiller, F. 2001. Fossilvergesellschaftungen, Paläoökologie und paläosynökologische Entwicklung im Oberen Anisium (Mittlere Trias) von Qingyan, insbesondre Bangtoupo, Provinz Guizhou, Südwestchina. *Münstersche Forschungen zur Geologie und Paläontologie* 92, 1-523.

Summons, R.E. and Powell, T.G. 1986. *Chlorobiaceae* in Palaeozoic seas revealed by biological markers, isotopes and geology. *Nature* 319, 763-765.

Sun, Y., Joachimski, M.M., Wignall, P.B., Yan, C., Chen, Y., Jiang, H., Wang, L. and Lai, X. 2012. Lethally hot temperatures during the Early Triassic greenhouse. *Science* 338, 366-370.

Svensen, H., Planke, S., Polozov, A.G., Schmidbauer, N., Corfu, F., Podladchikov, Y.Y. and Jamtveit, B. 2009. Siberian gas venting and the end-Permian environmental crisis. *Earth and Planetary Science Letters* 277, 490-500.

Sweet, W.C., Mosher, L.C., Clark, D.L., Collinson, J.W. and Hasenmueller, W.A. 1971. Conodont biostratigraphy of the Triassic. In: *Symposium on Conodont biostratigraphy*. Geological Society of America Memoirs 127, 499pp.

Szaniawski, H. and Malkowski, K. 1979. Conodonts from the Kapp Starostin Formation (Permian) of Spitsbergen. *Acta Palaeontologica Polonica* 24, 231-268.

Thomas, B.M., Willink, R.J., Grice, K., Twitchett, R.J., Purcell, R.R., Archbold, N.W., George, A.D., Tye, S., Alexander, R., Foster, C.B. and Barber, C.J. 2004. Unique marine Permian-Triassic boundary section from Western Australia. *Australian Journal of Earth Sciences* 51, 423-430.

Tong, J., Zakharov, Y.D., Orchard, M.J., Yin, H. and Hansen, H.J. 2003. A candidate of the Induan-Olenekian boundary Stratotype in the Tethyan region. *Science in China (Series D)* 46, 1182-1200.

Török, Á. 1998. Controls on development of Mid-Triassic ramps: examples from southern Hungary. In: Wright, V.P. and Burchette, T.P (eds). *Carbonate Ramps.* Geological Society, London, Special Publications, 149, 339-367.

Tucker, M.E. 2001. *Sedimentary Petrology, an introduction to the origin of Sedimentary Rocks.* Blackwell Scientific Publications, Oxford.

Tucker, M.E. 2011. *Sedimentary rocks in the field: A practical guide.* John Wiley and Sons, Chichester.

Twitchett, R.J. 1997. Palaeoenvironments of the Lower Triassic of the Dolomites, northern Italy. Unpublished PhD thesis, University of Leeds.

Twitchett, R.J. 1999. Palaeoenvironments and faunal recovery after the end-Permian mass extinction. *Palaeogeography, Palaeoclimatology, Palaeoecology* 154, 27-37.

Twitchett, R.J. 2000. A high resolution biostratigraphy for the Lower Triassic of northern Italy. *The Palaeontology Newsletter* 43, 19-22.

Twitchett, R.J. 2001. Incompleteness of the Permian-Triassic fossil record: a consequence of productivity decline? *Geological Journal* 36, 341-353.

Twitchett, R.J. 2006. The palaeoclimatology, palaeoecology and palaeoenvironmental analysis of mass extinction events. *Palaeogeography, Palaeoclimatology, Palaeoecology* 232, 190-213.

Twitchett, R.J. 2007. The Lilliput effect in the aftermath of the end-Permian extinction event. *Palaeogeography, Palaeoclimatology, Palaeoecology* 252, 132-144.

Twitchett, R.J and Barras, C.G. 2004. Trace fossils in the aftermath of mass extinction events. *Geological Society, London, Special Publications* 228, 397-418.

Twitchett, R.J. and Oji, T. 2005. Early Triassic recovery of echinoderms. *Comptes Rendus Palevol* 4, 531-542.

Twitchett, R.J. and Wignall, P.B. 1996. Trace fossils and the aftermath of the Permo-Triassic mass extinction: evidence from northern Italy. *Palaeogeography, Palaeoclimatology, Palaeoecology* 124, 137-151.

Twitchett, R.J., Looy, C.V, Morante, R., Visscher, H. and Wignall, P.B. 2001. Rapid and synchronous collapse of marine and terrestrial ecosystems during the end-Permian biotic crisis. *Geology* 29, 351-354.

Twitchett, R.J., Krystyn, L., Baud, A., Wheeley, J.R. and Richoz, S. 2004. Rapid marine recovery after the end-Permian mass-extinction event in the absence of marine anoxia. *Geology* 32, 805-808.

Twitchett, R.J., Feinberg, J.M., O'Conner, D.D., Alvarez, W. and McCollum, L.B. 2005. Early Triassic ophiuroids: their paleoecology taphonomy, and distribution. *Palaios* 20, 213-223.

Valentine, J.W. 1980. Determinants of diversity in higher taxonomic categories. *Paleobiology* 6, 440-450.

Velledits, F., Péró, C., Blau, J., Senowbari-Daryan, B., Kovács, S., Piros, O., Pocsai, T., Szügyi-Simon, H., Dumitricia, P. and Pálfy, J. 2011. The oldest Triassic platform margin reef from the Alpine-Carpathian region (Aggtelek, NE Hungary): platform evolution, reefal biota and biostratiagraphic framework. *Revista Italiana di Paleontologia e Stratigrafia* 117, 221-268.

Vermeij, G.J. 1977. The Mesozoic marine revolution: evidence from snails, predators and grazers. *Paleobiology* 3, 245-258.

Verschuen, D., Tibby, J., Sabbe, K. and Roberts, N. 2000. Effects of depth, salinity, and substrate on the invertebrate community of a fluctuating topical lake. *Ecology* 81, 164-182.

Vigran, J.O., Mangerud, G., Mork, A., Worsley, D. and Hochuli, P.A. 2014. Palynology and Geology of the Tiassic succession of Svalbard and the Barents Sea. *Geological Survey of norway Special Publication* 14.

Villéger, S., Novack-Gottshall, P.M. and Mouillot, D. 2011. The multidimensionality of the niche reveals functional diversity changes in benthic marine biotas across geological time. *Ecology Letters* 14, 561-568.

Visscher, H., Looy, C.V., Collinson, M.E., Brinkhuis, H., Konijnenburg-van Cittert, J.H.A., Kürschner, W.M. and Sephton, M.A. 2004. Environmental mutagenesis during the end-Permian ecological crisis. *PNAS* 101, 12952-12956.

Wade, B.S. and Twitchett, R.J. 2009. Extinction, dwarfing and the Lilliput effect. *Palaeogeography, Palaeoclimatology, Palaeoecology* 284, 1-3.

Waller, T.. and Stanley, G.D. 2005. Middle Triassic pteriomorphian Bivalvia (Mollusca) from the New Pass range, west-central Nevada: systematics, biostratigraphy, paleoecology, and paleobiogeography. *Journal of Paleontology* 7, 1-58.

Wang, C.Y. 1995. Conodonts of Permian-Triassic boundary beds and biostratigraphic boundary. *Acta Palaeontologica Sinica* 34, 129-151.

Wang, Y., Sadler, P.M., Shen, S-Z., Erwin, D.H., Zhang, Y-C., Wang, X-d., Wang, W., Crowley, J.L. and Henderson, C.M. 2014. Quantifying the process and abruptness of the end-Permian mass extinction. *Paleobiology* 40, 113-129.

Wasmer, M., Hautmann, M., Hermann, E., Ware, D., Roohi, G., Ur-Rehman, K., Yaseen, A. and Bucher, H. 2012. Olenekian (Early Triassic) bivalves from the Salt Range and Surghar Range, Pakistan. *Palaeontology* 55, 1043-1073.

Webb, A.E. and Leighton, L.R. 2011. Exploring the ecological dynamics of extinction. In: *Quantifying the Evolution of Early Life* 185, 185-220.

Wei, H., Shen, J., Schoepfer, S.D., Krystyn, L., Richoz, S. and Algeo, T.J. 2015. Environmental controls on marine ecosystem recovery following mass extinctions, with an example from the Early Triassic. *Earth-Science Reviews*. doi:10.1016/j.earscirev.2014.10.007.

Weidlich, O. 2002. Permian reefs re-examined: extrinsic control mechanisms of gradual and abrupt changes during 40 my of reef evolution. *Geobios* 35, 287–294.

Weidlich, O., Kiessling, W. and Flügel, E. 2003. Permian-Triassic boundary interval as a model for forcing marine ecosystem collapse by long-term atmospheric oxygen drop. *Geology* 31, 961-964.

Weitschat, W. and Lehmann, U. 1978. Biostratigraphy of the uppermost part of the Smithian stage (Lower Triassic) at the Botneheia, W-Spitsbergen, *Mitteilungen Geologisch-Paläontologischen Institut Universität Hamburg* 48, 85-100.

Wheeley, J.R. and Twitchett, R.J. 2005. Palaeoecological significance of a new Griesbachian (Early Triassic) gastropod assemblage from Oman. *Lethaia* 38, 37-45.

Wignall, P.B. 1993. Distinguishing between oxygen and substrate control in fossil benthic assemblages. *Journal of the geological Society of London* 150, 193-196.

Wignall, P.B. 2001. Large igneous provinces and mass extinctions. *Earth-Science Reviews* 53, 1-33.

Wignall, P.B. and Hallam, A. 1992. Anoxia as a cause of the Permian/Triassic mass extinction: facies evidence from Northern Italy and the western United States. *Palaeogeography, Palaeoclimatology, Palaeoecology* 93, 21-46.

Wignall, P.B. and Hallam, A. 1993. Griesbachian (Earliest Triassic) palaeoenvironmental changes in the Salt Range, Pakistan and southeast China and their bearing on the Permo-Triassic mass extinction. *Palaeogeography, Palaeoclimatology, Palaeoecology* 102, 215-237.

Wignall, P.B. and Twitchett, R.J. 1996. Oceanic anoxia and the end Permian mass extinction. *Science* 272, 1155-1158.

Wignall, P.B. and Twitchett, R.J. 1999. Unusual intraclastic limestones in Lower Triassic carbonates and their bearing on the aftermath of the end-Permian mass extinction. *Sedimentology* 46, 303-316.

Wignall, P.B. and Twitchett, R.J. 2002b. Extent, duration, and nature of the Permian-Triassic superanoxic event. *Geological Society of America Special Paper* 356, 395-413.

Wignall, P.B., Morante, R. and Newton, R. 1998. The Permo-Triassic transition in Spitsbergen: $\delta^{13}C_{org}$ chemostratigraphy, Fe and S geochemistry, facies, fauna and trace fossils. *Geological Magazine* 135, 47-62.

Wignall, P.B., Sun, Y., Bond, D.P.G., Izon, G., Newton, R.J., Védrine, S., Widdowson, M., Ali, J.., Lai, X-L., Jiang, H-S., Cope, H. and Bottrell, S.H. 2009. Volcanism, mass extinction, and carbon isotope fluctuations in the Middle Permian of China. *Science* 324, 1179-1182.

Wignall, P.B., Bond, D.P., Haas, J., Wand, W., Jiang, H., Lai, X., Altiner, D., Védrine, S., Hips, K., Zajzon, N., Sun, Y. and Newton, R.J. 2012. Capitanian (Middle Permian) mass extinction and recovery in western Tethys: A fossil, facies, and $\delta^{13}C$ study from Hungary and Hydra Island (Greece). *Palaios* 27, 78-89.

Wilson, M.A. and Palmer, T.J. 1989. Preparation of acetate peels. In: Feldmann, R.M, Chapman, R.E and Hannibal, J.T. *Paleotechniques*. The Paleontological Society, Special Publication 4, 142-146.

Worsley, D. and Mørk, A. 1978. The Triassic stratigraphy of southern Spitsbergen. *Nor. Polarinst. Arb* 43-60.

Worsley, D. and Mørk, A. 2001. The environmental significance of the trace fossil *Rhizocorallium jenense* in the Lower Triassic of western Spitsbergen. *Polar Research* 20, 37-48.

Wright, V.P. and Burchette, T.P. 1996. Shallow-water carbonate environments. In: Reading, H.G (ed). *Sedimentary environments: Processes, Facies and Stratigraphy*. Blackwell Science, Oxford. 325-392.

Yang, F., Peng, Y. and Gao, Y. 2001. Study on the late Permian *Claraia* in south China. *Scince in China (series D)* 44, 797-807.

Yang, H., Chen, Z-Q., Wang, Y., Tong, J., Song, H. and Chen, J. 2011. Composition and structure of microbialite ecosystems following the end-Permian mass extinction in South China. *Palaeogeography, palaeoclimatology, Palaeoecology* 308, 111-128.

Yin, H., He, W. and Xie, S. 2011. How severe is the modern biotic crisis? – A comparison of global change and biotic crisis between Permian-Triassic transition and modern times. *Frontiers in Earth Science* 5, 1-13.

Zatoń, M., Taylor, P.D. and Vinn, O. 2013. Early Triassic (Spathian) post-extinction microconchids from western Pangea. *Journal of Paleontology* 87, 159-165.

Zhang, L., Zhao, L., Chen, Z-Q., Algeo, T.J., Li, Y. and Cao, L. 2015. Amelioration of marine environments at the Smithian-Spathian boundary, Early Triassic. *Biogeosciences* 12, 1597-1613.

Zhao, X. and Tong, J. 2010. Two episodic changes of trace fossils through the Permian-Triassic transition in the Meishan cores, Zhejiang Province. *Science China Earth Sciences* 53, 1885-1893.

Zonneveld, J-P., Beatty, T.W. and Pemberton, S.G. 2007. Lingulide brachiopods and the trace fossil *Lingulichnus* from the Triassic of western Canada: implications for faunal recovery after the end-Permian mass extinction. *Palaios* 22, 74-97.

Zonneveld, J-P., Gingras, M.K., Beatty, T.W. 2010a. Diverse ichnofossil assemblages following the P-T mass extinction, Lower Triassic, Alberta and British Columbia, Canada: Evidence for shallow marine refugia on the northwestern coast of Pangea. *Palaios* 25, 368-392.

Zonneveld, J-P., MacNaughton, R.B., Utting, J., Beatty, T.W., Pemberton, S.G. and Henderson, C.M. 2010b. Sedimentology and ichnology of the Lower Triassic Montney Formation in the Pedigree-Ring/Border-Kahntah River area, northwestern Alberta and northeastern British Columbia. *Bulletin of Canadian Petroleum Geology* 58, 115-140.